Reading Between the Seams: Assessing Heat, Interference, and Opportunity in Flooded Mine Workings

Alexandra Sweeney

Reading Between the Seams: Assessing Heat, Interference, and Opportunity in Flooded Mine Workings

Alexandra Mary Wall Sweeney

A Thesis presented for the degree of
Doctor of Philosophy

Department of Earth Science
Durham University
United Kingdom
January 2026

Abstract

Mine water geothermal (MWG) systems can supply low-carbon heat by extracting energy from warm water in abandoned, flooded coal mines, but their wider deployment is constrained by uncertainty, including (i) where schemes are most feasible, (ii) how much heat can be sustainably extracted, and (iii) how neighbouring schemes should be managed where they share a connected mine water body. This thesis advances MWG development by improving prospectivity mapping, strengthening early-stage heat assessment, and proposing a practical basis for regulating thermal interactions between schemes.

First, emerging regional MWG prospectivity mapping methods are compared, including MiRAS, the Georesources Cornwall screening approach, the Mining Remediation Authority (MRA) opportunity mapping, and, conceptually, the more data-intensive Saxony methodology. Applied to Newcastle (UK), the methods highlight broadly similar favourable areas in but produce different spatial patterns and classifications because of divergent aims, thresholds, treatment of shallow workings, handling of mine water level data, and the inclusion, or exclusion, of heat demand.

Second, the thesis evaluates whether dynamic, mine-specific modelling adds value over common static heat-resource estimates. Using GEMSToolbox on a digitised two-seam coal mine (and an equivalent synthetic grid), results show that static methods can differ by orders of magnitude and do not capture key configuration controls (for example, shaft placement, connectivity, or collapse). Rapid scenario testing with GEMSToolbox provides time-dependent heat estimates and practical insight for feasibility-stage design and uncertainty management.

Finally, the thesis quantifies thermal interference between adjacent MWG schemes and introduces the heat extraction ratio (HER) as a simple, scheme-scale metric for expressing interference as a function of spacing, flow rate and operating lifetime. Building on international precedents and UK unitisation practice, two HER-based regulatory pathways are proposed: unitisation where feasible, or a simpler "yes/no" threshold approach. Together, these support transparent decision-making and improve investor confidence in long-term heat security.

Declaration

The work in this thesis is based on research carried out at the Department of Earth Science, Durham University, United Kingdom. No part of this thesis has been submitted elsewhere for any other degree or qualification and it is all my own work unless referenced to the contrary in the text.

Acknowledgements

I know many people enjoy and look forward to writing this section. I am not one of them, and I didn't. This is for two reasons:

1. I have already written a thesis and I don't want to write any more.

2. There are so many people I could, should, and would like to include, but I know I am going to forget someone. If your name is not below and you have actually bothered to read this, come back to this line: **I am thanking you personally and individually right now**. To be honest, I am gambling on nobody checking this.

The first people I must thank are my supervisory team: Jeroen, Julien, and Jon. Thank you for guiding me through this PhD, especially for helping me with my various modelling woes, and with the long slog of my first paper. Thanks also to Charlotte Adams for her advice, and to the many other people in the MRA and at Townrock Energy who gave advice along the way.

To Bex, Iolo, and Honor: I literally do not know what to say. There are no words to express how much fun I have had living with you. Please just imagine something deep and meaningful here.

Katie, I cannot thank you enough for all the good times we have had, and for all the logistical aid you have provided me. You are one of the best and most reliable friends in existence. I back you to do literally anything.

My GNZ pals, Jack, Zak, Joe, and Ella: thanks for keeping me going through many hours of online training, and for great field trip amusements. (P.S. I have actually written a thesis faster than I've finished that scrapbook.)

Emily and Sam, my safety team: ta for many a tea break. Gemma, my lady of leisure, I thank you for many late-night work distractions. More and more shout-outs to all my other department friends, including Adam, Janina, Saskia, and Annabelle.

Further thanks to my various long-distance motivators, including Helen, Sam, and Nick; Emily; Will; Marissa; Anaïs; and Hannah. Additionally, my family, who

have not only asked many questions and given advice, but also attended an hour-long talk I gave, which shows real commitment.

Special mention to everybody I lived with and knew in my first year at Ustinov: that was a great year of remembering how to socialise again post-pandemic.

To the Board Game Boys—Ali, Adarsh, Eoin, Josh, and Mike—you took every game far too seriously, and it was great fun the whole way. I hope I have been both a great and terrible influence on you all.

Contents

List of Figures

List of Tables

CHAPTER 1

Introduction

1.1 The need to decarbonise heat

By the early 2030s, global temperatures are expected to rise by 1.5 °C above pre-industrial levels (Intergovernmental Panel on Climate Change (IPCC), Core Writing Team; H. Lee and J. Romero (eds.) 2023). As warming continues, extreme weather events are becoming more severe and more frequent (Climate Change Committee, Adaptation Committee 2021). A more intense water cycle will bring both heavier rainfall and longer dry spells, ice and snow coverage are declining. Sea levels will continue to rise (Climate Change Committee, Adaptation Committee 2021), increasing the risk of flooding, while ocean waters will become increasingly acidic. Climate change is already harming human health, livelihoods, food and water security, and increasing displacement and inequality. Without action, these impacts will intensify, hitting vulnerable populations the hardest (Intergovernmental Panel on Climate Change (IPCC), Core Writing Team; H. Lee and J. Romero (eds.) 2023; Climate Change Committee, Adaptation Committee 2021).

The United Kingdom has committed to achieving net zero carbon emissions by 2050 through the 2019 amendment to the Climate Change Act. Meeting this legally

binding target requires a transition away from fossil fuels, which continue to provide the majority of the energy consumed in the UK (Energy Security & Net Zero 2025a). Space heating represents a particular challenge in this transition. It accounts for approximately 40 per cent of total energy consumption in the United Kingdom and produces around 34 per cent of national greenhouse gas emissions (Fraser-Harris et al. 2022). Approximately 90 per cent of households in England currently rely on fossil fuels, predominantly natural gas, for space heating (Energy Security & Net Zero 2025b). The scale of this reliance means that the decarbonisation of heating systems is critical to reducing green house gas emissions.

To decarbonise heat, low-carbon technologies will need to be deployed on a large scale. These include individual heat pumps, which would ideally operate on electricity from a decarbonised grid, as well as district heating networks supplied by low-carbon sources (e.g., waste-heat recovery, large-scale heat pumps, solar thermal, or potentially hydrogen boilers) (Department for Business 2020).

A range of renewable energy sources can support the energy transition, but each has limitations. Wind and solar photovoltaics are now central to electricity generation in the United Kingdom (Energy Security & Net Zero 2025a), yet both are intermittent and dependent on weather and seasonal variation, requiring significant grid balancing and storage capacity (Gonzalez et al. 2023). Biomass energy can provide both power and heat, but there are concerns over land use and supply chain sustainability (Destek et al. 2021). Marine energy, including tidal and wave power, has considerable theoretical potential but has not been deployed at significant scale in the UK (Coles et al. 2021; Jin and Greaves 2021). Solar thermal systems can supply hot water and supplementary heating, although their output is variable and most effective in the summer (Greco et al. 2020).

Geothermal energy offers several advantages compared with these more established renewables. Unlike solar and wind, geothermal provides a continuous baseload supply of energy that is not affected by weather or seasonal variation (Younger 2015). It also requires a relatively small surface footprint. Importantly, geothermal resources can be utilised not only for power generation but also directly for heating, offering a dual contribution to the United Kingdom's decarbonisation strategy.

1.2 What is geothermal energy?

Geothermal energy is heat contained in the Earth. This heat is a combination of primordial heat from the Earth's formation, heat generated by the decay of radioactive isotopes, and solar energy stored in the top meters of the crust. The difference in temperature between the Earth's convecting mantle and the surface results in the geothermal gradient. In general geothermal heat is accessed by running a fluid through the rocks of the target area to act as a carrier for the heat. This fluid may be naturally occurring, or injected, it may be contained within pipes, or not.

Geothermal energy resources can be classified in many different ways. Enthalpy is commonly used, dividing the resources into low, intermediate and high enthalpy. The values used to define these, however, are not standardised (Table 1.1). It is common to separate into 'shallow' and 'deep' geothermal resources, but the definition varies from country to country. In the UK, 300 - 500 m is the threshold between shallow and deep depending on the context (Abesser et al. 2018; Abesser et al. 2023; Department for Energy Security and Net Zero 2025b; *Infrastructure Act 2015* 2015). In the UK shallow geothermal covers low temperature heat resources of approximately 10 - 25°C. This heat resource can be contained in soils, groundwaters, or mines (see Section 1.3) and is usually exploited by a ground source heat pump (GSHP).

Table 1.1: Enthalpy classification of geothermal resources adapted from Dickson et al. 2005 with additional information from McClean and Pedersen 2021*. Temperatures are in °C.

	Low enthalpy resources	Intermediate enthalpy resources	High enthalpy resources
Muffler and Cataldi (1978)	< 90	90–150	> 150
Hochstein (1990)	< 125	125–225	> 225
Benderitter and Cormy (1990)	< 100	100–200	> 200
Nicholson (1993)	≤ 150	–	> 150
Axelsson and Gunnlaugsson (2000)	≤ 190	–	> 190
McClean and Pedersen (2021)*	≤ 100	100–150	> 150

Geothermal energy can be exploited in a variety of ways, although historically most development has taken place in regions close to plate boundaries where heat flow is elevated (Stelling et al. 2016). The United Kingdom is not located near a plate boundary, yet significant geothermal potential exists in several regions (Busby

2014).

One important resource type is granite contains high concentrations of heat-producing radioactive isotopes such as uranium, thorium, and potassium. These rocks can be exploited by targeting fracture networks that host warm groundwater, as demonstrated at United Downs in Cornwall, UK (Olver and Law 2025). Where natural permeability is insufficient, it can be enhanced using techniques such as acid dissolution, thermal fracturing, or hydraulic fracturing (Jia et al. 2022). Such approaches are collectively referred to as enhanced or engineered geothermal systems (EGS). These can be doublet systems such as United Downs (Olver and Law 2025), or co-axial systems such as at Eden Geothermal, Cornwall, UK (Horne et al. 2025).

Alternatively, closed-loop systems are not restricted to permeable reservoirs. A working fluid is circulated through a lined well and heat is transferred from the rock via conduction (White et al. 2024). Some closed loop systems are referred to as Advanced Geothermal Systems (AGS) (Beckers et al. 2022). This terminology, as often in geothermal, is not fully standardised and the term Deep Closed Loop Geothermal Systems is also used for closed loop systems which drill deep with the aim of accessing high temperatures, via conduction, to produce electricity (Kelly and McDermott 2022). The benefit of not relying on the geology of an area to have high fluid flow, or stimulation of the reservoir, is that the technology can theoretically be deployed anywhere (White et al. 2024; Beckers et al. 2022).

In addition, there is growing interest in the potential to repurpose existing oil and gas wells for geothermal applications, thereby extending the productive use of established subsurface infrastructure (Watson et al. 2020; Li et al. 2024; Soldo et al. 2020; Santos et al. 2022).

Hot sedimentary aquifers represent another category of resource. These conduction-dominated reservoirs within sedimentary basins are capable of supplying economically viable quantities of warm water (Brémaud et al. 2025; Comerford et al. 2018). A notable, and the only UK example, is the Southampton District Energy Scheme, which had a 2.8 MW geothermal capacity (Busby 2014) between 1988 and 2020 and is currently undergoing repair (Abesser and Walker 2022).

Ground Source Heat Pumps are the most common geothermal installation in the

UK. They extract heat from the near surface, usually in a closed loop system, from either shallow boreholes or trenches. This heat is then boosted with a heat pump (see Section 1.3.8 for details) to provide space heating.

1.3 Mine Water Geothermal

Mine water geothermal refers to the recovery, and in some cases storage, of heat using water contained within flooded underground mine workings. During active mining water is often pumped out to keep the working dry and allowing mining activity (Fernihough and O'Rourke 2021). However, operating the pumps is expensive, so following mine closure pumping ceases and voids such as roadways and shafts fill with groundwater, forming a permeable network that can be accessed by boreholes or existing shafts. This water is warmed by the natural heat flux of the earth and mineral oxidation (Raymond and Therrien 2008; Monaghan et al. 2025). Heat can be extracted either by pumping mine water to the surface (open-loop systems) or by circulating a working fluid through heat exchanger pipes placed within mine water or adjacent ground (closed-loop systems) (Banks et al. 2019b). Because mine water temperatures are generally 10 - 20 °C (Walls et al. 2024), heat pumps are typically required to deliver useful supply temperatures (see Section 1.3.8). The feasibility and sustainability of mine water geothermal depend on the available temperature and flow, hydrogeological connectivity, water chemistry, and practical access to mine workings. The following sections classify mine water geothermal systems into open-loop configurations with reinjection or discharge, shaft-based schemes, closed-loop approaches, and mine thermal energy storage, before discussing enabling mine conditions and key technical, regulatory, and socio-economic challenges.

1.3.1 Open loop with re-injection

In an open-loop reinjection system (Figure 1.1b), mine water is pumped directly from the workings to a surface heat exchanger (Banks et al. 2004). Abstraction is usually via purpose-drilled boreholes into the workings, or when open and available via existing mine entries, such as shafts. A heat exchanger is commonly used to

prevent fouling of the heat pump by metal precipitates and other suspended solids (Watzlaf and Ackman 2006). Heat from the mine water is then upgraded by a heat pump and delivered to the consumer at a higher temperature. Meanwhile, the cooled mine water is returned to the mine to re-equilibrate thermally. Reinjection is typically into a vertically or laterally distant part of the mine system, in order to minimise the risk that cooled water is re-abstracted before it has had time to warm (Banks et al. 2004; Banks et al. 2022; Walls et al. 2021).

Open-loop systems are generally more thermally efficient than closed-loop systems because the mine water remains in direct contact with the surrounding rock mass (Banks et al. 2004; Banks et al. 2022; Walls et al. 2021). However, they are more susceptible to scaling, clogging and corrosion (see Section 1.3.9), and pumping water to the surface can require substantial energy, with both energetic and financial costs increasing with depth (Oppelt et al. 2025).

This type of open-loop reinjection system forms the basis for most of the modelling presented in this thesis.

1.3.2 Open loop with surface discharge

In a surface discharge system, rather than being re-injected into the mine, water is discharged to a surface water body (Figure 1.1a). This has benefits because there is no risk of short-circuiting the system and re-abstracting cooled water, and less drilling is required.

There are sites where mine water naturally discharges at the surface (Walls et al. 2022), or is already pumped to the surface to protect drinking-water aquifers or surface waters from contamination, or to prevent flooding of surface infrastructure (Coal Authority 2024c; Bailey et al. 2013; Alvarado et al. 2022; Wyatt et al. 2023b). In such cases, extracting heat from water that is already being pumped, or that naturally emerges at the surface, can avoid the costs of new drilling and pumping.

However, if a new system is to be established, it may be difficult to obtain the necessary discharge licences, and mine water treatment may be required to address problematic water chemistry, which can be costly.

1.3.3 Open loop in shafts

An open-loop standing column system is a single-borehole or single-shaft open-loop arrangement in which groundwater is abstracted, passed through a heat exchanger (typically via a heat pump), and then re-injected into the same structure (borehole or shaft) at a different depth, so that the subsurface provides both the source and the sink for heat exchange (Banks et al. 2004). In a mine shaft application, water is abstracted from one depth in the shaft and returned to another depth within the same shaft (Figure 1.1e).

To operate as a standing column configuration without rapid thermal short-circuiting, the system requires either very low abstraction rates or sufficient ambient groundwater flow to advect injected water away from the abstraction intake (Walls et al. 2021). Here, 'strong' groundwater flow refers to conditions where advective transport within the mine workings is large enough that a substantial fraction of the reinjected water is displaced from the vicinity of the pump between injection and subsequent abstraction, relative to transport by mixing and dispersion alone.

1.3.4 Closed loop in shaft and surface water

A closed loop system in a mine shaft consists of a sealed pipe or pipe array installed within the shaft (Figure 1.1c). A working fluid is circulated through the pipework, typically a mixture of water and antifreeze (Banks et al. 2004). Heat is transferred from the mine water and surrounding rock to the working fluid through the pipe wall. The warmed fluid then returns to a heat pump, which raises its temperature to a level suitable for space heating, before it is recirculated through the shaft to acquire heat again (Banks et al. 2004).

Closed-loop systems rely on natural replenishment of heat within the mine water and surrounding rock to sustain operation over time. Replenishment may occur through processes such as natural circulation of mine water within the workings and conductive heat inflow from the rock mass, which act to restore temperatures in the vicinity of the closed-loop heat exchanger (Walls et al. 2021).

Closed-loop systems can also be installed in mine-related surface waters, such as

tailings ponds (Figure 1.1d), although these are likely to be at lower temperatures than water within the mine workings (Oppelt et al. 2025).

Closed-loop systems do not abstract mine water directly, so they do not experience the same clogging risks as open-loop systems (Section 1.3.9) and they often require fewer environmental permits (Walls et al. 2021). However, because heat transfer occurs via conduction across the pipe wall rather than by abstracting and cooling mine water directly, closed-loop systems typically have lower thermal capacities than open-loop systems (Banks et al. 2004), commonly on the order of tens of kilowatts (Walls et al. 2021).

1.3.5 Mine Thermal Energy Storage (MTES)

Rather than serving solely as a source of heating, the mined subsurface can also function as a reservoir for thermal energy, storing excess heat during periods of surplus relative to demand (Turnell et al. 2023). This can be achieved by using a heat exchanger to warm abstracted mine water before re-injecting it into the mine. The heat input may derive from excess solar energy (Koley et al. 2024), industrial waste heat, or residual heat from mine water previously used for cooling applications.

1.3.6 Coal Mines

This thesis focuses on mine water geothermal energy in coal mines. It is possible to use other types of mine for geothermal extraction, however due to their configuration and location coal mines are particularly prospective in the UK, and so are the focus of this thesis (Davies et al. 2023).

Coal has been used in the United Kingdom since the Bronze Age (Hatcher 1993a), with extraction on an industrial scale beginning in the 18th century. The development of coal mining played a central role in the growth of major urban and industrial centres (Fernihough and O'Rourke 2021), and its legacy remains evident today, with approximately one in four homes and businesses situated above former coalfields (North East LEP Mine Energy Taskforce 2024).

Coal seams in the UK are commonly given names (often local), and the same

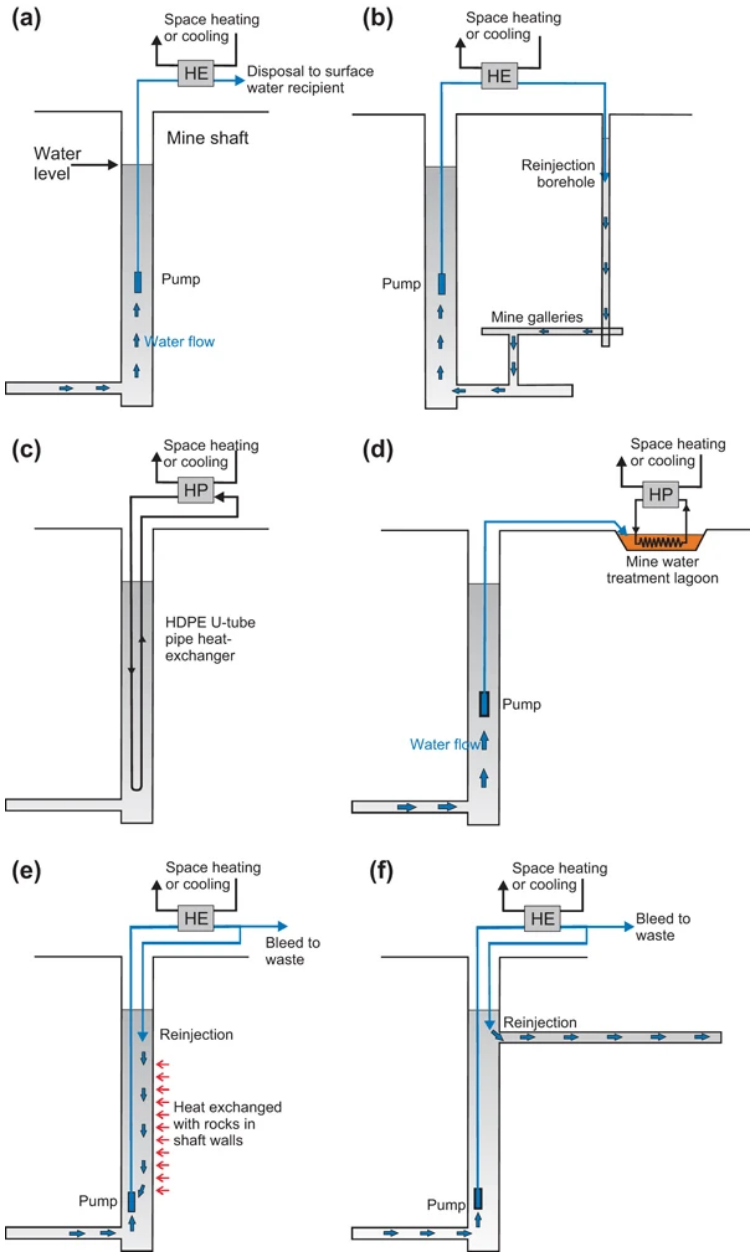

Figure 1.1: Different MWG configurations from Banks et al. (2019b). (a) Open loop with surface discharge, (b) Open loop with re-injection, (c) Closed loop in flooded shaft, (d) Closed loop in surface treatment pond, (e) Standing column with bleed and recirculation in shaft, (f) Standing column configuration, with large natural flow up shaft. HE heat exchanger or heat pump, HP heat pump.

seam may carry different names/aliases in different districts (Banks et al. 2022; McLean 2018).

As of 2024, only five underground coal mines remained operational in the United Kingdom with workforce of approximately 265 people (Department for Energy Security and Net Zero and Department for Business, Energy & Industrial Strategy 2025). Most abandoned workings are now flooded, with recorded mine areas extending over 15,000 km^2 (Wyatt et al. 2025). The Mining Remediation Authority currently treats around 120 billion litres of mine water annually, equivalent to 3800 L s^{-1} (Wyatt et al. 2023b). A reduction of just 5 K in this water could yield approximately 80 MW of heat flow. If a house is assumed to use 10,000 kWh per year for space heating (Phillips and Wilson 2024), 80 MW could heat 70,000 homes, demonstrating the scale of the potential resource already being brought to the surface. This is the easiest heat to access, but is only a portion of the total beneath the surface. The utilisation of mine water heat could therefore reduce greenhouse gas emissions, increase domestic energy production, and contribute to energy security. As many former coalfield areas are characterised by high levels of socio-economic deprivation (Beatty et al. 2019), the development of mine water geothermal schemes may also provide a means of addressing fuel poverty.

Mining Methods

There have been a variety of underground coal extraction methods used in the UK. Initially, where coal was exposed in hillsides workers would have dug this out until the hillside collapsed. This could be extended by digging a tunnel into the hill, following the seam. This type of mine was called a drift, but had various whimsical names that varied regionally, such as day-hole, 'in-gaun-e' en' ('ingoing eyes'), and bearmouth (Hatcher 1993a). Bellpits (Figure 1.2a) accessed coal vertically, a shaft would be sunk downward from the surface into a coal seam. The coal would then be dug out surrounding the shaft until it was at risk of collapse, at which point a new pit would be sunk adjacent to the first (Hatcher 1993a).

However, larger scale coal extraction was done by either room and pillar (also called stoop and room, pillar and stall, bord and pillar) (Figure 1.2) or longwall

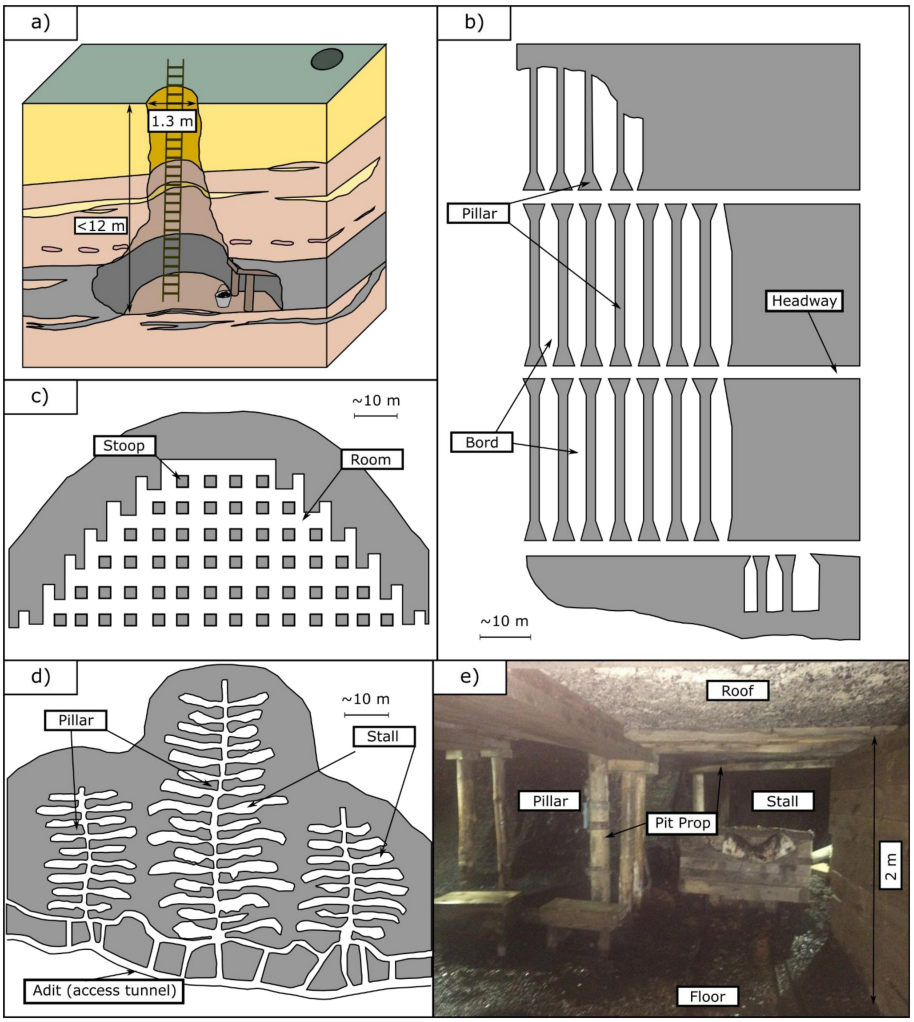

Figure 1.2: Coal mining methods (Andrews et al. 2020). a) Bell pit, b) Bord-and-pillar workings, Newcastle upon Tyne (17th Century), c) Stoop and room workings, Scotland (17th Century), d) Pillar and stall workings, South Wales (17th Century), e) Photograph of pillar and stall workings, Beamish open air museum.

mining (Figure 1.3).

Both of these methods are suitable for horizontal deposits (Hartman, 2002), which coal is commonly found as. In room and pillar (Figure 1.2) the coal is extracted in broadly straight lines, the rooms, which cross-cut each other at right angles, creating a chequerboard pattern, leaving 'pillars' of coal behind to support the roof (Younger and Adams 1999). Pillars can be recovered later (referred to as pillar robbing) when that section of the mine is no longer being used, allowing the roof to collapse (Younger and Adams 1999). The room and pillar method was the primary way of underground coal mining until the 20th century when longwall

mining became common (Younger and Adams 1999).

Longwall mining now uses a mechanical shearer which moves along the coal face with hydraulic supports holding up the roof as the machine shears. As the machine advances the supports move and the roof is allowed to collapse behind it (Hartman, 2002). Prior to mechanisation it would have been hewers (mine workers who extracted coal from the coal face) working simultaneously on the face instead of a shearer, and other mine workers using wood and waste rock to support the roof (Hatcher 1993a).

The collapsed roof material left behind is called goaf or gob (Bailey et al. 2016; Hatcher 1993a; Brune and Saki 2017). In room and pillar workings where the pillars have been left 50 % of the mine is left as void space, whereas in long wall mining only 20 % is void space (Younger and Adams 1999). The void space provides lateral connectivity for mine water to flow through when the water level rises, with shafts providing vertical connectivity.

In zones which have been longwalled or pillar robbed (where the coal pillars left to support the roof are later removed) the area can be said to have undergone total extraction (Galvin 2016; Andrews et al. 2020).

When establishing a mine water geothermal system knowing the mining method is important. Room and pillar zones may retain greater void space and therefore higher flow rates may be obtainable. However, the target areas for drilling are limited to the open voids of worked areas and are adjacent to rock (see Section 1.3.9).

Shaft Treatments

Drilling costs are a significant component of the capital expenditure for a mine water geothermal scheme. Where an existing shaft can be used instead of drilling a new well, substantial cost savings may be possible. The Mining Remediation Authority maintains datasets of known shafts and, where available, the state of abandonment and water level; the latter two are provided on a site by site request basis (Deeming et al. 2026). The method of shaft closure and the original shaft construction both influence accessibility. A range of closure methods has been used

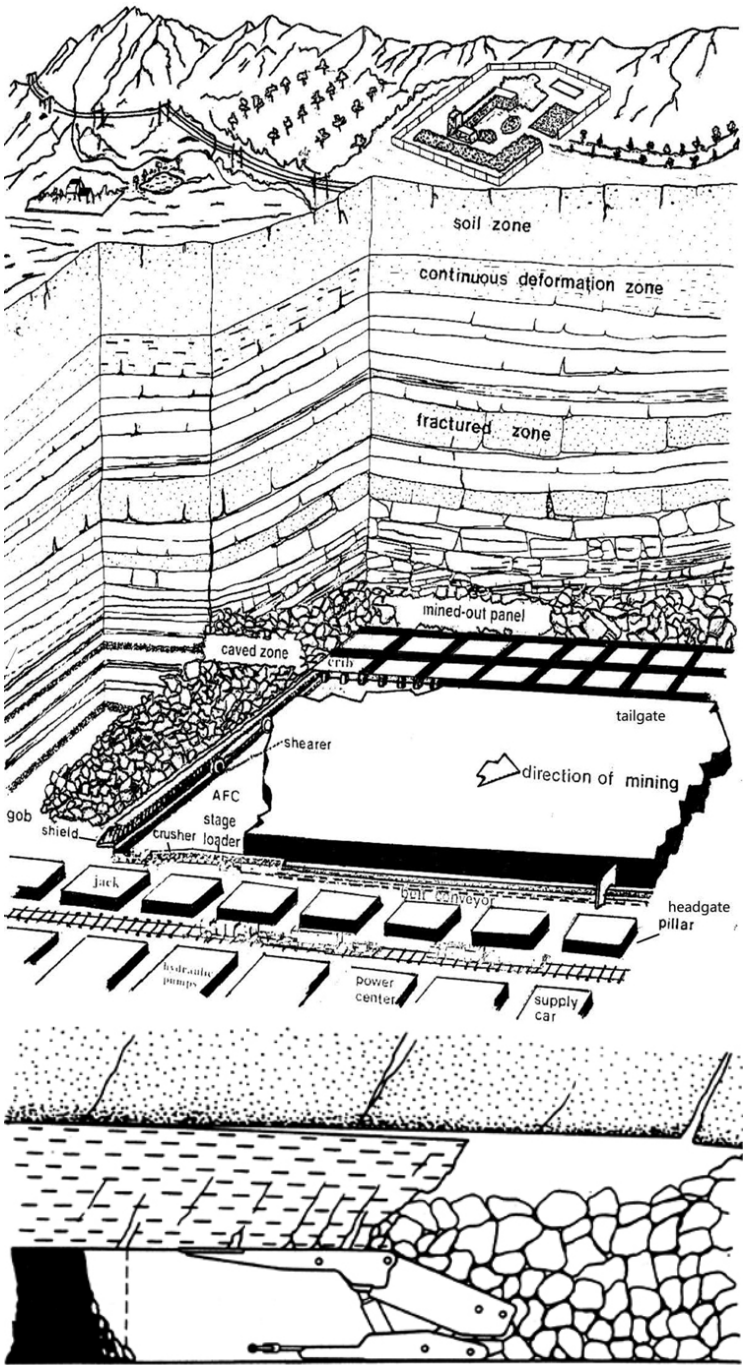

Figure 1.3: Vertical and horizontal view of longwall mining. In the upper section of the image there is room and pillar mining around the edge of a long wall pannel. The shearer is cutting away at the coal on the left and moving rightward. In the lower section the hydraulic support is holding up the roof as the shearer advances, allowing the goaf to collapse behind. From Peng (2019).

(Figure 1.4) (National Coal Board 1982). In older shafts the primary aim was often to level the surface, so convenient surface materials were placed as fill. Such materials may be toxic or prone to compression or decay, which can lead to instability. Mining equipment was sometimes used as fill, and shaft equipment such as cages may have been removed, left in place, or dropped to the bottom (National Coal Board 1982). Fill may extend the full depth of the shaft or only to an intermediate landing. To reduce expense, a platform was sometimes installed and used as a false bottom for filling; platforms could be made of wood or metal. Intersecting passages may or may not have been blocked, and if left open any disturbance can allow fill to migrate into the workings (National Coal Board 1982). More recent practice focuses on making the shaft safe and stable. Fill is designed and selected to suit the geology and shaft structure, and where possible barriers are constructed at intersections to prevent loss of fill into adjacent passages (National Coal Board 1982). The National Coal Board guidance recommends filling operations combined with a cover as best practice for abandoned shafts (National Coal Board 1982). Consequently, more recently treated shafts are likely to be blocked and are not straightforward targets for open loop mine water systems, although potentially still possible for high permeability fill (Deeming et al. 2026). Where a shaft has only been plugged or capped it may be more accessible, although the internal condition and any remaining equipment can still present significant challenges. Even shafts left open within an enclosure or under a grill may have accumulated debris that obstructs access. In addition, some older shafts have subsequently been built over (Deeming et al. 2026).

1.3.7 Mine water project examples

Although geothermal energy has a relatively low take up in comparison with other renewable energy technologies (Younger 2015), and mine water geothermal was until recently very low profile, there are examples both in the UK and around the world (Walls et al. 2021; Goudarzi et al. 2023).

One of the earliest mine water geothermal heating systems is in Spring Hills, Nova Scotia, Canada (Jessop et al. 1995). It was first investigated in the 1980s, there are still operational systems today, and the area is under consideration for

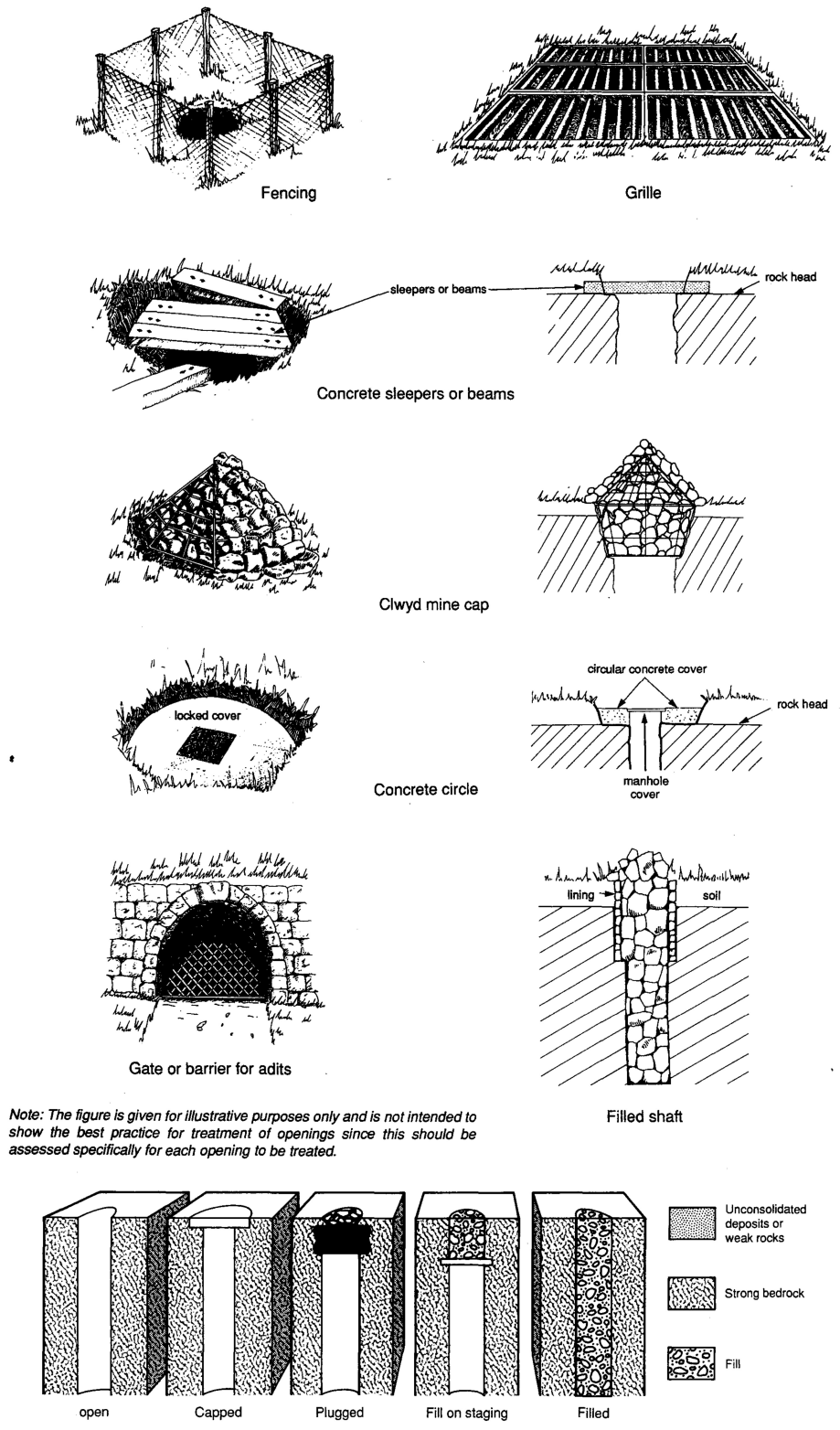

Figure 1.4: Possible shaft treatments (Department of the Environment and Welsh Office 1994)

further development (Jessop et al. 1995).

Possibly one of the most high-profile mine water systems is in Heerlen, Netherlands. In 2008 it began as a pilot district heating system using the coal mines beneath the city, and continues to operate, having undergone upgrades. It combines the heating and cooling of buildings (250,000 m^2 floor area) and uses the subsurface as thermal storage. There are two hot wells which have a temperature of 28°C at 700 m bgl, two cold wells, 16°C at 250 m, and an intermediate well at 500 m. As the underground is used as storage, all of the wells can be used for re-injection and abstraction (Verhoeven et al. 2014; Mijnwater Energy BV and IEA Geothermal 2023).

The UK has several mine water geothermal projects. There are three separate open loop with re-injection systems in Gateshead, UK. Two (Abbotsford Road and Nest Road) are operated by a private company 'Lanchester Wines' to heat warehouses and abstract from the Felling Colliery (Banks et al. 2022), and the third is operated by Gateshead Energy Company, on behalf of Gatehead Council (Gateshead Council et al. 2023). The third system feeds into a district heating system that supplies heat to several large building, such as a museum, as well as re-furbished council housing. As these systems are located in the same town, there is also a project run by the Mining Remediation Authority which has drilled boreholes in between the Gateshead Energy and Lanchester Wines systems to monitor the connection between these systems (Monaghan et al. 2025).

The Nest Road Lanchester Wines system abstracts 40 L s^{-1} water at 13-14°C, from one borehole at 131 m bgl, into the High Main Aquifer System (HMAS), which comprises of the High Main Seam and the High Main Post sandstone. A temperature decrease of 4 K is applied before re-injection into a single borehole at 280 m depth, into the Deep Mined Aquifer System (DMAS), which includes the Harvey, Beaumont and Hutton seams and is potentially connected to three overlying seams: Brass Thill, Six-Quarters and Maudlin-Bensham (Banks et al. 2022). The system was built in 2018 and still operates as of 2025.

The Abbotsford Road project was originally implemented in 2018. At the beginning, due to technicals issues, water was abstracted not from a mined seam, but

from a sandstone aquifer 110 m bgl, called the Upper Aquifer Sytem (UAS). One production well abstracted at 20 - 30 L s^{-1} at a temperature of 11-13°C (another two wells were drilled but had low yields). This water was re-injected at 155 m, into as the HMAS (Banks et al. 2022). The UAS is an oxidising system, this resulted in ochre precipitation issues (see Section 1.3.9), and also never produced flow rates as high as was desired. Therefore in 2022, a new exploration program began, drilling several exploration boreholes into the Felling Colliery. One of these wells was converted to full abstraction width and now the Abbotsford Road site abstracts from the DMAS at 265 m at temperature of 19°C. A ΔT of 8 K is removed at the heat pump and the mine water is reinjected through two boreholes into the HMAS. Importantly the DMAS is a reducing environment, limiting the problems with iron buildup (Mourik 2025). Reducing conditions imply little available oxygen, so iron is less likely to oxidise and precipitate as ochre; with less precipitation, there is less accumulation and clogging in wells, pipework, and reinjection zones.

The Gateshead project is a large 6.2 MW project with two abstraction wells and one re-injection well. Water is abstracted from 150 m at 15°C and re-injected at 50 m. There is also an additional well interconnecting the abstraction and re-injection horizons to facilitate increased yields from the abstraction wells. The total flow rate is up to 140 L s^{-1} (Gateshead Council et al. 2023).

In Seaham, approximately 22 km south-east of Gateshead, there is another scheme being built. Water, at 19 - 20°C, is already pumped at 150 L s^{-1} from the mine workings to protect the local drinking water aquifer (Walls et al. 2021). Heavy metals are removed, and the water is disposed of into the sea. A housing development is being built next to the treatment site, called Seaham Garden Village. When built the heat from the mine water will used in a district heating scheme to heat 750 homes (Durham County Council 2024). This will be an open loop with discharge scheme.

There is also a research facility in Glasgow, the UK Geoenergy Observatory (UKGEOS), which was built to investigate mine water geothermal energy (Monaghan et al. 2025). The UKGEOS Glasgow Observatory consists of 12 boreholes, including abstraction and reinjection wells as well as dedicated monitoring boreholes, drilled

to depths ranging from 16 to 199 m. These are equipped with distributed temperature sensing (DTS) cables, pressure and flow sensors, and downhole electrodes to enable four-dimensional electrical resistivity tomography (ERT) monitoring (British Geological Survey 2021). The facility supports controlled pumping and reinjection tests, the testing of heat pumps and chillers, and experimental investigations of thermal breakthrough and subsurface thermal storage (Gonzalez Quiros et al. 2025). In addition, it enables long-term monitoring of water chemistry, iron precipitation, and subsurface responses. The site also provides open-access datasets and gas monitoring, pre-drill soil chemistry, and surface water and groundwater geochemistry, as well as ground motion monitoring using InSAR reflectors.

The Lindsay mine water heat scheme (near Ammanford, Carmarthenshire) repurposes an existing mine-water treatment site by using heat exchangers submerged in a settlement pond used as part of a mine water treatment scheme. The recovered heat and supplies space heating and hot water to a nearby industrial unit.

At Markham Colliery (Markham No. 3 Shaft), near Bolsover, Derbyshire there is a standing column mine water heat-pump. Mine water is pumped from the flooded shaft, passed through a heat exchanger linked to a 20 kW heat pump, and then returned to the same shaft at a slightly different depth. Water was initially pumped from 235 m bgl, however in 2015 the pumps were raised to 170 m bgl as mine water levels had risen. The re-injection height was also raised from 250 m to 153 m bgl (Burnside et al. 2016).

1.3.8 Heat Pumps

A heat pump (Figure 1.5) takes a low-temperature input, either mine water or a secondary working fluid that has absorbed heat from the mine water via a heat exchanger, and raises it to a higher temperature suitable for space heating (Banks et al. 2004). The heat source, in this case the mine water, boils the refrigerant liquid at the evaporator, converting the liquid to a gas. The gas travels to the compressor, where the adiabatic compression causes the gas temperature to increase. This, now hot, gas travels to a condenser, where the heat is transferred to the space heating medium and upon cooling the gas returns to a liquid. The liquid travels through

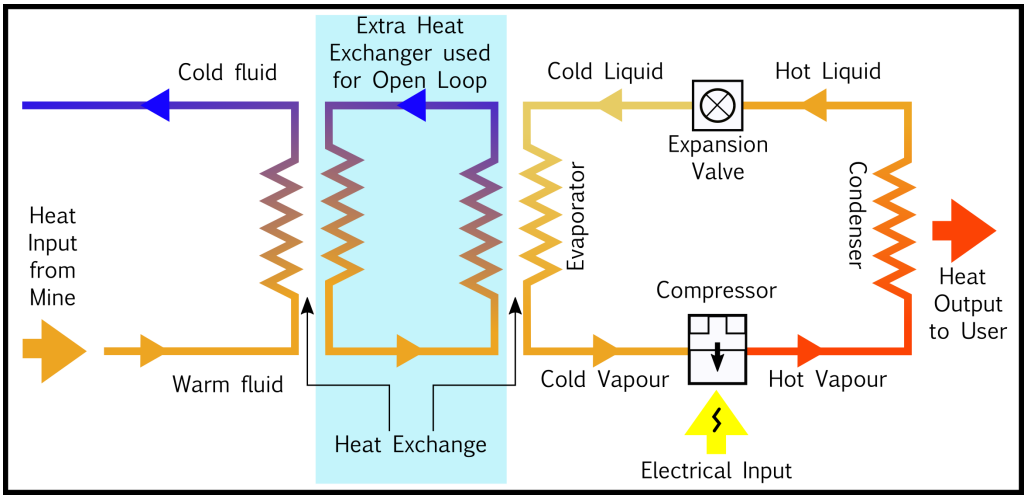

Figure 1.5: Diagram of heat exchanger and heat pump after Watzlaf and Ackman (2006).

the expansion valve, which drops the temperature before the liquid starts the cycle again (Watzlaf and Ackman 2006).

Modern heat pumps can raise temperatures around 50°C (Chua et al. 2010), enough to take 12°C mine water and raise it to 60°C to be used with standard radiators. Heat pumps can take 5°C out of the minewater at the evaporator stage, i.e., if the water abstracted was 12°C it would be re-injected at 7°C (Renz et al. 2009). The efficiency of a heat pump is termed the coefficient of performance or COP, which is usually from 3 – 6 for geothermal heat pumps (Behrooz et al. 2008). The COP is calculated by dividing the heat output of the pump by the amount of electrical energy input into the compressor, needed to raise the temperature (Watzlaf and Ackman 2006; Banks et al. 2004).

$$COP = \frac{Q}{P} \tag{1.1}$$

Q is the amount of heat outputted, P is the amount of electrical energy inputted. The COP is determined by the model of pump, and, crucially, the amount the temperature must be raised from the initial mine water temperature (Loredo et al. 2016). The less the heat pump needs to raise the temperature by, the more efficient the heat pump will be and the higher the COP. Sufficiently low COP values are vital for a mine water scheme to be financially viable (Ghoreishi Madiseh et al.

2012; Loredo et al. 2016). Using a low temperature form of heating can reduce the temperatures needed, for example, under floor heating requires input temperatures of less that 40°C (Østergaard et al. 2022). Targeting hotter mine waters is the other obvious solution. There is however a trade off in using hotter waters, these are usually from greater depths, leading to an increased energy (and cost) for pumping and can have a less favourable water chemistry (Walls et al. 2021).

1.3.9 Challenges in mine water geothermal

Mine water geothermal schemes can offer a reliable source of low-carbon heat, but moving from concept to long-term operation is often constrained by a set of interlinked technical, regulatory and socio-economic challenges. Flooded mine workings are inherently inaccessible, so uncertainty in connectivity, temperature distribution and sustainable abstraction rates can complicate MWG implementation. Operational risks are also strongly influenced by mine water chemistry, where dissolved iron, salts and gases may drive scaling, corrosion and clogging, increasing maintenance demands and threatening performance. In addition, developers must account for practical access and drilling constraints, legacy mine infrastructure and ground movement hazards, alongside project-specific permitting requirements for abstraction, discharge and reinjection. Finally, successful deployment depends on non-technical factors including public acceptance, clear governance and investment barriers. The following subsections review these challenges in turn, focusing on regulation, heat estimation, chemistry, ground movement, prospectivity mapping, drilling, public awareness and social impact, and financing.

Regulation

In the UK, unlike several other countries, there is no specific law that regulates geothermal energy. Instead geothermal energy comes under various different laws and regulations. These include the Town and Country planning regime (McClean and Pedersen 2023), Health and Safety laws (*Construction (Design and Management) Regulations 2015* 2015; *Provision and Use of Work Equipment Regulations 1998* 1998; *Management of Health and Safety at Work Regulations 1999* 1999), the

abstraction of water whcih is regulated by the various environment agencies of the UK, and access to the mines, which is controlled by the Mining Remediation Authority.

There are two key regulatory issues in the UK. One, is that a complicated regulatory landscape adds time (Li et al. 2025) and expense to a geothermal project (which is already capital expenditure (CapEx) heavy) making the project less attractive to investors. The second is, that in none of the applicable laws is heat considered ownable; it is either regulated as a pollutant (Abesser et al. 2018) or treated as a physical characteristic (McClean and Pedersen 2021). As a result, geothermal operators cannot be assured exclusive access to the heat resource over the lifetime of a project, since it may be appropriated or disrupted by nearby developments.

In Northern Ireland, Wales and England a licence is required to abstract more than 20 m^3 of water per day (Northern Ireland Environment Agency, Natural Resources Wales, Environment Agency) (*Water (Northern Ireland) Order 1999* 1999; *Water Resources Act 1991* 1991), however, in Scotland an abstraction licence is not required if the water is re-injected into the same geological formation after being used for geothermal energy extraction (*The Water Environment (Controlled Activities) (Scotland) Regulations 2011, General Binding Rule 17* 2011). The amount of heat abstracted can be limited as part of the licensing conditions, but this can only be done to protect the ground/surface water from a detrimental temperature change, not to protect against thermal interference (McClean and Pedersen 2023). If subsequent abstraction licences to other operators were to reduce the amount of water a prior licensee could abstract, they could claim damages. However, this does not apply if there were to be a reduction in heat (McClean and Pedersen 2023).

To access the majority of UK coal mines, permission is needed from the Mining Remediation Authority. The includes permission to drill, a mine water heat access agreement for long term use of the mine workings, and where the Mining Remediation Authority owns surface land in use, a property agreement will be required. The access agreement is in two parts, the first is for testing the system, and the second is for the long term operation of the project (Mining Remediation Authority 2024b). The access agreement is not designed to confirm that an applicant has the

ownership of any heat in the mine, it is to ensure public safety and protect property (Eynon 2024).

Heat estimation

Estimating the extractable heat from flooded mine workings is an iterative process that evolves as a project progresses from desk-based appraisal to detailed investigation and design (Watzlaf and Ackman 2006). The approach adopted at each stage is strongly influenced by the quantity and quality of available information on mine geometry, hydraulic connectivity, groundwater temperatures, and thermal and hydraulic properties (Monaghan et al. 2022; Chu et al. 2021). In most cases, these parameters are poorly constrained at the outset of a mine water geothermal assessment, requiring estimates to be progressively refined as new data become available (Grant 2014; Ciriaco et al. 2020).

At the earliest stages of a MWG project, before any exploration drilling, there is very little data available on the condition of the mines, or the water flow within. The mine plans are available from the Mining Remediation Authority in the UK, which will show the architecture as recorded, but as the mine can be hundreds of years old, how accurate this plans are, or how much degradation (e.g., collapse) may have occurred is unknown. In addition as discussed previously the treatment of any shafts linking the various levels of the mine is likely unknown. There may be data on the water levels and chemistry within the mine available from the Mining Remediation Authority, however this may not be from the same mine being investigated, and for some mine blocks there is no data at all.

Common early stage heat assessments are typically relatively simple, high-level methods that can be applied with limited data (Ciriaco et al. 2020). These methods often treat the mine as a bulk thermal resource characterised by an assumed temperature and effective volume of water and surrounding rock (Grant 2014; Quinao and Zarrouk 2014). Potential heat output is then estimated using assumed abstraction rates and allowable temperature drawdown (Grant 2014). Volumetric or stored-heat approaches are widely used in geothermal resource assessment because they are transparent and straightforward to apply (Ciriaco et al. 2020), but results

are highly sensitive to assumptions regarding geometry, connectivity, and parameter values (Grant 2014; Quinao and Zarrouk 2014). The methods are 'Heat-in-Place' style volumetric estimates or are based on potential flow rates (Gillespie et al. 2013).

During exploration, the acquisition of site-specific data enables refinement of heat estimates (Monaghan et al. 2022). Borehole temperature measurements, pumping tests, water level monitoring, and water chemitry data can be used to constrain the conceptual model and reduce uncertainty in hydraulic and thermal parameters (Walls et al. 2023; Monaghan et al. 2022).

As more data become available, and the resource can be better characterised, numerical modelling can be undertaken (see Section 1.3.10) for explanation of modelling). In addition to requiring the newly acquired data, this is also more computationally expensive. Numerical models allow explicit representation of mine geometry, boundary conditions, and spatial variability in hydraulic and thermal properties (Andrés et al. 2017). They are particularly valuable for assessing behaviour such as thermal drawdown around abstraction points, the influence of reinjection, and long-term system sustainability (Andrés et al. 2017; Chu et al. 2021).

Chemistry

Mine water chemistry can vary considerably. It can be acidic, neutral or alkaline and can be metal rich (Banks et al. 2019b; Walls et al. 2022). Two problems associated with the chemistry are corrosion and fouling/clogging. Mine waters commonly contain significant dissolved iron. Oxidised water can precipitate out hydrated iron oxides, 'ochre' (Figure 1.6). Ochre can clog up pumps, pipes, heat exchangers, boreholes, which can result in frequent maintenance to clean out the ochre. This can make schemes unviable. Preventing contact with atmospheric oxygen can prevent ochre precipitation. However, there are mine waters where ochre has already precipitated (Banks et al. 2019b). If the ochre is present in low enough concentrations this may be manageable.

Corrosion of the MWG infrastructure can have multiple causes. Acidic mine waters are very common and acidity is corrosive to carbon steel. Dissolved H_2S can corrode multiple metals as can highly reducing and saline waters (Walls et al. 2021).

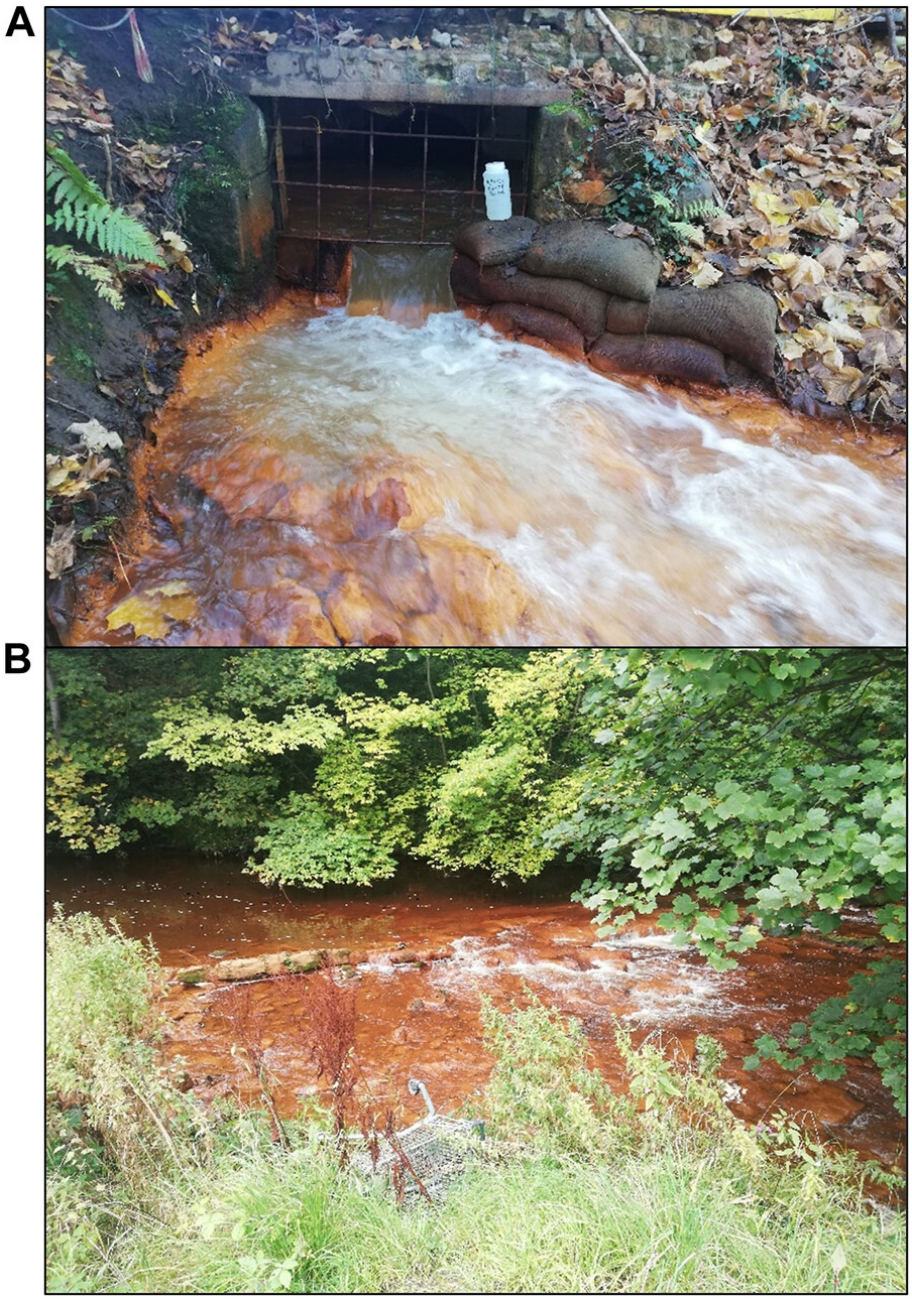

Figure 1.6: Images of Old Fordell ("Junkie's Adit") mine water discharge (A), which contains high iron loading (1L bottle for scale), and the resulting downstream ochre precipitation on the River South Esk (B) (Walls et al. 2022).

Additionally, changes in temperature can drive chemical reactions independently of other factors. For example, experiments in a gneiss-hosted silver mine showed that heating (analogous to the injection of waste heat) led to the precipitation of goethite and gypsum (Stemmle et al. 2025).

Ground movement

Areas of coal mining can experience ground movement both during and post mining. This can be ground subsidence, during and post mining (McCay et al. 2018), and surface uplift as the mines flood post-exploitation (Zhao and Konietzky 2021; Dudek et al. 2020). The collapse of entries and roadway intersections can cause sink holes at the surface, while the areas of total extraction can produce troughs at the surface. Room and Pillar mines which may have been left intact (not robbed) can still produce subsidence (Donnelly 2020). Roof supports can fail (especially, older wooden supports), pillars can spall (pieces of rock break off) and collapse, the seam floor can burst up, and the roof can collapse down. The unsupported void that is produced can migrate to the surface producing subsidence, or if the workings are very shallow, potentially a sink hole (Andrews et al. 2020; Donnelly 2020). The flow of water can enhance the deterioration (Donnelly 2020; Andrews et al. 2020).

A mine water scheme could negatively interact with these processes. Room and pillar mine working may not have the high permeabilities expected because of the presence of low permeability collapse material, reducing potential flow rates. Also, dewatering from the scheme could trigger collapse, potentially damaging wells and causing surface subsidence (Andrews et al. 2020).

Avoiding the use of, or drilling through, shallow mine workings can also reduce the risk of surface subsidence (Walls et al. 2024).

Prospectivity mapping

MWG opportunities are spatially uneven and site-specific: temperature, hydraulic connectivity, water chemistry, access to shafts and roadways, surface constraints, and proximity to heat demand vary. These characteristics make early-stage decision-making challenging, particularly for non-specialists and for public- or private-sector

organisations attempting to prioritise feasibility work across many potential locations.

Prospectivity mapping provides a systematic way to translate complex subsurface information into spatially explicit evidence that can support early-stage screening and investment decisions. The outputs typically take the form of maps, indices, or ranked classes indicating where a resource may be more or less favourable, often accompanied by notes on data coverage and uncertainty. Importantly, these outputs do not replace site investigation; rather, they are intended to help stakeholders identify priority areas for further work, raise the profile of said resource, and stimulate investment (Nurmi 2020; ACIL Allen Consulting 2022; Partington et al. 2016).

Resource mapping and prospectivity workflows are well established in mineral exploration were subsurface information is incomplete and exploration is costly. Spatial prospectivity tools are commonly used to narrow the search space before committing to detailed site work. National geological agencies have used GIS-based modelling to translate datasets into comparable prospectivity layers that can be communicated to industry and policy stakeholders. The Mineral Potential Mapper in Australia provides a prominent example, where the creation of new datasets and prospectivity maps has been associated with improved targeting and favourable returns on public investment (ACIL Allen Consulting 2022). Similar state-led initiatives in New Zealand and Finland have used mineral prospectivity mapping to support exploration promotion and greenfield targeting (Partington et al. 2016; Nurmi 2020). These precedents show how mapped prospectivity can convert complex subsurface evidence into actionable screening information, helping to de-risk the earliest investment decisions.

Analogous approaches are relevant to MWG, where a comparable challenge exists. As MWG has become more widely recognised over the past few years, several organisations have begun to produce MWG prospectivity maps and screening tools that highlight areas of potential and provide non-specialists with accessible information to decide where projects should progress to feasibility studies. These maps include some combination of information characterising the subsurface resource, and in some cases, the surface heat demand (Walls et al. 2024; Coal Authority 2024d;

Coal Authority 2024c; Ebel et al. 2025).

Drilling

Drilling into mines can be challenging and there are various risks. Drilling through mine workings shallower than the target can cause complications and expense (Walls et al. 2021). These workings may need to be grouted. If the workings are open and the bit drops into void space there is a risk of losing verticality. In some cases this can also result in the drill string becoming stuck which may lead to the loss of both the drill string and the borehole. Void space, whether due to abandoned mine workings, mining induced fractures, natural fractures, or fractures created during drilling when drilling fluid hydrostatic pressure exceeds the surrounding formation pressure, can cause loss of drilling fluid circulation (Walls et al. 2021). Replacing lost fluid increases operational cost and also introduces physical risks. If cuttings cannot be transported away from the bit they may accumulate in the borehole, restricting movement of the drill string and reducing drilling efficiency. In addition, without fluid support there is an increased risk of borehole collapse. Loss of verticality in a borehole planned to be vertical can also result in the target being missed. For example, when targeting a roadway in a mine that may be only about 2 m wide and located between 30 m and several hundred metres below ground level, even a small deviation can result in failure to intersect the void. Where two seams are present in the area, drilling can continue to the deeper seam if the upper target is missed, thereby reducing the chance of a wasted borehole (Wyatt et al. 2025). Targeting mine workings is further complicated by uncertainty in historical mine plans, which may be several hundred years old, contain inherent inaccuracies, and be difficult to georeference to modern mapping systems (Wyatt et al. 2025). Missing the mine void can result in a non productive borehole. However, if the borehole is believed to be close to the target there are techniques to break through into the void and establish hydraulic connection. For example, the Mining Remediation Authority has reported success using a water jet mounted on the drill string to cut an opening approximately 120 to 150 mm wide and 300 mm high into the coal seam, thereby breaking through into adjacent workings. In one case this increased borehole yield

from < 0.01 L s^{-1} to > 30 L s^{-1} (Wyatt et al. 2023b).

Drilling into coal seams or abandoned mine workings carries the additional risk of encountering hazardous gases such as methane, carbon dioxide, carbon monoxide or hydrogen sulphide (Coal Authority et al. 2019). Methane can accumulate within voids or unworked coal and may be released suddenly when penetrated by a borehole. The main risk of methane is fire/explosion, but it is also an asphyxiant (Coal Authority et al. 2019; Department of the Environment and Welsh Office 1994). Carbon dioxide can collect in mine workings or voids and displace oxygen, creating an asphyxiation risk in confined spaces or at the surface (Coal Authority et al. 2019; Department of the Environment and Welsh Office 1994). Carbon monoxide can be generated through mine fires and usually only present in low levels in mine workings, but it has been found at 200 ppm. It is toxic, flammable and explosive (Coal Authority et al. 2019). Hydrogen sulphide, which can occur where sulphide minerals are present, is both toxic and can lead to unconsciousness and death (Coal Authority et al. 2019; Department of the Environment and Welsh Office 1994). Hydrogen, although rare, has also been detected in coal mines and presents an additional explosion hazard (Coal Authority et al. 2019).

Public awareness and social impact

Levels of public awareness of geothermal energy in the UK remain very low. There are only limited mentions in legislation and government plans. Awareness is, however, beginning to grow, with geothermal energy appearing more often in TV and radio coverage. When projects do occur, it is important to gain and maintain a Social Licence to Operate (SLO). SLO refers to the intangible, implied consent and, in some cases, support from a community towards a project (Barich et al. 2022; Tost et al. 2021). The concept was first developed in relation to the mining industry (though it is now used more widely) and is regularly highlighted as one of the key risks to mining projects. A project may be described as having SLO if the community merely accepts it. At the highest level, SLO implies a situation of mutual benefit, in which the community perceives the project as part of its in-group and actively defends it against external criticism (Tost et al. 2021; Barich et al. 2022).

Conversely, if a project fails to secure or loses SLO, this can lead to boycotts, protest, legal challenges, and in extreme cases, sabotage or violence (Tost et al. 2021; Barich et al. 2022). Geothermal energy, particularly for heat, offers some advantages in seeking public acceptance. Once operating, its surface footprint is small compared to other renewable technologies, it can operate in all weather conditions, and it can contribute to energy security (Shirani et al. 2020). There can also be a sense of pride in communities in reusing the legacy of coal mining (Li et al. 2025; Shirani et al. 2020). Geothermal heat has the benefit of being inherently local. Unlike electricity, it cannot be fed into a national grid and must be used close to the point of extraction. This means that benefits should, in principle, remain geographically close to the community where heat is abstracted. However, the fact that heat must be used locally does not necessarily mean it will be used by the local population. Communities often worry that if there is an initial financial outlay, those who cannot afford it will be excluded. This concern is acute in coalfield areas, which experience high levels of deprivation and fuel poverty (Li et al. 2025; Beatty et al. 2019). Research around a mine water project in Wales found that the local community recognised the long-term benefits of the scheme but, given the limited financial resources of the area, believed that participation would only be attractive if the heat was cheaper than alternatives (Shirani et al. 2020). New housing developments can feed into the issue of financial barriers. If new builds are connected to a mine water heating scheme while the pre-existing housing stock is not, and if the new housing is priced higher, there is a danger that the indigenous community will be excluded from the benefits of a local resource. Common public concerns about geothermal energy include water usage, seismicity, subsidence, and pollution (Carr-Cornish and Romanach 2014; Shirani et al. 2020; Ioannou et al. 2023a). Research has also shown that people often prefer geothermal projects to be located away from their own communities, which is problematic for heat schemes that must operate close to users (Carr-Cornish and Romanach 2014). Effective and transparent communication between project developers and local communities is essential (Barich et al. 2022; Shirani et al. 2020). In September 2025, a deep geothermal electricity producing plant was refused planning permission on the grounds that it would harm the natural and historic character of

the area (Falmouth Packet 2025). This decision followed community concerns about potential river pollution, impacts on the heritage landscape, and seismicity. Notably, these concerns were raised even though the Environment Agency, Natural England, and the local council's ecologists, flood authority, and planning officers were satisfied with the planning conditions intended to protect the environment. There were accusations from the community that the geothermal company and the local planning authority had not been communicative or done enough to engage the community. This case illustrates both the risks posed by SLO and the importance of actively maintaining it.

Financing

MWG projects, like geothermal projects generally, are characterised by high upfront capital expenditure relative to their total lifecycle costs (Nur et al. 2023). A substantial share of costs is incurred before any heat is sold. For example 20% of the capital expenditure is incurred by the end of exploration drilling and testing (David Townsend, TownRock Energy, personal communication, June 2025). There is a particular concern about the magnitude of the capital required for exploratory drilling (Li et al. 2025). This pattern of front-loaded, largely irreversible expenditure is one of the defining financing challenges for MWG.

The cost profile of MWG is compounded by regulatory uncertainty. A lack of clear and stable regulations has been identified as a deterrent to investment in geothermal energy (Goodman et al. 2007; Manzella et al. 2018). Similar issues arise for MWG in the UK, where uncertainties around the legal status of subsurface heat, complicated licensing pathways, and a lack of ownership rules resulting in the risk of thermal interference between schemes can all discourage investment (Abesser et al. 2023; McClean and Pedersen 2021; McClean and Pedersen 2023). For potential investors, whether local authorities, private companies, housing associations or infrastructure funds, an early and central concern is whether sufficient accessible heat is available at an acceptable level of technical and financial risk. Assessing the magnitude and sustainability of the heat resource is crucial for judging project feasibility and determining whether the expected heat supply is sufficient to justify

the financial and operational risks associated with developing a MWG scheme (Ciriaco et al. 2020). In the geothermal sector broadly, exploration risk and regulatory complexity are repeatedly identified as major obstacles to raising project finance (Compernolle et al. 2019; International Renewable Energy Agency (IRENA) 2017). As a result, project financing is widely regarded as one of the principal barriers to the wider deployment of geothermal energy technologies.

Risk is not constant over a geothermal project lifecycle, financing structures evolve as projects move from concept to operation (Nur et al. 2023). A simplified sequence for the initiation of a MWG (and geothermal projects more generally) begins with desk and feasibility studies which involve obtaining mine plans, hydrogeological assessment, and preliminary heat assessments. This is typically funded from developer balance sheets, small public grants, or in-kind support. If prospective this can move on to exploration drilling and testing, which includes pump tests and water chemistry analysis. This is where around 20 % of total project CAPEX may already be deployed, with resource risk still relatively high. Commercial lenders are reluctant to accept this level of risk, so early-stage high risk expenditure generally relies on equity-based financing or quasi-equity capital, often complemented by grants or concessional public funds(Dewi et al. 2020; Nur et al. 2023).

The Final Investment Decision (FID) typically occurs after exploration and initial drilling have demonstrated that the resource is technically and economically viable. At this point, resource risk is reduced (Kępińska et al. 2021). The bulk of external finance is usually raised at or just after FID, predominantly in the form of debt (project finance or corporate loans), alongside sponsor equity. This allows for the constructing of the production wells and surface infrastructure.

In this structure, the exploration and testing phase is the central financing bottleneck. High-risk expenditures in this phase generally cannot be financed with standard commercial debt and therefore depend on equity and public co-funding.

De-risking early project stages has a disproportionate influence on financing conditions because exploration risk is so central (Compernolle et al. 2019; International Renewable Energy Agency (IRENA) 2017). Reducing resource and drilling risks enhances project economics and makes it easier to attract capital (Sanyal and Koenig

1995). For MWG, de-risking measures can be grouped into:

1. Technical de-risking: improved mine-water characterisation, staged drilling strategies (for example slim-hole exploration wells prior to production diameter wells), enhanced numerical modelling and monitoring.

2. Regulatory de-risking: clearer licensing routes for subsurface heat and mine water use, transparent rules heat ownership/use, and predictable treatment of heat networks and tariffs (Goodman et al. 2007; Manzella et al. 2018; Abesser et al. 2023).

3. Financial de-risking instruments: public grants, subordinated loans, loan guarantees, and risk insurance schemes that specifically target exploration risk.

By reducing uncertainty about both the resource and the regulatory framework, de-risking can expand the pool of potential investors, and it tends to improve the terms of both equity and debt.

Several countries have developed explicit financial instruments to tackle the resource risk for geothermal schemes. France, Germany, Iceland, The Netherlands, Denmark, and Switzerland have public insurance schemes (Dumas et al. 2019; Kępińska et al. 2021). There funding agencies and banks in Latin America, Mexico, Chile, and Eastern Africa that have also set up risk mitigation schemes, usually in the forms of grants for capital costs (Dumas et al. 2019). In non-grant type schemes there are two main forms of mitigation. In insurance schemes after a risk has occurred, the insuring body provides reimbursement according to the terms of the agreement. In guaranteed loans, the project pays back the loan if successful, if the resource risk occurs, then the loan is forgiven (Dumas et al. 2019).

There is also the possibility of alternative, community based financing. The CROWDTHERMAL project investigates the use of crowdfunding and community investment, combined with professional risk mitigation, as a means to raise capital for high-risk phases while also building local acceptance (Ioannou et al. 2023b; Fernández Fuentes et al. 2022).

1.3.10 Modelling

As explained earlier in this chapter, the coal mines in the UK which are of interest for MWG are flooded and have in some cases been abandoned for hundreds of years. This means the mines are inaccessible prior to drilling and installing infrastructure, and their condition (collapse, backfill, etc.) is relatively unknown. Modelling can aid in assessing whether a mine system is viable for MWG, prior to expensive groundworks commencing (Mouli-Castillo et al. 2024). Two types of model have been used for MWG, analytical and numerical.

1.3.11 Analytical models

Analytical models use mathematical solutions and are much faster to run and are easy to implement (Loredo et al. 2016). Due to their speed they can be used at the scale of a whole mine system (Mouli-Castillo et al. 2024). However, they are simplified approaches that suit homogenous systems with simple processes (Loredo et al. 2016; Birdsell et al. 2024) and cannot accurately reflect the real world conditions of a mine (Mouli-Castillo et al. 2024).

1.3.12 Numerical models

Numerical methods are more complicated and therefore computationally intense than analytical, but can more accurately reflect real world conditions (Mouli-Castillo et al. 2024; Birdsell et al. 2024). Three different types of numerical modelling techniques have been applied to modelling the fluid flow, heat transfer, and sometimes additional processes within flooded mines (Mouli-Castillo et al. 2024). These are Finite Difference Method (FDM), Finite Volume Method (FVM), and Finite Element Method (FEM). These methods essentially work by converting a continuous physical problem into a set of discrete algebraic equations (Loredo et al. 2016). These equations are all solved simultaneously to determine the condition being investigated. What makes each method unique is the way in which the problem is discretised and the way the system is represented.

1.3.13 GEMSToolbox

In this thesis GEMSToolbox is used (described fully in Mouli-Castillo et al. (2024)) to model heat transfer and fluid flow. GEMSToolbox is a numerical framework using semi-analytical solutions. It has the speed of an analytical approach, but is adaptable enough to apply to real mine architechure.

GEMSToolbox represents a flooded mine as a one-dimensional network of cylindrical pipes (galleries, roadways, rooms) connected at nodes (junctions, shafts and wells). This is based on EPANET 2, a software package developed by the U.S. Environmental Protection Agency for simulating hydraulics and water quality in drinking water distribution networks. The hydraulic modelling is based on the work of Todini and Rossman (2013), and the heat transfer modelling is adapted from Rodríguez and Díaz (2009) and Loredo et al. (2017).

For a chosen configuration of abstraction and injection wells, GEMSToolbox first solves a steady-state hydraulic problem: conservation of mass is enforced at every node, and Bernoulli's equation with a Darcy–Weisbach head-loss term is applied along each pipe (Todini and Rossman 2013), yielding hydraulic heads, flow rates and travel times throughout the network. This establishes a hydraulic pressure gradient and therefore flow around the mine. All water is modelled as flowing through the "pipes", under the assumption that the mine voids have a much higher ability to transmit water than the surrounding rock mass.

Once the flow field is known, GEMSToolbox applies semi-analytical solutions for advective–conductive heat transfer along each pipe. A radial model represents heat exchange between the mine water and the surrounding rock, and a complementary planar formulation, combined with a geometric weighting scheme, accounts for thermal interference between neighbouring galleries in densely worked seams. As water flows through the system, any temperature difference between the rock and water drives heat exchange, causing the mine water to warm as it moves along the network. The model calculates the temperature at every node, including the designated abstraction node(s), over the specified simulation time. As heat is transferred from the rock to the water, the rock face cools, creating a thermal gradient from the water–rock interface into the rock mass, and heat subsequently diffuses back

towards the pipes.

This combination of pipe-network hydraulics and semi-analytical heat transfer allows complex multi-seam geometries to be simulated much more quickly than with fully three-dimensional coupled codes, making the tool particularly suited to feasibility-stage screening of mine-water geothermal schemes.

To run GEMSToolbox, the user supplies an input CSV file describing the mine geometry (either via GIS shapefiles or via an idealised grid); the hydraulic configuration (injection and abstraction nodes and their constant flow rates, any fixed-head boundary nodes, pipe diameters and roughness, and optional porous-pipe parameters to represent backfill or collapse material); the rock and water thermal properties (thermal conductivity, specific heat capacity, density); the geothermal gradient used to initialise rock temperature; injection temperature(s) at the wells; and the total simulation time.

Users can also choose which nodal and pipe variables are written to an output that can be used in visualisation software (VTK files), for example temperatures, flow rates and travel times.

1.4 Research Questions

The principal aim of this thesis is to advance the development of mine water geothermal energy by improving methods for identifying suitable sites, refining approaches for early-stage heat assessment, and proposing strategies to ensure the sustainable regulation of thermal interactions between systems. A lack of investor confidence currently represents a key barrier to the large-scale implementation of MWG. By addressing the research questions set out in this thesis, the work seeks to provide both methodological and practical contributions that support the wider uptake of mine water geothermal resources and reduce uncertainty for investors.

RQ1: What are the key differences in mine water geothermal prospectivity mapping methods in terms of aims, data requirements, and the areas they identify as high or low prospectivity?

RQ2: Does the use of GEMSToolbox provide added value in estimating extractable heat for mine water geothermal projects compared with commonly used static methods?

RQ3: How should thermal interference between neighbouring mine water geothermal systems be regulated, and what approaches could be appropriate in a UK context?

1.5 Thesis Outline

Chapter 2 presents a comparison of different screening tools for identifying prospective areas for mine water geothermal systems. Chapter 3 examines the relative merits of dynamic versus static heat assessment methods applied early in a mine water geothermal project. Chapter 4 investigates and proposes approaches to regulate thermal interference between mine water geothermal systems. Chapter 5 provides the overall conclusions of the thesis.

Chapters 3 and 4 of this thesis have been prepared in the format of journal articles. Chapter 4 has been peer reviewed and published in the Quarterly Journal of Engineering Geology and Hydrogeology, while Chapter 3 peer reviewed and accepted in Geomachanics and Geophysics for Geo-Energy and Geo-Resources. As the chapters have been submitted to different journals, some minor inconsistencies in formatting and spelling may remain, although these have been standardised wherever possible. Whilst co-authors provided advice and assistance during data analysis and interpretation, and contributed to manuscript framing, structuring, and editing, I was the primary author and was responsible for the majority of the research and writing within these manuscripts.

CHAPTER 2

Comparing different methods of mine water potential assessment

2.1 Introduction

The United Kingdom has a statutory commitment to achieve net zero greenhouse gas emissions by 2050 under the Climate Change Act and its 2019 amendment. Heating activities account for 42% of UK energy consumption, with space heating alone responsible for 25% (Department for Energy Security and Net Zero 2025a). Decarbonising heating is therefore important to delivering national climate targets.

Mine water geothermal (MWG) systems, which extract low-grade heat from warm water in abandoned flooded mine workings and upgrade it using heat pumps, offer a low-carbon, locally available and secure heat source in former coalfield areas (Gluyas et al. 2020; Walls et al. 2021; Monaghan et al. 2025). Around a quarter of UK homes and businesses are estimated to sit above former coal mines, indicating a substantial technical resource that could support the expansion of heat networks and contribute to the decarbonisation of building heat demand (Gluyas et al. 2020).

Experience from the minerals sector shows that systematic resource mapping and prospectivity analysis can play an important role in steering investment. For

example, Geoscience Australia's Mineral Potential Mapper has generated new geoscientific datasets and minerals potential maps that have been credited with improving exploration targeting and contributing to recent discoveries, while delivering strong benefit–cost ratios for public investment (ACIL Allen Consulting 2022). In New Zealand, the government has used mineral prospectivity modelling using geographic information systems (GIS) to promote minerals exploration (Partington et al. 2016). Similarly, the Geological Survey of Finland has developed mineral potential mapping to encourage greenfield exploration (Nurmi 2020). These examples illustrate how spatially explicit prospectivity outputs can de-risk early decisions and encourage investment in subsurface resources.

As MWG has become more widely recognised over the past few years, several organisations have begun to produce MWG prospectivity maps and screening tools that highlight areas of potential and provide non-specialists with accessible information to decide where projects should progress to feasibility studies. This chapter compares a set of these emerging MWG mapping methodologies, examining their data requirements and classification schemes.

Four different regional assessment methodologies are compared, three of which (see * below) are applied to the case study area of Newcastle, in the UK (Figure 2.1).

1. Mine Water Geothermal Resource Atlas for Scotland (MiRAS)*,
2. Georesources Cornwall (GRC) Geothermal Energy Screening Assessment*,
3. Mining Remediation Authority (MRA), Mine Water Heat Opportunity Mapping*,
4. Saxony Mine Water Potential Study,

Newcastle was selected because it is one of ten cities identified by the Department for Energy Security and Net Zero as having, or having the potential to develop, one or more heat networks situated above former coal mines.

Newcastle is a city in the North east of England, UK, with a population of ∼300,000 (Nomis 2025). There is evidence of a significant trade of coal from the

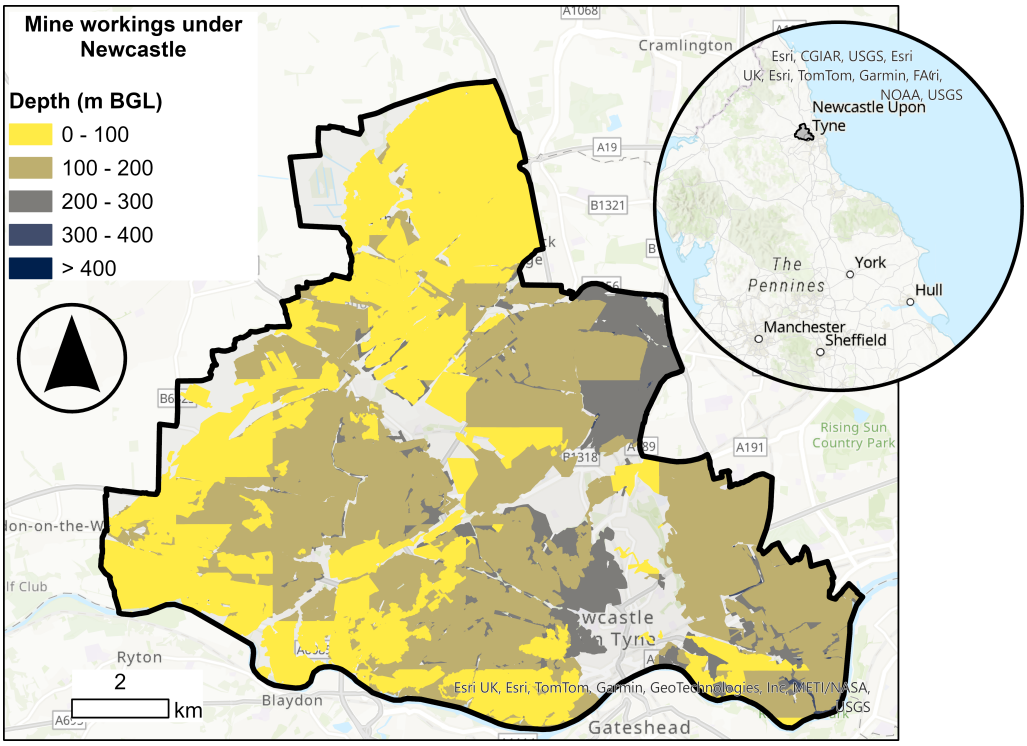

Figure 2.1: Location of Newcastle and extent of mine workings beneath the city. The mine workings are grouped in 100 m bgl depth categories. The shallower categories are drawn on top of the deeper categories. Reproduced with the permission of © The Mining Remediation Authority. All rights reserved.

Newcastle area since the early 13th century (Hatcher 1993b) and the last coal mine under urban Newcastle closed in 1959 (Westaway and Younger 2016). With over 600 years of coal mining the majority of Newcastle is underlain by coal workings, as can been seen in Figure 2.1.

The aims of the different assessed methods are:

Mine Water Geothermal Resource Atlas for Scotland (MiRAS): Enable stakeholders without specialist geological background to screen areas for open-loop mine water projects (with re-injection) and highlight optimal zones; designed to sit alongside national heat-demand mapping.

Georesources Cornwall Geothermal (GRC) Energy Screening Assessment: Correlate possible mine water heat resources (open loop) with existing and potential heat demand across Cornwall, focusing on deep mines and demand clusters.

Mining Remediation Authority (MRA), Mine Water Heat Opportunity Mapping: The aim of this mapping is to identify and classify areas into 'good', 'possible' and 'challenging' within Wales and 10 English cities where open loop mine water heat schemes are likely to be feasible, so that planners, consultants and energy officers know where to focus more detailed feasibility studies and potential heat-network development.

Saxony Mine Water Potential Study: To analyse and classify locations in order to derive mine water geothermal potential (open or closed loop) in a user facing GIS by combining underground conditions with surface heat demand, and to provide practical information and a decision-making aid for mine water geothermal project development.

2.1.1 MiRAS

Walls et al. (2024) designed MiRAS for the Midland Valley of Scotland and prioritised evaluating data that contributes heavily to the OPEX and CAPEX of a MWG project. As such it identified the optimal MWG site as having at least two overlapping coal seams, to provide vertical distance between abstraction and injection site, increasing the length of the flow path and reducing the risk of thermal feedback; no shallow (<30 m bgl) seams to minimise subsidence risk; a resting mine water head

Table 2.1: Data required for the different mine water geothermal opportunity mapping methods.

	MiRAS	MRA	GRC	Saxony
Location of mine workings	✓	✓	✓	✓
Depth of mine workings	✓	✓	✓	
Age of the mine				✓
Mine volume				✓
Mine plan documentation quality				✓
Mine water depth	✓	✓		✓
Mine water surface temperature				✓
Mine water chemistry				✓
Mine water recovery		✓		
Mine accessibility				✓
Mine drainage system				✓
Opencast workings		✓		
Heat Demand			✓	✓

of <60 m bgl to keep pumping energy/cost acceptable; and target seams <250 m bgl to control drilling costs.

The MiRAS workflow begins by identifying areas where at least two coal seams overlap, while excluding zones where seams occur at depths of less than 30 metres below ground level in order to minimise subsidence risk. The analysis then constructs a continuous surface representing the mine water level by interpolating measured heads from discharges and boreholes. Subtracting this surface from a digital terrain model generates a map of mine water depth, classified in 10 metre intervals and limited to depths of 60 metres or less, reflecting acceptable pumping requirements.

Each dataset is handled as a raster, meaning the study area is represented as a grid of cells, with each cell storing a single value of the relevant parameter.

Depths to target coal seams are similarly derived by converting seam level measurements from metres Ordnance Datum to metres below ground level and interpolating a continuous seam-depth surface using inverse distance weighting. These depths are then classified into those shallower and deeper than 250 metres, given the influence of drilling depth on project cost.

The final prospectivity output is produced by combining the three rasters, coal seam overlap, depth to mine water level and depth to target seams on a cell-by-cell basis.

2.1.2 GRC, Geothermal Screening Assessment

This method was designed for the underground metal mines in Cornwall in 2018 and was based around access for mine water schemes being through open shafts or boreholes (EGS Energy Ltd and Carrak Consulting Ltd 2019). Its aim was to identify areas with possible mine water heat resources with areas of existing or potential heat demand by overlaying deep-mine locations against existing/prospective heat demand to identify target areas.

The mine depths were divided into > 500 m, 300-500 m, 200-300 m and were a proxy for temperature. The local Cornish geothermal gradient of 36°C km^{-1} and a surface temperature of 10°C was used to calculate the temperatures and the 3 depth categories correspond to > 25°C, ∼19 - 25°C, and ∼16 - 19 °C, respectively. Only the mines deeper than 300 m, predicted to be hotter than 19°C, were shown on the final map. Heat demand was taken from a report for Cornwall Council on the heat demand and infrastructure of Cornwall (Happold 2015), locations Cornwall Council had identified for future building growth (Council 2019), and sites landowners have suggested for future housing growth (Council 2016).

2.1.3 MRA, Mine Water Opportunity Maps

The MRA mine water opportunity maps provide a high-level screening of mine water geothermal potential across Wales and selected English cities. For Wales, opportunity maps were produced for each local authority area on behalf of the Welsh Government, while a separate set of maps was prepared for ten English cities (Birmingham, Bristol, Coventry, Leeds, Greater Manchester, Newcastle, Nottingham, Sheffield, Stoke-on-Trent, Sunderland) commissioned by the Department of Energy Security and Net Zero (Coal Authority 2024d; Coal Authority 2024c). The English cities were selected because they both overlie coalfield areas and participated in the Heat Network Zoning Pilot and Advanced Zoning programmes. In each case, mapped zones are classified into three categories of opportunity, labelled good, possible and challenging. The criteria defining these categories are summarised in Table 2.2, and the overall mapping workflow is shown in Figure 2.2.

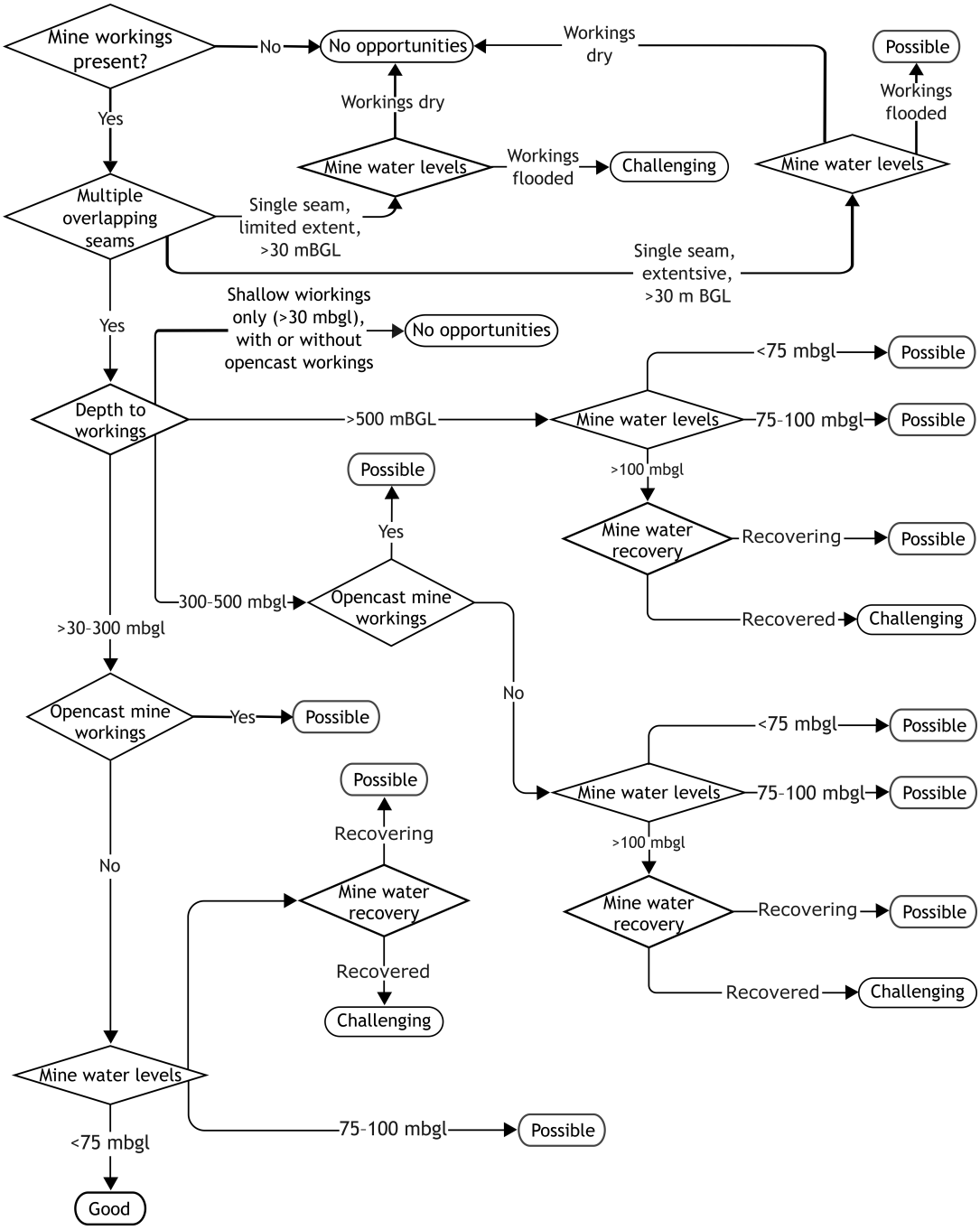

Figure 2.2: Flowchart of the MRA's mine water heat opportunity assessment protocol redrawn from Coal Authority (2024c) and Coal Authority (2024d). Mine water recovery refers to the rise of mine water levels, if the mine water is rising, the water levels are recovering (Whitworth 2002). During active mining, many workings required ongoing dewatering because they were naturally wet. However, given the high cost of pumping, dewatering commonly ceased after closure, permitting water levels to rise.

Table 2.2: Criteria for the MRA categories of 'Good', 'Possible', 'Challenging'.

Category	**Criteria (summarised)**
Good	All of: overlapping workings; flooded; workings 30-300 m bgl; water level $\lesssim$ 75 m bgl; water levels recovered or recovering.
Possible	Overlapping *and* flooded workings, plus at least one of: (i) workings $\leq$ 500 m bgl; (ii) water level 75-100 m bgl (recovered/recovering); (iii) water level $>$ 100 m bgl but recovering; (iv) evidence of opencast with workings 30-500 m.
Challenging	Any one of: not flooded; only $<$ 30 m bgl; only $>$ 500 m bgl with no shallower targets; water level $>$ 100 m bgl and recovered; known mine gas; single, fully flooded seam not impacted by opencast (short-circuit risk).
No opportunities	Where workings exist and either: opencast with workings $<$ 30 m only; or a single seam of limited extent. (Areas with no workings are not included.)

2.1.4 Saxony Mine Water Potential Study

In the state of Saxony, Germany, a series of 14 municipalities with current or past mining were assessed. The surface heat demand was considered as well as data about mines. The different underground parameters were assessed and each given a score of 1 to 5 (5 being the best). These were weighted and combined to produce an overall ranking of the underground potential of a municipality, also of 1 to 5, which is attached to the mined area. The underground parameters assessed are in Table 2.3.

Table 2.3: Parameters evaluated in the Saxony methodology. Importance weighting given in parentheses (). (Ebel et al. 2025).

Parameters and ratings	**Reason**
Mine Age *(3)*	The period during which most mining activity occurred. More recent workings generally have better structural integrity, larger tunnel cross-sections, and more comprehensive documentation.
1– before 1500	
2– 1500–1700	
3– 1700–1800	
4– 1800–1945	
5– from 1945	
Mine drainage system *(17)*	Drainage tunnels concentrate mine water flow; the system is rated by volume flow. Higher flows allow higher usable heat output. The top rating is > 2 MW ($\Delta T = 5$ K). Areas without drainage systems receive the lowest rating.
1– Not available	
2– Decentralised system, < 10 m^3/h	
3– Decentralised system, 10–100 m^3/h	
4– Centralised system, $>$ 100–500 m^3/h	
5– Centralised system, > 500 m^3/h	
Mine water depth *(11)*	The depth of the mine water to be pumped effects operating costs, as well as initial drilling and pipework costs. A depth of 200 m or more results in the worst rating, which increases at 50 m intervals.
1– $>$ 200 m	
2– 150–200 m	
3– 100–150 m	
4– 50–100 m	
5– $<$ 50 m	
Mine volume *(6)*	The volume reflects the amount of mine water available and the extent of workings, which determines the abstraction and reinjection options. The lower limit of 10,000 m^3 corresponds to large artificial heat-storage facilities.
1– to 10,000 m^3	
2– to 50,000 m^3	
3– to 100,000 m^3	
4– up to 1,000,000 m^3	
5– from 1,000,000 m^3	

Parameters and ratings	Reason
Mine plan documentation *(22)* **1**– No plans available **2**– Analogue plans prior to 1800 **3**– Analogue plans before and after 1800 **4**– Digital georeferenced plans **5**– Plans in digital vectorised format	The rating is for the age and format of survey information. The accuracy and amount of information is generally higher in more recent maps.
Mine water surface temperature *(8)* **1**– $< 12\,^{\circ}\mathrm{C}$ **2**– 12–15 °C **3**– 15–20 °C **4**– 20–25 °C **5**– $> 25\,^{\circ}\mathrm{C}$	Mine water temperature is controlled by depth, inflow, and mixing, with deep levels being warmer and shallow levels dominated by surface-water infiltration.
Mine water chemistry *(14)* **1**– Heavily polluted (radioactive) **2**– Heavily polluted (high mineralisation) **3**– Moderately polluted (moderate mineralisation) **4**– Low contamination (low mineralisation) **5**– Drinking water quality	Harsh mine water chemistry can effect the infrastructure used (corrosion, fouling, etc.) and lead to environmental and legal risks .
Mine accessibility *(19)* **1**– Abandoned, shaft access unlikely **2**– Abandoned, shaft access possible **3**– Abandonment ongoing **4**– Parts abandoned **5**– Mine largely active	The lowest accessibility rating is when safety concerns prevent the opening of shafts or tunnels. The highest rating is given to fully active mines where accessibility to potential locations for mine water utilisation is available.

Heat demand (DBI GTI 2023) is mapped for each municipal area using 0.25

km^{-2} hexagons, with each hexagon colour coded by its heat demand. Values are grouped into five categories (GWh yr^{-1}): <0.2, 0.2-0.8, 0.8-2.1, 2.1-5.0, and >5.0.

Only hexagons that overlap mapped mine workings are kept, because these are the areas where mine water is potentially available. The map is then further simplified by keeping only the main continuous cluster of hexagons associated with the largest mined zone, and removing small, isolated patches. The heat-demand potential rankings are then combined with the underground potential value to produce a map of hexagons that ranks overall mine water potential from Very Low (1) to Very Good (5).

Criteria review and potential adaptation of the Saxony Mine Water Potential Study

Due to time constraints and data availability, the Saxonian method could not be tested on the case study area. Below is a consideration of the method and how it could be adapted to apply to a UK setting.

Comparing the data used for the methodologies used to produce the maps here to the Saxony methodology shows some notable differences (Table 2.1). The Saxony methodology is considerably more in-depth than the British methodologies, with 8 different parameters, all ranked 1-5, before being combined together into a weighted average, and then combined with surface heat demand to produce a GIS map of suitability got mine geothermal use.

The **age of the mine workings** is a factor considered by the Saxionian method, and is suggested as future work by Walls et al. (2024) and mentioned by Coal Authority (2024c) as information to be considered in site specific feasibility studies. Age is considered as older workings are more likely to have undergone collapse and have smaller roadway cross-sections. Additionally, younger mines may be better mapped. The 1 - 5 value is decided based on when the largest proportion of mining took place within a municipality. While in the UK the same areas have undergone coal mining for centuries, in some cases with 200 year old maps referencing 'old workings', the Mining Remediation Authority does have a downloadable dataset called 'Working Date'. This identifies the year coal was mined at a specific point,

for a specific seam. This could be used at a town or city scale (as in the Saxonian method), i.e. for the whole of Newcastle, by producing an average mine age map, as done for mine water depth, or mine depth in the MiRAS method, before calculating the average over the whole area. Or, as this data set provides the seam code, the mine depth calculation could be done as was in the GRC and MRA methods, extracting the points that overlie the mine polygons from the underground working dataset, and matching the point to polygons on the basis of seam code. A grid could then be produced and a mean age extracted for each grid square. This would then allow for this assessment at a finer scale. The age categories used should also be considered, for example after the nationalisation of the majority of the UK coal industry in 1947, the National Coal Board drove forward the mechanisation of the industry on the 1960s, leading to more long wall mining and a change in mine geometry (Vernon 2024).

The **mine drainage system** is one of the most important parameters in the Saxonian methods, with a centralised drainage system with high flow rates being the most prospective (Table 2.3). Drainage adits have a long history of use in both coal and metal mining (Younger 2004). Recent work has documented the discharge of drainage adits to the surface for the purpose of identifying geothermal opportunities (Walls et al. 2022; Coal Authority 2024d) and for recognising locations associated with environmental harm (Banks and Banks 2001). For example, the Old Fordell discharge in Scotland has a flow rate of 88 L s^{-1} and a heating potential of 2.49 MW (Walls et al. 2022). In the UK, major mine roadways, which are typically larger and better maintained than worked panels, have been considered attractive drilling targets for mine water geothermal schemes (Burnside et al. 2023). However, this author is not aware of any projects that have specifically targeted drainage tunnels within mine workings.

Estimating the **volume of the mine workings** for the method would be difficult. One approach would be to estimate the quantity of coal removed by examining historical production records (Jessop et al. 1995), or by reviewing the mine plans individually. However, accessing the plans held by the MRA involves cost and time, and each plan would then need to be digitised before any volumetric interpretation

could be made (see Chapter 3). An alternative would be to use the Underground Workings (UW) dataset (Coal Authority 2024g). Each polygon in the dataset is associated with a seam thickness, so it would be possible to multiply the thickness by the area of each polygon and sum the results to obtain an approximate worked volume (over an appropriately defined area), applying a correction factor for compaction. This would, however, produce an overestimate, because the polygons do not capture internal working detail; in areas of partial extraction they do not account for coal left in pillars or unworked zones. Unfortunately, without examining the individual mine plans there is no reliable way to determine the specific working methods used. Age could potentially serve as a rough proxy (Walls et al. 2024), but it would remain an approximation.

The categories for the **mine plan** parameter would need to be reworked because the plans held by the MRA for coal mines, although scanned and available as images, are not supplied in a georeferenced form. More recent plans usually include British National Grid lines, whereas older plans are far more difficult to georeference; this typically requires matching identifiable buildings or geographical features to Ordnance Survey maps. Some key dates to consider as category limits would be 1850, when the Coal Mines Inspection Act required an owner to keep a plan at each mine, and 1872, when depositing these plans with the Secretary of State became a statutory requirement (British Geological Survey 2024a; *Coal Mines Regulation Act 1872* 1872). Plans produced during this period often showed only the boundaries of the workings and contained little additional detail. In 1954 the Mines and Quarries Act was passed, introducing more stringent requirements for the content and accuracy of mine plans (*Mines and Quarries Act 1954* 1954).

The **temperature** categories at the mine water level are directly applicable to mine water temperatures in the United Kingdom. Farr et al. (2021) reports both measured and estimated temperatures at 100 metre intervals for mine water blocks across the country. These data could be combined with water level information to estimate the temperature at the mine water surface. Some areas contain little or no monitoring data, so further data collection would improve the reliability of these estimates.

Mine water chemistry is the fourth most important category in the Saxonian method. The categories run from 5, drinking water quality, to 1, heavily polluted and radioactive water. Radioactivity is not a major concern within coal mine water in the UK , so the categories for the water chemistry parameter could be redesigned to suit the UK better. The mine block reports provide some water quality data on salinity, iron, and alkalinity (Wyatt et al. 2023a). While salinity, total iron and alkalinity do not capture the full range of water quality issues relevant to mine water heat schemes (for example manganese, pH, temperature, dissolved oxygen, suspended solids and microbiological activity all influence bio-fouling and corrosion (Abeywickrama et al. 2021; Ebel et al. 2025; Banks et al. 2019b)), they are still useful indicators of risk. Salinity gives a first approximation of how aggressive the water may be to metallic components through chloride-driven corrosion; alkalinity provides an indication of the tendency for carbonate scaling on heat exchanger surfaces; and total iron highlights the likelihood of ochre formation and associated clogging of submersible pumps, pipework and heat exchangers (Walls et al. 2021).

The **accessibility** categories, which are based on the operational or abandoned status of mines and on the ability to access mine shafts, are not directly applicable in a UK context. As of 2025, the UK has only one significant operating underground coal mine (Aberpergwm) and a small number of minor drift or freeminer operations in Ayle and the Forest of Dean (Mining Remediation Authority 2025a). The Mining Remediation Authority's Mine Entries dataset records approximately 172,000 mine entries, although treatment information is absent for about 70 percent of these features (Coal Authority 2024a). If this accessibilty parameter were to be adapted for UK use, it could either be removed, because nearly all UK coal mines would fall into a single category (abandoned with inaccessible or unknown shafts), or it could be reconceptualised entirely. A more relevant interpretation of accessibility may instead be the availability of surface land suitable for drilling above target mine workings. This would require GIS-based analysis to identify land parcels of adequate size that also have suitable road access. Consultation with drilling contractors who have experience working in abandoned coal mines is strongly recommended.

2.2 Application of mapping methods

The MiRAS, Georesources Cornwall, and MRA Mine Water Heat Opportunity Mapping methods were tested on Newcastle (Figure 2.1).

There is significant overlap in the original data (Table 2.4) used in each mapping method, but the type and amount of processing required for each method varies. For each method a series of rasters are created in ArcGIS expressing the data required (Table 2.1). These maps are then combined, either visually (GRC), mathematically (MiRAS) or through a series of decision rules (MRA). The details of how each dataset was processed, turned into a map, and combined together is discussed for each method assessed below.

2.2.1 MiRAS

The MiRAS method operates by creating 3 maps (rasters) which represent the 4 criteria MiRAS uses to identify optimal mine water areas. The first of these (C12) identifies areas with overlapping mine workings, and has the areas with shallow workings (<30 m bgl) removed. The second (C3) shows areas where the depth to mine water is shallower than 60 m bgl. The third shows an average depth to mine workings, classified as >250 m bgl or <250 m bgl.

How each of these maps is created is described below and the flowchart of how Walls et al. (2024) did this is in Figure 2.3.

Overlapping mine workings without shallow workings

The C12 map combines the first two criteria: areas of overlapping workings (C1) with workings shallower than 30 m bgl (C2) excluded.

C1 is derived from the Underground Workings dataset (Table 2.4). This dataset comprises a series of polygons representing mined seams. GIS analysis was used to identify locations where these polygons overlap.

Areas where the 'Shallow coal workings' dataset is present (a separate polygon dataset showing only workings shallower than 30 m bgl) were then removed. The resulting C12 map therefore shows single or overlapping seams, with areas of shallow

Table 2.4: Data used for the different mine water geothermal opportunity mapping methods.

Data	**Dataset (source)**	**Methods**
Mine workings	Underground workings dataset (Coal Authority 2024g)	MiRAS, GRC, MRA
Shallow (>30 m) mine workings	Shallow coal workings dataset (UK Government 2024)	MiRAS
Depth of workings	In seam levels dataset (Coal Authority 2024f)	MiRAS, GRC, MRA
Mine water discharge points	Hydrogeological Conceptual Model reports for the mine blocks (Wyatt 2022a; Wyatt 2022b; Marchi-Smith 2022; Wyatt 2022c; Wyatt 2022d; Marchi-Smith and Wyatt 2022a; Wyatt 2022e; Marchi-Smith and Wyatt 2024a; Wyatt 2022f; Cowley 2022; Marchi-Smith and Wyatt 2022b; Wyatt 2022g; Wyatt 2022h; Wyatt 2022i; Wyatt 2022j; Marchi-Smith and Wyatt 2024b)	MiRAS, MRA
Mine water monitoring points	Hydrogeological Conceptual Model reports for the mine blocks (Wyatt 2022a; Wyatt 2022b; Marchi-Smith 2022; Wyatt 2022c; Wyatt 2022d; Marchi-Smith and Wyatt 2022a; Wyatt 2022e; Marchi-Smith and Wyatt 2024a; Wyatt 2022f; Cowley 2022; Marchi-Smith and Wyatt 2022b; Wyatt 2022g; Wyatt 2022h; Wyatt 2022i; Wyatt 2022j; Marchi-Smith and Wyatt 2024b)	MiRAS, MRA
Opencast workings	Unlicensed opencast coal mining dataset (Coal Authority 2024h)	MRA
Mine water recovery	Hydrogeology of the North East England Coalfield conceptual model (Wyatt et al. 2023a)	MRA
Digital Terrain Model	OS Terrain 5 DTM (Ordnance Survey 2025)	MiRAS, GRC, MRA
Heat demand	Peta 5 heat demand layers (Möller et al. 2022)	GRC

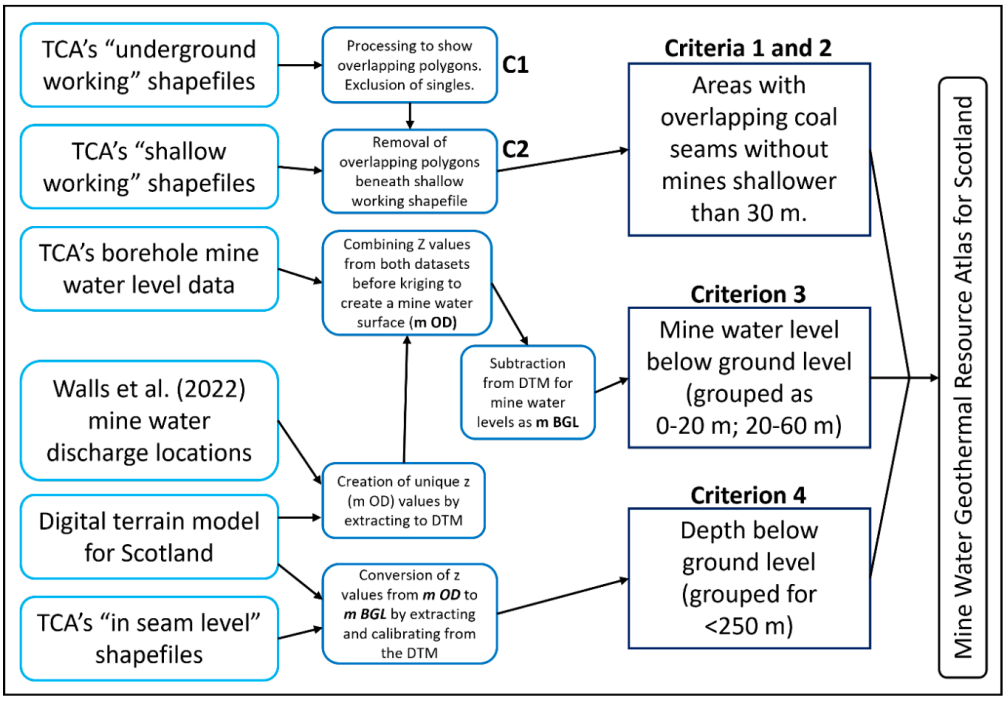

Figure 2.3: MiRAS flowchart of methodology (Walls et al. 2024) The 6 boxes on the left-hand side are the data inputs Walls et al. (2024) used in this method. The three boxes on the right-hand side are the 3 criteria maps that are combined together to produce the final map (the far right box).

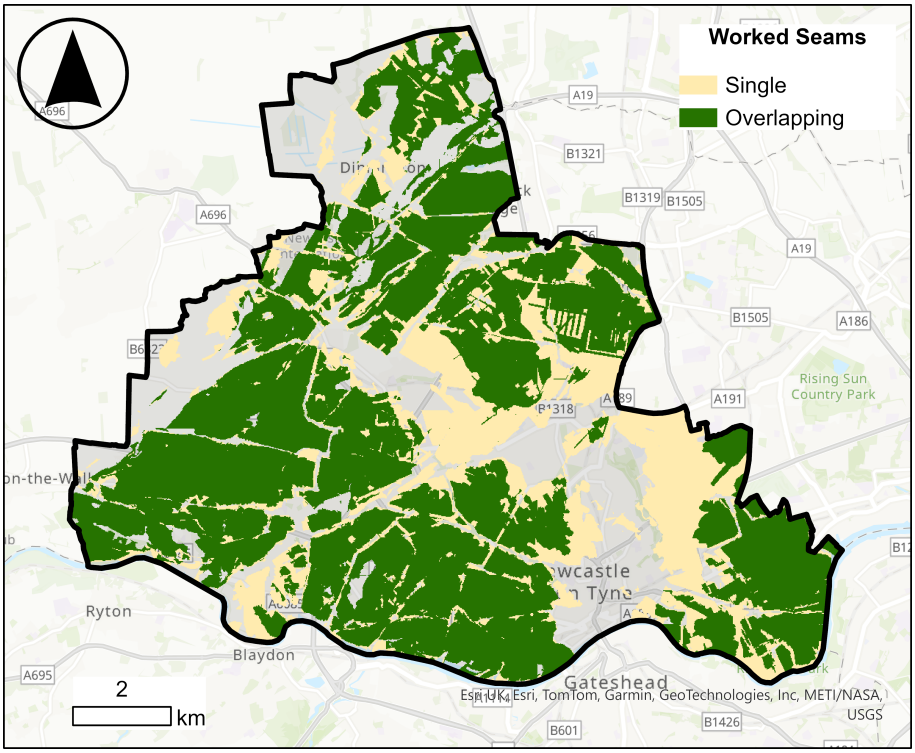

Figure 2.4: Map of MiRAS criteria 1 and 2 (C12) in Newcastle, it shows the presence of single and overlapping seams (C1) with areas with shallow workings, <30 m bgl, removed (C2). Reproduced with the permission of © The Mining Remediation Authority. All rights reserved

mine workings excluded (Figure 2.4).

Figure 2.4 indicates that mine workings underlie most of Newcastle and that, in the majority of locations where workings occur, multiple seams overlap. Comparing Figure 2.4 with Figure 2.1 shows that shallow workings are concentrated mainly along the western edge of Newcastle: these areas appear blank in Figure 2.4, but mine workings are visible in Figure 2.1.

Depth to mine water

C3 identifies locations where the mine water head is >60 m bgl. To achieve this, a dataset of mine water depth values was compiled and interpolated to produce a continuous mine water surface, which was then classified into depth bands.

Mine water head data were compiled from a series of Mining Remediation Authority hydrogeology reports covering the mine water blocks in the region (Wyatt 2022a; Wyatt 2022b; Marchi-Smith 2022; Wyatt 2022c; Wyatt 2022d; Marchi-Smith

and Wyatt 2022a; Wyatt 2022e; Marchi-Smith and Wyatt 2024a; Wyatt 2022f; Cowley 2022; Marchi-Smith and Wyatt 2022b; Wyatt 2022g; Wyatt 2022h; Wyatt 2022i; Wyatt 2022j; Marchi-Smith and Wyatt 2024b). For each block, the report map showing sampling locations was georeferenced and digitised to create a new dataset, with water depths extracted from the reports. Where multiple measurements existed for the same location, the most recent value was retained and earlier values were discarded. Where surface discharge locations were reported without a head elevation, the head was assumed to be at ground surface at that point.

These water depths were then interpolated to create a mine water head surface in m OD, consistent with the original MRA data. This was converted to m bgl by subtracting the interpolated head surface from a Digital Terrain Model (DTM), representing ground-surface elevation.

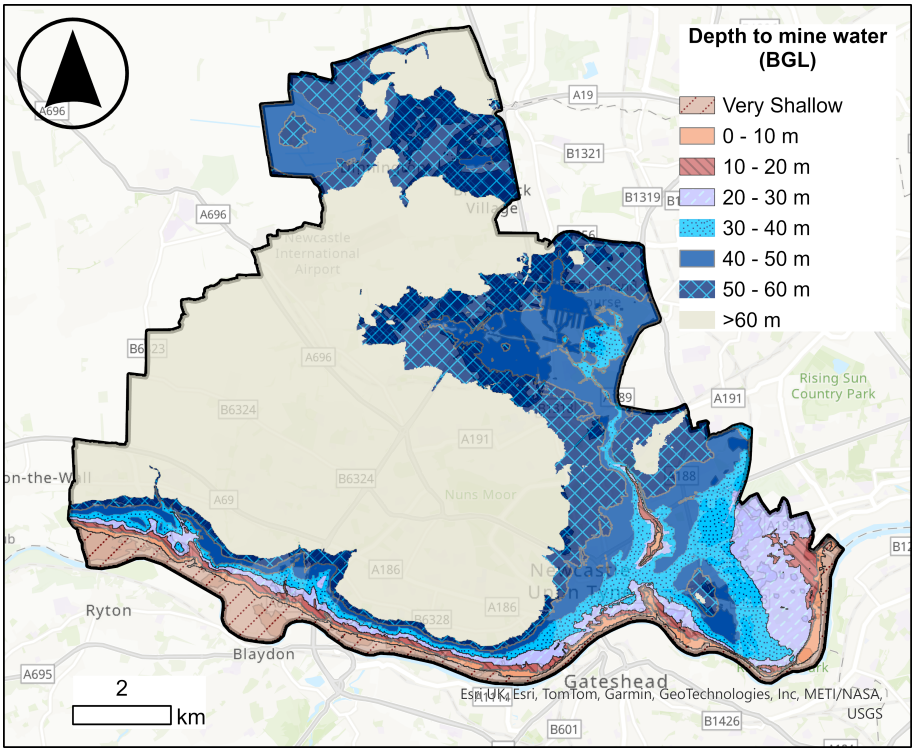

Figure 2.5: Map of MiRAS criteria 3 (C3), identifying where the depth to mine water is <60 m across Newcastle. Areas where the depth to mine water is <60 m bgl are concentrated along three rivers; the River Tyne (west to east at the southern edge of the map), the Ouseburn (which joins the Tyne on the eastern side of the map), and the Seaton Burn (which runs west to east across the north of the map). Reproduced with the permission of © The Mining Remediation Authority. All rights reserved.

The resulting mine water depths were classified into 10 m depth bands from >0

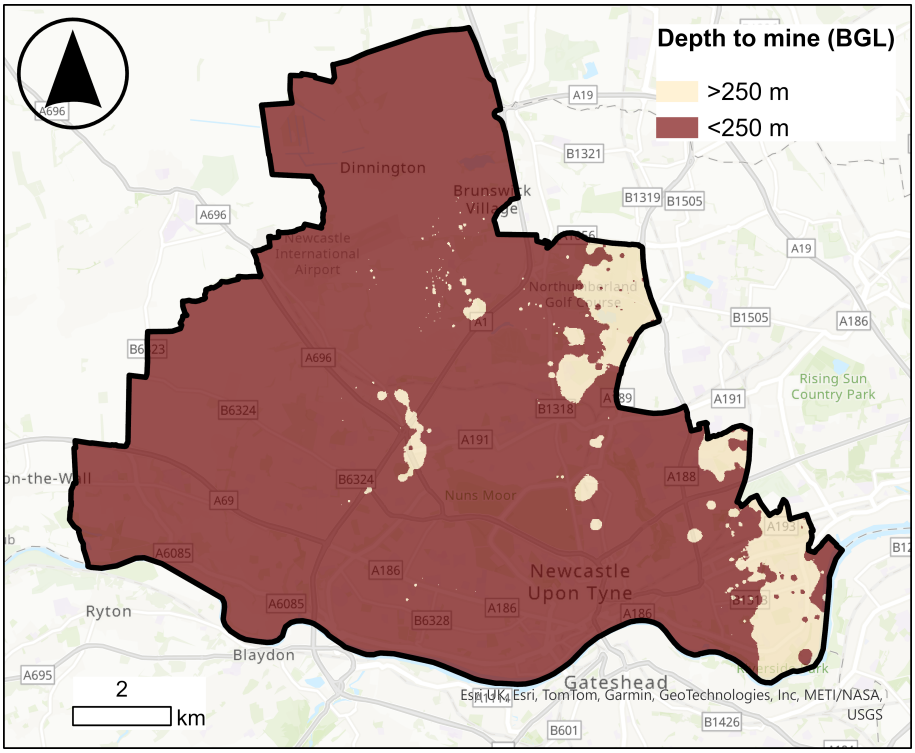

Figure 2.6: Map of MiRAS criteria 4 (C4), identifying where the average depth to the mines is above and below 250 m bgl across Newcastle. Reproduced with the permission of © The Mining Remediation Authority. All rights reserved.

to 60 m bgl. The result is a map that retains only locations with acceptable head depth (<60 m bgl), in 10 m increments for subsequent combination with the other criteria (Figure 2.5).

The middle and western parts of the city have depths to mine water greater than 60 m bgl, so they cannot be classified as optimal areas (Figure 2.5). The most suitable areas are concentrated along the rivers (Figure 2.5). Presumably this is because the surface elvation is lower next to the rivers.

Mine working depths

C4 identifies locations where worked seams are not excessively deep. To create this layer, worked seam elevation points, given relative to Ordnance Datum (In seam level dataset), are converted to m bgl using the the DTM. For each point, the ground level was sampled from the DTM and the depth to the worked seam was calculated by subtracting the seam elevation from the ground elevation.

These point depths were then interpolated into continuous map allowing depth

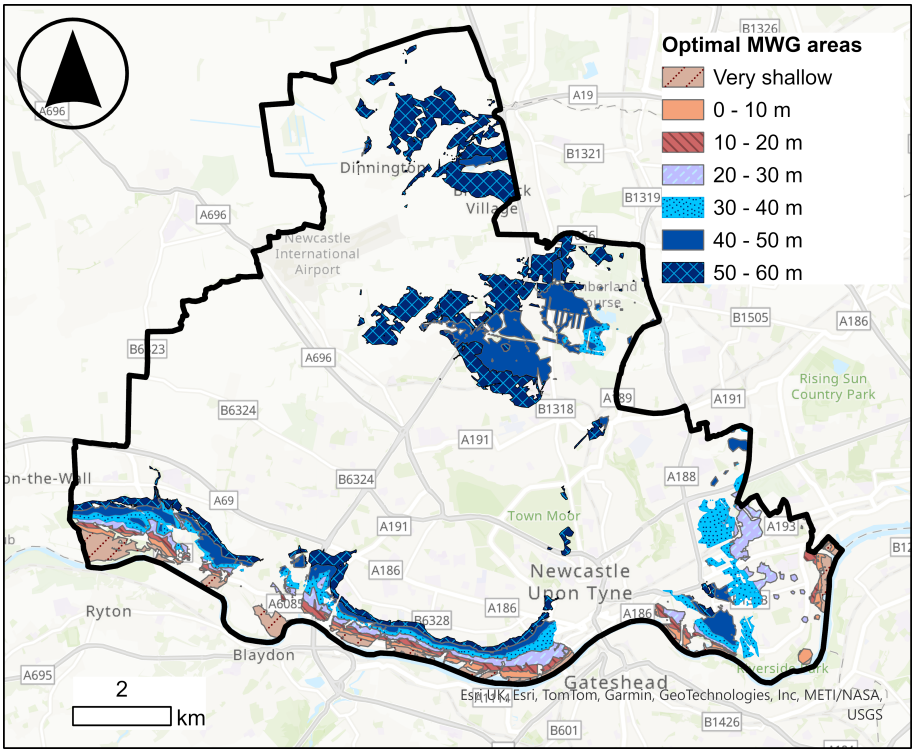

Figure 2.7: The final map of Newcastle produced following the MiRAS method combining the three previous maps. The optimal areas are displayed with the depths to mine water. The most optimal sites are 20 - 60 m bgl (blue). Reproduced with the permission of © The Mining Remediation Authority. All rights reserved.

to be estimated between data points. Finally, the map was divided into areas where workings are shallower than 250 m bgl and areas where workings are deeper than 250 m (Figure 2.6). The substantial majority of the area is <250 m bgl, with depths >250 m bgl concentrated mainly along the eastern edge.

Final map

These three maps are multiplied together to produce the final map. This output shows only areas with no shallow workings and multiple overlapping seams, where mine workings are shallower than 250 m bgl and depth to mine water is less than 60 m bgl, displayed in 10 m bands (Figure 2.7).

As stated by Walls et al. (2024), the areas with mine water >20 m bgl are more optimal for an open loop with re-injection scheme, as at shallower depths there is a risk of localised water level rise. It is possible that an open loop with discharge scheme may be suited, but the additional risks and costs of discharging to the surface

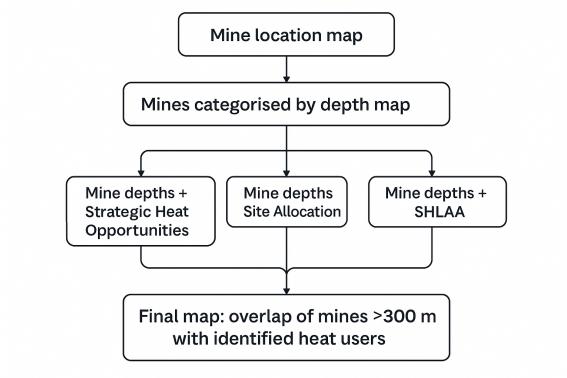

Figure 2.8: Georesources Cornwall methodology flowchart (EGS Energy Ltd and Carrak Consulting Ltd 2019).

need to be considered. The best areas using this method are shown to be in the North of Newcastle, the South but set back from the river Tyne, and the Southeast.

2.2.2 GRC, Geothermal Screening Assessment

The GRC method requires the locations of the mines in the target area, the depths of the mine workings, the geothermal gradient, and the current and potential future heat demand in the areas being evaluated. Two maps are created, the first shows the location and the depths of the mines, classified into depths that translate into <16°C, 16-19°C, and 19-23°C. The second, displays heat demand. These are then combined to allow for a visual assessment of where the areas of highest heat demand coincide with the areas of the deepest, and hottest mines. Figure 2.8 shows how the original application of this method was done in Cornwall.

Mine locations and depths

The MRA Underground Workings dataset is used to map where mine workings are located. However, the mine polygons do not include depth information. Unlike the MiRAS approach, which builds a continuous depth surface, this method uses discrete depth data.

To add depth information, the In Seam Level dataset was used. Where a depth data point overlaps a mine working polygon and both relate to the same coal seam, the depth value is assigned to that polygon. If multiple depth points occur within

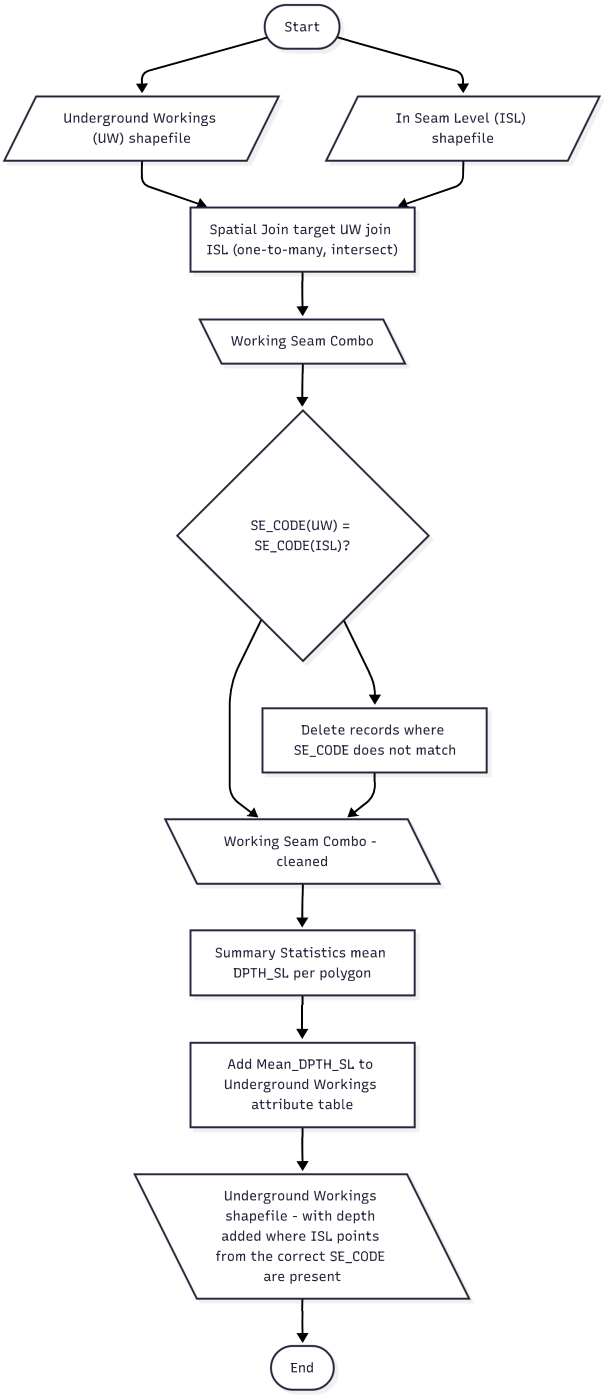

Figure 2.9: Process created to add depth data from In seam level (ISL) data set to the Underground workings (UW) mine polygons. The SE_CODE is a property that both datasets have that identifies which coal seam the data is from. In this instance SL (sea level) refers to depths from Ordnance Datum. This is used for the GRC and MRA method.

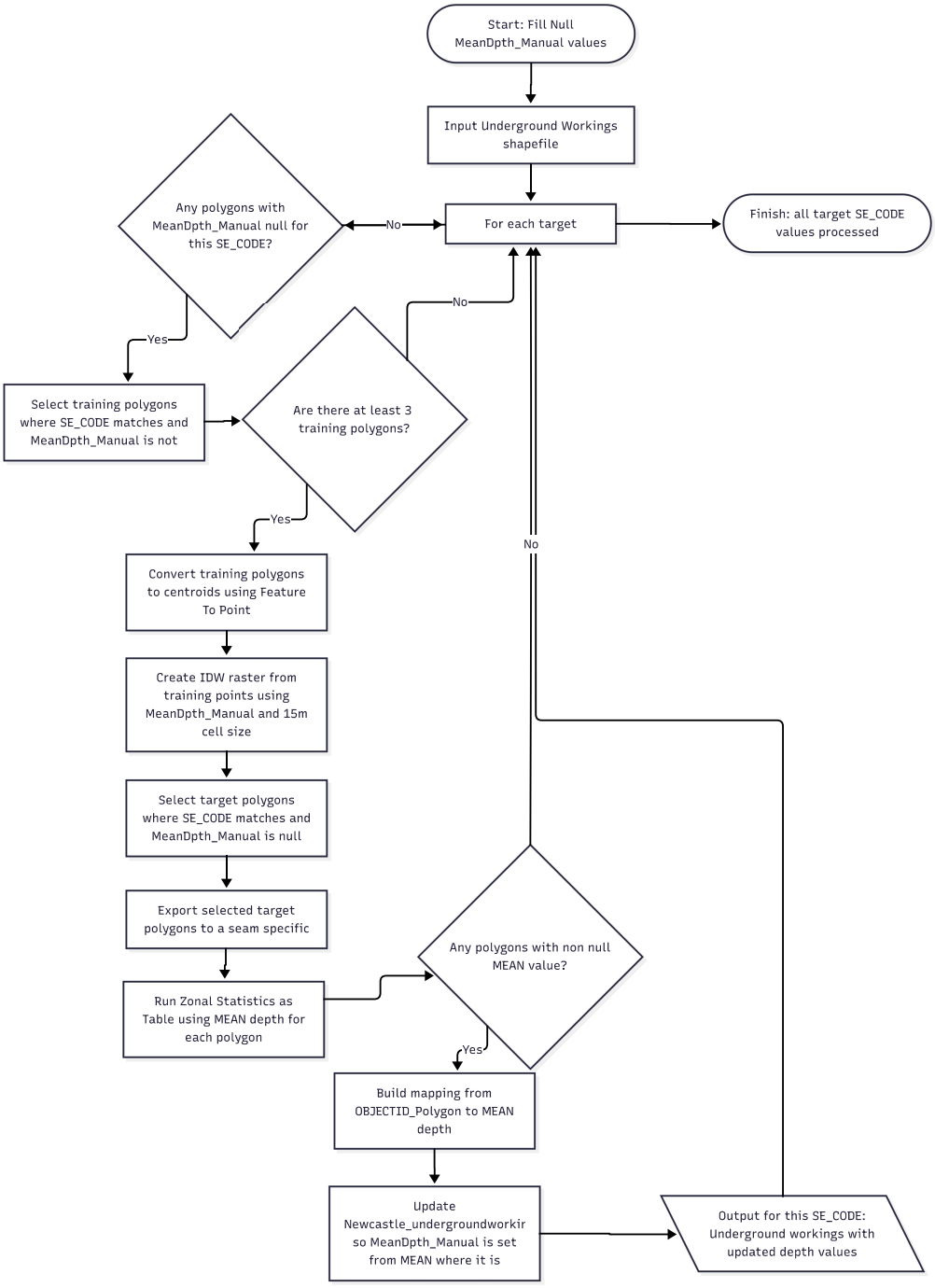

Figure 2.10: Process created to add depth data to the mine workings polygons that do not have associated depth data directly from In seam level points. For each seam the depth values are interpolated to form a depth map. Polygons of the same seam with missing depths are then assigned the mean interpolated depth within their area. This is used for the GRC and MRA method.

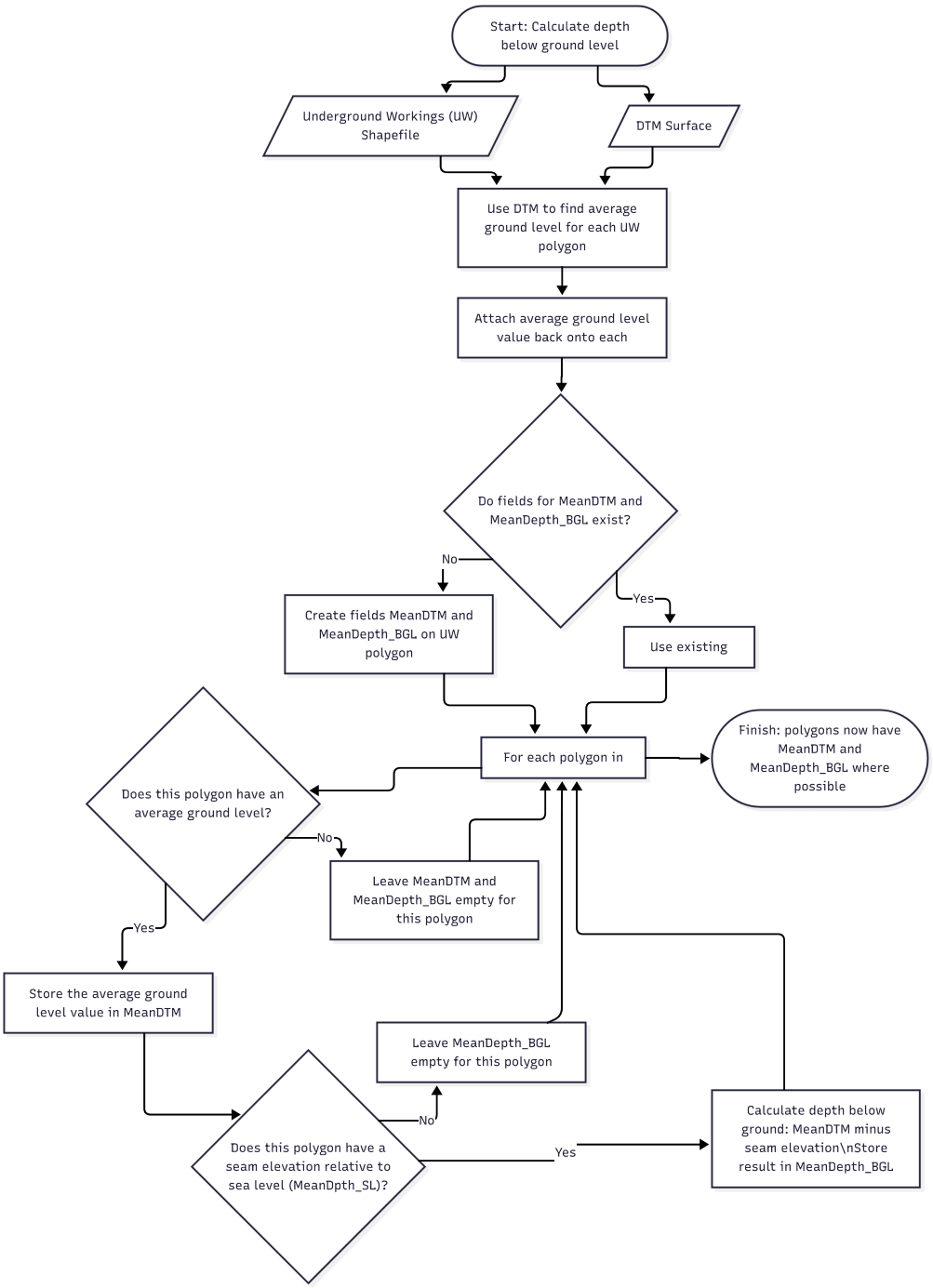

Figure 2.11: Process created to convert the underground workings polygons into m bgl. This is used for the GRC and MRA method.

a single polygon, the mean depth is used (Figure 2.9).

Some mine working polygons have no associated seam depth data (865 of 2719 in the Newcastle case study). For these polygons, depth is estimated in a second step (Figure 2.10). For each seam, polygons with existing depth values are used to build a seam-specific depth map by interpolation between known values. This depth map is then used to assign depths to polygons of the same seam that lack measurements by calculating the mean estimated depth across each polygon area. These estimated depths are written back into the mine working polygon dataset. This produces a single mine working polygon layer in which all polygons have depth values.

Finally, depths were converted to metres below ground level using the DTM (Figure 2.11) and grouped into three depth ranges: <203.5 m bgl, 203.5–290.7 m bgl, and 290.7–405.9 m bgl. These depth ranges correspond to approximate temperature ranges of <16°C, 16–19°C, and 19–23°C, assuming an average surface temperature of 9°C and a local geothermal gradient of 34.4°C km^{-1} (Farr et al. 2021). The original method also includes a >25°C category, but no mines in this study area are predicted to exceed 23°C. Mine workings shallower that 203.5 m bgl are not displayed as <16°C is considered too cold in the original method (Figure 2.12).

Comparing Figure 2.12 with Figure 2.1 indicates that shallower workings (<203.5 m bgl) are concentrated along the western edge of the map, with additional areas in the centre and on the eastern side, immediately west of the A188. The deeper workings are predominantly located along the eastern edge of the map.

Heat Demand

Heat demand was mapped using the Heat Demand Densities layer from Möller et al. (2022) which maps the demand (in TJ km^{-1}) from the residential and service sector as was in 2015 (Figure 2.13).

Figure 2.13 shows that heat demand is below 50 TJ km^{-2} in the west, which is predominantly agricultural land. The highest heat demand occurs in the south-east of Newcastle, corresponding to the city's commercial centre.

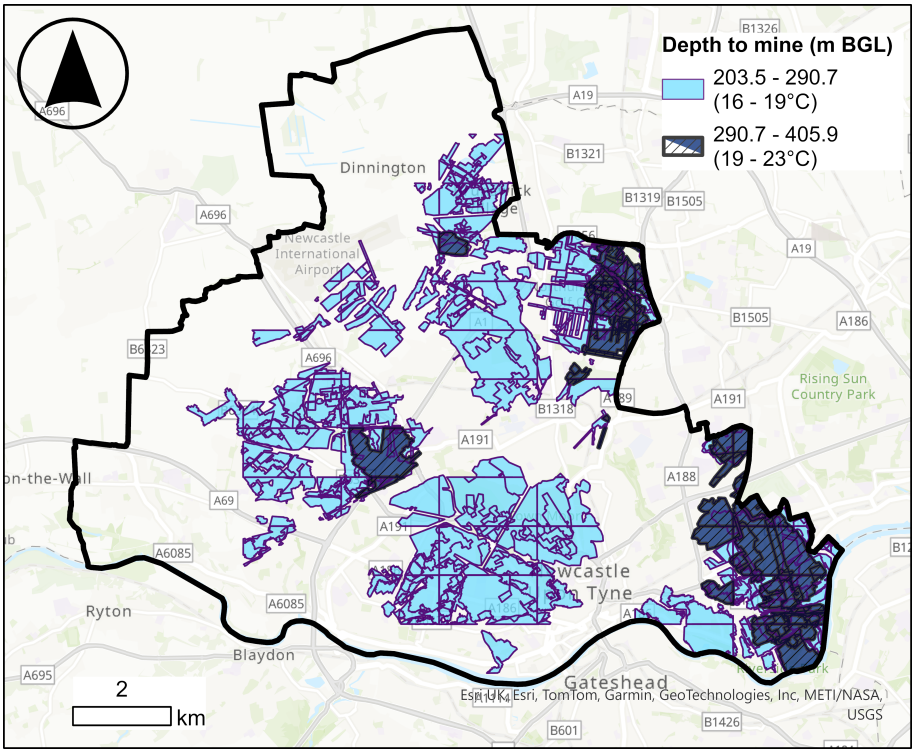

Figure 2.12: Map of the Newcastle mines for the GRC method. Mines <203.5 m bgl are not displayed as they are predicted to be <16°C. Reproduced with the permission of © The Mining Remediation Authority. All rights reserved.

Final map

The final map shows the heat demand and the mine workings within each depth category. The deeper, hotter, more prospective mines are drawn on top of the shallower mines to allow the more prospective areas to be more easily identified (Figure 2.14). Then a visual assessment is used to identify the most prospective areas (Figure 2.15).

The annotated final map (Figure 2.15 produced by following the Georesources Cornwall method highlights the two most optimal areas, where high heat demand and deeper hotter mines coincide. The Northwest side of the map is noticeably empty. In regards to heat demand, this is where Newcastle transitions from being suburban housing to agricultural land. The mines in this area are also shallower than 203 metres (this can be see comparing Figures 2.12 and 2.17) and are therefore not shown.

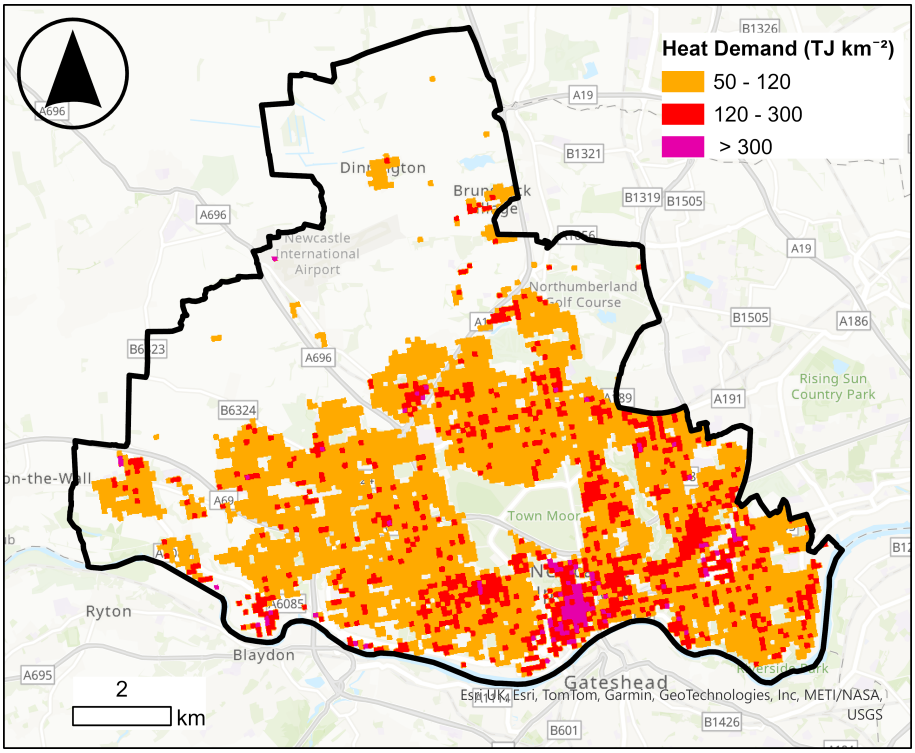

Figure 2.13: Map of heat demand across Newcastle for the GRC method. Heat demand data from Möller et al. (2022). Reproduced with the permission of © The Mining Remediation Authority. All rights reserved.

2.2.3 MRA, Mine Water Heat Opportunity Mapping

The MRA method uses 7 maps to go through the decision process flowchart in Figure 2.2 to produce the final map. How each of these maps was produced is described below. These are then combined through a series of decision rules.

Mine workings present

The underground workings file is converted to a raster which shows where workings are present (Figure 2.16).

Multiple overlapping seams

The same analysis is used here as in the MiRAS C1 assessment, identifying where the overlapping seams are (Figure 2.17).

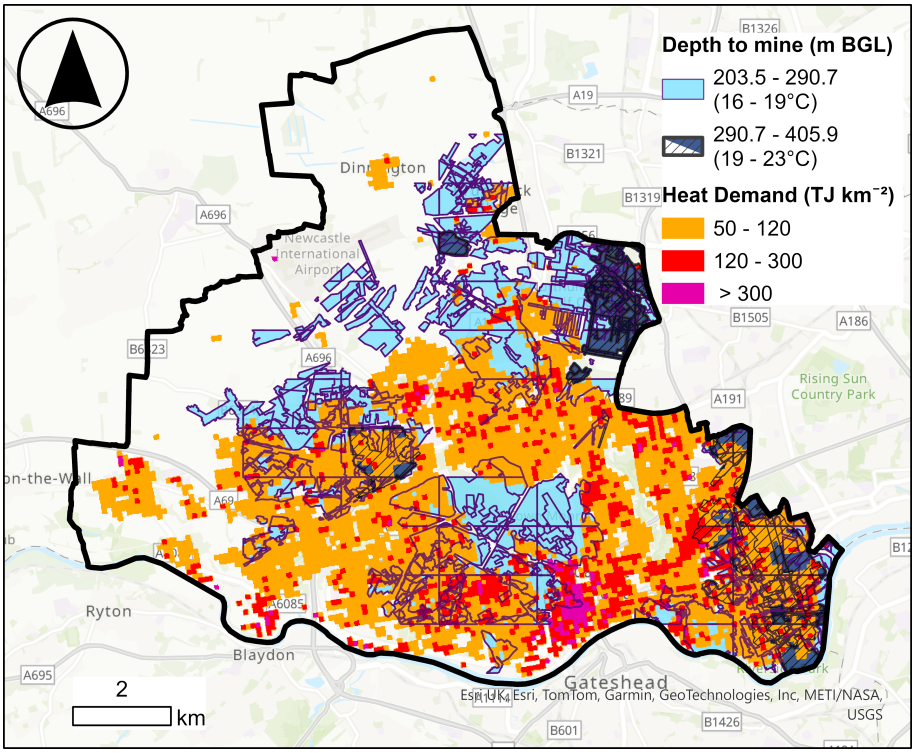

Figure 2.14: Map of Newcastle displaying heat demand and mine depth data for visual identification of the best MWG sites (GRC method). Reproduced with the permission of © The Mining Remediation Authority. All rights reserved.

Depth to workings

The process of finding the depth of each mine working polygon is the same as that used for the GRC method (Figures 2.9, 2.10, 2.11). After determining the depth for each mine working polygon the depths are classified. The MRA method uses shallow workings only (<30 m bgl), >30 - 300 m bgl, 300 - 500 m bgl, and >500 m bgl. The area being assessed is broken down into cells. For each cell the depths of every mine polygon that is present in the cell is assessed. If there are only workings shallower than 30 m, that is classed as category 0. If there is at least one seam between 30 and 300 m bgl, the cell is category 1. If the cell does not meet the test for category 0, or 1, but has at least one mine polygon between 300 - 500 m bgl, it becomes category 2. If the cell does not meet the test for category 0, 1, or 2, but has at least one mine polygon > 500 m bgl, it becomes category 3 (Figure 2.18).

Figure 2.18 shows mine working depth classes (m bgl). The classes are areas with only shallow workings (<30 m), areas with at least one working between 30

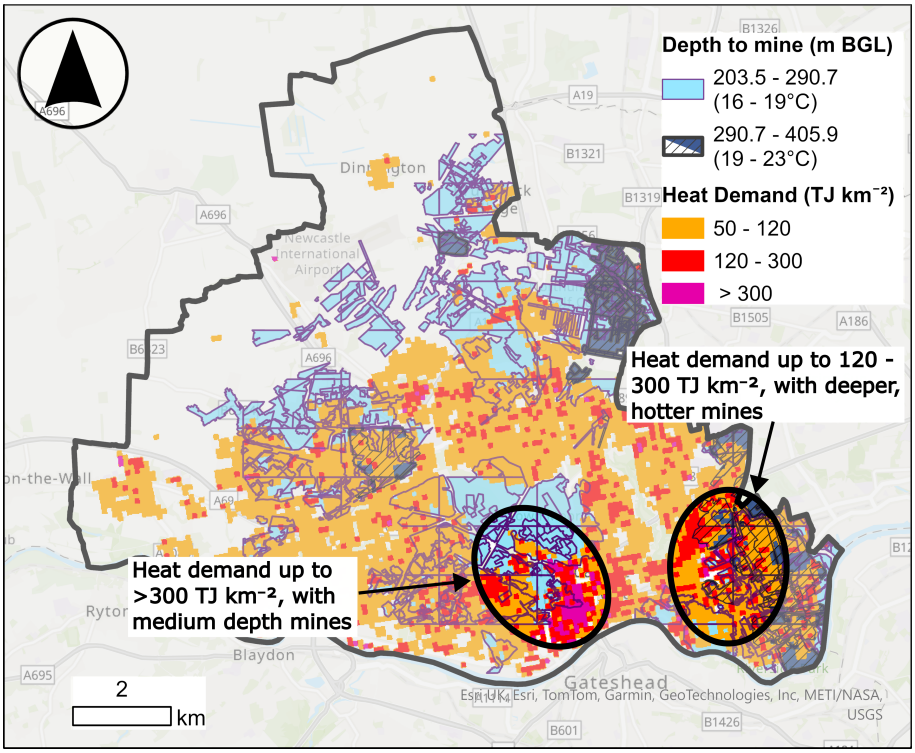

Figure 2.15: The GRC final map of Newcastle, produced from the GRC method, identifying two sites with the greatest potential. Reproduced with the permission of © The Mining Remediation Authority. All rights reserved.

– 300 m, and areas that do not meet either of these criteria but have at least one working between 300 – 500 m bgl. The vast majority of Newcastle has workings in the 30 – 300 m bgl range, which is the ideal depth range in the MRA method.

Opencast workings

The Unlicenced Opencast workings dataset from the MRA was used to identify areas of opencast workings (Figure 2.19).

Opencast mine workings cover only a small proportion of the Newcastle area and are largely restricted to the western side, as shown in Figure 2.19.

Depth to mine water

Mine water depth data is from the Mining Remediation Authority (2024a) and the series of hydrogeological reports produced by the MRA, for the NE of England, and the mine block there within (Wyatt 2022a; Wyatt 2022b; Marchi-Smith 2022; Wyatt 2022c; Wyatt 2022d; Marchi-Smith and Wyatt 2022a; Wyatt 2022e; Marchi-

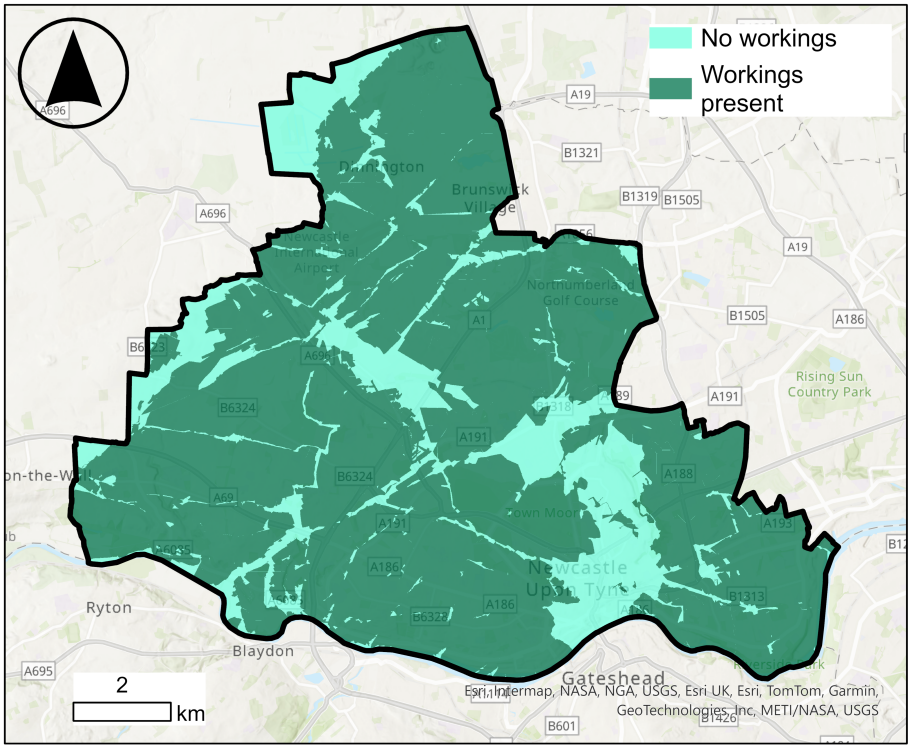

Figure 2.16: Map of all the underground mine workings present in Newcastle for the MRA methodology. Reproduced with the permission of © The Mining Remediation Authority. All rights reserved.

Smith and Wyatt 2024a; Wyatt 2022f; Cowley 2022; Marchi-Smith and Wyatt 2022b; Wyatt 2022g; Wyatt 2022h; Wyatt 2022i; Wyatt 2022j; Marchi-Smith and Wyatt 2024b; Wyatt et al. 2023a). The maps showing the mine blocks and the locations of discharge and monitoring points are imported into GIS software, georeferenced and digitised. The mine water heights contained in the report are reported in m OD. If there was a discharge point with no associated height, it was presumed to be at ground level. The water level in each mine block is considered separately. If there is only one data point this is taken as the mine water height across the whole mine block. If there are 3 or fewer points, a mean value is taken. If there are more than 3 data point mine water depth was interpolated across the block. These were joined together and subtracted from the regional DTM to create a mine water surface in m bgl. This was then classified according to the MRA conditions, <75 m bgl, 75 - 100 m bgl, and >100 m bgl (Figure 2.20).

Predicted mine water depth across Newcastle is shown in Figure 2.20. The greatest depths occur in the south-central and south-west parts of the map. Most

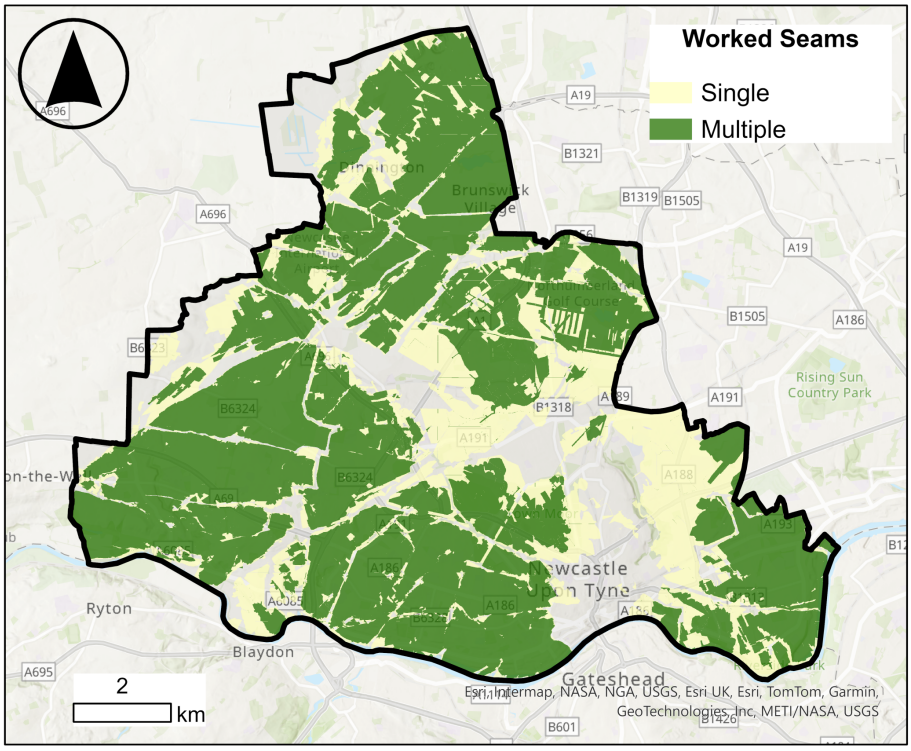

Figure 2.17: Map identifying the where single and overlapping seams are present in Newcastle for MRA methodology. Reproduced with the permission of © The Mining Remediation Authority. All rights reserved.

other areas are <75 m bgl, which is the preferred depth in the MRA method.

Recovery

The recovery status (whether the water level is still rising, or has ceased to rise) of the mine water block is assessed using information from the Hydrogeology of the North East England Coalfield report (Wyatt et al. 2023a). For the purposes of the methodology, water levels must be classified as either recovering or recovered. However, the report explicitly assigns these categories to only a limited number of mine blocks. It is therefore interpreted that areas where pumping is actively used to control water levels are unlikely to have pumping reduced to permit further recovery; such areas can consequently be considered artificially "recovered". All remaining areas are also classified as recovered to avoid overestimating the opportunities available (Table 2.5). The recovery status is attached to each mine block (Figure 2.21).

Figure 2.21 shows that mine water level has recovered across all mine blocks in Newcastle.

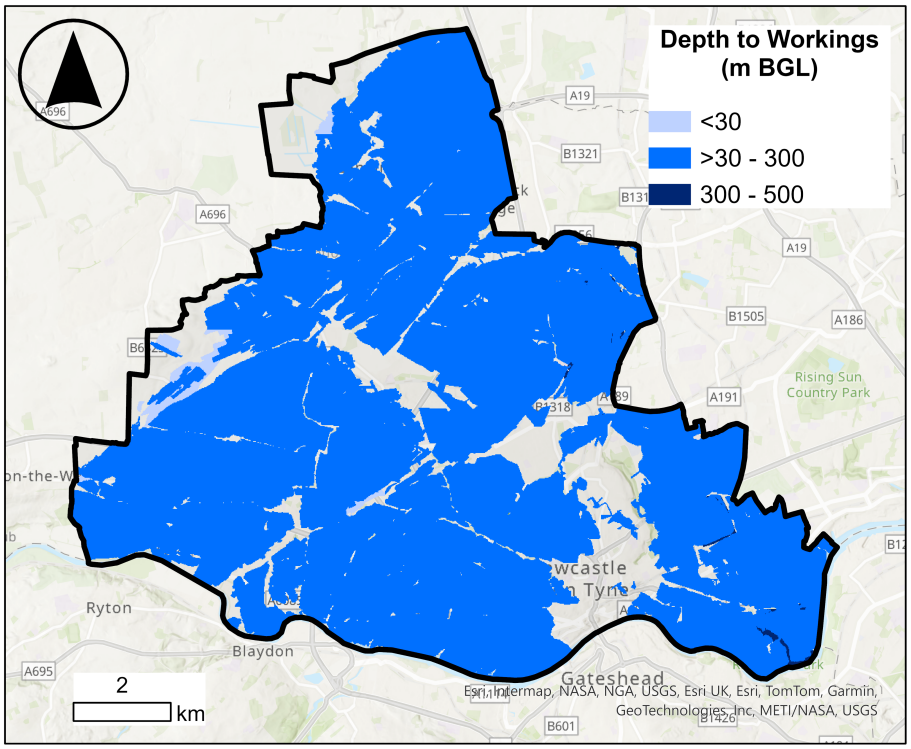

Figure 2.18: Mine working depth in Newcastle (MRA methodology): <30 m bgl only; 30-300 m bgl if present (takes precedence over 300-500 m); 300-500 m bgl only if no workings occur above 300 m (see text for further explanation of the classification). Reproduced with the permission of © The Mining Remediation Authority. All rights reserved.

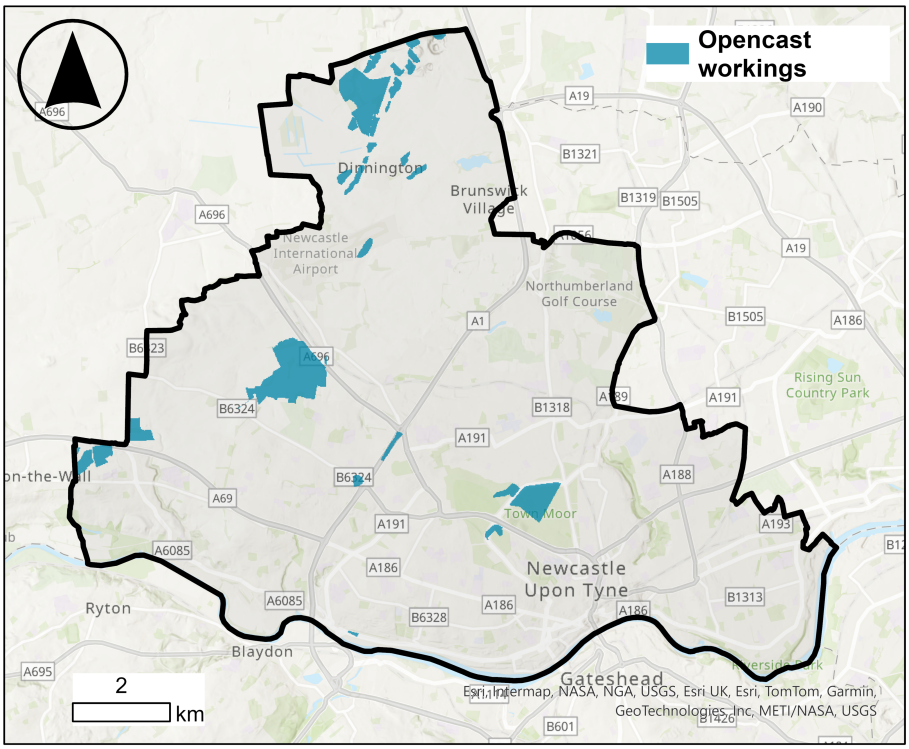

Figure 2.19: Opencast mine workings in Newcastle for the MRA methodology. Reproduced with the permission of © The Mining Remediation Authority. All rights reserved.

Flooding

The last map required is to assess whether the mines are flooded.

First, mine working depths were grouped into four bands: <30 m bgl, 30–300 m bgl, 300–500 m bgl, and >500 m bgl. The map is then divided into a grid and for each cell the depths of the mine workings are compared to the depth of the mine water. Where the mine water depth is shallower than the mine working depth, those working are considered flooded. Each cell is assigned a single category based on the deepest flooded depth band present, using a simple priority scheme (deeper bands take priority). The output categories are: no flooded workings, flooded workings <30 m bgl only, at least one flooded working at 30–300 m bgl (even if shallower flooded workings are also present), no flooded workings at 30–300 m bgl but at least one at 300–500 m bgl, and no flooded workings in the shallower bands but at least one >500 m bgl (Figure 2.22).

When Figure 2.22 is compared with Figure 2.16, which shows the distribution

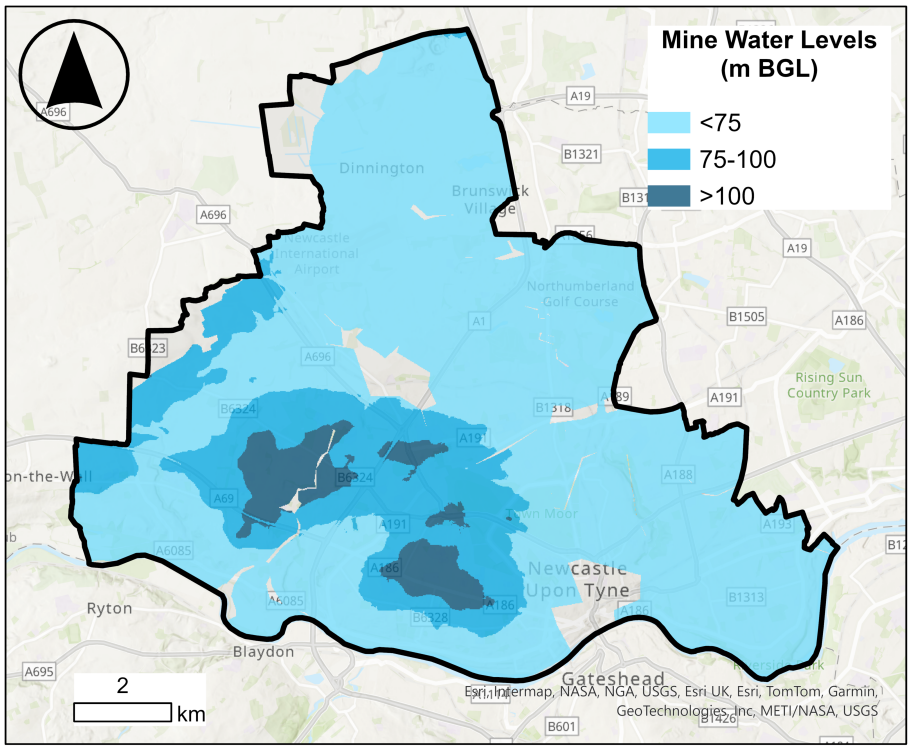

Figure 2.20: Depth to mine water in Newcastle, assessed per mine block, for the MRA method. Reproduced with the permission of © The Mining Remediation Authority. All rights reserved.

of mine workings, it is clear that most workings are flooded and that flooding predominantly occurs in the 30–300 m bgl depth range.

Final map

Using all of the above maps an ordered set of rules is applied across the whole area following the MRA flowchart (Figure 2.2). In summary, cells were assigned to four classes (good = 4, possible = 3, challenging = 2, no opportunity = 1) according to combinations of: the presence of underground workings, whether multiple seams are present,the depth band of the workings,the presence of opencast workings, the mine water level and flooding status, and the mine water recovery status (Figure 2.23).

The final MWG opportunity map produced by following the MRA method displays the results ranked into ‘good’, ‘possible’ and ‘challenging’. There is also ‘uncategorised’, these are locations where the outcomes did not fit into the definitions the different opportunity levels. A more in depth consideration of the categories is presented in the discussion, but the uncategorised sections here are produced by

Table 2.5: Recovery classification of mine water blocks.

Block name	Hydrology report description	Classification
Central Durham North	Pumped and gravity discharge	Recovered
Algernon-Hebburn	Uncertain, possible gravity discharges	Recovered
Bates	Pumped	Recovered
Newcastle High Main	Unknown if this is a separate block or related to the Central Durham North or Walker blocks; considered as recovered to match Central Durham North	Recovered
Kenton	Possible overflow	Recovered
Walker	Recovered	Recovered
Blaydon	Gravity discharge	Recovered
East Walbottle	Uncertain	Recovered
Throckley	Gravity discharge	Recovered

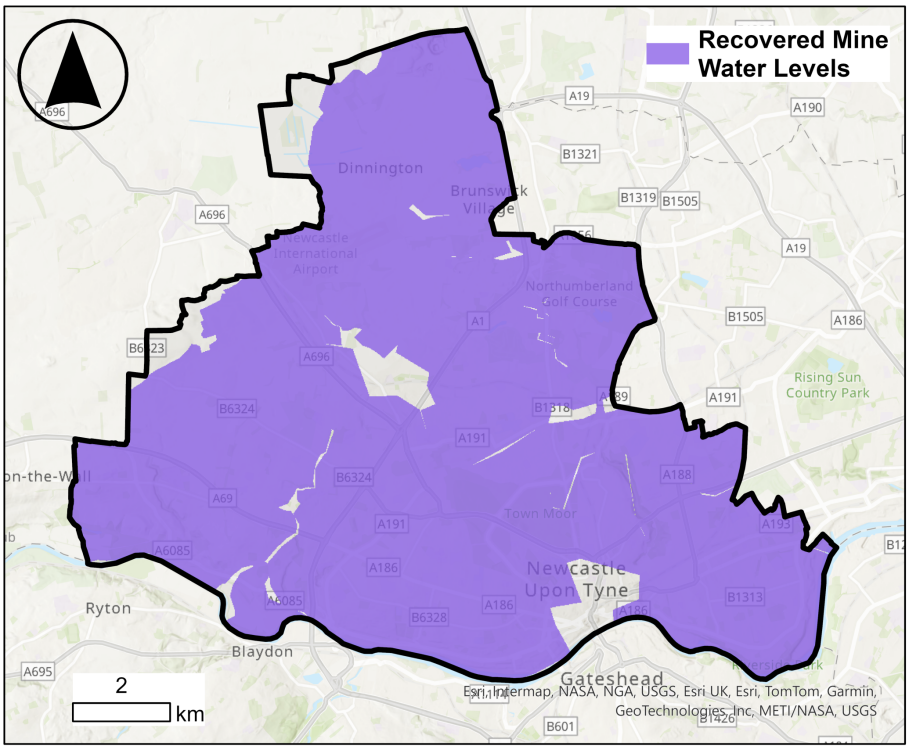

Figure 2.21: Map showing that the water level in all of the mine blocks in Newcastle is assessed to have recovered for the MRA method. Reproduced with the permission of © The Mining Remediation Authority. All rights reserved.

slight mis-alignments between the different raster layers.

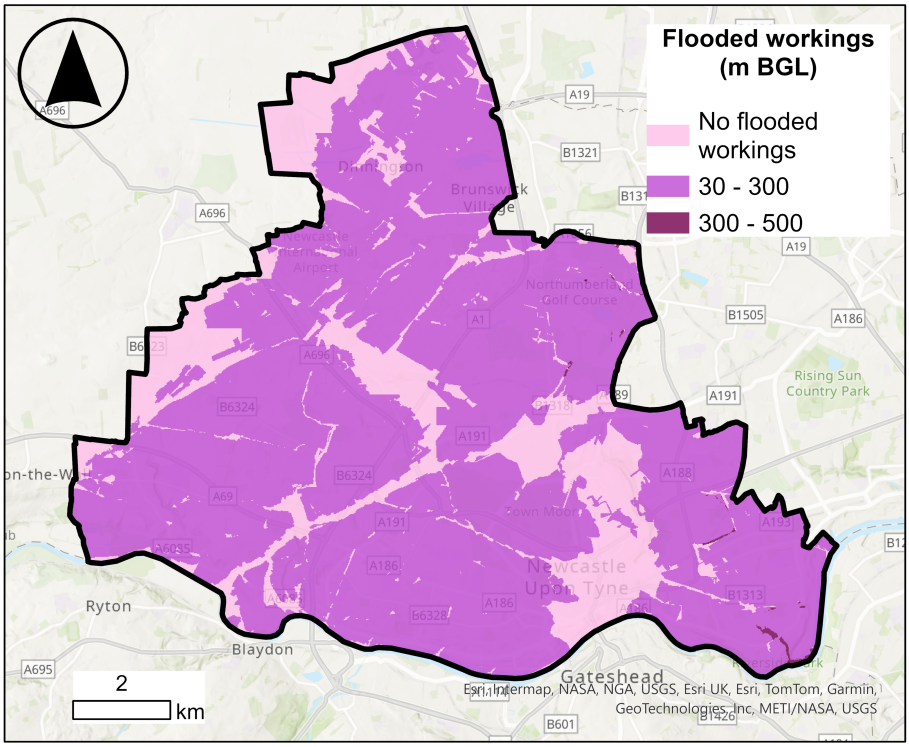

Figure 2.22: Flooded mine workings (mine water depth < mine working depth) in Newcastle (MRA methodology). Classified into: no flooded workings, only mines <30 m bgl which are flooded (none present), any flooding 30-300 m bgl (even if other flooded depths are also present), flooding within 30-300 m bgl. Reproduced with the permission of © The Mining Remediation Authority. All rights reserved.

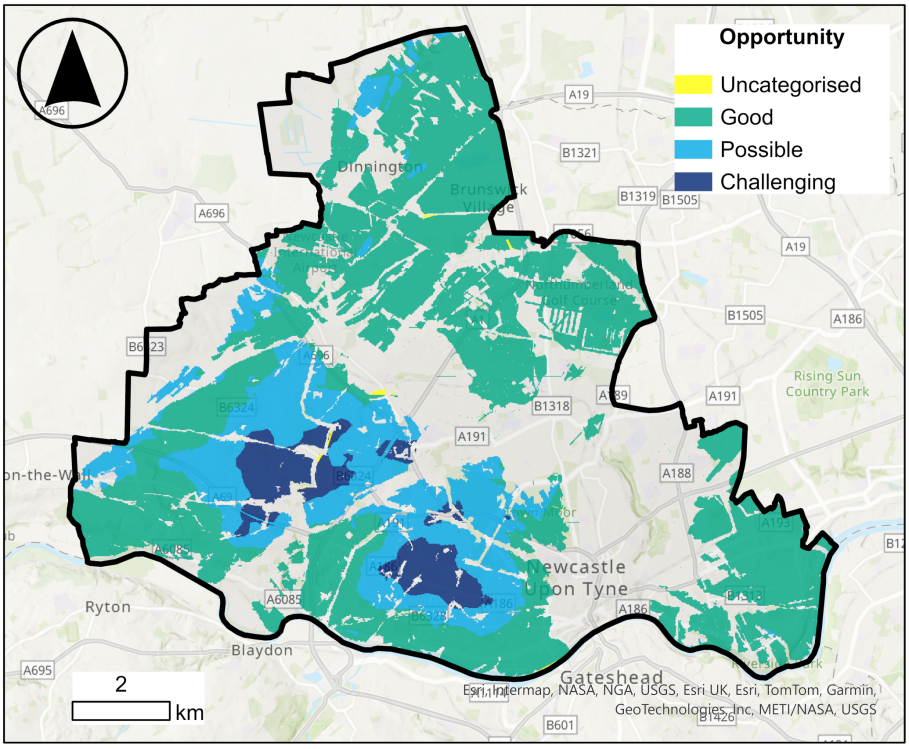

Figure 2.23: The final MWG opportunity map of Newcastle produced following the MRA method. Areas are divided into 'Good', 'Possible' and 'Challenging';'No opportunity' areas are not shown. 'Uncategorised' indicates where the decision tree did not return one of these categories, in this case due to slight misalignment between map layers. Reproduced with the permission of © The Mining Remediation Authority. All rights reserved.

2.3 Discussion

2.3.1 MiRAS

The final map produced using the MiRAS method identifies only a very limited area (Figure 2.7). Most of the study area has average mine working depths above 250 m (Figure 2.6), and the extent of multiple seams, even after shallow seams are excluded, is still much larger than the area shown in the final map (Figure 2.4). This indicates that the depth to mine water is the main factor constraining the size of the mapped area in this case (Figure 2.5).

The MiRAS method is clear, and although it does require data processing such as data interpolation (discussed in Sections 2.3.4 and 2.3.5), it is relatively easy to implement.

2.3.2 GRC, Geothermal Screening Assessment

The GRC assessment (Figure 2.15) highlights two areas suitable for MWGH, one where there is the highest heat demand (over 300 TJ km^{-2}) and mines between 16 and 19°C, and another where the deepest and hottest class of mine (19 - 23 °C) are co-located with an areas of heat demand between 120 - 300 TJ km^{-2}. Both of these area are close to the Tyne and Ouseburn, as are some optimal areas in the MiRAS final map (Figure 2.7). However this is because the areas of highest heat demand are close to the River Tyne, rather than the depth to the mine water, as in the MiRAS method.

The main advantage of the GRC method is its speed: it requires very little input data (only heat demand, mine depth and location, and an estimate of the geothermal gradient) and involves no raster calculations. Due to its simplicity it can be applied across wide areas. However, since it does not incorporate the technical detail captured by the other methods, its greatest value may lie in being simplified even further. By mapping only mine locations alongside heat demand, it could serve as a first-pass tool for identifying areas where there may be economically viable heat demand.

2.3.3 MRA, Mine Water Heat Opportunity Mapping

The MRA method identifies the widest area of 'opportunity' (Figure 2.23). This is because the MRA method is not just looking for the very best sites (the 'good' category), but also considers areas where MWG could be 'possible' or even 'challenging'. However, even when comparing just the 'good' category, the MRA map shows a larger area than the other methods.

There are several reasons for this in the Newcastle case study area. Overall, the parameters that are the same in both the MRA and MiRAS methods (e.g. depth to mine workings and overlapping seams) have more generous limits in the MRA method (Table 2.2). For example, the cut-off depth to the mines is 300 m bgl for the 'good' in the MRA method, but 250 m bgl in the MiRAS method. While the 'Good' category in the MRA requires overlapping seams, like the optimal areas in the MiRAS method, the MRA method allows for shallow seams, whereas the MiRAS method removes them (Figure 2.4). The differences in the depth to mine water also contribute to the greater area marked as a good opportunity (Figure 2.24), with the cut-off being <75 m bgl in the MRA method, but only <60 m bgl in the MiRAS method.

The MRA method includes more parameters than the other mapped methods and allows for more complexity. For example, by considering mine water recovery, areas in which the mine water is still recovering (rising) but may not yet be in the best <75 m bgl category can still be considered, as the water level may be shallower in the future.

2.3.4 Depth to mine water

In both the MiRAS and MRA mapping there are issues with the mine water depth map. While both maps (Figure 2.5 and 2.20) are made slightly differently, both rely on interpolating data points. The first issue is that there are a limited number of data points. There are only 8 within the Newcastle boundary (the rest are in the surrounding areas) and in the case of the MRA method (which builds a depth to mine water layer for each mine water block) some mine blocks had no direct data

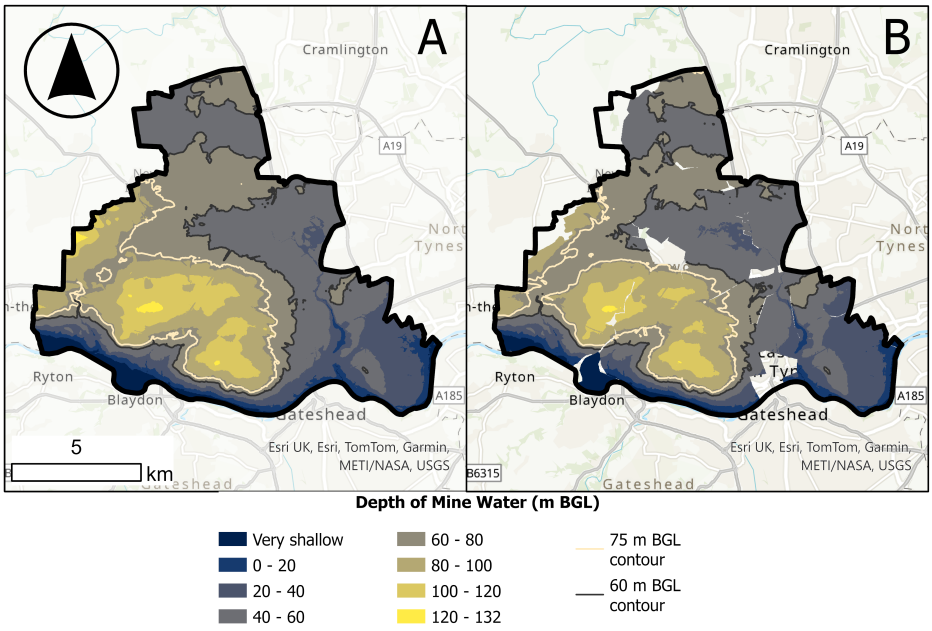

Figure 2.24: Comparison between the mine water level maps produced using the MiRAS method (A) and the MRA method (B). The optimal areas have depth to mine water of <65 m bgl in the MiRAS method and the 'good' areas in the MRA method have a depth to mine water of <75 m bgl. Reproduced with the permission of © The Mining Remediation Authority. All rights reserved.

at all (East Walbottle and Kenton).

Secondly, the data points were obtained by importing images of the maps from the individual mine block hydrological reports, georeferencing them, and manually adding the mine water heights (and other data). There may be errors in the georeferencing, although this error is unlikely to be significant in comparison to the size of the area being mapped.

Thirdly, the mine water depth surfaces in both methods had to be converted from AOD to bgl. This was done by subtracting the mine water surface from the DTM. There are areas in which the resulting mine water bgl depth would suggest that the mine water is above the ground level. This is most often around the rivers. The Blaydon mine water block has a greater preponderance of above ground level areas. This may be related to only having discharge points in this block. Having water about ground level was identified as an issue in the MiRAS workflow and was categorised as 'very shallow'.

The MRA method defines one of the opportunity ranking criteria as 'known mine water levels across mine water blocks', so for this method the water level was defined per block. This does lead to a difference in mine water depth between the MRA and MiRAS methods as shown in Figure 2.24. The MiRAS method used interpolation to create one surface across the whole area, whereas the MRA map was made by creating a surface for each mine block and joining them together. Comparing Figures 2.20 and 2.5, this is apparent as there are areas of no mine water level in Figure 2.20 which have values in the MiRAS method. However, this is accounted for by the inclusion of the worked seams (Figure 2.4) which removes the areas that have not been mined from the final map.

However, what appears to make more difference in terms of water level is the depth cut-off values used. In the MiRAS method no depths below 60 m bgl are considered optimal, in the MRA method the cut-off for 'good' opportunities is >75 m bgl. When looking at Figure 2.24, a larger area is available to be classed as good using the 75 m contour cut-off, than if the 60 m contour from MiRAS is used.

The depth to mine water is important for a mine water geothermal scheme because of the ongoing cost of pumping and the risk of surface flooding. During reinjection, the water level can rise, either locally around the reinjection point or on a more regional scale. This means that if the resting water level is too shallow, reinjection may cause new surface discharges (i.e., flooding) (Wieber and Stemke 2019; Banks et al. 2022). For this reason, the MiRAS method identifies areas with water depths of 20–60 m below ground level (bgl) as most optimal for open loop schemes with reinjection, and cautions that areas with water depth less than 20 m bgl may be more suitable for open loop schemes with discharge, depending on the transmissivity of the mine workings (Walls et al. 2024). On the other hand, the deeper the water level, the greater the ongoing pumping costs.

The cost of pumping can be calculated following Walls et al. (2021):

$$P = \frac{h\,\rho_w\,g\,q}{\zeta} \tag{2.1}$$

$$C_{£/\text{year}} = \frac{P\,t\,p}{100} \tag{2.2}$$

where P is the electrical power consumed by the pump (kW), h is the pumping head to be overcome (m), ρ_w is the density of water ($\mathrm{kg\,m^{-3}}$), g is gravitational acceleration (9.81 $\mathrm{m\,s^{-2}}$), q is the flow rate (50 $\mathrm{L\,s^{-1}}$), ζ is the pump efficiency (65%), $C_{£/\mathrm{year}}$ is the annual pumping cost, t is the number of hours the pump runs per year (assumed to be 3500), and p is the electricity price (25.94 $\mathrm{p\,kWh^{-1}}$ (National Statistics 2025)).

Using these values, pumping against a head of 50 m bgl (the best number in the Saxony methodology) results in an annual cost of approximately £29,000. A head of 60 m bgl results in an annual cost of approximately £41,000, a head of 75 m bgl corresponds to approximately £52,000, and heads greater than 100 m bgl lead to costs exceeding £68,000. Additionally, when abstracting water, the water level can draw down around the abstraction borehole (Wieber and Stemke 2019; Banks et al. 2019a; Banks et al. 2022), which increases the pumping head and therefore the cost of pumping.

2.3.5 Depth to mine workings

The depth to the mine workings is calculated differently in the MiRAS method than in the MRA or GRC methods.

The MiRAS method interpolates the mine depth (In seam level) together to form one, continuous surface. While this is quick and efficient using an average depth to mine workings, may misclassify areas as above or below the 250 m bgl cut-off. In principle, an area could contain two or more workings shallower than 250 m yet still have a higher average depth than 250 m bgl, if there are numerous deeper seams.

The document summarising the GRC method does not specifically state whether the 'mine depths' used are the maximum depths. However, in this replication each individual mine working is matched to its depth, to cover all possibilities.

The depths used in the GRC method are proxies form the mine water temperature (Figure 2.12). However, when the temperatures used are compared to those in operational mine water geothermal schemes (Peralta Ramos et al. 2015; Wang et al. 2024; Walls et al. 2021; Oppelt et al. 2025), the temperature ranges appear to be too high for widespread use. Most operating schemes use mine water temperatures

between 12 - 25°C. With a local geothermal gradient in Newcastle of 34.4°C km^{-1} and an average annual air temperature of 9 °C (Farr et al. 2021), 12°C is predicted at a depth of approximately 87 m bgl. This is substantially shallower than the ∼200 m bgl (16°C) cut-off in the method, and would significantly broaden the areas of potential.

In the MRA method, the depth to workings decision point has 4 options (Figure 2.2). The 'shallow workings only (<30 m bgl), with or without opencast workings', '>30 - 300', '300 - 500', and '>500'. It is not stated how many or what proportion of workings have to be within a category to determine the classification. Given that, in the text, it is stated that shallow workings can be mitigated for when drilling to deeper targets, it was decided that only when there are no workings deeper than 30 m should the '<30 m' be used. Additionally, as the text discusses, single seam exploitations, open loop with re-injection, and open loop with discharge, when there is ≥1 working between >30 - 300, the area goes into that category and this follows on for the deeper categories.

In comparison to the GRC method, significantly shallower mine depths are acceptable in the MRA method (>30 m vs ∼200 m). However, comparing the 'good' opportunities to MiRAS's optimal sites, the MiRAS cut-off is 250 m, vs the MRA 'good' cut-off of 30 - 300 m. The <250 m bgl cut-off leads to several portions along the western of the MiRAS map not being considered optimal, whereas in the MRA map, the same areas are all in the ideal >30 - 300 m bgl category. Additionally, in the MRA method, areas where there are <30 m seams are not removed, as they would be in the MiRAS method. This does not add a very large area, but the difference is noticeable when comparing Figures 2.4 and 2.17, particularly in the northwestern portion of the maps.

2.3.6 Comprehensive flowchart

The MRA methodology has the most parameters of the methods mapped, and provides a flowchart (Figure 2.2) to follow the series of decisions used to define the MWG opportunities available . However, with a highly parameterised methodology there is a risk that some plausible site-specific scenarios (i.e., edge cases that do not

fit neatly within the defined thresholds) are not captured. Some examples are given below.

- A single seam, shallower the 30 m bgl is not an option on the flowchart.
- The term 'extensive' is used to separate single seams (>30 m bgl) into two different groups, but the term 'extensive' is not defined in the published methodology. In this case study, the single seams were therefore treated as not 'extensive'. However, comparison of the map of single versus multiple seams (Figure 2.17) with the MRA output for Newcastle (Figure 2.25) suggests that these seams were treated as 'extensive' within the MRA. A subsequent clarification indicates that 'extensive' refers to workings with areas of $>\sim$8 km^2 (personal comm. Gareth Farr, 2025), based on the assumption that a seam thickness of $\sim$1 m, collapsed to 0.2 m, over an area of 8 km^2 could supply $\sim$60 L s^{-1} at ΔT of 5 K (approximately 1 MW of heat).
- Although the method requires flooded workings for both 'good' and 'possible' opportunities, the flowchart checks flooding only for single-seam workings. For multiple workings at >30-500 m, sites are classified as 'Possible' if opencast workings are present without considering mine water, and otherwise mine water is assessed only by water-level depth (<75 m bgl, 75-100 m, >100 m) rather than flooding status. This leaves an ambiguity: workings may be unflooded at depths >30 m while the mine water level still falls within the <75 m bgl category.
- A 'challenging opportunity' is defined as an area that is unfavourable for developing MWG and may not improve in the future. The text description classes areas where the mines are not flooded as 'challenging'; however, if the mines are not flooded then a mine water heat scheme is not possible and the area should be classed as 'no opportunities' rather than 'challenging'. While recovering mine water levels could flood currently dry workings in the future, the methodology states that the assessment should be revised every two years to account for this possibility.

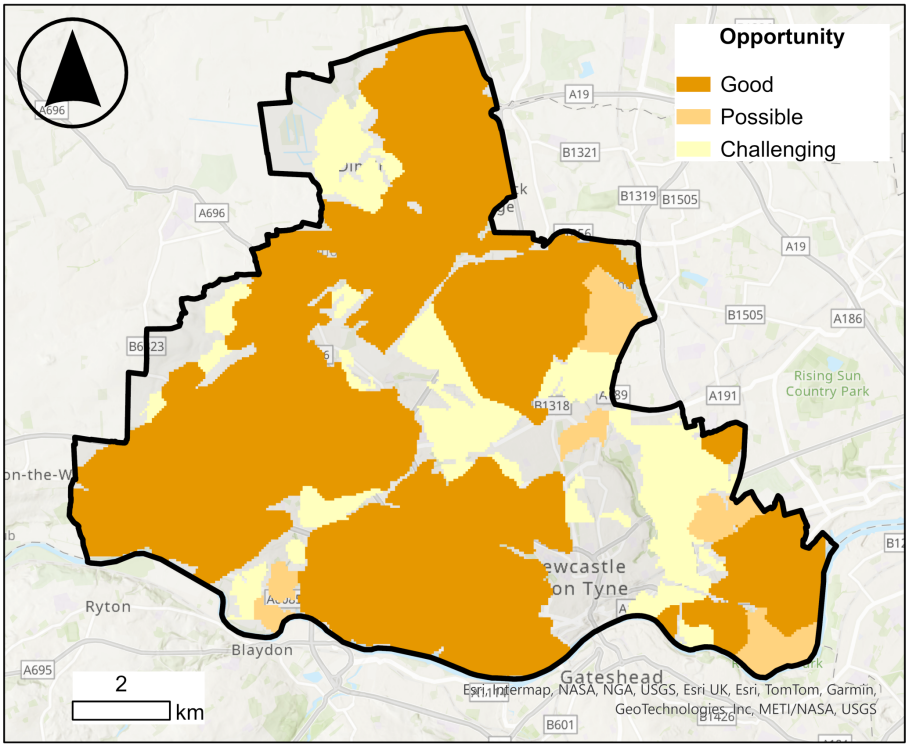

Figure 2.25: The opportunity map produced by the MRA for Newcastle (Coal Authority 2024e). Reproduced with the permission of © The Mining Remediation Authority. All rights reserved.

2.4 Conclusions

All three mapping methods highlight areas for mine water heating opportunities in the south-east of Newcastle, although the overall extent of the identified zones varies significantly. The inclusion of heat demand alters the most favourable localities, as do the cut-off values for mine depth and depth to mine water.

The lack of mine water level data is a source of uncertainty in all methods that use water level as a criterion (MRA, MiRAS and, if implemented, the Saxonian method). The collection of additional water level data would improve confidence in the outputs, particularly for mine blocks where values are currently missing.

Additional publicly available information on the cost of drilling into mine workings and on the cost of water pumping in operational mine water geothermal projects would be beneficial for validating the cut-off values used.

The MRA method produces not only a wider range of areas classified as 'good', due to more generous cut-off values, but also a substantially larger total area by dis-

playing less favourable sites as possible or challenging. The MRA method considers more complex situations than the other mapped methods, but the methodology could be improved with further clarifications.

The GRC method is most appropriate as a rapid, very high-level tool for comparing the presence of mine workings with heat demand. Its utility could be improved if an acceptable distance between heat demand and the most prospective mines could be defined.

The MiRAS method is reasonably straightforward to understand and implement but the use of an average depth to mine workings may lead to some misclassifications.

The Saxonian method is more detailed and would require considerably more time and data, although it has the potential to provide a more holistic assessment. Some parameters could be removed or redesigned to better reflect conditions in the United Kingdom, such as mine accessibility. Possible considerations for revised categories and data sources have been suggested in this chapter.

CHAPTER 3

The benefit of using dynamic rather than static heat assessment methods early in a mine water energy project

This chapter has been published by Geomechanics and Geophysics for Geo-Energy and Geo-Resources. The modelling and production of the manuscript were done by A. Sweeney who would like to acknowledge the useful discussions, training and support provided by her co-authors.

A. Sweeney, J. van Hunen, J. Mouli-Castillo, and J. Gluyas, "The benefit of using dynamic rather than static heat assessment methods early in a mine water energy project," Geomechanics and Geophysics for Geo-Energy and Geo-Resources, 2026. https://doi.org/10.1007/s40948-025-01099-y

Author Contributions

- A.S.: conceptualisation; data curation; formal analysis; investigation; methodology; project administration; validation; visualisation; writing – original draft; writing – review & editing.
- J.G.: writing – review & editing.
- J.M.-C.: software; writing – review & editing.

- J.v.H.: software; writing – review & editing.

3.1 Abstract

Mine water geothermal (MWG) heating offers a low-carbon solution for space heating, helping to reduce greenhouse gas emissions. To assess the feasibility of an MWG scheme, an estimate of extractable heat is required to size the system, to determine if it meets surface demand, and evaluate economic viability. In early project stages, where data are limited, static methods, such as geothermal heat flow, mine water volume, rock volume, and flow rate, are commonly used. However, these methods do not account for mine geometry.

GEMSToolbox is a streamlined dynamic model, purpose built for MWG, that operates with the same limited data as static methods but also incorporates digitised mine plans. It allows rapid modelling of scenarios such as roadway collapse and shaft treatments, and helps identify optimal injection and abstraction points.

We apply GEMSToolbox to a digitised two-seam coal mine and to a simplified synthetic grid model of similar size. The resulting dynamic heat estimates are compared with those from static methods, revealing order of magnitude differences, from 4,200 MWh to 210,000 MWh over 40 years.

Using dynamic modelling early in project development improves targeting of exploration wells, enables site-specific mitigation planning, and reduces uncertainty. GEMSToolbox offers a practical alternative to static methods, enhancing both technical confidence and investment readiness in MWG projects.

3.2 Introduction

The decarbonisation of space heating is vital for reducing greenhouse gas emissions. In the EU 40 % of energy consumed is for space and water heating (Zeyen et al. 2021). Mine water geothermal (MWG) offers a low-carbon solution for space heating in buildings located near abandoned and flooded mines (Monaghan et al. 2022; Oppelt et al. 2022; Chu et al. 2021; Oppelt et al. 2025; Walls et al. 2021; Banks

et al. 2022; Verhoeven et al. 2014; Jessop et al. 1995). Since the presence of coal drove economic development and therefore the growth of towns and cities near coalfields (Fernihough and O'Rourke 2021), there is now a significant and under-utilised resource of warm mine water located near population centres. These flooded mine workings are predominantly heated by the geothermal heat flux from Earth's primordial heat and radiogenic decay of minerals in the crust (Monaghan et al. 2025). There are additional inputs from solar heat (0 - ∼20 m BGL) and exothermic geochemical reactions (Monaghan et al. 2025). The geothermal gradient in British coal fields varies between 17.3 and 34.3°C km^{-1}, with the median being 24.1°C km^{-1} (Farr et al. 2021). In the UK, the Mining Remediation Authority estimates that a quarter of homes and businesses are located above coalfields (North East LEP Mine Energy Taskforce 2024). When considering the use of a MWG system, one of the first questions to address is how much heat is present and accessible within the mines. This question is critical for investors, whether local authorities, private companies, or other organisations, to determine the feasibility of MWG systems and whether the potential heat supply justifies the financial and operational risks of developing a MWG scheme (Ciriaco et al. 2020). This is particularly important because, like other forms of geothermal energy extraction technologies, MWG typically involves high upfront capital costs (Townsend et al. 2020; Walls et al. 2023).

In the early stages of exploration, and before any drilling has taken place, there is often very limited information available regarding the current state of old abandoned mines or groundwater flow (Watzlaf and Ackman 2006; Whittington et al. 2025). In some cases, further information cannot be obtained without drilling, as geophysical methods may be unsuitable for urban environments, or incapable of producing reliable results at the relevant depths and scales (Kearey et al. 2002), since useable mine cavities are often only a few metres wide and can be >1000 m below ground level (bgl) in the UK (Wyatt et al. 2025).

Consequently, initial estimates of useable heat must rely on sparse data, typically just mine plans and published literature, such as geothermal gradients and porosity data. Several methods exist for estimating the thermal potential of mine systems, which can be broadly divided into static and dynamic approaches (Tian et al. 2024).

Static methods are simpler, relying on straightforward mathematical calculations that do not consider the response of the reservoir to heat extraction (Shah et al. 2022). In contrast, dynamic methods use modelling to consider temporal effects, such as heat depletion and recharge, and can incorporate the geometry of the mines, which influences heat accessibility (Chu et al. 2021; Tian et al. 2024).

We propose that our streamlined dynamic modelling approach (GEMS Toolbox) offers a practical alternative to static estimation methods commonly used in the early stages of mine energy project development. While traditional dynamic models are typically applied later due to their high data requirements, computational cost, and runtimes in the order of hours to weeks, our approach offers runtimes in the order of seconds to hours and is compatible with early-stage data constraints. Using the same limited input data as static methods, it enables scenario testing based on actual mine geometry, allowing users to explore conditions such as roadway collapses, additional shafts, or different well configurations. This capability supports early uncertainty reduction, proactive mitigation planning, and more targeted exploration. To assess its performance, we compare our approach with several static estimation methods using both digitised coal mine plans from County Durham, UK, and a synthetic grid-based representation of the same site. The modelled mine follows a room-and-pillar layout with no backfill and the heat recovery system is simulated as an open loop system with reinjection (Figure 3.1).

3.3 Methods

To allow for a robust comparison between the different methods of heat estimation all methods were tested on the same section of mine workings. The demonstrator area is a section of a room and pillar coal mine underneath the city of Durham, UK. It covers a section of the Hutton Seam, part of Elvet Colliery, and Busty Seam, part of Littleburn Colliery. The coal is part of the Pennine Coal Measures Formation, deposited between 318 and 309.5 Ma (British Geological Survey 2025). This area is used as data has already been secured for a previous study (Mouli-Castillo et al. 2024). Goaf areas (collapsed workings) are excluded from the analysis.

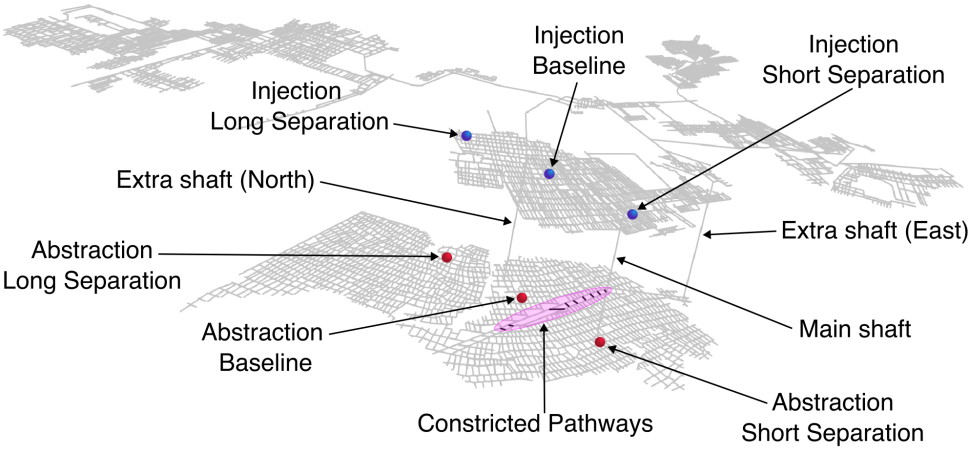

Figure 3.1: Digitised mining map showing the different geometric variables that were tested: additional shafts, alternate injection and abstraction sites, areas of constricted pathways. The upper seam is the Hutton, and the lower seam is the Busty. Width of the model is approximately 1500 m and there is a 72 m separation between the seams. Reproduced with the permission of © The Mining Remediation Authority. All rights reserved.

In these sections, longwall mining or pillar robbing has caused roof failure and left extensive debris. Since we are proposing an open loop system the artificially induced flow field that will develop will prioritise areas of the mine with no obstruction, hence goaf areas experience negligible flow. The maps are accessed from the Mining Remediation Authority (catalogue number 5161 and 11562) and are georeferenced and digitised.

The depths of the two seams are taken from borehole data available using the BGS borehole viewer. Constant, year-round, heat extraction over 40 years was modelled. This assumption is made because the study is concerned with long-term heat availability rather than shorter-term or seasonal variations. The decline in reservoir temperature is governed primarily by the total amount of heat removed, whether this extraction is distributed throughout the year or concentrated into a shorter operating period. After this 40-year period, the infrastructure (e.g., pumps, heat exchangers, etc.) is assumed to require replacement.

In both the digitised mine plans and the synthetic grid set up, water is abstracted

from the deeper, warmer seam (the Busty Seam in the digitised mine plans, 13.6 °C) and re-injected into the shallower, colder seam (Hutton Seam, 11.1 °C).

All of the methods used and scenario variants investigated are listed in Table 3.1.

Table 3.1: Summary of modelling approaches and scenario variants used in this study. The table distinguishes simple static heat-resource estimates from dynamic GEMSToolbox simulations based on mine plans and an idealised synthetic grid, and briefly describes the purpose of each scenario.

Model	**Description**
	Static
Geothermal Heat Flow	Heat supplied only by background geothermal flux across the mined footprint.
Volume of Water in Mines	Heat stored in the water currently filling the mine voids.
Rock Volume	
No Porosity	Heat stored in a solid rock block with no pore space or water.
Mine Void Porosity	Heat stored in rock plus water in mining-induced voids only.
Matrix Porosity	Heat stored in rock including only matrix porosity of the Pennine Coal Measures.
Combined Porosity	Heat stored in rock and water using both matrix and mining-induced porosity.
	Dynamic - GEMSToolbox
Mine Plans	
Baseline Map	Dynamic model using the digitised mine layout and current shaft configuration.
Long Separation	Wells placed further apart to increase flow path length through the mine.
Short Separation	Wells placed close together to test short-circuiting of cold reinjected water.
Extra Shaft (North)	Scenario with an extra northern connecting shaft opened between seams.
Extra Shaft (East)	Scenario with an extra eastern connecting shaft opened between seams.
Dual Extra Shafts	Scenario with both additional shafts open simultaneously.
Constricted Pathways	Selected galleries narrowed to represent collapse and constricted flow pathways.
Synthetic Grid	Dynamic model of an idealised two-seam grid mine matching the real mine's size and flow path length.

3.3.1 Static Modelling

This section presents the different static modelling methods that will be compared against the dynamic method in this work. In geoenergy, the term volumetric is often used rather than static, however, one of the methods we investigate is independent of geology, and there is no volume, so static is used instead of volumetric. The different static methods evaluated are: "geothermal heat flow", "water volume in the mine voids", "rock volume", and "flow rate". When the methods require an amount of heat to be removed, ΔT, 5.6°C is used. This is the difference between the temperature of the abstracted water (in the static method, this is the temperature of the Busty Seam, 13.6 °C, which is effectively the reservoir) and the injection temperature (which is the same in the dynamic modelling), 8 °C (Table 3.2).

Geothermal Heat Flow

Geothermal heat flow is the amount of heat transferred over an area from the Earth's interior. The sources of this heat are secular cooling of the Earth and the decay of long-lived radiogenic isotopes. To calculate the useable heat the geothermal heat flux can be multiplied by the area of the mined zone being considered for heat extraction (Equation 3.1) (Todd et al. 2019; Gillespie et al. 2013). In this case, the area corresponds to the union of the Busty and Hutton Seams in plan view. Since these seams overlap vertically, their combined footprint is not the sum of their individual areas. Although geothermal heat flux varies throughout the UK (Farr et al. 2021), a value of 65 $\mathrm{mW, m^{-2}}$, representing the average continental crustal heat flux, is used here (Todd et al. 2019).

$$Q = 10^{-6} q_H A_a \tag{3.1}$$

Where Q is the useable heat extraction rate, in MW, q_H is the geothermal heat flux, $\mathrm{W\,m^{-2}}$, and A_a is the aerial view mine area, $\mathrm{m^2}$. All parameters used in this and subsequent equations are used in Tables 3.2 and 3.3.

Volume of Water in Mine Voids

The amount of available heat in the water contained within the mine voids is calculated by taking the total length of the digitised mine voids and multiplying this by the cross-sectional area of the rooms (3.97 m^2) (Mouli-Castillo et al. 2024) to produce a volume of water. 5.6 °C is removed from the water to produce the useable heat (Equation 3.2).

$$Q = 10^{-6} \frac{V_m \rho_w c_w \Delta T}{t} \tag{3.2}$$

Where V_m is the volume of water in the mine voids, m^3, c_w is the heat capacity of water (assumed equal to that of pure liquid water), $J\,kg^{-1}K^{-1}$, ρ_w is the density of water, $kg\,m^{-3}$, ΔT is the difference in water temperature before and after heat removal, K, and t is the heat extraction period in seconds.

Rock Volume

Rather than considering only the useable heat within the water-filled mine voids, the heat stored in the surrounding rock mass can also be estimated (Gillespie et al. 2013). To do this, the volume of the rock contributing heat must first be determined. This volume is calculated by multiplying the surface area of the mined zone (as seen from above) by the effective distance over which heat can be transferred from the rock. The extent of this heat extraction distance is given by Equation 3.3:

$$\Delta x_h \propto \sqrt{tK} \tag{3.3}$$

Where Δx_h is the heat diffusion length, m and K is the diffusivity coefficient of sandstone, $10^{-6} m^2 s^{-1}$. This produces in a distance of 35.5 m. Therefore the rock volume is calculated by Equation 3.4:

$$V_r = 2\Delta x_h \left(A_b + A_h\right) \tag{3.4}$$

Where V_r is the rock volume, m^3, A_b is the area of the Busty seam, m^2, and A_h is the area of the Hutton seam, m^2. This makes the assumption that, as in this case, the two seams are further apart than $2\Delta x_h$. If this were not the case, the equation

would need to be modified, so that any vertically overlapping area is not counted twice. The heat in this block is calculated:

$$Q = 10^{-6} \frac{V_r \rho_r c_r \Delta T F}{t} \tag{3.5}$$

Where ρ_r is rock density $\mathrm{kg\,m^{-3}}$, c_r is rock heat capacity, $\mathrm{J\,kg^{-1}K^{-1}}$, F is the recovery factor.

It is not possible to extract all of the heat in the reservoir, the recovery factor compensates for this (Ciriaco et al. 2020). The recovery factor is the ratio of the thermal energy extracted at the surface to the total thermal energy contained within the reservoir. The recovery factor accounts for physical and geological variables not explicitly included in the method (Ciriaco et al. 2020), such as effective porosity and permeability (Williams et al. 2008). It also reflects that due to the diffusive nature of thermal conduction, the entire reservoir will not cool uniformly to the injection temperature. Instead, heat extraction will be localised near the flow paths, and volumes of rock may remain unexploited.

$$F = \frac{Q_e}{Q_t} \tag{3.6}$$

Where Q_e is the rate of heat extracted at the surface, and Q_t is the total rate of heat theoretically in the reservoir. A recovery factor of 0.1 was used (Ciriaco et al. 2020; Grant 2014).

Equation 3.5 does not consider the effect of any porosity within the block of rock, but mines are known to have several different types of porosity (Andrés et al. 2017). To account for porosity effects in the rock mass and mine voids, three porosity scenarios were evaluated in addition to a zero porosity scenario. The first scenario used a matrix porosity of 0.14, based on average values for sandstone in the Pennine Coal Measures (Mallin Martin and Smedley 2021). The second assumed fully open mine voids with a porosity of 1.00, and no porosity in the rock mass surrounding the mine workings. Given that the mines make up a very small proportion of the total volume of the block, this corresponded to an effective bulk porosity of 0.004. The third scenario incorporated both the mine void and the matrix porosity in the

surrounding rock mass (Pennine coal measure porosity) using a volume-weighted average, resulting in a combined bulk porosity of 0.1435 (Equation 3.7).

$$\phi_c = \frac{V_r - V_m}{V_r}\phi_p + \frac{V_m}{V_r}\phi_v \tag{3.7}$$

Where ϕ_c is the combined porosity, ϕ_p is the porosity of the Pennine coal measures, ϕ_v is the porosity of void space. The calculation of the useable heat extraction rate, Q, from the rock volume including the water is:

$$Q = 10^{-6}\frac{\left[\phi\rho_w c_w + (1-\phi)\rho_r c_r\right] V_r \Delta T F}{t} \tag{3.8}$$

Where ϕ is porosity.

Flow Rate

Where there is an anticipated flow rate the useable heat extraction rate, Q, can be calculated using the flow rate, specific heat capacity of water and the reduction in the temperature of the water (Equation 3.9) (Gillespie et al. 2013). An abstraction flow rate of 25 L s^{-1} was used as a representative value of a medium scale mine water scheme (Walls et al. 2021; Gillespie et al. 2013; Banks et al. 2022).

$$Q = 10^{-6} c_w \, q_F \, \Delta T \tag{3.9}$$

Where q_F is the flow rate L s^{-1}.

3.3.2 Dynamic Modelling

The dynamic modelling uses GEMSToolbox (Mouli-Castillo et al. 2024). It is a middle ground between large, detailed, 3D numerical models and simple analytical models. To achieve this the code is purpose-designed for MWG allowing it to make additional assumptions in terms of processes and geometry that conventional multi-physics software do not do. It is designed to be used at the feasibility stage when the main data available are mine maps and generic rock properties.

GEMSToolbox models a flooded mine as a network of pipes (galleries/room-

Table 3.2: Geometrical parameters. The 'Method' column indicates which of the modelling approaches described use each variable. The numbers may appear singly or in combination. Geothermal Heat Flow = 1, Volume of Water in Mine Voids = 2, Rock Volume = 3, Flow Rate = 4, Dynamic Modelling with GEMSToolbox = 5, A for the just the synthetic grid. *The Busty and Hutton areas include a 35.5 m lateral buffer around each seam perimeter, corresponding to the thermal diffusion length (Equation 3.3), representing the zone of surrounding rock from which heat is assumed to be accessible laterally from the mine. References: [c],Mouli-Castillo et al. 2024, [d] Farr et al. 2021, [e], Todd et al. 2019, [f], Mallin Martin and Smedley 2021, [g], Ciriaco et al. 2020; Grant 2014.

Variable	**Symbol**	**Value**	**Unit**	**Method**
Useable heat extraction rate	Q		MW	
Busty area *	A_b	690,000	m^2	3
Hutton area *	A_h	1,500,000	m^2	3
Aerial view mine area	A_a	1,900,000	m^2	1
Total seam area		2,200,000	m^2	5A
Distance between seams	x_s	72.46	m	5
Default room diameter[c]		2.25	m	2, 5
Diffusion length	Δx_h	35.5	m	3
Flow rate	q_F	25	$L\ s^{-1}$	4, 5
Geothermal gradient[d]		34.3	$°C\,km^{-1}$	5
Geothermal heat flux[e]	q_H	65	$mW\,m^{-2}$	1
Heat removed	ΔT	5.6	°C	2 3 4
Injection temperature		8	°C	5
Mean water reservoir temperature	T_w	13.6	°C	2 3 4
Combined porosity	ϕ_c	0.1435		3
Porosity of void space	ϕ_v	1		3
Porosity of Pennine coal measures[f]	ϕ_p	0.14		3
Rock volume	V_r	160,000,000	m^3	3
Recovery Factor[g]	F	0.1		3
Time	t	40	years	2, 3, 4, 5
Volume of water in the mine voids	V_m	640000	m^3	2 3

Table 3.3: Physical parameters. The 'Method' column indicates which of the modelling approaches described use each variable. The numbers may appear singly or in combination. Geothermal Heat Flow = 1, Volume of Water in Mine Voids = 2, Rock Volume = 3, Flow Rate = 4, Dynamic Modelling with GEMSToolbox = 5. Reference [a] refers to Carslaw and Jaeger 1959, [b] refers to Rodríguez and Díaz 2009.

Variable	**Symbol**	**Value**	**Unit**	**Method**
Diffusivity coefficient[a]	K	10^{-6}	$\mathrm{m^2\,s^{-1}}$	3
Rock density[b]	ρ_r	2500	$\mathrm{kg\,m^{-3}}$	3 5
Rock heat capacity[b]	C_r	800	$\mathrm{J\,kg^{-1}\,K^{-1}}$	3 5
Water density[b]	ρ_w	1000	$\mathrm{kg\,m^{-3}}$	2 3 4 5
Water heat capacity[b]	C_w	4186	$\mathrm{J\,kg^{-1}\,K^{-1}}$	2 3 4 5

s/roadways) and nodes (crossroads/wells). The network geometry can be built directly from digitised mine plans or from a simplified grid layout. For a given configuration of abstraction and reinjection wells, the tool first solves a steady-state hydraulic problem to obtain flow rates, hydraulic heads, and travel times in all galleries, using standard pipe-flow equations with head loss. These flows are then used to calculate how heat is exchanged between the mine water and the surrounding rock over time. Semi-analytical solutions are used for advective–conductive heat transfer along each gallery, including radial exchange around individual workings and additional planar terms to capture thermal interference between neighbouring galleries. Each scenario is defined through a small set of input files describing the geometry, rock and water properties, and operating conditions, and the model outputs time series of temperatures and flows together with fields suitable for visualisation (Mouli-Castillo et al. 2024).

Mine Plans

GEMSToolbox was applied to a section of the abandoned mine workings beneath the city of Durham, UK. The mine plans do not show any shafts connecting the two seams in the vicinity. However, the Mining Remediation Authority data shows that there are shafts in the area. Post mine closure shafts may have been 'treated'. This treatment can vary from being capped with planks of wood, to completely filled with concrete. One of the shafts identified is not confirmed to be filled in, so for this

comparison it is considered open and is implemented in the model.

Injection and abstraction wells are usually placed relatively close together on the surface to minimise surface infrastructure. Therefore, areas where the two seams overlapped are targeted and paired injection and abstraction wells that are laterally close to one another, but on different seams are created. Three different well pairs are selected: a close pair, 34 m from pair to shaft, a medium pair, 224 m from pair to shaft, and a far pair, 478 m from pair to shaft (Figure 3.1). These well pairs are all run for 1, 5, 10, 20, 40 years. They are referred to as Short Separation, Baseline Map, and Long Separation respectively.

Due to the inherent uncertainty surrounding the current state of the flooded mines, it is important to evaluate how deviations from the expected mine architecture could influence system behaviour. For instance, deterioration of supporting pillars may lead to a reduction in the size of mine voids. Additionally, there may be uncertainty regarding the precise locations of mine shafts and the nature of their treatment. The impact of these uncertainties on extractable heat can be explored through dynamic modelling.

To investigate the impact of uncertain shaft configurations, three scenarios are developed by introducing two hypothetical shafts: (1) 'Extra shaft (North)', (2) 'Extra Shaft (East)', and (3) both extra shafts, 'Dual Extra Shafts'. Separately, to assess the effects of reduced void space, the diameters of rooms are reduced to 1 m (Figure 3.1). This area of reduced void space is located in the flow path in between the injection and abstraction wells, and there are very few galleries/roadways aligned in this orientation (parallel to flow), see Figure 3.1. A reduction in diameter, for example due to roof subsidence (Malolepszy 2003), could alter flow paths and therefore affect the abstraction temperature, making it an important scenario to test.

Synthetic Grid

Rather than inputting the digitised geometry of mine workings into GEMSToolbox a simplified synthetic grid can be created within the software. Using a synthetic grid can avoid the laborious and time consuming step of digitising the mine plans

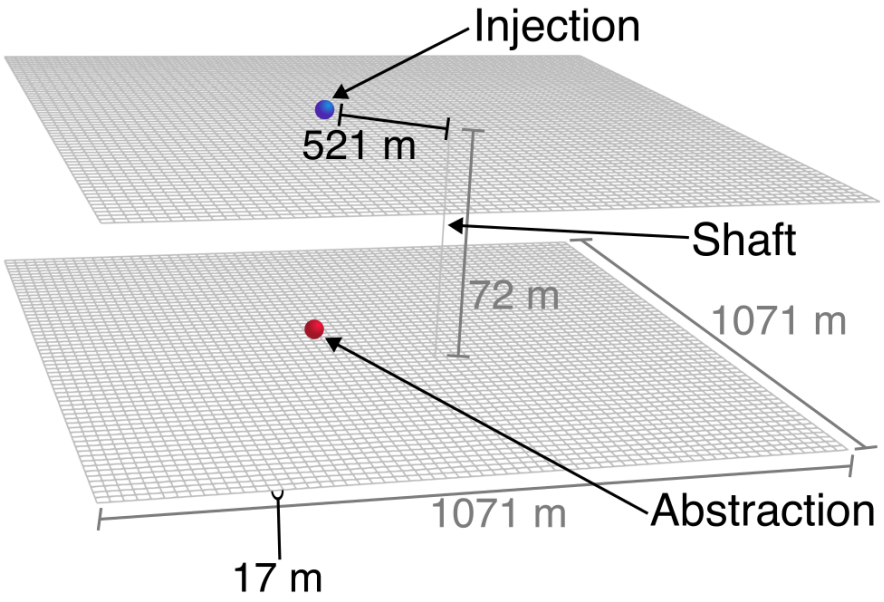

Figure 3.2: Synthetic grid model layout.

and removes the need for GIS software as the data needed can be measured directly off the plans.

In this case a square, two seam, synthetic mine is created with the same total area and number of seams as in the mine plans (Figure 3.2). The distance between each crossroad intersection is 17 m, which is the average distance taken from the mine plans. The flow path from the injection well to the shaft and then to the abstraction well is identified and measured on the Baseline Map, resulting in a total distance of 521 m. This distance is then replicated in the synthetic mine, which is run for 1, 5, 10, 20, and 40 years.

3.4 Results

All methods evaluated in this study use a consistent temperature difference (ΔT) of 5.6 °C based on the assumed initial temperature of the Busty Seam, 13.6 °C, and an injection temperature of 8 °C. Each system is modelled to operate continuously over a 40-year period. The results presented here are intended to illustrate the performance of each method within the specific context of the study area and should not be interpreted as universally applicable. They are valid for the room and pillar

mining sections of the Durham coalfield that are the focus of this analysis.

3.4.1 Static modelling

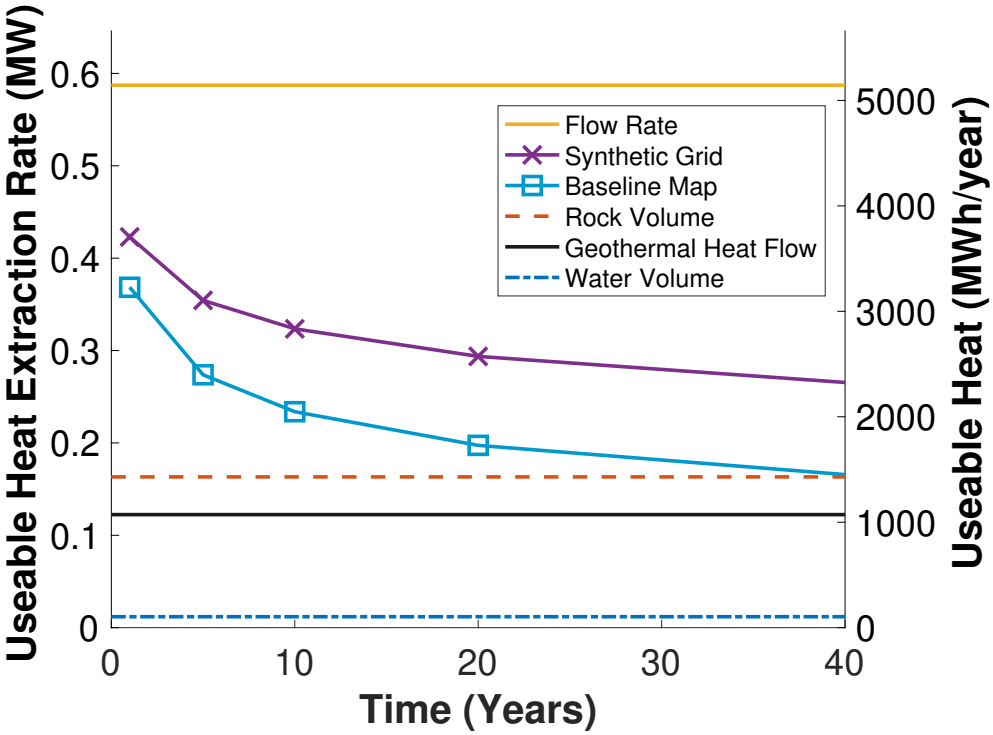

Figure 3.3: Useable heat per year calculated using different methodologies. The left Y axis shows the rate of heat being produced, the right Y axis shows the amount of heat being produced per year.

Geothermal Heat Flow

The geothermal heat flow results in low useable heat, producing approximately 0.12 MW and a total of 43,000 MWh over 40 years (Figure 3.3).

Volume of Water in Mine Voids

The volume of water in the mine produces the least useable heat (Figure 3.3), with heat extraction of approximately 0.012 MW and a total of 4,200 MWh over 40 years.

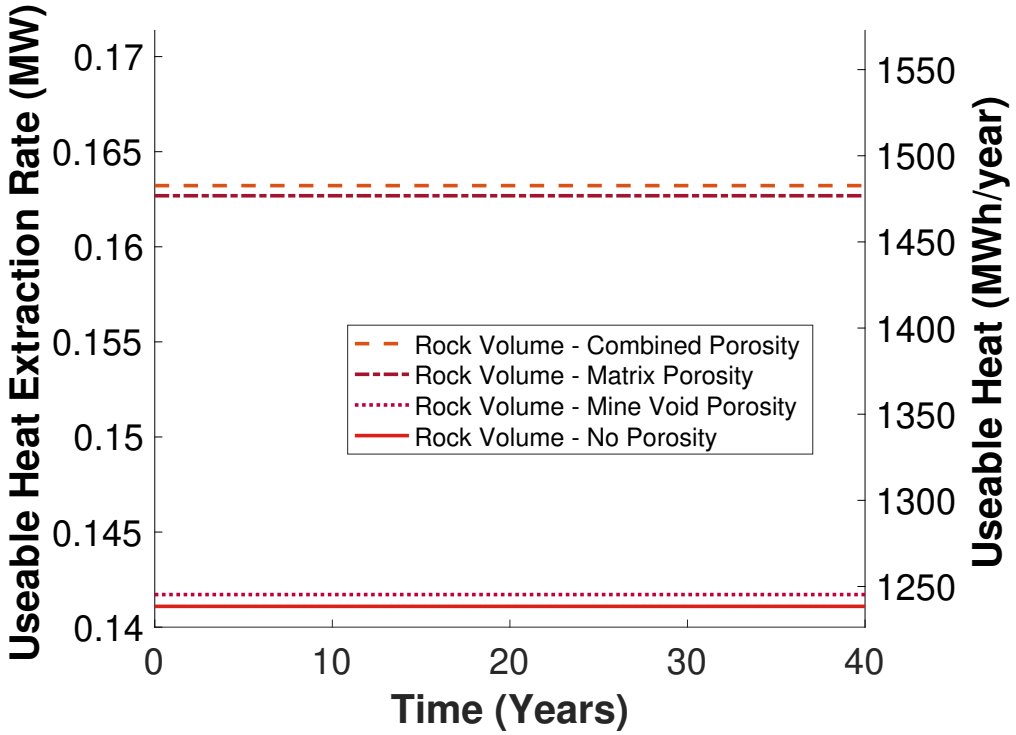

Figure 3.4: Useable heat per year calculated using the rock volume method with different porosity values. Note the y-axis is from 0.14 to 0.17 MW. This shows that the porosity does not significantly impact the ranking of the heat estimate relative to the other methods explored.

Rock Volume

The rock volume method estimates that there is more useable heat than the water volume and geothermal heat flow methods, but it is still lower than both the dynamic modelling methods and the flow rate method. The rock volume method yields 0.16 MW (Figure 3.3), with a total useable heat of $57,000$ MWh. This approach considers the porosity generated from mining activities as well as the primary porosity of the rock (combined porosity in Figure 3.4). Additionally, scenarios that assume no porosity, only mining-induced porosity, and only primary rock porosity are tested, resulting in a heat extraction rate of 0.14, 0.14, and 0.16 MW, respectively.

Flow Rate

The highest amount of useable heat is indicated by the flow rate method, which produces 0.59 MW and a total of $210,000$ MWh over 40 years. This is over 3.5 times

greater than that produced from the Rock Volume method, and approximately 1.5 times greater than the Synthetic Grid model predicts as the maximum useable heat (Figure 3.3).

3.4.2 Dynamic modelling

Both dynamic modelling methods show a similar pattern, with the highest heat extraction occurring in the first year and gradually decreasing over time. In the Baseline Map setup, useable heat extraction rate starts at 0.37 MW in the first year. By year 5, the rate declines to 0.27 MW, and by year 10, it further decreases to 0.23 MW. The sharp decline in extraction during the first 5 years transitions into a more gradual decline at longer timescales (20–40 years), reaching 0.17 MW at 40 years. The total useable heat in the Baseline Map setup is estimated by integrating the heat availability curve which produces 73, 000 MWh.

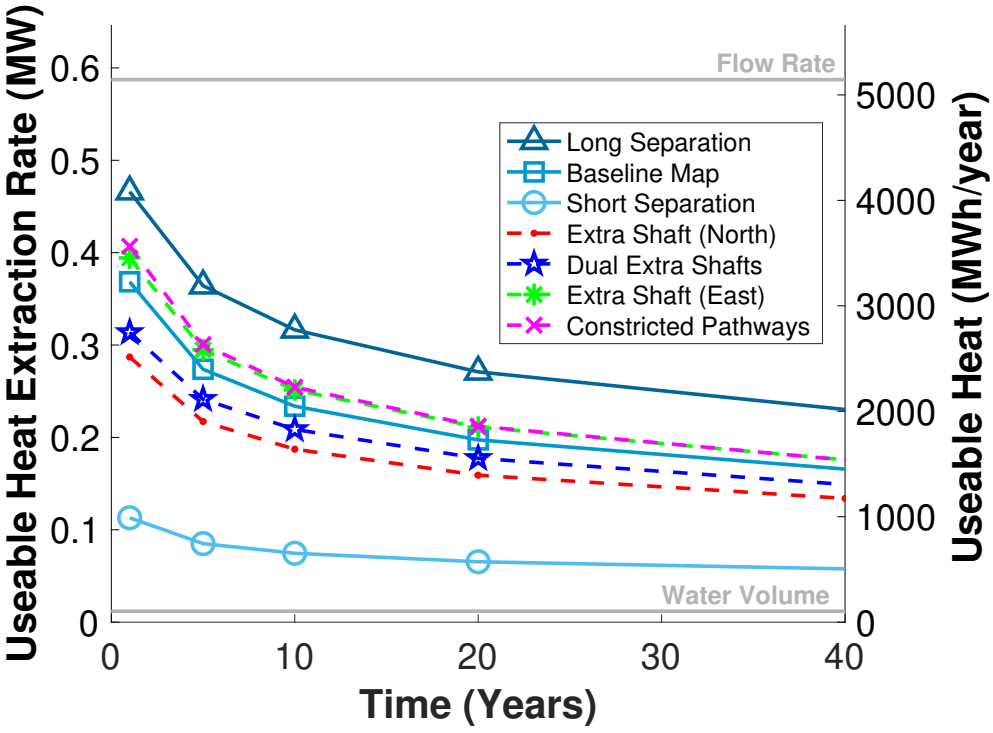

Figure 3.5: Available heat per year produced by different digitised map model set ups.

Similarly, the Synthetic Grid model also exhibits a decreasing trend, though with a slightly different pattern. At year 1, it starts at a lower value of 0.42 MW,

but remains relatively close to the Baseline Map. The useable heat extraction rate decreases more gradually than in the Baseline Map, reaching 0.35 MW at 10 years and ending at 0.27 MW at 40 years. The total useable heat is 100,000 MWh.

Figure 3.5 demonstrates the ability of modelling to test different potential injection and abstraction setups and the effect of additional connecting shafts. All results follow the same pattern, showing a reduction in useable heat over time.

Moving the injection/abstraction point further away (Long Separation) produces a higher useable heat extraction rate at all timescales, starting at 0.47 MW and ending at 0.23 MW at 40 years. Conversely, moving the injection/abstraction point closer (Short Separation) results in consistently lower heat extraction values, with 0.11 MW at 1 year and 0.058 MW at 40 years.

Adding additional connecting shafts can result in either lower or higher useable heat values. The Extra Shaft (North) setup modifies the system by introducing an extra connecting shaft (Figure 3.1). At 1 year, the useable heat extraction rate is lower than the standard Baseline Map, measuring 0.29 MW, and decreases to 0.13 MW. On the other hand, adding a shaft in a different location, Extra Shaft (East), results in higher useable heat extraction rate. At year 1, it is 0.39 MW, and by 40 years, it is 0.18 MW.

The Dual Extra Shafts setup combines both Extra Shaft North and East into a single configuration, resulting in three shafts in total. The rate of useable heat output begins at 0.31 MW at 1 year, consistently remaining below the Baseline Map setup, but above Extra Shaft (North), and ending at 40 years at 0.15 MW.

Changing the diameters of the rooms (or shafts, or roadways) can affect the flow pathways in the mine and affect the heat output, as shown in Figure 3.5 by the Constricted Pathways line. In this case, the diameter is reduced to 1 m (Figure 3.1), and the rate of heat output for year one increases to 0.41 MW in comparison to the Baseline Map, and remains higher than the Baseline Map at 40 years, reaching 0.18 MW.

3.5 Discussion

3.5.1 Geothermal Heat Flow

Using this method, the amount of useable heat over the mined area is directly dependent on the geothermal heat flux value applied. Here we used the average continental value of 65 $\mathrm{mW\,m^{-2}}$, but this value does vary depending on location. For example, to the North West of the Durham test area lies the North Pennine Batholith (Bott and Smith 2018), where there is locally higher crustal radiogenic heat production which increases the heat flux to up to 99 $\mathrm{mW\,m^{-2}}$ (British Geological Survey 2024b). However, the local geothermal gradient reported by Farr et al. 2021 validates the use of 65 $\mathrm{mW\,m^{-2}}$ as a reasonable representative value.

Low values such as $1,100$ MWh $\mathrm{y^{-1}}$ (Figure 3.3) are to be expected, because this approach effectively restricts heat extraction to the background geothermal heat flux and does not draw on the finite stored heat in the mine–rock system, or consider other forms of recharge (O'Sullivan et al. 2010; Axelsson et al. 2015). For comparison, the average UK household requires a space-heating load of 18 $\mathrm{Wm^{-2}}$ (Fraser-Harris et al. 2022), versus a geothermal heat flux of 65 $\mathrm{mWm^{-2}}$ (Todd et al. 2019). Under such a constraint, the mine footprint would need to be roughly 280 times larger than the heated floor area. This calculation should therefore be interpreted as the minimum heat available (Raymond and Therrien 2008), and a conservative theoretical estimate of the background recharge rate to compare other methods against.

3.5.2 Mine Void Water Volume

The first step in this method is to estimate the volume of water in the mines. Here we estimate this volume from the digitised mine plan, but there are alternate methods. If there are records of the mass of coal extracted, this can be multiplied by the density of coal to produce a volume (Jessop et al. 1995). This method requires very little waste rock to be extracted, or the amount of waste rock must be known (Malolepszy 2003). In addition, there can be variations in the density of the coal (Younger and Adams 1999) and the production figures must link to the specific section of the mine

being investigated. The other option is to estimate the mined area of each targeted seam and multiply by the corresponding seam thickness (Jessop et al. 1995).

This method does not access any heat stored in the surrounding rock, which is why the rate of heat extraction is relatively low, 0.012 MW.

3.5.3 Rock Volume

This method calculates the amount of heat contained in the block of rock surrounding the mine and applies a recovery factor to estimate the amount of heat that can be practically extracted.

The recovery factor used to determine the practically extractable heat is strongly influential on the amount of heat estimated to be available. There is a wide variation in recovery factors used ranging from 0 to 0.5 (Ciriaco et al. 2020), where 0 means no is heat recoverable from the reservoir, and 0.5 means 50 % of the heat in the reservoir is extractable at the surface. A value of 0.25 is commonly used but it appears to be too high compared to values reported from operating fields (Ciriaco et al. 2020; Grant 2014). A recovery factor of 0.1 is used to reflect observed results (Grant 2014). However, while reported values are from various types of geothermal reservoir none are specific to mine water reservoirs. This recovery factor accounts for the fact that not all of the heat in the system will be recoverable, but currently it cannot reflect the actual reservoir being investigated and it is therefore difficult to establish if a realistic value has been selected. In the future, it would be valuable to assess recovery factors directly from operational mine water projects to provide more representative estimates.

As shown in Figure 3.4, variations in porosity directly influence the resulting heat output. This is because the pore volume is assumed to be water-filled. For the same temperature difference, the heat contained in that volume is solely governed by the specific heat capacity times density. The ratio of those terms for rock to water is 0.48. This indicates that for a constant volume and temperature difference a volume of rock contains 48 % less heat than the equivalent volume of water. (Table 3.3). Consequently, as there is no water assumed in the 'no porosity' scenario it yields the lowest heat extraction rate of 0.14 MW. The anthropogenic aquifer created by

mining contributes a very small volume relative to the total rock volume, resulting in a porosity of just 0.004 and a slightly higher heat output ('Mined Porosity'). In contrast, the Pennine Coal Measures, with a porosity of 0.14, produces a significantly greater heat output. The 'Combined Porosity' case, which incorporates both the mined voids and the formation porosity, results in a total porosity of 0.1435 and the highest heat output of 1.63 MW, due to the greater proportion of water assumed present. The 'no porosity' scenario reveals that 86 % of the heat (according to the rock volume method) is coming from the rock, with the remaining 14 % coming from the fluid in the void space. These are similar values to those produced by Quinao and Zarrouk 2014 (88 % and 12 % respectively) for an idealised electricity producing reservoir.

Using the Rock Volume produces the second highest static estimate of the useable heat, regardless of the porosity used. It yields significantly more heat than the water volume method, nearly 14 times more MWh per year. This is because the rock volume is 250 times greater than the volume of water in the mine voids.

3.5.4 Flow Rate

Using the flow rate method yields the highest estimate of the useable heat extraction rate, 0.59 MW. This value is approximately 50 times greater than the estimate derived from the static volume of water stored within the mine, which is 0.012 MW. This discrepancy is expected, as the total volume of water circulated over a 40-year period at a continuous flow rate of 25 L s^{-1} is approximately 50 times larger than the initial volume of water calculated to be present in the mine voids.

The flow rate method produces an estimate that is approximately 3.5 times higher than that of the rock volume method. This is due to the interplay between three factors. First, The volume of water is approximately 20 % less than volume of rock - which would favour the rock volume method. Second however, as explained above the difference in density and heat capacity between water and rock leads to less heat present in the reservoir of rock, than if it was water. Third, and on top of this the recovery factor of 0.1 applied in the rock volume method means that only 10 % of that heat is predicted to be extractable at the surface (see Table 3.3).

A key limitation of the flow rate method arises when there is no historical flow rate data, for example, from prior drilling, mine dewatering operations, or natural surface discharges. In such cases, the flow rate used in calculations becomes arbitrary and disconnected from the physical realities of the subsurface reservoir. If an unrealistically low flow rate is selected (e.g., 10 L s^{-1}), the thermal resource may be underutilized. Conversely, assuming a high flow rate (e.g., 350 L s^{-1}) may lead to overestimation and rapid thermal depletion of the system.

Furthermore, this method does not account for the architecture of the mined aquifer. Flow paths can vary significantly within the same mine, and identical flow rates may yield very different thermal outputs depending on their route through the system (see Figure 3.5).

This method also assumes that the abstraction temperature does not decrease over time, or at least that the selected ΔT can be maintained over time. In reality, without anthropogenic recharge or substantial natural groundwater recharge (see Section 3.5.5), the mine water resource will cool (Sweeney et al. 2025). This progressive temperature decline can reduce the recoverable heat and may make the scheme uneconomic.

Overall, this method is best suited to locations with natural or managed surface discharges, where both flow rate and temperature data are available (Walls et al. 2022). In these cases, such as Seaham Garden Village, UK, the heat pump system can be directly applied to the available flows without requiring reinjection, providing a practical and efficient means of energy recovery (Mining Remediation Authority 2025b).

3.5.5 Heat Recharge

In a mine water heating system, heat is removed from the reservoir as warm water is abstracted and colder water is reinjected (Banks et al. 2019b). However, heat can also be returned to the system through several mechanisms: the natural geothermal heat flux (which is always present), the inflow of warmer groundwater from surrounding areas, and the injection of heat from anthropogenic sources (Monaghan et al. 2025).

The extent to which these modes of heat recharge are accounted for varies across the static methods. At one end of the spectrum is the flow rate method, which, by assuming a constant flow rate and constant rate of heat extraction, implicitly assumes ongoing heat recharge but does not specify its source. This method does not consider any potential cooling of the mine system, effectively implying that the extracted heat is continuously replenished. However, without long-term hydrogeological and thermal data, this assumption may not hold, and the sustainability of the heat supply remains uncertain.

At the other end of the spectrum are the rock volume and water volume methods, neither of which consider recharge from groundwater nor deep geothermal heat. While this may be reasonable over very short timescales, thermal recharge from surrounding rocks (and potentially other sources) may make more of a contribution over the lifetime of a system (Monaghan et al. 2025). These methods may be most appropriate in settings with very low groundwater flow and no planned reinjection, although they still neglect the contribution from geothermal heat flux.

The geothermal heat flow method sits between these extremes, as it inherently accounts for the geothermal heat flux but excludes groundwater and anthropogenic heat recharge. It should be noted that if anthropogenic heat recharge is required to ensure the long term viability of a scheme it does not have to start synchronously with heat extraction. Fraser-Harris et al. 2022 identified that heat recharge can be implemented years after heat extraction has begun to prevent a damaging thermal drawdown.

In our dynamic method, recharge, such as groundwater flow is not included (Mouli-Castillo et al. 2024), but anthropogenic heat recharge can be implemented. Even aside from differences in how recharge is handled, one of the fundamental distinctions between the static and dynamic approaches is that static methods do not incorporate the actual geometry of the mine. As a result, they cannot provide insight into how the spatial architecture of the mine could influence the performance of a geothermal scheme.

3.5.6 Dynamic modelling

Grid vs Maps

The synthetic grid model (Figure 3.6) produces more useable heat than the digitised mine maps (Figures 3.3 and 3.6). However, it is closer to the digitised Baseline Map than static methods and captures the expected reduction in heat extraction over time due to the absence of heat recharge. An advantage of using synthetic grids is the reduced time and effort required to estimate useable heat. Instead of digitising the entire mine, which is time consuming, a reasonable estimate can be obtained using only a few key parameters: the surface area, an estimated length of the dominant flow path, seam depths, the geothermal gradient, and an approximation of the average gallery spacing. This approach offers a more representative estimate than static calculations. Nonetheless, the primary advantage of using fully digitised maps remains the ability to evaluate a range of scenarios informed by the geometry and structural characteristics of a specific mine layout.

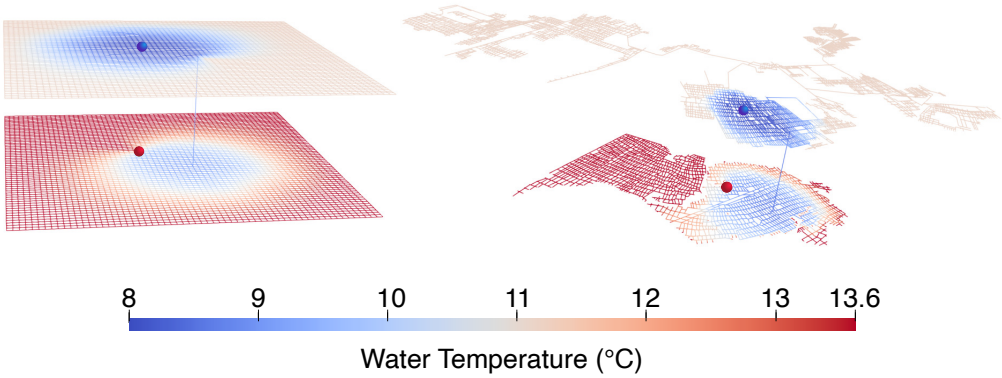

Figure 3.6: Temperature inside the Synthetic Grid model and the Baseline Map model. Water is injected at 25 Ls^{-1} into the upper seam (blue sphere) and abstracted on the lower seam (red sphere). Both images are the results after 20 years. Reproduced with the permission of © The Mining Remediation Authority. All rights reserved

Distance

As has been found previously (Sweeney et al. 2025), increasing the distance the water travels from injection to abstraction increases the amount of useable heat. With a

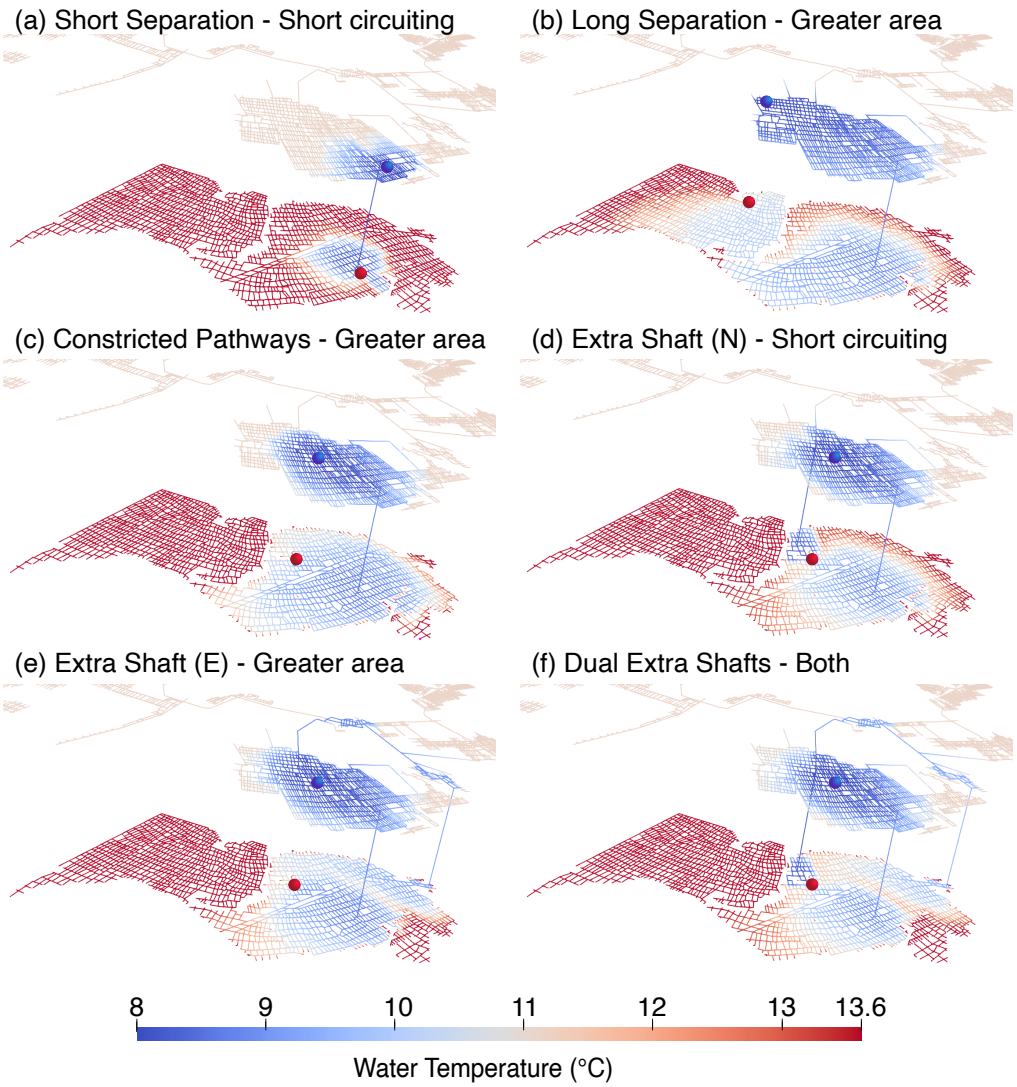

Figure 3.7: Temperature inside the mine in the different modelled scenarios. Water is injected at 25 L s^{-1} into the upper seam (blue sphere) and abstracted on the lower seam (red sphere). All images are the results at 20 years. A) Injection and abstraction point in the close position. Cold (blue) water is being produced at the abstraction point. B) Injection and abstraction point in the far position. The flow path on the lower seam is being funnelled around a break in the mine workings. C) The rooms across the centre are reduced in diameter to 1 m (Figure 3.1). This causes water to flow around the edges and increases the area of the mine heat is being extracted from. D) Extra Shaft (North) implemented causing the cold injected water to reach the abstraction well quickly. E) Extra Shaft (East) implemented causing the water to flow over a greater area of the mine. F) Both Extra Shaft (North) and Extra Shaft (East) implemented causing both a greater area of the mine to be used, but also cold water to reach the abstraction well quickly. Reproduced with the permission of © The Mining Remediation Authority. All rights reserved.

longer travel distance heat is extracted over a wider area of the mine and the risk of short circuiting is reduced (Walls et al. 2021). In this case, when the distance

is increased from Baseline Map to Long Separation the useable heat increases both after 1 year, and at the end, after 40 years of heat extraction (Figure 3.5). When the distance is decreased from the Baseline Map setup to the Short Separation, the useable heat decreases, there is also a difference in the heat extraction over time. In the Baseline Map and Long Separation setups there is a rapid decrease in useable heat per year for the first 5 years, after which the rate of decline decreases overtime, although does not completely flatten off within the 40 years. In the Short Separation setup the decrease in useable heat per year is much reduced and there is a flattening off. This is because the system short circuits very quickly (Figure 3.7) as evidenced by the cold water completely encircling the injection and extraction wells, and therefore the cold water being injected at the fixed temperature of 8°C is being produced. It should be noted that the distance from the abstraction/injection point in the shaft when viewed from the surface does not always reflect the subsurface flow path. For example, as in Long Separation, the water may traverse a longer route underground, flowing around structural discontinuities, increasing the area of the mine heat is extracted from.

Additional Shafts

The presence of additional shafts can both increase and decrease the useable heat. 'Extra Shaft (North)' decreases the heat, 'Extra Shaft (East)' increases the heat, and the presence of both reduces the heat, but not by as much as just Extra Shaft (North) (Figure 3.5). These variations are due to the changes in flow paths that the presence of the additional shafts induces. Adding Extra Shaft (North) creates a short circuit between the injection and abstraction well, while adding Extra Shaft (East) causes water to flow through a new section of the mine (Figure 3.7). The combination of both still accesses an increased area of the mine, but the short circuiting is also present. This highlights the importance of explicitly modelling the presence of any potentially open additional shafts as they can either enhance or impair heat extraction. In the mine water project in Gateshead, UK, an additional borehole was drilled to connect the seams used for abstraction and re-injection in order to establish a flow cell capable of sustaining the required flow rates (Adams

et al. 2023). An intervention of this kind can improve hydraulic connectivity but could also have the risk creating a short-circuit flow path between the abstraction and re-injection wells. This kind of intervention is well suited to evaluation with scenario-based numerical modelling.

Reduction in Room Diameter

The reduction of the room diameter in between the shaft and the abstraction point causes the flow paths of the 'Constricted Pathways' set-up to diverge from the 'Baseline Map' set-up. The flow spreads around the area of reduced diameter, lengthening the flow path, delaying the time at which the cold front reaches the abstraction point, and increasing the area of the mine heat is extracted from. In this 'Constricted Pathways' set-up, the useable heat is higher in comparison to Baseline Map at year 1 but the difference between the two decreases over time. However, in another scenario, the reduction in diameter could lead to an area being cut off, and a reduction in the area of the mine heat can be extracted from. This example highlights a specific vulnerability of the system; in real-world applications, a more extensive analysis would be required to explore a broader set of scenarios and uncertainties.

Risk reduction

We have demonstrated the use of dynamic modelling with GEMSToolbox to support scenario analysis during the early stages of mine water geothermal project development. This approach enables the optimisation of exploration targets and the development of mitigation strategies tailored to the specific conditions of the underground mine. Here we have investigated specific, user driven scenarios, to demonstrate the potential uses of fast dynamic modelling. However, it would also be prudent to investigate randomly generated scenarios to ensure that no critical risks have been missed. By reducing project uncertainty earlier in the development timeline, dynamic modelling can lower investment risk during the pre-production stages. This risk reduction is particularly important for securing funding, as early activities, such as exploration drilling, often require equity-based financing (Dewi et al. 2020). While the final investment decision (FID) typically occurs after exploration,

and is associated with raising the bulk of project financing (usually debt-based), de-risking earlier stages can expand the pool of potential investors and improve the terms of both equity and debt financing (Sanyal and Koenig 1995). As one of the main barriers to the widespread use of geothermal energy is project financing, it is important to reduce risk (Compernolle et al. 2019; International Renewable Energy Agency (IRENA) 2017). Figure 3.8 illustrates how the use of dynamic modelling tools such as GEMSToolbox can influence the project risk curve and enhance investment readiness from the outset.

The cumulative cost curve begins relatively low, reflecting expenditures associated with a desk-based feasibility study. Costs increase substantially during the exploration drilling and testing phase, with approximately 20 % of the capital expenditure incurred by the end of this step (David Townsend, TownRock Energy, personal communication, June 2025). They continue to rise through the drilling of production-diameter wells, which often involves reaming pre-existing exploration wells, and through the construction of surface infrastructure. Costs then decline during the installation and commissioning phases. During the operations and maintenance phase, ongoing expenses are largely limited to maintenance and the power required to operate the pump. It is at this point that income starts to rise, as heat is produced and sold.

The quantity of available data begins to increase during the feasibility study, when mine plans, local hydrogeological reports, geothermal gradient assessments, mine closure documents, shaft treatment information, and firsthand accounts are gathered and analysed. A significant increase in data occurs during exploration drilling and testing, which provides the first direct information on mine conditions, the accuracy and georeferencing of mine plans, water temperatures, chemistry, and initial pumping and reinjection performance (Kępińska et al. 2021). These data can help determine whether a strong hydraulic connection exists between the injection and abstraction wells. Further information becomes available when production-diameter wells are drilled, allowing for the confirmation of flow volumes and thus the actual amount of useable heat.

Relatively few additional data are collected during surface construction and com-

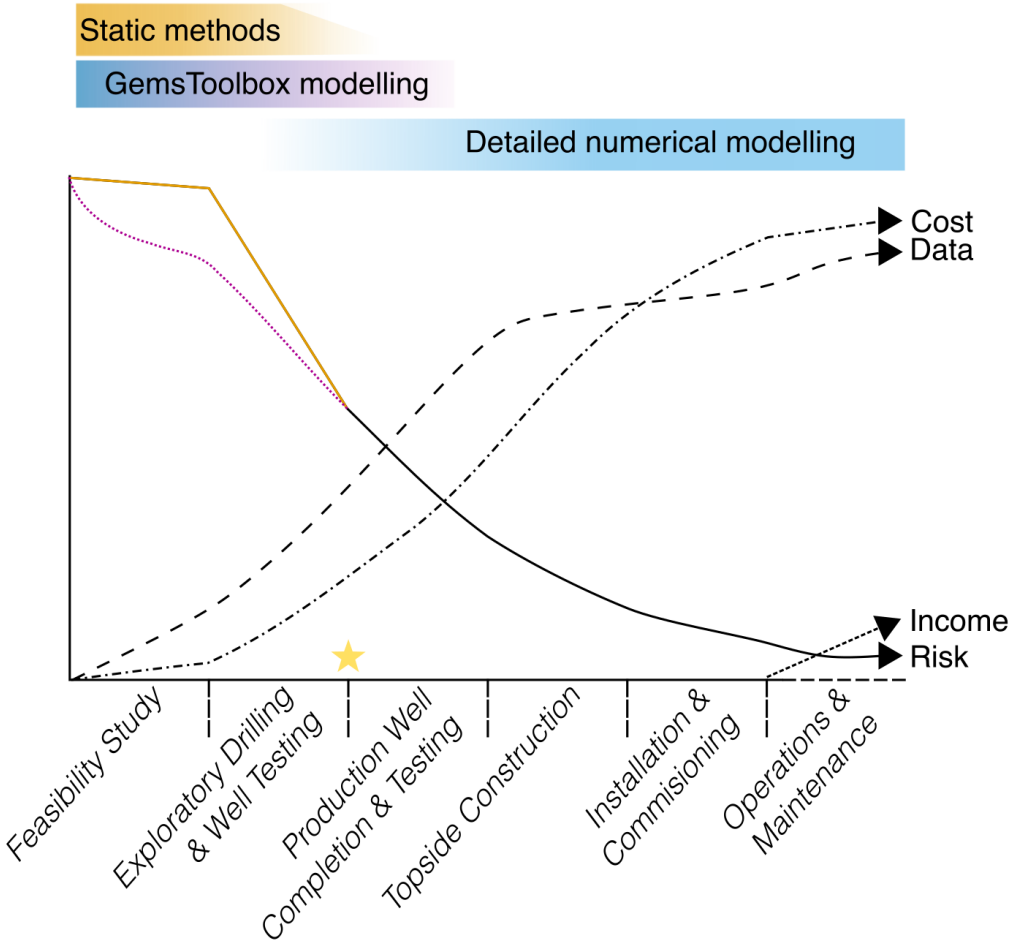

Figure 3.8: A representative drilled mine water geothermal project timeline, showing the cumulative cost, data, risk and income across the stages, and when different heat estimation tools are used. Solid orange line is risk using static methods, dotted purple line is risk when using dynamic modelling methods. Yellow star is final investment decision (FID). This does not include planning, licensing, regulator approvals, or community engagement, while these are not physical risks to the project, they are risks in themselves and can take time and money, especially if there are delays in this process. This also does not include the costs of a the construction of a heat network. The flow rate method is an unusual static method, in that it is most appropriate either at the beginning stage of a feasibility study if there is prior data on possible extraction rates, or after the exploratory well testing when the first flow rate data from the project will be known. Exploration boreholes in the 'Exploratory Drilling & Well Testing' stage are not the same diameter as a production well, they are slim-hole, and are reamed out to production width if deemed successful. Adapted from Gehringer and Loksha 2012.

missioning. However, the operations and maintenance phase provides opportunities for ongoing data acquisition. Parameters such as pumping rate, water level, tem-

perature, and chemistry can be monitored continuously, helping to validate models and support long-term performance forecasting.

Risk is high at the outset of any drilled geothermal project but decreases significantly as data from the exploratory phase are obtained (Kępińska et al. 2021). Drilling and testing of production wells further reduce risk. Although some reduction continues through surface construction and commissioning, the rate becomes more gradual. In the operations and maintenance phase, risk remains low but may continue to decline slightly over time as additional performance data are gathered.

Static heat estimation methods are commonly applied during the feasibility stage. These methods typically yield a single value representing the heat in place or, if combined with a recovery factor, the recoverable heat. However, they do not account for system lifetime, mine geometry, or actual flow paths, and therefore offer limited potential for reducing uncertainty. In contrast, the GEMSToolbox modelling approach can be applied at the same project stage using similar input data. It incorporates temporal effects and allows for the simulation of multiple scenarios. This enables a reduction in uncertainty earlier in the project, supports more effective targeting of exploration zones, and facilitates early-stage mitigation planning.

GEMSToolbox offers a streamlined numerical framework based on semi-analytical solutions, which significantly reduces computational requirements. As a result, models can be run quickly and inexpensively, enabling rapid sensitivity analysis and scenario exploration, even on a standard laptop. This contrasts with fully numerical models, such as those based on finite difference, finite volume, or finite element methods, which demand extensive computational time and detailed input data. Such models are more appropriate once a substantial amount of site-specific data have been collected and greater financial resources are available. In that context, they offer higher spatial and temporal resolution and can support more complex flow and heat transport simulations. However, for early-stage decision-making, GEMSToolbox provides a fast, cost-effective, and sufficiently accurate means of reducing uncertainty and guiding project development.

Another benefit of the GEMSToolbox modelling is the visual output. As seen in Figures 3.6 and 3.7 the temperature distribution, injection and abstraction place-

ment (and other information such as flow rate, water velocity, head, and more) can be displayed simply in 3D. This presents complex data in a commonly comprehensible way, which helps in clear communication.

3.6 Conclusion

This study highlights the value of using dynamic modelling with the GEMSToolbox to support early-stage decision-making in mine water geothermal projects. While it relies on nearly the same input data as static estimation methods, the GEMSToolbox requires only a small additional investment of time and effort to produce far more informative results. These include time-dependent heat estimates and the ability to simulate different operational scenarios, both of which provide a more realistic understanding of system behaviour. This allows for improved targeting of exploration activities and the design of mitigation strategies that are specific to the conditions of the underground mine. Reducing uncertainty at this stage lowers the overall project risk and increases the potential to attract investment. This is particularly important during the early phases when funding is often needed for exploration drilling and typically comes from equity sources. As the project progresses toward the point at which most capital is raised, often through debt financing, earlier risk reduction can also lead to more favourable financial terms and a wider range of potential investors. Dynamic modelling with the GEMSToolbox can therefore play a critical role in improving both technical confidence and investment readiness in mine water geothermal development.

CHAPTER 4

The need to regulate thermal interference between mine water geothermal systems: a UK perspective

This chapter has been published in the Quarterly Journal of Engineering Geology and Hydrogeology. Sweeney et al. 2025. The modelling and production of the manuscript were done by A. Sweeney who would like to acknowledge the useful discussions, training and support provided by her co-authors.

A. Sweeney, J. van Hunen, J. Mouli-Castillo, and J. Gluyas, "The need to regulate thermal interference between mine water geothermal systems: a UK perspective," Quarterly Journal of Engineering Geology and Hydrogeology, vol. 58, no. 2, pp. qjegh2024–185, 2025. https://doi.org/10.1144/qjegh2024-18

Author Contributions

- A.S.: conceptualisation (lead); formal analysis (lead); investigation (lead); methodology (lead); project administration (lead); validation (lead); visualisation (lead); writing – original draft (lead); writing – review & editing (lead).
- J.G.: writing – review & editing (equal).

- J.H.: conceptualisation (equal); formal analysis (supporting); software (equal); writing – review & editing (equal).
- J.M.-C.: formal analysis (supporting); software (equal); writing – review & editing (equal).

4.1 Abstract

The lack of regulations concerning potential subsurface thermal interference between mine water geothermal systems is hindering wider adoption of the technology. Using the GEMSToolbox modelling tool, we examined a generic room and pillar coal mine to assess the impact of thermal interference between adjacent MWG systems. The modelling quantifies the thermal interference occurring between two operators sharing a contiguous water body within a mine block. High water abstraction rates and smaller distances between the MWG wells increase the risk of significant interference, which worsens the longer the systems operate. We introduce the 'heat extraction ratio' to quantify thermal interference, defined as the ratio of heat produced with two users present compared with a single user. This metric can aid regulators in establishing acceptable levels of thermal interference between MWG systems. Drawing on regulations from geothermal energy-producing countries, ground source heat pump guidelines and UK oil and gas laws, we propose two potential policies for managing MWG thermal interference. The first policy requires unitisation when thermal interference systems if they would breach the regulatory threshold.

4.2 Introduction

The UK is legally bound to reduce its greenhouse gas emissions to net zero by 2050, as set out in the Climate Change Act 2008 (as amended by the 2050 Target Amendment Order 2019). Heating is responsible for 23 % of the UK's emissions (BEIS 2021) and mine water geothermal (MWG) heating is an opportunity to decarbonize some of the space heating sector. The UK has an estimated 23 000 disused coal mines (Gluyas et al. 2020), often considered a liability, but they are also an oppor-

tunity, to help supply the heat demands of the 25 % of homes and businesses located in coal-mining areas (Gluyas et al. 2020). There are currently only a few operating MWG systems in the UK, including Nest Road and Abbotsford Road operated by Lanchester Wines, and a scheme operated by Gateshead Council (Banks et al. 2022; Coal Authority 2024b). These three lie within the Gateshead Council area in NE England. In addition, there is a research facility, UK Geoenergy Observatory, in Glasgow, Scotland (Monaghan et al. 2022) and a scheme being built in Seaham, County Durham, NE England. However, a lack of clear regulations has been identified as a deterrent to investment in geothermal energy (Goodman et al. 2007; Manzella et al. 2018). In the UK, heat is considered a pollutant (Abesser et al. 2018) or a physical characteristic (McClean and Pedersen 2021), but is not an ownable resource. This means that the operators of a geothermal scheme cannot guarantee that the heat resource they are using will remain available to them over the lifetime of the geothermal operation. There is a danger that it might be appropriated or disturbed by another operator located too close by. To implement a coal MWG system in the UK, a mine water heat access agreement must be acquired from the Mining Remediation Authority to access the flooded and abandoned coal mine workings, but this does not guarantee any heat. A water abstraction licence is also required from the appropriate environment agency (Natural Resources Wales, NRW; Northern Ireland Environment Agency, NIEA; and, in England, the Environment Agency, EA) (Water Resources Act 1991, Chapter 57; Water (Northern Ireland) Order 1999, SI 1999 No. 662 (NI)). However, in Scotland, under General Binding Rule 17 (GBR 17) of The Water Environment (Controlled Activities) (Scotland) Regulations 2011 (CAR), an abstraction licence is not required if the water is re-injected into the same geological formation after being used for geothermal energy extraction. When granting a water abstraction licence, the licensing authority can limit the amount of heat to be extracted, but this can only be done to protect ground or surface water from a change in temperature that would negatively harm the environment, not to prevent thermal interference between geothermal systems (McClean and Pedersen 2023). If the owner of an abstraction licence experiences a reduction in the amount of water they can abstract because of the permitting of further abstraction licences,

they may be able to claim damages, but this does not apply to a reduction in heat (McClean and Pedersen 2023). An obvious potential problem of having multiple operators extracting heat from an interconnected mine system is the possibility of a rapid depletion of the heat available and/or one system extracting the cold water re-injected by another. However, it is also important to consider the opposite; if mine water heating is to contribute to the UK's energy mix, mine water systems should not be artificially spaced out, wasting potential heat resources. For example, previously the Mining Remediation Authority rules only allowed one geothermal system per mine block (Coal Authority 2022). A mine block is defined as a mine or set of mines that are hydrologically disconnected from the surrounding mines. This disconnection may be complete, or there may be a limited hydraulic connection but not enough to let water levels between the adjacent blocks equalize (Coal Authority 2018). These blocks can be tens of square kilometres and there have been MWG schemes that have operated at $<$10 L s^{-1} (Walls et al. 2021). Such a scenario would not draw significant quantities of heat from the mine block, and if a second system was not allowed in a such a mine block, a huge volume of heat could potentially be underdeveloped. The current Mining Remediation Authority approach is to consider new applications on a case-by-case basis (Mining Remediation Authority, pers. comm., 20 February 2025).

The aim of this paper is threefold: (1) we review international geothermal regulations and regulations from other industries; (2) we quantify the thermal interference between two mine geothermal heating systems; (3) we combine these results to suggest policy options for regulating thermal interference between mine water geothermal heating systems. This is applicable to the UK and other countries with heat extraction schemes in room and pillar coal mines.

4.3 Regulatory Context

Whereas the UK does not have a regulatory regime for considering the needs of multiple operators in one geothermal resource (Abesser and Walker 2022), other countries have a longer history of commercial more geothermal energy, and as such,

in most cases, have developed regulatory regimes. These regulations may be instructive for the UK to develop its own geothermal regulations. Likewise, there are examples in the oil and gas industry, which also deals with a valuable fluid that can flow from one area to another and does not respect human surface infrastructure or licensing blocks (Kemp 2013). Ground source heat pumps (GSHPs) have grown in popularity in Europe, with 2.19 million GSHPs installed as of 2023 (European Geothermal Energy Council 2023). Regulations specifically for GSHPs (which often are separate from other geothermal regulations) can also provide insight, as heat interference between increasingly densely packed GSHP systems is a growing problem (Belliardi, Soma, et al. 2022).

4.3.1 Oil and gas unitisation rules in the UK

Unitization in the oil and gas industry refers to organizations with the right to extract petroleum in a reservoir co-operating to operate the reservoir. It is common around the world, including in the UK. The purpose of unitization is to decrease economic and physical waste, and to ensure that the operators all receive their 'fair share' (Asmus and Weaver 2006). If the UK Minister (for Energy Security and Net Zero, as January 2025) decides that any section of a licenced area is part of a single oilfield that contains other granted licences, the Minister can order that the licensees in the affected field co-operate to extract the petroleum. The Minister can do this as it is in the national interest to 'secure maximum ultimate recovery of petroleum and in order to avoid unnecessary competitive drilling' (The Petroleum (Current Model Clauses) Order 1999, SI 1999/160). Although this national interest supersedes the need for fairness (Asmus and Weaver 2006), the regulations state that the unitization should be fair and equitable (The Petroleum (Production)(Landward Areas) Regulations 1995, SI 1995/1436). However, the North Sea Transition Authority, previously the Oil and Gas Authority, states that the final decision to accept or reject a field development programme will be based on the plan producing the maximum economic recovery of oil and gas (North Sea Transition Authority 2018). If there is no wastage, the government will not force the licensees to unitize, even if that leads to unequitable extraction between licensees (Asmus and Weaver 2006).

The UK does not consider petroleum to be privately ownable until it has been extracted, as all rights to unextracted petroleum are vested in the Crown (Gordon 2015; North Sea Transition Authority 2018). Therefore, issues of fairness cannot be enforced while the petroleum remains in place within the reservoir (Asmus and Weaver 2006; North Sea Transition Authority 2018). Although the UK Government has the power to enforce unitization, this power has not been exercised, although the existing regulations have led to many voluntary unitizations (Gordon 2015).

4.3.2 Review of national geothermal regulations in 11 countries

The use of mine water geothermal heating is not prevalent enough around the world (Chu et al. 2021) for there to be many laws or regulations that directly deal with thermal interference in MWG. However, the problem of heat sharing is relevant to multiple types of geothermal technologies, including GSHPs and deep/high temperature geothermal energy. For example, if a company is targeting a permeable fault structure for open-loop power production and a rival company targets the same fault structure further downstrike there will be similar issues of heat resource degradation to those a mine water geothermal system would experience. Regulations from various countries were investigated in this study. Although a comprehensive review of global regulations was not the objective, a selection of countries was chosen based on their geothermal energy production and regulatory frameworks. The analysis focuses on the top seven geothermal-producing countries as of 2022 (Richter 2023): the USA, Indonesia, the Philippines, Turkey, New Zealand, Mexico and Kenya.

Additionally, regulations from several other countries were reviewed because of unique regulatory approaches or noteworthy geothermal developments. Iceland was included as it is renowned for its extensive geothermal energy utilization. The Netherlands was examined for its well-developed regulatory framework and successful implementation of mine geothermal systems (Verhoeven et al. 2014). Poland, with its numerous operating coal mines, presents significant potential for mine geothermal projects post-closure. Czechia was also analysed because of its interesting regulatory structure. The countries' regulations can be classified into three

categories: (1) regulations do not mention competing usage; (2) regulations mention competing usage but do not provide a framework for dealing with it; (3) regulations provide a framework for competing usage.

Regulations do not mention competing usage.

Neither Indonesia nor Kenya mention competing usage or thermal interference in the Law of the Republic of Indonesia No. 21 of 2014 about Geothermal or the Energy Act (2019) of Kenya, respectively. In Turkey, multiple licences can be found over one geothermal reservoir as the licencing areas do not relate to the geothermal reservoir being exploited (Aydin et al. 2020), so the thermal interaction problem is not addressed. This has resulted in significant amounts of thermal interference between wells (Aydin et al. 2020).

Regulations mention competing usage but do not provide a framework for addressing it.

In Czechia using 'dry heat' (from the Earth) for 'industrial purposes' requires a permit under the Mining Activity Act. When applying for this there must be documentation proving the settlement of conflicts (Szalewska 2021), although no further detail on how to settle the conflicts has been given. To explore for a geothermal resource in Iceland, a Prospecting Licence must be granted by Orkustofnun (National Energy Authority), and then, to use the resource, a Utilisation Licence is required. Conditions can be attached to the Prospecting Licence if there are concerns about interference with pre-existing exploitation. A Utilisation Licence can be rejected or have conditions attached if the Minister (responsibility delegated to Orkustofnun) is concerned about pre-existing use of the resource, with Article 17 of the Act on the survey and utilization of ground resources (1998) (No. 57/1998) stating: 'In granting utilisation licences care should be taken that... account is taken of any utilisation already begun in the vicinity. If the Minister is of the opinion that the applicant for a utilisation licence does not meet these requirements, the Minister may refuse to grant the licence or insert special conditions in the licence.' The Netherlands Mining Act (Wet van 13 oktober 2022 tot wijziging van de Mijnbouwwet 2022, Stb 2022

438) states that an application for a geothermal search area, start-up permit and follow-up permit may be rejected if there is a geothermal energy search area allocation, a geothermal energy starting permit or a follow-up geothermal energy permit that already applies to the area in question. When applying for a search or start-up permit, the applicant must estimate any temperature or pressure interference with other geothermal projects. This demonstrates that thermal interference is considered in the Dutch system, but the law does not state when this thermal interference will or will not be acceptable. The Geothermal Service Contract of the Department of Energy (2019) in the Philippines states that the developer will 'Have a free and unimpeded use of Geothermal Resources within the Contract Area in view of the Geothermal Operations, Additional Investments and New Investments in regard of which, the DEPARTMENT (of Energy) shall ensure that rights, privileges and other authorizations it may grant to third parties will not defeat or impair such use'. The obligation is on the Philippines Government to ensure that any licence that is issued does not have an impact on prior use.

Regulations provide a framework for competing usage

The Polish Geological and Mining Law (2011) covers licensing for the extraction of thermal waters. Article 30 states that the 'concession' must include 'the area within which the intended activity is to be pursued', and Article 29 1a states that the concession granting authority will refuse to grant the concession if there is already a concession for the same type of activity in the same area. If the concession area includes the whole area that water and heat are extracted from and the areas cannot overlap, then that should theoretically mean that there is no thermal interference between adjacent systems. Mexico, New Zealand and some parts of the USA all provide for unitization to manage multiple operators in one geothermal reservoir. In Mexico this comes from the Geothermal Energy Law of Mexico (2014), which states that the Secretariat of Energy has the responsibility to resolve disputes arising from the interference of granted concessions. If the Secretariat determines the joint operation is required to avoid damage to third parties, enforce national security, serve public interest, ensure efficient use of the geothermal resource and/or avoid environ-

mental damage, the involved parties are required to come to an agreement for joint operation. If after 90 days the parties do not agree, the Secretariat will determine the joint operating agreement. In the USA there are both federal and state laws regarding geothermal energy. The Energy Policy Act of 2005 states that on federal land the Bureau of Land Management can both approve voluntary unitization agreements and compel unitization agreements (Doris et al. 2009). The rules for state land vary from state to state. In Utah, for example, the power to regulate geothermal resources (natural heat of the Earth from higher temperature sources, >120°C) is given to the Division of Water Rights in the Geothermal Resource Conservation Act. If the reservoir underlies multiple rights owners, each owner has the right to a proportionate amount of the resource. The Division of Water Rights can order unitization if it believes it is needed to 'prevent waste, correlative rights, prevent drilling of unnecessary wells', subject to a two-thirds supporting vote from the owners (Geothermal Resources 1982). In New Zealand Deep Geothermal Systems (DGS) were originally operated as one consent holder systems. However, in 2006 a court case between the Waikato Regional Council and several private operators changed this. The Waikato Regional Council rules stated that for 'large takes and discharges' there should be a single consent holder to provide a single point of responsibility and control. However, the Environment Court decided that a single operator system was not the best way to regulate sustainable development and in reality there were already cases of multiple consent holders in several systems (Environment Court New Zealand 2006, Decision No. A047/2006). The Court's decision was that DGS did need to be managed in an integrated manner and provided the components required in an 'integrated management system'. This included a 'Multiple Operator Agreement' in which multiple operators must co-operate to address the efficient use of the resource, resolve conflicts and have accountability for adverse effects (Environment Court New Zealand 2006, Decision No. A047/2006). Malafeh and Sharp (2015) identified this as compulsory unitization.

4.4 GSHP regulations

Ground source heat pumps are a method of space heating or cooling that are becoming increasingly popular (Lund et al. 2022). Heat is exchanged with the ground using vertical borehole heat exchangers, or lateral coils of tubing, before the temperature is elevated using a heat pump. Although many countries do not have regulations regarding the prevention of thermal interference between GSHPs (Tsagarakis, Efthymiou, et al. 2020; Perego et al. 2022), some do. These are often in the form of minimum distances between the GSHP and either the property line or the next geothermal system (Haehnlein et al. 2010; Somogyi et al. 2017). Countries that have such regulations include China, Germany, Lichtenstein, Sweden and Switzerland, and the distances vary from 3 to 20 m (Haehnlein et al. 2010). Whether these or similar regulations apply to GSHPs and underground thermal energy storage depends on the country. In some cases, depth and/or temperature limits place these technologies under different regulatory frameworks. However, several countries have established minimum distance regulations for shallow open-loop geothermal systems. For example, Czechia, Greece and Sweden have specific requirements, with mandated distances ranging from 5 to 30 m (Haehnlein et al. 2010). Although there is significant work investigating thermal interference between systems (Fascì et al. 2019; Belliardi, Soma, et al. 2022; Perego et al. 2022; De Paoli et al. 2023; Duijff et al. 2023; Stemmle et al. 2024), the regulations are rarely based on this work (Somogyi et al. 2017). The evidence base on which the regulation is based was not readily available after a literature review.

4.4.1 Mine water thermal modelling method

The aim of the modelling was to quantify the impact of having two MWG systems present in a mine and assess the effects of flow rate, distance and the timescale the systems operate for. These parameters are investigated because they vary between systems and can be controlled by the system operators, unlike the underlying geometric and geological characteristics of the mines.

Conceptual model

The model is configured for an open loop with re-injection geothermal heating system in a room and pillar coal mine (Figure 4.1). In this set-up warm water is pumped from a deeper, warmer seam to the surface, passed through a heat exchanger and the now cool mine water is disposed of back into a shallower seam in the mine to re-heat before being abstracted again. Room and pillar mining is a style of mining common to coal mines, where the coal is removed creating 'rooms', while 'pillars' of coal are left to act as structural supports. In the model the rooms are assumed to be open (have not collapsed or been backfilled) and provide a direct hydraulic connection between the injection and abstraction points.

For these experiments, representative synthetic mines were created, rather than using real mine maps. Each mine system has a unique geometry, but many room and pillar coal mines share similar characteristics. We created a general, geometrically simple mine system that is representative of many existing mine systems.

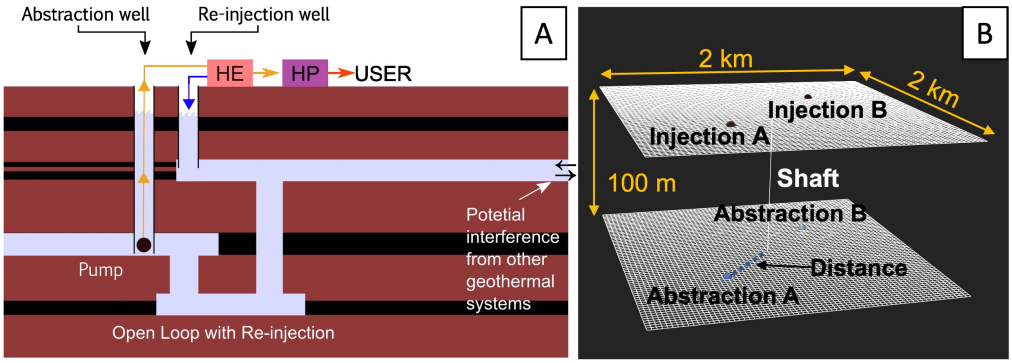

Figure 4.1: (a) Diagram of a hypothetical open loop with re-injection coal mine geothermal system. Arrow colours indicate temperatures, where red is greater than orange, which is greater than blue. HE, heat exchanger; HP, heat pump. (b) Our model set-up, showing two injection and abstraction points placed symmetrically around a central shaft in a two-seam system.

The synthetic mine has two seams with a single central, connecting shaft (Figure 4.1), allowing water to flow between the two seams. The need for this was demonstrated by the Gateshead mine water project, which required an additional borehole to be drilled, connecting the injection and abstraction seams, to ensure a flow cell (Adams et al. 2023). The synthetic seams are approximately 2 km by 2 km,

with 100 m vertical spacing. Further physical parameters are given in Table 4.1. Water is abstracted from the deeper seam and re-injected into the shallower seam. This is typical in a heating system, as the lower seam will be warmer owing to the geothermal gradient (Verhoeven et al. 2014; Banks et al. 2019b; Walls et al. 2021). Having the injection and abstraction wells close to each other reduces the amount of surface infrastructure needed and land required. Different distances between the wells and the shaft were tested, and as the mine dimensions are limited the water flow of the systems positioned closest to the boundary will be affected by the mine edge. This limitation is applied to replicate the real-world physical constraints of a mine.

4.4.2 Modelling with GEMSToolbox

Table 4.1: Physical parameters used in the experiments. a, Rodríguez and Díaz (2009); b, Walls et al. (2021); c, (Mouli-Castillo et al. 2024); d, (Gregory 1983); e, (Hartman 2002).

Parameter	**Value**	**Units**	**Reference**
Thermal conductivity of the rock mass surrounding mine	2.78	$\mathrm{W\,m^{-1}\,K^{-1}}$	a
Specific heat capacity of the rock mass surrounding mine	800	$\mathrm{J\,kg^{-1}\,K^{-1}}$	a
Density of the rock mass surrounding mine	2500	$\mathrm{kg\,m^{-3}}$	a
Thermal conductivity of the water in the mine	0.58	$\mathrm{W\,m^{-1}\,K^{-1}}$	a
Specific heat capacity of the water in the mine	4186	$\mathrm{J\,kg^{-1}\,K^{-1}}$	a
Density of the water in the mine	1000	$\mathrm{kg\,m^{-3}}$	a
Dynamic viscosity of the water in the mine	1.0×10^{-3}	$\mathrm{Pa\,s}$	a
Injection temperature of water	10	°C	b
Initial temperature of the rock mass surrounding the mine at the shallower seam	15	°C	b
Pipe diameter (void space is modelled as pipes)	2.25	m	c
Distance between crossroads	30	m	d, e

The modelling tool GEMSToolbox is used (Mouli-Castillo et al. 2024), building

on (Todini and Pilati 1988), (Rodríguez and Díaz 2009), (Ferket et al. 2011) and (Loredo et al. 2016). It is designed to be a compromise between very detailed large-scale 3D numerical models and simple analytical models. It is targeted at the feasibility stage of a project when there are few data available other than mine maps and generic rock properties to test different injection and abstraction points. Owing to the lack of available data for such projects, detailed 3D models are not warranted at the feasibility stage, when exploring the impact of parameter uncertainty on project risk is more valuable. As the model runs quickly it can be used to analyse many possible scenarios. Each run of the representative grid takes approximately 20 s on a MacBook Pro 2020, with an M1 chip.

The void spaces (rooms and roadways) are modelled as interconnected cylindrical pipes, interconnected at nodes (Rossman 2000). The user specifies the injection and abstraction locations and associated flow rates. This establishes a hydraulic pressure gradient and therefore flow around the mine. All water is modelled as flowing through the 'pipes' rather than the surrounding rock as it is assumed that the galleries have a much higher ability to transfer water than the surrounding rocks. Additionally, there is limited research on the thermal and hydraulic properties of groundwater flow in mines (Monaghan et al. 2025). As a result, we were unable to parameterize the water flow for input into the GEMSToolbox model.

As the water flows through the mines, heat is exchanged with the surrounding rock, owing to the temperature difference between the two, causing the mine water to warm as it moves through the system. The user sets the injection temperature, which remains fixed for the duration of the model run. The model calculates the temperature at every node, including the designated abstraction node(s) at the end of the run time. As the heat is transferred from the rock to the water, the rock face cools, creating a thermal gradient from the water–rock interface into the rock mass. Heat then diffuses towards the pipes. Because there is no external groundwater flow, no additional heat replenishment occurs within the mine.

4.4.3 Quantification

The thermal power output Q (kW) produced by a system is as calculated by Preene and Younger (2014):

$$Q = q\rho_w C_w \Delta T \tag{4.1}$$

where q is the flow rate through the heat exchanger ($m^3\ s^{-1}$), ρ_w is the density of water (kg m^3), C_w is the heat capacity of water (4.18 kW $kg^{-1}K^{-1}$) and T is the change in temperature (amount of warming that occurs) between the injection temperature and the abstraction temperature (K) (it should be noted that ΔT, representing a temperature difference, is measured in kelvins, whereas all individual temperature values are given in degrees Celsius). Because the injection temperature remains constant throughout the model run time, a decrease in abstraction temperature will lead to a corresponding decrease in ΔT. This assumption is based on re-injection temperature requirements conceivably being set in permits or environmental regulations. The practical implication would be an increase in power requirement of the heat pump over its lifetime to maintain equivalent heat output to the end users despite a reducing ΔT. The surface pipework is assumed to be perfectly insulated, with no heat loss. Given that the abstraction temperature is taken at the model end time (i.e. if the model ran for 50 years the abstraction temperature is from the end of the 50th year), it will underestimate the actual amount of energy produced, as the abstraction temperature would have been higher in the early years.

To evaluate the impact on an initial system (System A) of adding a second system (System B) to a mine, the heat extraction ratio (HER) was coined. This is a measure of how much the heat energy produced by System A over the entire simulation period decreases (or increases) on addition of System B. The higher the HER value, the less interference there is between systems.

$$\text{heat extraction ratio} = \frac{Q_{AB}}{Q_A} \tag{4.2}$$

where Q_{AB} is the Q of System A when System B is present in the system and QA is the Q of System A when it is in the only system present.

To assess the impact of flow rate, distance between the central shaft and re-

injection location and operating time, these parameters were varied, respectively, from 1 to L s^{-1}, 42 to 1018 m and 1 to 50 years. We tested scenarios where the flow rates of the two systems matched, as well as scenarios where they varied.

Each configuration was run twice to calculate the HER, once with only System A, and once with both Systems A and B.

4.5 Results

The results of a model run are displayed in Figure 4.2. The cold re-injected water can be seen around injection points A and B before it flows towards and down the shaft, warming up as it travels towards abstraction points A and B.

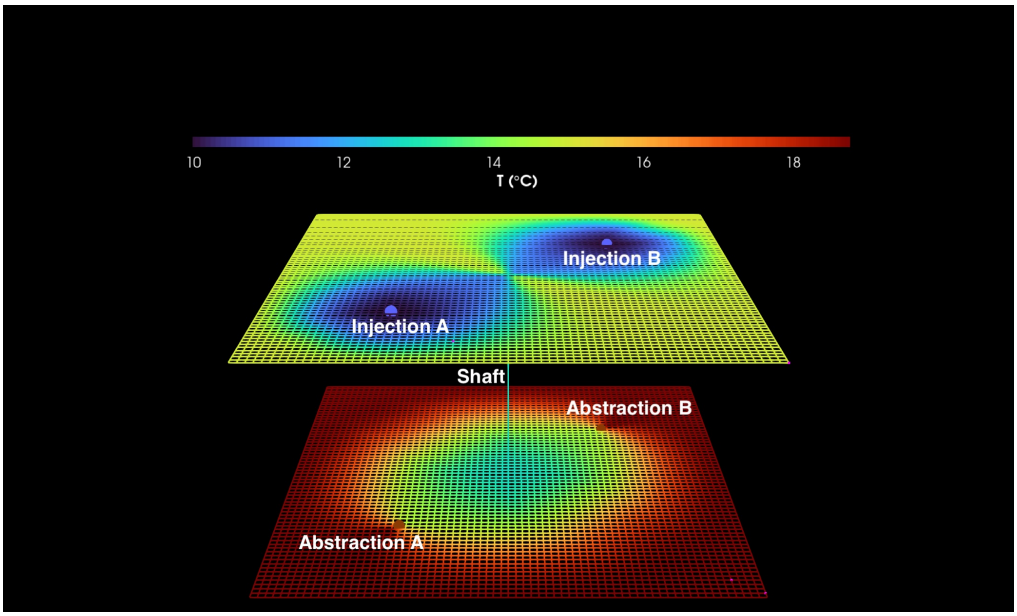

Figure 4.2: GEMSToolbox model results displayed showing two systems, each with one injection and one abstraction point, with a central shaft. Vertical height not to scale. Both systems are operating at 50 L s^{-1} for 20 years and are 679 m from the shaft. The seams are separated by 100 m, the initial top seam temperature is 15°C and the bottom seam temperature is 18.76°C. The distance between crossroads is 30 m.

For each calculation the model is run twice, once with only one system present and once with two systems present (Figure 4.3). The model provides the abstraction temperature for each system present (Figure 4.2), which allows the calculation of the amount of warming that is occurring (ΔT) and the HER (Figure 4.3) of System

A using equation (4.2).

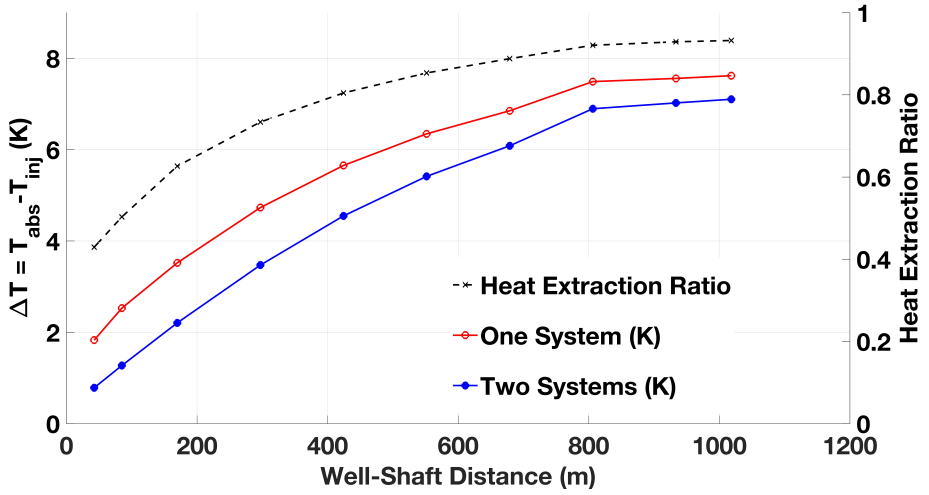

Figure 4.3: The amount of System A warming (abstraction temperature–injection temperature, ΔT) at different distances, and the resultant heat extraction ratio (of System A). In this model run both systems operate at 50 L s^{-1}, operating for 20 years. When there is the least difference between the abstraction temperature–injection temperature of the one-system model and the two-system model, the HER is the highest. This reflects the minimal impact of adding a second system when they are separated by the greatest distance.

The ΔT of System A increases as the distance between the wells and shaft increases, and therefore the distance to System B also increases (Figure 4.3). The difference between the T values of one versus two systems also decreases with distance, demonstrating that at larger distances there is less impact on the thermal resource of System A if an additional system is added. This is reflected by the heat extraction ratio being closest to one (0.93) at the greatest distance tested (1018 m). The boundaries of the mine influence the water flow at the greatest well–shaft distances, where the injection and abstraction wells are closest to the edge. When the mine size increased from approximately 2 × 2 km to 4 × 4 km, the rise in abstraction temperature ranged from 1.11 × 10 5 to 9.7 %, with the largest effect observed in systems with high flow rates positioned closest to the edge of the mine. This effect is consistent with real-world conditions, as mines are not infinite in size.

Figure 4.4 compares the effect of distance on the ΔT and the HER of System A, when System B is at three different flow rates (Figure 4.4a-c). As the distance between System A and System B increases, the T of System A increases. The steepest

rate of change occurs at low distances, before the gradient starts to reduce and then flattens off, with insignificant incremental gain in temperature when the distance increases. For 1 year and a flow rate of 25 L s^{-1}, this happens at approximately 800 m (Figure 4.4a). The same pattern occurs at all the flow rates (25, 50, 75 L s^{-1}) and timescales (1–50 years). These results are expected: for longer flow paths, the water can receive heat for longer from the surrounding rock, and the water temperature will asymptotically approach the rock temperature.

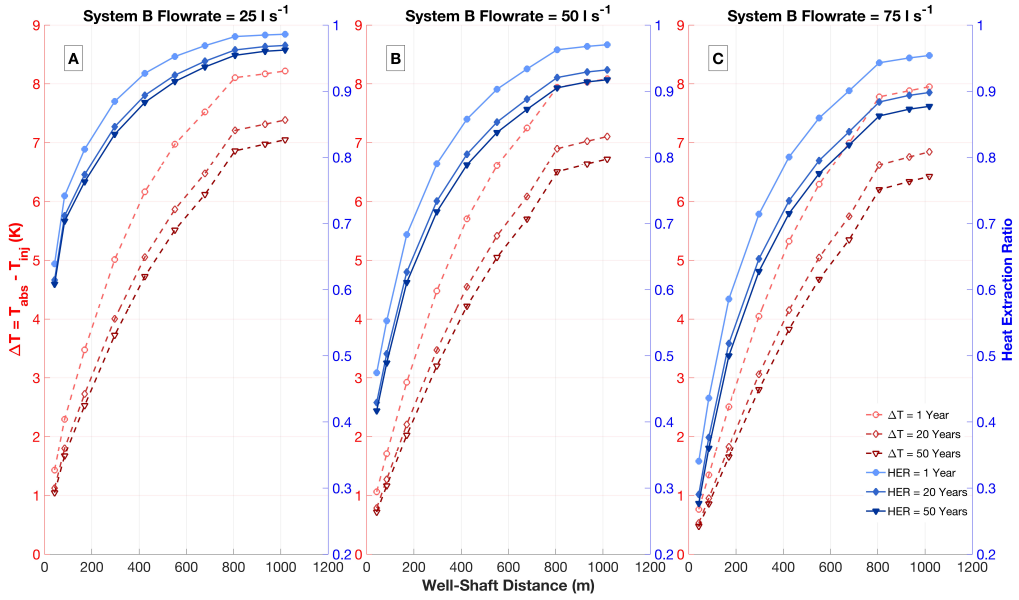

Figure 4.4: (a–c) Comparison of System A warming and heat extraction ratio (HER; blue continuous lines) for different System B flow rates and operational timescales (monochromatic shades). As the distance increases, the ΔT (red dashed lines) of System A increases, showing that systems located close together will have more thermal interference (i.e. a lower HER) than those further apart. The System A temperature does stop increasing though, indicating that, eventually, increasing the distance stops being an efficient method of reducing interference between systems. The same pattern is seen for all flow rates and timescales, although shorter timescales reduce System A's temperature less, and higher flow rates require the systems to be further apart to reduce the interference. Higher flow rates have lower HERs for all timescales; the higher System B's flow rate, the more thermal interference there is, and the more heat energy System A loses. In all cases, as the distance between the systems increases the amount of heat System A loses decreases.

Figure 4.4 also demonstrates that increased operating times result in less warming occurring, and that without the addition of heat from an outside source the system will cool eventually, and this will occur faster at higher flow rates. Larger distances between the systems and the central shaft (and therefore the other system)

result in higher HER values, and therefore less interference between the systems. The greatest rate of change occurs at the smaller distances, but the curve flattens off as the distances increase. There is a point at which increasing the distance between the systems and the shaft is not an impactful way of reducing the systems' influence on each other.

The higher the flow rates, the further away the systems need to be for this to happen. The higher the flow rate the greater the impact on the HER and the greater the change of HER with distance.

The effect of the operating time on the HER is also displayed in Figure 4.4. Longer operating times result in a lower T and lower HER values, meaning there is more interaction between the systems when they run for longer. The longer the systems operate for, and the higher the System B flow rate, the greater the impact on System A.

Figure 4.5 illustrates the relation between flow rate and operation time for a given well–shaft distance. At low flow rates, two systems can run for a long time without significant interference, but for higher flow rates, interference becomes significant sooner.

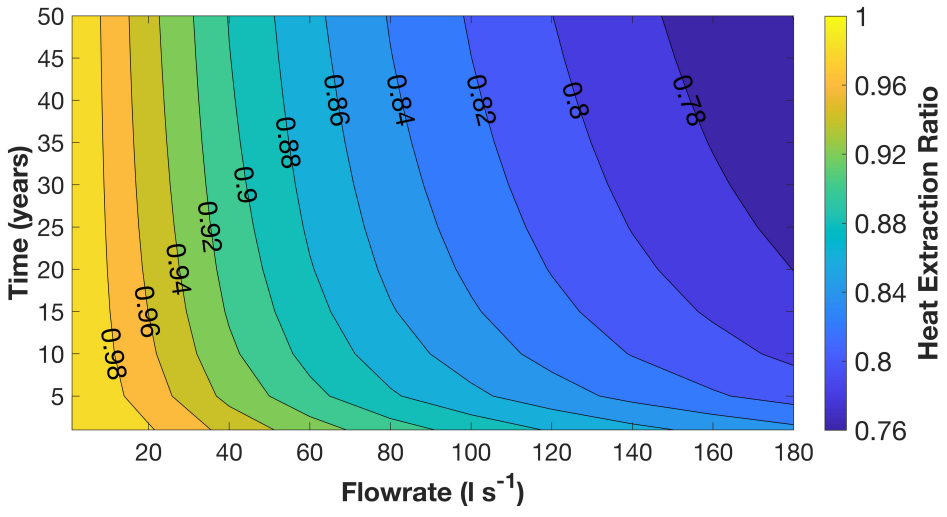

Figure 4.5: Heat extraction ratio as a function of the time that two systems run for, and the flow rates used. Higher flow rates lead to a lower HER, as more interference occurs, as do increased run times, although this is more apparent at higher flow rates.

4.5.1 Interference predictive model

A multiple linear regression analysis was performed to relate the ΔT to the natural logarithms of the input parameters. This provides a useful equation to predict abstraction temperatures without the need for further numerical modelling. For this analysis, both System A and System B had the same flow rate, varying from 12.5 to 75 L s^{-1}, the timescales range from 1 to 50 years and the well–shaft distance from 42 to 1018 m.

Multiple linear regression was used to find the relationship between the input parameters (distance, flow rate, time) and the amount of warming (ΔT). Natural logarithms of the input parameters were used:

$$\Delta T = \Delta T_0 + A_2 \ln(x) + B_2 \ln(q) + C_2 \ln(t) \tag{4.3}$$

The best fitting parameters for this system are T0 = 3.704 K, A2 = 2.396, B2 = 1.255 and C2 = 0.293; x is the distance (m), q is the flow rate (m^3 s^{-1}) and t is the time (years). These parameters give an r^2 of 0.964.

The predicted ΔT results are plotted versus the actual model runs in Figure 4.6. All the predicted curves start with a steep gradient, which decreases as distance increases but does not flatten off. As the distance increases, the ΔT_{max} also increases. However, at greater distances, the rate at which ΔT_{max} increases diminishes, matching the pattern of the modelled values. At longer operating times ΔT_{max} is reduced.

The results are truncated between ΔT_{min} and ΔT_{max} as this reflects the physical limits of the system; the water cannot cool below the injection temperature, or warm above the initial rock temperature.

4.6 Discussion

4.6.1 HER and regulatory pathways

The modelling results show that adjacent mine geothermal systems could experience negative interference, but that under the correct circumstances this can be minimized. Regulation can be used to ensure that systems are at an appropriate

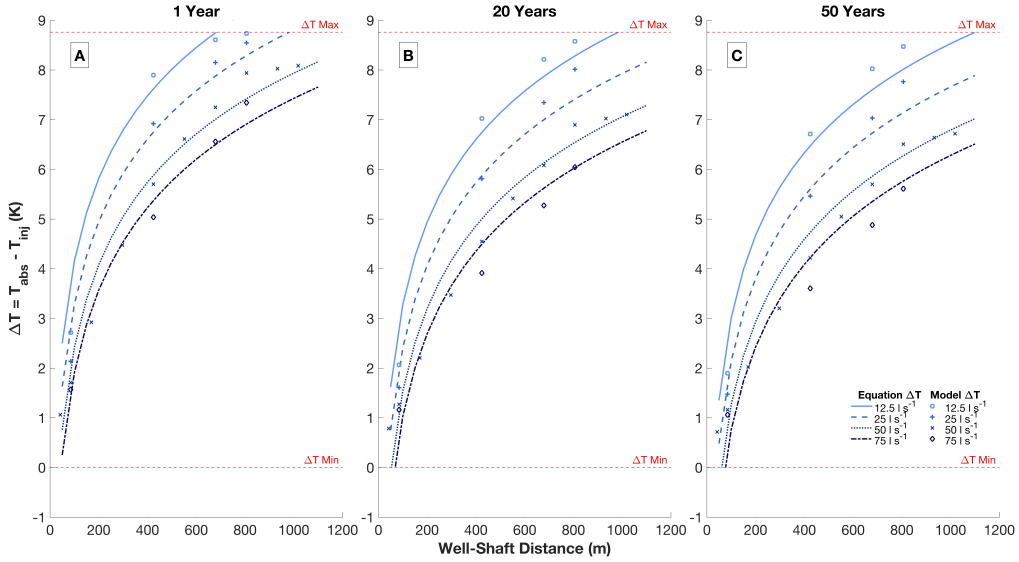

Figure 4.6: (a–c) Equation predicted temperatures compared with modelling results for 1, 20 and 50 years, with Systems A and B having matching flow rates.

distance and the use of acceptable flow rates can reduce interference. The HER can be used by regulators to quantify the amount of interference between systems. A threshold value can be set, with any value below this threshold predicting an unacceptable amount of interference (Figure 4.7).

The HER can be calculated without modelling the systems directly using equation (4.3). The use of this equation is most suitable in systems with a reasonably regular geometry. If an MWG system is already in place, then the difference between the abstraction and the injection temperature is known. The ΔT when an additional system has been added can be estimated with the equation, and the heat extraction ratio can be calculated to quantify the impact of the additional system.

It should be noted that the models, by their nature, are simplified geometries and we recommend future work comparing the model systems with real systems to better understand variability in the predicted heat extraction ratio. The generic models presented here offer a first estimate of the interference between systems, and a more careful analysis can be achieved using tailored models, if desired. This might be particularly beneficial when mine plans deviate significantly from the regular set-up used here. Additional future areas of study would be to consider the impact of greater numbers of systems, groundwater flow and the effect of porous media, either from longwall mining or backfilling room and pillar mines.

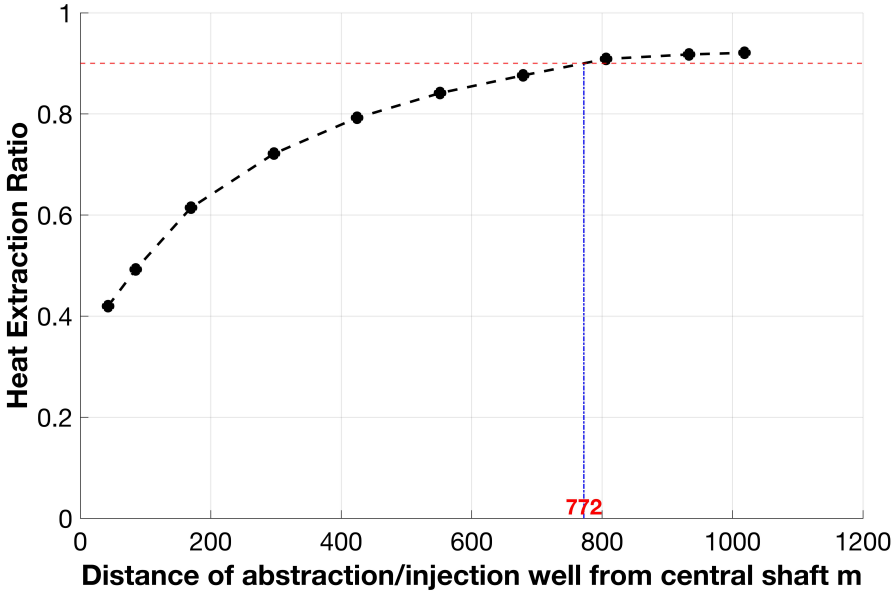

Figure 4.7: Graph showing the potential to use the HER as a regulatory tool. This example uses a system with a flow rate of 50 L s^{-1} and operation time of 40 years. Using a threshold HER of 0.9 suggests a minimum well–shaft distance of 772 m. System A has an HER of 0.42, meaning it has lost almost 60 % of its energy, when the two systems are 42 m from the central shaft. However, when the systems are over 1000 m from the shaft, and therefore 2 km from each other, System A's ratio is 0.92, meaning it has lost only 8 % of its heat energy. Here the threshold value is at 0.9; System A cannot lose more than 10 % of its heat after the addition of System B. The modelling indicates that System B should not be allowed if it is nearer than 772 m.

Although the HER can be used to predict and quantify thermal interference, how to regulate thermal interference is a different question. The review of regulations indicates several possible options, ranging from not regulating interference at all, to unitization, to not allowing any interference. Having no interference regulations is likely to continue the status quo of deterring investors (Goodman et al. 2007; Manzella et al. 2018), especially as we have demonstrated that systems can interfere with each other.

As we have shown that it is possible to have systems adjacent to each other without significant negative interference, one-system mine blocks are inappropriate as this leaves large amounts of heat resource inaccessible. Although there are many potential regulatory approaches, the HER provides a quantitative basis for assessing thermal interference. Based on this, we propose two possible policy options (Fig-

ure 4.8)). We believe that any further recommendation with regard to how to apply the HER to a regulatory approach requires further work, such as techno-economic modelling and the addition of thermal storage and waste heat disposal.

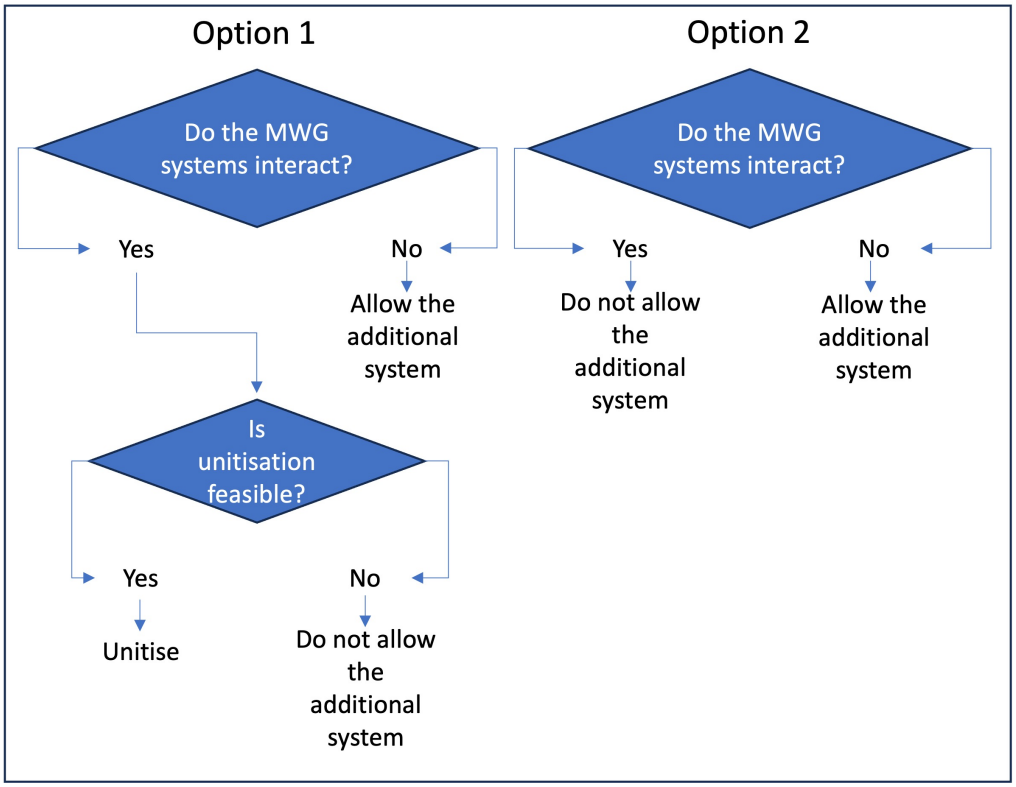

Figure 4.8: Flowchart of the two suggested policy options to regulate the interference of MWG systems. 1, a unitization-based approach; 2, a simple yes or no approach.

Option 1 is a unitization-based approach, as used in New Zealand, Mexico and Utah. There is knowledge of how to regulate unitization agreements given the UK's long history of oil and gas extraction in the North Sea in which unitization is prevalent. However, given that heat is less transportable than electricity or oil, unitization may not always be feasible. In the UK, if a renewable power company produced electricity at a site, the electricity would be sent to the electrical grid and that amount of power could then be sold to customers all over the country. Likewise, if petroleum was being produced, pipelines and/or tankers can be used to transport the product all over the world. Therefore, a unitized operation could provide power to customers regardless of their location. However, if two MWG operations unitized, this could result in increasing the abstraction and injection rates from a single site

or moving the boreholes' infrastructure from the planned sites. This could result in an increased distance from the intended customers. If heat is being transferred over increased distances (Molar-Cruz et al. 2022), there can be significant costs in building pipes, such as obtaining appropriate permissions and excavating roads. These costs may be too great for small-scale schemes (e.g. of a few houses). However, in practice, this may not prove to be a problem, as we have demonstrated that the lower flow rates of small schemes are less likely to cause thermal interference.

Unitization may, however, be especially practical for MWG schemes associated with district heating systems where there is an inbuilt heat transfer network.

Using Option 2, without unitization, there is the potential that a pre-existing small system could prevent a much larger system from being built, which would provide decarbonized heating to a larger user base and be a more efficient use of the subsurface resource. Similar issues occur in minerals planning, and regulations have been developed accordingly.

In minerals planning the term 'sterilized' is used to refer to a situation where a surface development above or adjacent to a deposit prevents any future extraction. In this hypothetical case, it is somewhat different, as the sterilization would be by prior geothermal extraction. To prevent mineral sterilization, some countries (Austria, Czechia, Spain, Greece, Poland, Portugal, UK, Southern Australia and Maryland, USA; Wrighton et al. 2014; Gugerell et al. 2020) have implemented minerals safeguarding policies.

In the UK, these policies are the designation of mineral safeguarding areas (MSAs), which are areas of known resources, permitted reserves, quarries and infrastructure sites, and mineral consultation areas (MCAs), areas based on MSAs but including a wider buffer zone. An MSA or MCA does not mean that mineral development (the winning and working of minerals or the depositing of mineral waste; Ministry of Housing, Communities and Local Government 2014) will happen, or that non-mineral development cannot happen. An MSA or MCA requires a non-mineral developer to prove either that mineral development would not be viable or that the non-mineral development is of greater strategic importance (The Mineral Products Association and The Planning Officers' Society 2019).

A similar system could be developed for mine water geothermal areas, where regulators could have the right to refuse the installation of geothermal systems in zones that have the potential to provide large amounts of heat, to preserve that potential for future large-scale systems. Of course, to do this, there would have to be an assessment of potential mine water geothermal areas and a mechanism to decide what a suitable-sized geothermal system would be.

4.6.2 Interference predictive model

To allow for prediction of the ΔT and HER without modelling, multiple linear regression analysis was performed to produce a simplified equation, using the well–shaft distance, flow rate and operating time to calculate ΔT.

The physically plausible values of ΔT are between zero and the ΔT_{max}, where the ΔT_{max} is the temperature difference between the initial rock temperature and the injection temperature. The water cannot heat beyond the warmest rock temperature and cannot become colder than the injection temperature. The equation does not reflect these physical limits, and, therefore, values obtained from this equation should be truncated between zero and ΔT_{max}.

This does not affect the usefulness of the equation as values close to zero illustrate a scenario that obviously needs to be avoided, and for values close to ΔT_{max} the system is already working close to optimal.

4.7 Conclusions

Our model simulations demonstrate that thermal interference of neighbouring MWG systems can be quantified. This interference increases with flow rate, time and a reduced distance between systems. To increase confidence in the technology and therefore increase the use of mine water geothermal systems, regulation is required to manage the thermal interference. The heat extraction ratio is proposed as a novel method to quantify thermal interference and can be used to set threshold values.

We propose two policy options to regulate the thermal inference:

(1) a unitisation-based approach: when an additional system would have too

significant an impact on the first system present, unitisation is required if feasible;

(2) a simplified yes or no approach: if an additional system would have too significant an impact on the first system present, the second system should not be allowed. If this system is used, highly prospective areas may need to be preserved for large-scale schemes.

CHAPTER 5

Conclusions

This thesis advances a multi-scale understanding of mine water geothermal (MWG) resources, from regional opportunity to scheme–scheme interaction. It first critically evaluates alternative regional prospectivity mapping methodologies, highlighting methodological limitations, and data requirements. It then assesses the benefits of dynamic, mine-specific heat assessment using GEMSToolbox compared with conventional static methods at the scheme scale, and finally quantifies thermal interference between neighbouring schemes and develops regulatory concepts to manage cumulative impacts and ensure the long-term sustainability of MWG deployment.

The research questions for this thesis, and their key findings, are as follows:

RQ1: What are the differences in mine water geothermal prospectivity mapping methods in terms of aims, data requirements, and the areas they identify as high or low prospectivity?

The comparison between assessed methods shows that they broadly share a common overarching aim of providing early stage screening and decision support, but differ in their data requirements and the way they express prospectivity, and that these choices strongly influence which areas are highlighted as favourable. MiRAS and the MRA maps both target planners and non-specialists who need to know

where open loop schemes are likely to be feasible, and use overlapping worked seams, mine water depth and mine depth as key controls. MiRAS applies relatively strict thresholds (for example 20–60 m water depth and workings shallower than 250 m) to delineate a small set of "optimal" zones, whereas the MRA mapping uses broader depth bands and additional categories such as "possible" and "challenging", resulting in a much larger area being flagged as having some opportunity. In contrast, the Georesources Cornwall method is deliberately simple, driven mainly by mine depth as a proxy for temperature and by mapped heat demand, and therefore serves as a coarse, high level overlay of deep mines and demand clusters rather than a detailed technical screen. Conceptual comparison with the Saxony methodology highlights a further step change in complexity, with multiple ranked underground parameters (including mine age, drainage, volume, plan quality, chemistry and accessibility) combined with heat demand in a weighted scheme to give a more holistic, but far more data intensive, assessment.

Applied to Newcastle, these methodological differences translate into distinct prospectivity patterns. All three implemented methods identify parts of the south and south east as favourable, but MiRAS maps only limited optimal areas, the Georesources Cornwall method highlights two principal clusters where deeper workings coincide with higher demand, and the MRA mapping shows the widest distribution of "good", "possible" and "challenging" zones. Differences in cut off values for mine and water depth, treatment of shallow workings, handling of missing water level data and the inclusion or exclusion of heat demand all contribute to these contrasting outputs, and in some cases lead to internally inconsistent categories (for example, areas with no mine water being classed as "challenging"). Overall, the comparison demonstrates that current MWG prospectivity methods span a spectrum from rapid but coarse mapping to more detailed, multi parameter frameworks, and that greater clarity, consistency and data availability are needed if their outputs are to be robustly compared and used to guide investment and planning.

RQ2: Does the use of GEMSToolbox provide added value in estimating extractable heat for mine water geothermal projects compared with

commonly used static methods?

This thesis finds that using GEMSToolbox provides added value for extractable heat estimation in mine water geothermal projects. Application of GEMSToolbox to a digitised two seam coal mine and to an equivalent synthetic grid model, and comparison with commonly used static methods (geothermal heat flow, mine water volume, rock volume and flow rate based approaches), shows that estimates of extractable heat for the same system and operating period can vary by orders of magnitude. Unlike static methods, GEMSToolbox explicitly evaluates the dynamic contribution of flow to heat extraction, while incorporating assumptions regarding heat recharge, in addition to the parameters required by conventional approaches. As a result, it is expected to provide more reliable estimates of extractable heat. GEMSToolbox delivers a more realistic, time-dependent representation of the extractable heat while relying largely on the same early stage data as static methods, supplemented by digitised mine geometry, and therefore improves the assessments without greatly increasing data requirements. The explicit representation of mine workings also enhances visualisation, providing intuitive three dimensional outputs that are useful for communicating scheme behaviour to non specialists, regulators and investors.

The work further demonstrates that the scenario testing capabilities within GEMSToolbox offer practical insight into scheme design and uncertainty. Alternative abstraction and injection locations, additional shafts and roadway collapse scenarios are explored (Figures 3.5 and 3.7), illustrating how these factors influence long term heat delivery and where schemes become particularly sensitive to geometric or operational assumptions. Fundamentally, changes in mine geometry change the length of flow path and the area of the mine that heat is accessed from. The scenario modelling demonstrates that when the flow path is lengthened (as occurs in the scenarios 'Long Separation', 'Constricted Pathways', and 'Extra Shaft (E)'), resulting in the re-injected water having a longer time to re-heat and a larger area to access heat from, the useable heat abstracted increases. Conversely, when the flow pathway decreases in length (scenarios 'Short Separation', 'Extra Shaft (N)', 'Dual Extra Shafts'), the usable heat abstracted decreases and the cold water from

the re-injection well will 'breakthrough' to the abstraction well sooner. The ability to test different scenarios and use the real mine plan geometry is particularly valuable given that flow pathways are among the most uncertain and computationally demanding aspects to constrain in a MWG system.

Benchmarking against commonly applied static estimation methods, alongside scenario-based evaluations undertaken using GEMSToolbox, highlights the value of a dynamic, geometry-explicit modelling approach that enables both assessment against established methods and systematic exploration of uncertainty in MWG systems.

Short runtimes and straightforward workflows mean that such dynamic assessments are viable at feasibility and pre-feasibility stages, where they can guide targeting of exploration, support mitigation planning and provide a more robust and transparent basis for assessing whether a scheme is likely to meet demand.

RQ3: How should thermal interference between neighbouring mine water systems be regulated, and what approaches could be appropriate in a UK context?

This thesis shows that thermal interference between neighbouring MWG schemes can and should be regulated using explicitly quantitative criteria grounded in scheme-scale modelling. Using GEMSToolbox, it is demonstrated that interference can be quantified through the heat extraction ratio (HER), which expresses the change in heat output from an existing scheme following the introduction of a new one. This provides regulators with a simple threshold metric, informed by distance, flow rate and operating lifetime, for judging whether a proposed development would cause an unacceptable loss of heat to an existing system. A review of international geothermal regulations, ground source heat pump guidance and UK oil and gas unitisation practice indicates that there are clear precedents for managing competing subsurface uses. Building on these insights and the modelling results, this thesis proposes two HER-based regulatory pathways suited to the UK context: a unitisation-style approach, in which schemes that would otherwise interfere beyond an agreed HER threshold are required to cooperate where feasible; and a simpler "yes/no" test, in

which applications that would breach the threshold are refused and, where necessary, highly prospective areas are safeguarded for larger future schemes. Together, these proposals outline a practical route for moving from implicit, water-centred licensing towards explicit, interference-based regulation of MWG heat extraction.

5.1 Improving investor confidence

Mine water geothermal (MWG) is a proven technology, with multiple operational schemes in the UK and internationally that deliver heating, cooling and thermal storage at up to multi megawatt scales. Nevertheless, the current number of MWG schemes remains small relative to the scale of the resource. A key barrier identified in this thesis and in the wider literature is a lack of investor confidence, arising from uncertainty in resource assessment, scheme performance and the regulatory environment.

Several aspects of this work contribute directly to reducing that uncertainty. First, the thesis highlights shortcomings in existing MWG prospectivity mapping methodologies and shows how methodological choices and data limitations can affect confidence in their outputs. By identifying the data types required for robust mapping and by proposing revised categorisation approaches, it points towards prospectivity frameworks that are more transparent, reproducible and transferable. If adopted, these improvements would support the development of a consistent, national MWG prospectivity map for UK coalfields, analogous to mineral prospectivity maps that have successfully raised the profile of other subsurface resources and attracted exploration investment.

Second, the thesis shows the benefits of incorporating dynamic, mine specific modelling into early stage heat assessment. Using GEMSToolbox, a streamlined numerical model purpose built for MWG that operates with similar data requirements to static screening methods but also includes digitised mine geometry, the work demonstrates that heat estimates from static vary by orders of magnitude and fail to capture key configuration effects such as shaft placement, roadway connectivity and potential collapse scenarios. Rapid dynamic simulations enable scheme design-

ers and investors to test realistic operating scenarios, explore uncertainty ranges and identify more resilient well configurations, which in turn improves the reliability of feasibility assessments and reduces perceived technical risk.

Third, the thesis addresses the risk of thermal interference between neighbouring MWG schemes and the current absence of regulations explicitly managing this risk. By quantifying how interference varies with spacing, flow rate and operational lifetime, and by introducing the heat extraction ratio (HER) as a simple metric to express the impact of a new scheme on an existing one, the work provides a practical basis for regulatory decision making. The proposed policy options, which use HER thresholds to trigger either unitisation or restrictions on new developments, illustrate how transparent and predictable rules could be formulated to manage cumulative impacts. In doing so, they respond directly to investor concerns about future crowding of the resource and the security of long term heat offtake.

Taken together, these contributions help strengthen the technical and regulatory evidence base for MWG, from the identification of prospective areas through to project scale performance assessment and the management of interactions between neighbouring schemes. This combination of improved screening, more realistic resource estimation and clearer regulatory concepts has the potential to increase investor confidence and support the wider deployment of MWG as part of a low carbon heat transition.

5.2 Recommendations for future data collection, analysis, and publication

Across this thesis, several important data gaps have been identified that constrain the assessment, design and regulation of mine water geothermal (MWG) schemes. Closing these gaps would substantially improve the robustness and transparency of future work in the field.

Depth to mine water is a critical control on MWG feasibility at both the regional (prospectivity mapping) and project feasibility stages. If the water level lies below the target workings and the workings are dry, no mine water scheme is possible.

Where workings are flooded, water depth is the primary control on ongoing pumping costs, while excessively shallow water levels may increase the risk of flooding. However, many mine water blocks lack any recorded water level data. There is a similar issue for temperature, with some mine blocks containing no measurements of mine water or host rock temperature. Hopefully the MRA's recent and ongoing drill program to monitor mine water will provide data for this (Mining Remediation Authority 2024c).

Depth of the targeted workings also strongly affects drilling cost, together with geology and the presence of shallower seams that must be drilled through. Practical challenges include hard rock, wellbore collapse and loss of drilling fluid. Walls et al. 2024 uses a cut-off value of 250 m for mine depth, based on drilling cost predictions provided by TownRock Energy, but these cost estimates are not in the public domain. The MRA does not state why its own depth cut-off values were selected, noting only that deeper workings are often younger and better recorded but more expensive to drill to. There is therefore a clear need for a systematic, publicly available review of drilling costs for both exploration and production-scale wells into mine workings. Such a dataset would improve the credibility and reproducibility of MWG prospectivity mapping methods.

With improved access to water level, temperature and drilling cost data, it would be feasible to develop a consistent MWG prospectivity map for all coal mining areas of the UK, rather than the current piecemeal situation, and to make this resource publicly available.

A future improvement to GEMSToolbox would be the ability to represent external groundwater flow entering and leaving the mine system. At present, if mine plans indicate that water flows through a roadway connected to workings that are not being modelled, this location can be represented as an injection node. This approach is valid where the inflow can reasonably be balanced by removing an equivalent volume of water elsewhere in the model. However, this method is suited only to scenarios where the unmodelled workings are hydraulically connected or where a discrete inflow–outflow balance can be approximated. It does not capture situations in which water enters or leaves the system diffusely through natural rock perme-

ability, which cannot currently be modelled. Modelling groundwater is important for both estimating extractable heat (Chapter 3) and predicting thermal interference (Chapter 4). Although some areas exhibit low groundwater flow, where flow is present it can provide additional heat recharge. Infiltrating groundwater can acquire heat from surrounding strata as it migrates towards mine workings, thereby slowing the rate at which a mine water geothermal system cools. This effect is not captured under the current modelling regime. Groundwater flow may also influence thermal interference between systems. For example, if System A reinjects cooled water upstream of System B's abstraction point, the resulting cold plume may reach System B sooner than predicted by models that do not incorporate advective transport. Results from Chapter 4 indicate that a mine water geothermal system should cool over time in the absence of reinjected heat. However, the Lanchester Wines systems at Abbottsford Road and Nest Road have not reported any decline in abstraction temperature since commissioning in 2018. Several explanations are possible:

1. The systems switch off during summer, allowing background geothermal fluxes to recharge the mines between heating seasons. Given the megawatt scale of the systems, this is unlikely.

2. The abstraction and reinjection points may be sufficiently far apart that the cold plume (as shown in Figure 4.2) has not yet reached the abstraction wells.

3. Natural groundwater flow may be recharging the systems, supplying heat and dispersing the cold plume.

The first step in investigating this is to model each system individually using GEMSToolbox, establishing the thermal front that would be expected to reach the abstraction wells from their respective reinjection wells. The second step is to assess local groundwater flow to determine its potential influence. Project Groundwater Northumbria (Kearsey et al. 2025), which recently mapped the hydrogeology in the area, may provide initial data for this.

A related question is whether the Lanchester Wines sites and the Gateshead system may experience thermal interference. The sites are known to be hydrogeologically connected (Banks et al. 2022; Monaghan et al. 2025). Modelling the

systems together would allow an initial assessment of whether cooling from one system is advected towards another. If groundwater replenishes heat to an upstream system, there is a risk that its cold plume could be transported towards a downstream site. To complement the modelling and establish whether water is exchanged between sites in addition to the known hydraulic pressure connection (Monaghan et al. 2025), a tracer test could be undertaken. The tracer test should be conducted both when the Abbottsford Road and Nest Road systems are switched off during the non heating season and when they are operating. Testing during shutdown would provide a baseline and insight into background groundwater flow. Testing during operation would show how pumping perturbs flow paths and the potential for future heat exchange. If no tracer is detected at the receiver sites, this would indicate that, despite hydraulic connectivity, water is not being directly exchanged. In such a case, advective heat transfer would not occur. Given the 700 m distance between Nest Road and Abbottsford Road, and the 1.9 km distance between Nest Road and the Gateshead system, conductive heat transfer would not occur over the operational lifetime of the systems, and thermal interference would not be a concern.

Bibliography

Abesser, C., Stacia Ryder, and Melanie Rohse (2023). *Considering Geothermal Energy Regulations in the UK*. Research brief. Unconventional Hydrocarbons in the UK Energy System (UKUH) Programme. URL: http://www.ukuh.org/media/sites/researchwebsites/2ukuh/Considering%20geothermal%20energy%20regulations%20in%20the%20UK_final.pdf.

Abesser, C. and A. Walker (2022). *Geothermal energy*. Tech. rep. 46. UK Parliamentary Office of Science and Technology. URL: https://researchbriefings.files.parliament.uk/documents/POST-PB-0046/POST-PB-0046.pdf.

Abesser, C. et al. (2018). *Who owns (Geothermal) heat?* Tech. rep. British Geological Survey. URL: https://www.bgs.ac.uk/download/science-briefing-paper-who-owns-geothermal-heat/.

Abeywickrama, Janith et al. (2021). "Geochemical characterization of fouling on mine water driven plate heat exchangers in Saxon mining region, Germany". In: *International Journal of Heat and Mass Transfer* 176, p. 121486. ISSN: 0017-9310. DOI: https://doi.org/10.1016/j.ijheatmasstransfer.2021.121486. URL: https://www.sciencedirect.com/science/article/pii/S0017931021005895.

ACIL Allen Consulting (2022). *Mineral Potential Mapper: A Geoscience Australia Case Study*. ACIL Allen Consulting. URL: https://acilallen.com.au/uploads/projects/809/ACILAllen_MineralPotentialMapper2022.pdf.

Act on the Survey and Utilisation of Ground Resources (1998). Secondary source referencing Act No. 57/1998 (use where direct act text is unavailable). Republic of Iceland. URL: https://www.wto.org/english/tratop_e/tpr_e/s273-04_e.doc (visited on 12/23/2025).

Adams, C., J. Gordon, and K. Parker (2023). "The Gateshead Mine Water Heat Scheme". In: *SPE Aberdeen Geothermal Seminar*.

Alvarado, Edgardo Jose et al. (2022). "Geothermal energy potential of active northern underground mines: designing a system relying on mine water". In: *Mine Water and the Environment* 41.4, pp. 1055–1081.

Andrés, C, A Ordóñez, and R Álvarez (2017). "Hydraulic and thermal modelling of an underground mining reservoir". In: *Mine water and the environment* 36.1, p. 24. DOI: 10.1007/s10230-015-0365-1.

Andrews, Billy J. et al. (2020). "Collapse processes in abandoned pillar and stall coal mines: Implications for shallow mine geothermal energy". In: *Geothermics* 88, p. 101904. ISSN: 0375-6505. DOI: 10.1016/j.geothermics.2020.101904. URL: https://www.sciencedirect.com/science/article/pii/S0375650520301966.

Asmus, D. and J.L. Weaver (2006). "Unitizing Oil and Gas Fields around the World: a comparative analysis of National Laws and Private Contracts". In: *Houston Journal of International Law* 28.

Axelsson, G and E Gunnlaugsson (2000). "Background: Geothermal utilization, management and monitoring". In: *Long-term monitoring of high-and low enthalpy fields under exploitation, WGC*, pp. 3–10.

Axelsson, Gudni et al. (2015). "Renewability assessment of the Reykjanes geothermal system, SW-Iceland". In: *Proceedings of the World Geothermal Congress 2015*.

Aydin, H. et al. (2020). "Evaluation of production capacity of geothermal power plants in Turkey". In: *GRC Transactions* 40, pp. 163–174.

Bailey, MT, AML Moorhouse, and IA Watson (2013). "Heat extraction from hypersaline mine water at the Dawdon mine water treatment site". In: *Mine Closure 2013: Proceedings of the Eighth International Seminar on Mine Closure*. Ed. by M Tibbett, AB Fourie, and C Digby. Cornwall: Australian Centre for Geomechanics, pp. 559–570. DOI: 10.36487/ACG_rep/1352_47_Bailey. URL: https://papers.acg.uwa.edu.au/p/1352_47_Bailey/.

Bailey, MT et al. (2016). "Heat recovery potential of mine water treatment systems in Great Britain". In: *International Journal of Coal Geology* 164, pp. 77–84. DOI: 10.1016/j.coal.2016.03.007. URL: https://www.sciencedirect.com/science/article/pii/S0166516216300490.

Banks, D. et al. (2004). "Heat pumps as a tool for energy recovery from mining wastes". In: *Geological Society, London, Special Publications* 236.1, pp. 499–513. DOI: 10.1144/GSL.SP.2004.236.01.27. eprint: https://www.lyellcollection.org/doi/pdf/10.1144/GSL.SP.2004.236.01.27. URL: https://www.lyellcollection.org/doi/abs/10.1144/GSL.SP.2004.236.01.27.

Banks, D. et al. (2019a). "A combined pumping test and heat extraction/recirculation trial in an abandoned haematite ore mine shaft, Egremont, Cumbria, UK". In: *Sustainable Water Resources Management* 5, pp. 51–69. DOI: 10.1007/s40899-017-0165-9. URL: https://doi.org/10.1007/s40899-017-0165-9.

Banks, D. et al. (2019b). "Water from abandoned mines as a heat source: practical experiences of open- and closed-loop strategies, United Kingdom". In: *Sustainable Water Resources Management* 5, pp. 29–50. DOI: 10.1007/s40899-017-0094-7.

Banks, D. et al. (2022). "Conceptual modelling of two large-scale Mine Water Geothermal Energy Schemes: Felling, Gateshead, UK". In: *International Journal of Environmental Research and Public Health* 19, p. 1643. DOI: 10.3390/ijerph19031643.

Banks, S.B and D Banks (2001). "Abandoned mines drainage: impact assessment and mitigation of discharges from coal mines in the UK". In: *Engineering Geology* 60.1. Geoenvironmental Engineering, pp. 31–37. ISSN: 0013-7952. DOI: https://doi.org/10.1016/S0013-7952(00)00086-7. URL: https://www.sciencedirect.com/science/article/pii/S0013795200000867.

Barich, Amel et al. (2022). "Social License to Operate in Geothermal Energy". In: *Energies* 15.1. ISSN: 1996-1073. DOI: 10.3390/en15010139. URL: https://www.mdpi.com/1996-1073/15/1/139.

Beatty, Christina, Stephen Fothergill, and Anthony Gore (2019). *The state of the coalfields 2019: Economic and social conditions in the former coalfields of England, Scotland and Wales*. Sheffield Hallam Universiuty.

Beckers, Koenraad F. et al. (2022). "Techno-Economic Performance of Closed-Loop Geothermal Systems for Heat Production and Electricity Generation". In: *Geothermics* 100, p. 102318. ISSN: 0375-6505. DOI: https://doi.org/10.1016/j.geothermics.2021.102318. URL: https://www.sciencedirect.com/science/article/pii/S037565052100273X.

Behrooz, Bazargan Sabet, Demollin Elianne, and Van Bergermeer Jan-Jaap (2008). "Geothermal use of deep flooded mines". In: *International symposium on post-mining, Nancy, France*, pp. 1–10.

BEIS (2021). *Final UK Greenhouse Gas Emissions National Statistics: 1990 to 2019*. Tech. rep. URL: https://assets.publishing.service.gov.uk/media/63e131dde90e07626846bdf9/greenhouse-gas-emissions-statistical-release-2021.pdf.

Belliardi, M., L. Soma, et al. (2022). "Application of a method for the sustainable planning and management of ground source heat pump systems in an urban environment, considering the effects of reciprocal thermal interference". In: *Open Research Europe* 2. DOI: 10.12688/openreseurope.14665.2.

Benderitter, Y and G Cormy (1990). "Possible approach to geothermal research and relative costs". In: *Small geothermal resources: A guide to development and utilization, UNITAR, New York*, pp. 59–69.

Birdsell, Daniel T. et al. (2024). "Analytical solutions to evaluate the geothermal energy generation potential from sedimentary-basin reservoirs". In: *Geothermics* 116, p. 102843. ISSN: 0375-6505. DOI: https://doi.org/10.1016/j.geothermics.2023.102843. URL: https://www.sciencedirect.com/science/article/pii/S0375650523001980.

Bott, Martin H. P. and Frederick W. Smith (2018). "The role of the Devonian Weardale Granite in the emplacement of the North Pennine mineralization". In: *Proceedings of the Yorkshire Geological Society* 62.1, pp. 1–15. DOI: 10.1144/pygs2017-391. eprint: https://www.lyellcollection.org/doi/pdf/10.1144/pygs2017-391. URL: https://www.lyellcollection.org/doi/abs/10.1144/pygs2017-391.

Brémaud, Maëlle et al. (2025). "International database of hot sedimentary aquifer geothermal projects: de-risking future projects by identifying key success and failure criteria". In: *Geoenergy* 3.1, geoenergy2024–031. DOI: 10.1144/geoenergy2024-031. eprint: https://www.lyellcollection.org/doi/pdf/10.1144/geoenergy2024-031. URL: https://www.lyellcollection.org/doi/abs/10.1144/geoenergy2024-031.

British Geological Survey (2021). *The Glasgow Observatory: A new open-access mine water energy research and innovation facility*. Accessed: 2025-09-19. URL: https://cms.ukgeos.ac.uk/opportunities/assets/docs/UKGEOS_Glasgow_observatory_brochure-min.pdf.

British Geological Survey (2024a). *Mining plans*. https://www.bgs.ac.uk/information-hub/scanned-records/mining-plans-2/. Accessed: 2025-12-08.
— (2024b). *UK Digital Geothermal Catalogue, Version 1*. Accessed: 2025-07-23. DOI: 10.5285/05569ed5-db0e-4587-807c-58e39ee240fa.
— (2025). *BGS Geology Viewer*. https://geologyviewer.bgs.ac.uk/. Contains British Geological Survey materials © UKRI. Accessed 6 November 2025.
Brune, Jürgen F. and Saqib A. Saki (2017). "Prevention of gob ignitions and explosions in longwall mining using dynamic seals". In: *International Journal of Mining Science and Technology* 27.6, pp. 999–1003. ISSN: 2095-2686. DOI: https://doi.org/10.1016/j.ijmst.2017.06.026. URL: https://www.sciencedirect.com/science/article/pii/S2095268617305220.
Burnside, N.M. et al. (2016). "Hydrochemistry and stable isotopes as tools for understanding the sustainability of minewater geothermal energy production from a 'standing column'heat pump system: Markham Colliery, Bolsover, Derbyshire, UK". In: *International Journal of Coal Geology* 165, pp. 223–230.
Burnside, N.M. et al. (2023). "Lessons from mine water geothermal projects across Central Scotland". In: *Proceedings of the World Geothermal Congress 2023*. Conference paper. Beijing, China. URL: https://strathprints.strath.ac.uk/87400/.
Busby, Jon (2014). "Geothermal energy in sedimentary basins in the UK". In: *Hydrogeology Journal* 22.1, pp. 129–141. DOI: 10.1007/s10040-013-1054-4. URL: https://doi.org/10.1007/s10040-013-1054-4.
Carr-Cornish, Simone and Lygia Romanach (2014). "Differences in Public Perceptions of Geothermal Energy Technology in Australia". In: *Energies* 7.3, pp. 1555–1575. ISSN: 1996-1073. DOI: 10.3390/en7031555. URL: https://www.mdpi.com/1996-1073/7/3/1555.
Carslaw, H. S. and J. C. Jaeger (1959). *Conduction of Heat in Solids*. 2nd. Oxford: Clarendon Press.
Chu, Z. et al. (2021). "Mine-oriented low-enthalpy geothermal exploitation: a review from spatio-temporal perspective". In: *Energy Conversion and Management* 237, p. 114123. DOI: 10.1016/j.enconman.2021.114123.
Chua, K.J., S.K. Chou, and W.M. Yang (2010). "Advances in heat pump systems: A review". In: *Applied Energy* 87.12, pp. 3611–3624. ISSN: 0306-2619. DOI: 10.1016/j.apenergy.2010.06.014. URL: https://www.sciencedirect.com/science/article/pii/S030626191000228X.
Ciriaco, Anthony E, Sadiq J Zarrouk, and Golbon Zakeri (2020). "Geothermal resource and reserve assessment methodology: Overview, analysis and future directions". In: *Renewable and Sustainable Energy Reviews* 119, p. 109515. DOI: 10.1016/j.rser.2019.109515.
Climate Change Committee, Adaptation Committee (June 2021). *Independent Assessment of UK Climate Risk: Advice to Government for the UK's Third Climate Change Risk Assessment (CCRA3)*. Accessible at the CCC's website; published 16June2021. London, United Kingdom: Climate Change Committee.
Coal Authority (2018). *Mine water block factsheets*. Accessed: 2023-07-12. URL: https://www.gov.uk/government/publications/mine-water-block-factsheets.
— (2022). *Written Evidence Submitted by the Coal Authority (GEO0032)*. Tech. rep. Environmental Audit Committee.

Coal Authority (2024a). *Mine entries data set: User guide*. https://www.gov.uk/government/publications/coal-mining-data-mine-entries/mine-entries-dataset-user-guide. Updated 9 February 2024, accessed 8 December 2025.
— (2024b). *Mine water energy scheme at Gateshead*. Accessed: 2024-06-21. URL: https://www2.groundstability.com/major-grant-to-connect-gateshead-homes-to-coal-authority-mine-water-energy-scheme/.
— (2024c). *Mine Water Heat Opportunity Mapping for 10 Cities in England: Overarching Report and Methodology*. Tech. rep. Accessed: 1 December 2025. Mansfield, UK: Coal Authority.
— (2024d). *Mine Water Heat Opportunity Maps for Wales: User Guide and Methodology*. Tech. rep. Prepared for the Welsh Government. Accessed: 1 December 2025. Mansfield, UK: Coal Authority.
— (2024e). *Newcastle Opportunity Map*. Geopackage. Resource in: Mine Water Heat Opportunity Mapping for 10 Cities in England (data.gov.uk). Data created/last updated 2024-09-19. Licence: Open Government Licence (OGL). URL: https://ckan.publishing.service.gov.uk/dataset/mine-water-heat-opportunity-mapping-for-10-cities-in-england/resource/d4f33daf-b77b-4ab1-882b-e23700bbde29 (visited on 12/19/2025).
— (2024f). *User Guide: In Seam Levels Dataset*. Coal Authority. Version 2.
— (2024g). *User Guide: Underground Working Dataset*. Coal Authority. Version 2.
— (2024h). *User Guide: Unlicensed Opencast Dataset*. Coal Authority. Version 2.
Coal Authority et al. (2019). *Guidance on Managing the Risk of Hazardous Gases when Drilling or Piling Near Coal: Version 2*. URL: https://assets.publishing.service.gov.uk/media/5d0b5af3ed915d09440c15aa/Guidance_on_managing_the_risk_of_hazardous_gases_when_drilling_or_piling_near_coal.pdf.
Coal Mines Regulation Act 1872 (1872). https://www.legislation.gov.uk/ukpga/Vict/35-36/76/pdfs/ukpga_18720076_en.pdf. Accessed: 2025-12-08.
Coles, Daniel et al. (Nov. 2021). "A review of the UK and British Channel Islands practical tidal stream energy resource". In: *Proceedings of the Royal Society A: Mathematical, Physical and Engineering Sciences* 477.2255, p. 20210469. ISSN: 1364-5021. DOI: 10.1098/rspa.2021.0469. eprint: https://royalsocietypublishing.org/rspa/article-pdf/doi/10.1098/rspa.2021.0469/726719/rspa.2021.0469.pdf. URL: https://doi.org/10.1098/rspa.2021.0469.
Comerford, A. et al. (2018). "Controls on geothermal heat recovery from a hot sedimentary aquifer in Guardbridge, Scotland: Field measurements, modelling and long term sustainability". In: *Geothermics* 76, pp. 125–140. ISSN: 0375-6505. DOI: https://doi.org/10.1016/j.geothermics.2018.07.004. URL: https://www.sciencedirect.com/science/article/pii/S0375650518300397.
Compernolle, Tine et al. (2019). "The impact of policy measures on profitability and risk in geothermal energy investments". In: *Energy Economics* 84, p. 104524. DOI: 10.1016/j.eneco.2019.104524.
Construction (Design and Management) Regulations 2015 (2015). Statutory Instrument 2015/51. UK legislation. URL: https://www.legislation.gov.uk/uksi/2015/51/contents/made.
Council, Cornwall (2016). *Cornwall Strategic Housing Land Availability Assessment (SHLAA)*. Cornwall Council, January 2016. Available online.

Council, Cornwall (2019). *Cornwall Site Allocations Development Plan Document*. Adopted 26 November 2019, Cornwall Council. Available online.

Cowley, Luke (Aug. 2022). *Hydrogeological Conceptual Model for Silksworth Mine Water Block (No. 34): Technical Note*. Tech. rep. Draft 1.1. Coal Authority and Environment Agency.

Davies, G. et al. (2023). "Evaluation of low temperature waste heat as a low carbon heat resource in the UK". In: *Applied Thermal Engineering* 235, p. 121283. ISSN: 1359-4311. DOI: https://doi.org/10.1016/j.applthermaleng.2023.121283. URL: https://www.sciencedirect.com/science/article/pii/S1359431123013121.

DBI GTI (2023). "Methodology Description of GIS Analyses". Unpublished contract description. Freiberg, Germany.

De Paoli, C. et al. (2023). "Modelling interactions between Three Aquifer Thermal Energy Storage (ATES) Systems in Brussels (Belgium)". In: *Applied Sciences* 13, p. 2934. DOI: 10.3390/app13052934.

Deeming, K. B. et al. (2026). "Screening of mine shafts for future energy technologies: a case study from the Scottish coalfields". In: *Energy Geoscience Conference Series* 1.1, egc1-2024–50. DOI: 10.1144/egc1-2024-50. eprint: https://www.lyellcollection.org/doi/pdf/10.1144/egc1-2024-50. URL: https://www.lyellcollection.org/doi/abs/10.1144/egc1-2024-50.

Department for Business, Energy & Industrial Strategy (2020). *Powering our Net Zero Future: Energy White Paper*. Command Paper Cm 9707. "Powering our Net Zero Future" – the UK Government's Energy White Paper. Her Majesty's Government. URL: https://assets.publishing.service.gov.uk/media/5fdc61e2d3bf7f3a3bdc8cbf/201216_BEIS_EWP_Command_Paper_Accessible.pdf.

Department for Energy Security and Net Zero (2025a). *Energy Consumption in the United Kingdom (ECUK): 2025 End Use data tables*. https://www.data.gov.uk/dataset/26afb14b-be9a-4722-916e-10655d0edc38/energy-consumption-in-the-uk. Dataset: *Energy Consumption in the UK*. Published 25 September 2025.

— (2025b). *UK Geothermal Platform: Summary layers methodology and user guidance*. Technical report. UK Government. URL: https://assets.publishing.service.gov.uk/media/68920a0cdc6688ed50878476/uk-geothermal-platform-summary-layers.pdf.

Department for Energy Security and Net Zero and Department for Business, Energy & Industrial Strategy (2025). *Historical coal data: coal production, availability and consumption, 1853 to 2024*. Last updated 31 July 2025. URL: %5Curl%7Bhttps://www.gov.uk/government/statistical-data-sets/historical-coal-data-coal-production-availability-and-consumption%7D.

Department of the Environment and Welsh Office (1994). *Mineral Planning Guidance 12: Treatment of Disused Mine Openings and Availability of Information on Mined Ground*. Mineral Planning Guidance MPG 12. London: Department of the Environment; Welsh Office. URL: https://www.gov.wales/sites/default/files/publications/2019-01/minerals-planning-guidance-12.pdf.

Destek, Mehmet Akif, Samuel Asumadu Sarkodie, and Ernest Frimpong Asamoah (2021). "Does biomass energy drive environmental sustainability? An SDG perspective for top five biomass consuming countries". In: *Biomass and Bioenergy* 149, p. 106076. ISSN: 0961-9534. DOI: https://doi.org/10.1016/j.biombioe.

2021.106076. URL: https://www.sciencedirect.com/science/article/pii/S0961953421001136.

Dewi, Marmelia P., Andri D. Setiawan, and Yusuf Latief (2020). "Developing a Sustainable Financing Model for Geothermal Projects: A Conceptual Framework". In: *Proceedings of the 3rd Asia Pacific Conference on Research in Industrial and Systems Engineering*. APCORISE '20. Depok, Indonesia: Association for Computing Machinery, pp. 355–360. ISBN: 9781450376006. DOI: 10.1145/3400934.3400999. URL: 10.1145/3400934.3400999.

Dickson, Mary H. et al. (2005). *Geothermal energy: utilization and technology*. eng. 1st ed. London: Routledge. ISBN: 9781138991880.

Donnelly, Laurance (2020). "Chapter 11Coal mining subsidence in the UK". In: *Geological Society, London, Engineering Geology Special Publications* 29.1, pp. 291–309. DOI: 10.1144/EGSP29.11. eprint: https://www.lyellcollection.org/doi/pdf/10.1144/EGSP29.11. URL: https://www.lyellcollection.org/doi/abs/10.1144/EGSP29.11.

Doris, E., C. Kreycik, and K. Young (2009). *Policy Overview and Options for Maximizing the Role of Policy in Geothermal Electricity Development*. Tech. rep. Golden, CO: National Renewable Energy Laboratory. DOI: 10.2172/1219322.

Dudek, Mateusz et al. (2020). "Predicting of land surface uplift caused by the flooding of underground coal mines – A case study". In: *International Journal of Rock Mechanics and Mining Sciences* 132, p. 104377. ISSN: 1365-1609. DOI: https://doi.org/10.1016/j.ijrmms.2020.104377. URL: https://www.sciencedirect.com/science/article/pii/S1365160919307038.

Duijff, R., M. Bloemendal, and M. Bakker (2023). "Interaction effects between aquifer thermal energy storage systems". In: *Groundwater* 61, pp. 173–182. DOI: 10.1111/gwat.13163.

Dumas, Philippe et al. (June 2019). "Risk Mitigation and Insurance Schemes Adapted to Geothermal Market Maturity: The Right Scheme for my Market". In.

Durham County Council (2024). *Milestone in mine water heat project as work starts*. https://www.durham.gov.uk/article/32588/News-Milestone-in-mine-water-heat-project-as-work-starts. News article. (Visited on 09/15/2025).

Ebel, Tom et al. (2025). *Grubenwasserpotenzialstudie Sachsen: Kategorisierung und Analyse von Grubenwässern in stillgelegten Bergwerken Sachsens hinsichtlich ihres geothermischen Potenzials*. Abschlussbericht, Schriftenreihe des LfULG. Sächsisches Landesamt für Umwelt, Landwirtschaft und Geologie.

EGS Energy Ltd and Carrak Consulting Ltd (2019). "Geothermal Energy Screening Assessment: Heat resource potential from abandoned metal mines in Cornwall". In: *Georesources Cornwall: Recommendations for development of the Georesources sector in Cornwall. Working Paper, Version 10 October 2019*. Ed. by Frances Wall and Alexandra Sweeney. Appendix to Section 3. Penryn, Cornwall: Camborne School of Mines, University of Exeter.

Energy Security & Net Zero, Department for (2025a). *Energy Trends UK, January to March 2025*. Statistical Release Energy Trends, June 2025. Statistical release covering UK energy production, trade, and consumption by fuel type. Her Majesty's Government. URL: https://assets.publishing.service.gov.uk/media/685bda130433072fce0e0fe1/Energy_Trends_June_2025.pdf.

Energy Security & Net Zero, Department for (2025b). *English Housing Survey 2023-24: Low Carbon Technologies in English Homes*. https://www.gov.uk/government/statistics/english-housing-survey-2023-to-2024-low-carbon-technologies-in-english-homes-fact-sheet. Household use of heating systems by fuel type.

European Geothermal Energy Council (2023). *2022 EGEC Geothermal Market Report Key Findings*. Tech. rep.

Eynon, Joanne (2024). "Understanding Mine Water Heat Access Agreements: Purpose and Requirements". In: *2024 Mine Water Geothermal Energy Symposium*. Conference presentation, available on YouTube. IEA Geothermal. URL: https://www.youtube.com/watch?v=DRZ6l-Wvf9Q (visited on 09/25/2025).

Falmouth Packet (2025). "Fate heavily criticised as geothermal plant decided". In: *Falmouth Packet*. Accessed: 2025-09-26. URL: https://www.falmouthpacket.co.uk/news/25495088.fate-heavily-criticised-geothermal-plant-decided/.

Farr, G et al. (2021). "The temperature of Britain's coalfields". In: *Quarterly Journal of Engineering Geology and Hydrogeology* 54.3, qjegh2020–109. DOI: 10.1144/qjegh2020-109.

Fascì, M.L. et al. (2019). "Analysis of the thermal interference between ground source heat pump systems in dense neighborhoods". In: *Science and Technology for the Built Environment* 25, pp. 1069–1080. DOI: 10.1080/23744731.2019.1648130.

Ferket, H., L. Ben, and P. Tongeren (2011). "Transforming flooded coal mines to large-scale geothermal and heat storage reservoirs: what can we expect?" In: *Mine Water Managing the Challenges*. Ed. by T.R. Rüde, A. Freund, and C. Wolkersdorfer. 11th International Mine Water Association Congress. Aachen, Germany, pp. 171–175.

Fernández Fuentes, Isabel et al. (2022). "The CROWDTHERMAL Project: Creating Public Acceptance of Geothermal Energy and Opportunities for Community Financing". In: *Energies* 15.21. ISSN: 1996-1073. DOI: 10.3390/en15218310. URL: https://www.mdpi.com/1996-1073/15/21/8310.

Fernihough, Alan and Kevin Hjortshøj O'Rourke (2021). "Coal and the European industrial revolution". In: *The Economic Journal* 131.635, pp. 1135–1149. DOI: 10.1093/ej/ueaa117.

Fraser-Harris, Andrew et al. (2022). "The geobattery concept: a geothermal circular heat network for the sustainable development of near surface low enthalpy geothermal energy to decarbonise heating". In: *Earth Science, Systems and Society* 2.1, p. 10047. DOI: 10.3389/esss.2022.10047.

Galvin, J. M. (2016). "Pillar Extraction". In: *Ground Engineering - Principles and Practices for Underground Coal Mining*. Cham: Springer International Publishing, pp. 309–358. ISBN: 978-3-319-25005-2. DOI: 10.1007/978-3-319-25005-2_8. URL: https://doi.org/10.1007/978-3-319-25005-2_8.

Gateshead Council, Coal Authority, and IEA Geothermal (2023). *Mine Water Heat Network, UK*. Tech. rep. Case study prepared for the IEA Geothermal Case Studies series. Gateshead Energy Company (GEC). URL: https://drive.google.com/file/d/1xlVCiyqM3b7JQsYJHfJl0YzTugweSL_Q/view (visited on 09/15/2025).

Gehringer, Magnus and Victor Loksha (2012). *Geothermal Handbook: Planning and Financing Power Generation*. ESMAP Technical Report 002/12. © World Bank.

License: CC BY 3.0 IGO. Washington, DC: World Bank. URL: https://openknowledge.worldbank.org/handle/10986/23712.

Ghoreishi Madiseh, S. A. et al. (May 2012). "Sustainable heat extraction from abandoned mine tunnels: A numerical model". In: *Journal of Renewable and Sustainable Energy* 4.3, p. 033102. ISSN: 1941-7012. DOI: 10.1063/1.4712055. eprint: https://pubs.aip.org/aip/jrse/article-pdf/doi/10.1063/1.4712055/13658533/033102_1_online.pdf. URL: 10.1063/1.4712055.

Gillespie, MR, EJ Crane, and HF Barron (2013). "Study into the potential for deep geothermal energy in Scotland". In: *British Geological Survey Commissioned Report*. URL: https://nora.nerc.ac.uk/id/eprint/507992/1/00437996.pdf.

Gluyas, J.G., C.A. Adams, and I.A.G. Wilson (2020). "The theoretical potential for large-scale underground thermal energy storage (UTES) within the UK". In: *Energy Reports* 6, pp. 229–237. DOI: 10.1016/j.egyr.2020.12.006.

Gonzalez, J. M., J. E. Tomlinson, E. A. Martínez Ceseña, et al. (2023). "Designing diversified renewable energy systems to balance multisector performance". In: *Nature Sustainability* 6, pp. 415–427. DOI: 10.1038/s41893-022-01033-0. URL: https://doi.org/10.1038/s41893-022-01033-0.

Gonzalez Quiros, Andres et al. (2025). "Influence of mine geometry and working type on groundwater flow and heat transport for geothermal exploitation". In: URL: https://www.imwa.info/docs/imwa_2025/IMWA2025_GonzalezQuiros_377.pdf.

Goodman, R. et al. (2007). "GTR-H-Geothermal Regulations in Europe, the Kistelek process". In: *Proceedings European Geothermal Congress*. Unterhaching, Germany.

Gordon, G.W. (2015). "Production licensing on the UK Continental Shelf: Ministerial Powers and controls". In: *LSU Journal of Energy Law and Resources* 4, p. 75. URL: https://digitalcommons.law.lsu.edu/jelr/vol4/iss1/8.

Goudarzi, ESHAGH et al. (2023). "Mine water utilization as a secondary heat source and heat storage in a smart local heating and cooling distribution system". In: *9th International Conference on Smart Local Energy Systems*.

Grant, MA (2014). "Stored-heat assessments: a review in the light of field experience". In: *Geothermal Energy Science* 2.1, pp. 49–54. DOI: 10.5194/gtes-2-49-2014.

Greco, Adriana et al. (2020). "A Comparative Study on the Performances of Flat Plate and Evacuated Tube Collectors Deployable in Domestic Solar Water Heating Systems in Different Climate Areas". In: *Climate* 8.6. ISSN: 2225-1154. DOI: 10.3390/cli8060078. URL: https://www.mdpi.com/2225-1154/8/6/78.

Gregory, C.E. (1983). *Rudiments of Mining Practice*. Trans Tech Publications.

Haehnlein, S., P. Bayer, and P. Blum (2010). "International legal status of the use of shallow geothermal energy". In: *Renewable and Sustainable Energy Reviews* 14, pp. 2611–2625. DOI: 10.1016/j.rser.2010.07.069.

Happold, Buro (2015). *Cornwall Strategic Heat Opportunities Study*. Commissioned by Cornwall Council. Unpublished report.

Hartman, H.L. (2002). *Introductory Mining Engineering*. Hoboken, NJ: Wiley.

Hatcher, John (June 1993a). "187Mines and the Techniques of Mining". In: *The History of the British Coal Industry: Volume 1: Before 1700: Towards the Age of Coal*. Oxford University Press. ISBN: 9780198282822. DOI: 10.1093/acprof:

oso/9780198282822.003.0006. eprint: https://academic.oup.com/book/0/chapter/197491183/chapter-ag-pdf/44605705/book_27522_section_197491183.ag.pdf. URL: https://doi.org/10.1093/acprof:oso/9780198282822.003.0006.

Hatcher, John (June 1993b). "The Coalfields of Britain". In: *The History of the British Coal Industry: Volume 1: Before 1700: Towards the Age of Coal*. Oxford University Press. ISBN: 9780198282822. DOI: 10.1093/acprof:oso/9780198282822.003.0005. eprint: https://academic.oup.com/book/0/chapter/197486501/chapter-ag-pdf/44605721/book_27522_section_197486501.ag.pdf. URL: https://doi.org/10.1093/acprof:oso/9780198282822.003.0005.

Hochstein, Manfred P (1990). "Classification and assessment of geothermal resources". In: *Small geothermal resources: A guide to development and utilization, UNITAR, New York*, pp. 31–57.

Horne, R., A. Genter, M. McClure, et al. (2025). "Enhanced geothermal systems for clean firm energy generation". In: *Nature Reviews Clean Technology* 1, pp. 148–160. DOI: 10.1038/s44359-024-00019-9.

Infrastructure Act 2015 (2015). https://www.legislation.gov.uk/ukpga/2015/7/contents/enacted. UK Public General Acts, 2015 c. 7.

Intergovernmental Panel on Climate Change (IPCC), Core Writing Team; H. Lee and J. Romero (eds.) (2023). *Summary for Policy Makers. In: Climate Change2023: Synthesis Report*. IPCC Synthesis Report – Summary for Policymakers. Geneva, Switzerland: World Meteorological Organization; United Nations Environment Programme, pp. 1–34. DOI: 10.59327/IPCC/AR6-9789291691647.001.

International Renewable Energy Agency (IRENA) (2017). *Geothermal Power: Technology Brief*. IRENA Technology Brief E01, August 2017. Abu Dhabi: International Renewable Energy Agency. URL: https://www.irena.org/-/media/Files/IRENA/Agency/Publication/2017/Aug/IRENA_Geothermal_Power_2017.pdf.

Ioannou, Anastasia et al. (2023a). "A Decision Support Tool for Social Engagement, Alternative Financing and Risk Mitigation of Geothermal Energy Projects". In: *Energies* 16.3. ISSN: 1996-1073. URL: https://www.mdpi.com/1996-1073/16/3/1280.

— (2023b). "A Decision Support Tool for Social Engagement, Alternative Financing and Risk Mitigation of Geothermal Energy Projects". In: *Energies* 16.3. ISSN: 1996-1073. DOI: 10.3390/en16031280. URL: https://www.mdpi.com/1996-1073/16/3/1280.

Jessop, Alan M, Jack K MacDonald, and Howard Spence (1995). "Clean energy from abandoned mines at Springhill, Nova Scotia". In: *Energy Sources* 17.1, pp. 93–106. DOI: 10.1080/00908319508946072.

Jia, Y., C. F. Tsang, A. Hammar, et al. (2022). "Hydraulic stimulation strategies in enhanced geothermal systems (EGS): a review". In: *Geomechanics and Geophysics for Geo-Energy and Geo-Resources* 8, p. 211. DOI: 10.1007/s40948-022-00516-w.

Jin, Siya and Deborah Greaves (2021). "Wave energy in the UK: Status review and future perspectives". In: *Renewable and Sustainable Energy Reviews* 143, p. 110932. ISSN: 1364-0321. DOI: https://doi.org/10.1016/j.rser.2021.110932. URL: https://www.sciencedirect.com/science/article/pii/S1364032121002240.

Kearey, Philip, Michael Brooks, and Ian Hill (2002). *An introduction to geophysical exploration*. Vol. 4. John Wiley & Sons.

Kearsey, T et al. (2025). *Bedrock Sandstone channel subsurface mapping for the Gateshead area-Project Groundwater Northumbria*. Tech. rep. British Geological Survey.

Kelly, Joseph J. and Christopher I. McDermott (2022). "Numerical modelling of a deep closed-loop geothermal system: evaluating the Eavor-Loop". In: *AIMS Geosciences* 8.2, pp. 175–212. ISSN: 2471-2132. DOI: 10.3934/geosci.2022011. URL: https://www.aimspress.com/article/doi/10.3934/geosci.2022011.

Kemp, A. (2013). *The Official History of North Sea Oil and Gas: Volume I: The Growing Dominance of the State*. Routledge.

Kępińska, Beata et al. (2021). "Risk insurance fund for geothermal energy projects in selected European countries–operational and financial simulation". In: *gospodarka surowcami mineralnymi* 37.3. DOI: DOI:10.24425/gsm.2021.138654.

Koley, Susmita et al. (2024). "Experimental parametric evaluation of adsorption characteristics for silica gel - water based open-bed system for seasonal thermal energy storage". In: *Journal of Energy Storage* 89, p. 111812. ISSN: 2352-152X. DOI: https://doi.org/10.1016/j.est.2024.111812. URL: https://www.sciencedirect.com/science/article/pii/S2352152X24013975.

Law of the Republic of Indonesia Number 21 of 2014 on Geothermal (Sept. 17, 2014). English text PDF. House of Representatives of the Republic of Indonesia. URL: https://policy.asiapacificenergy.org/sites/default/files/Geothermal%20Law.pdf (visited on 12/23/2025).

Li, Jingyi, Cathy Hollis, and Alejandro Gallego-Schmid (2025). "Equity or profit? Understanding the social sustainability challenges of mine water heating network implementation". In: *Energy Research & Social Science* 124, p. 104062. ISSN: 2214-6296. DOI: https://doi.org/10.1016/j.erss.2025.104062. URL: https://www.sciencedirect.com/science/article/pii/S2214629625001434.

Li, Jingyi et al. (2024). "Life cycle assessment of repurposing abandoned onshore oil and gas wells for geothermal power generation". In: *Science of The Total Environment* 907, p. 167843. ISSN: 0048-9697. DOI: https://doi.org/10.1016/j.scitotenv.2023.167843. URL: https://www.sciencedirect.com/science/article/pii/S0048969723064707.

Loredo, C., N. Roqueñí, and A. Ordóñez (2016). "Modelling flow and heat transfer in flooded mines for geothermal energy use: a review". In: *International Journal of Coal Geology* 164, pp. 115–122. DOI: 10.1016/j.coal.2016.04.013.

Loredo, Covadonga, David Banks, and Nieves Roqueñí (2017). "Evaluation of analytical models for heat transfer in mine tunnels". In: *Geothermics* 69, pp. 153–164. ISSN: 0375-6505. DOI: https://doi.org/10.1016/j.geothermics.2017.06.001. URL: https://www.sciencedirect.com/science/article/pii/S0375650517301955.

Malafeh, S. and B. Sharp (2015). "Role of royalties in sustainable geothermal energy development". In: *Energy Policy* 85, pp. 235–242. DOI: 10.1016/j.enpol.2015.06.023.

Mallin Martin, D. and L. Smedley P. (2021). *Baseline groundwater chemistry: the Pennine Coal Measures of the East Midlands and South Yorkshire*. Open Report OR/21/023. Keyworth, Nottingham: British Geological Survey. URL: https://nora.nerc.ac.uk/id/eprint/531736/1/OR21023.pdf.

Malolepszy, Zbigniew (2003). "Low temperature, man-made geothermal reservoirs in abandoned workings of underground mines". In: *Proceedings of the 28th workshop on geothermal reservoir engineering, Stanford University, USA*. URL: https://pangea.stanford.edu/ERE/pdf/IGAstandard/SGW/2003/Malolepszy.pdf.

Management of Health and Safety at Work Regulations 1999 (1999). Statutory Instrument 1999/3242. UK legislation. URL: https://www.legislation.gov.uk/uksi/1999/3242/contents/made.

Manzella, A., A. Allansdottir, and A. Pellizzone (2018). *Geothermal Energy and Society*. Cham: Springer.

Marchi-Smith, Rhiannon (Aug. 2022). *Hydrogeological Conceptual Model for Bowburn–Trimdon Grange Mine Water Block (No. 38): Technical Note*. Tech. rep. Draft 1.1. Coal Authority and Environment Agency.

Marchi-Smith, Rhiannon and Lee Wyatt (Aug. 2022a). *Hydrogeological Conceptual Model for Dawdon–Horden Mine Water Block (No. 35): Technical Note*. Tech. rep. Draft 1.1. Coal Authority and Environment Agency.

— (Aug. 2022b). *Hydrogeological Conceptual Model for South of Butterknowle Fault Mine Water Block (No. 40): Technical Note*. Tech. rep. Draft 1.1. Coal Authority and Environment Agency.

— (Nov. 2024a). *Hydrogeological Conceptual Model for Lumley Mine Water Block (No. 26): Technical Note*. Tech. rep. Draft 1.2. Coal Authority and Environment Agency.

— (Nov. 2024b). *Hydrogeological Conceptual Model for Westoe–Wearmouth Mine Water Block (No. 27): Technical Note*. Tech. rep. Draft 1.3. Coal Authority and Environment Agency.

McCay, Alistair T., Manousos Valyrakis, and Paul L. Younger (2018). "A meta-analysis of coal mining induced subsidence data and implications for their use in the carbon industry". In: *International Journal of Coal Geology* 192, pp. 91–101. ISSN: 0166-5162. DOI: https://doi.org/10.1016/j.coal.2018.03.013. URL: https://www.sciencedirect.com/science/article/pii/S0166516217307000.

McClean, A. and O.W. Pedersen (2021). "Who owns the heat? The scope for geothermal heat to contribute to net zero". In: *Journal of Environmental Law* 34, pp. 343–351. DOI: 10.1093/jel/eqab038.

— (2023). "The role of regulation in geothermal energy in the UK". In: *Energy Policy* 173, p. 113378. DOI: 10.1016/j.enpol.2022.113378.

McLean, W. S. (2018). *Scottish coal seam names and correlations*. Open Report OR/18/027. Unpublished. Nottingham, UK: British Geological Survey, p. 19. URL: https://nora.nerc.ac.uk/id/eprint/520887/1/OR18027.pdf.

Mijnwater Energy BV and IEA Geothermal (2023). *Mine Water Geothermal: Heerlen District Energy Scheme*. Tech. rep. Case study prepared for the IEA Geothermal Case Studies series. Mijnwater Energy BV. URL: https://www.mijnwater.com/en/about-mijnwater (visited on 09/15/2025).

Mines and Quarries Act 1954 (1954). https://www.legislation.gov.uk/ukpga/Eliz2/2-3/70/contents. 2 & 3 Eliz. 2 c. 70, Section 17: Plans of workings.

Mining Remediation Authority (2024a). *Mine Water Discharge Points Dataset*. Data service via Digimap. Accessed via Digimap.

Mining Remediation Authority (Dec. 2024b). *Mine water heat access agreement: Information on mine water heat access agreements*. GOV.UK. Guidance, last updated 13 December 2024. URL: https://www.gov.uk/government/publications/mine-water-heat-access-agreement/information-on-mine-water-heat-access-agreements (visited on 09/25/2025).

— (2024c). *Upcoming opportunity for contractors*. Accessed: 2026-05-18. URL: https://www.miningremediation.co.uk/upcoming-opportunity-for-contractors/.

— (2025a). *Coal mining production and manpower returns from January to March 2025*. Accessed: 08 December 2025.

— (Mar. 2025b). *Further breakthrough in using mine water to provide green heat*. Accessed: 2025-05-29. URL: https://www.gov.uk/government/news/further-breakthrough-in-using-mine-water-to-provide-green-heat.

Möller, Bernd et al. (2022). *Peta: The Pan-European Thermal Atlas, version 5.2: developed as part of the sEEnergies project*. Interactive web map. Heat demand layer. URL: https://www.seenergies.eu/peta5/.

Monaghan, Alison A et al. (2022). "Drilling into mines for heat: geological synthesis of the UK Geoenergy Observatory in Glasgow and implications for mine water heat resources". In: *Quarterly Journal of Engineering Geology and Hydrogeology* 55, qjegh2021–033. DOI: 10.1144/qjegh2021-033.

Monaghan, Alison A et al. (2025). "Geological factors in the sustainable management of mine water heating, cooling and thermal storage resources in the UK". In: *Energy Geoscience Conference Series* 1, egc1-2023–39. DOI: 10.1144/egc1-2023-39.

Mouli-Castillo, J. et al. (2024). "GEMSToolbox: a novel modelling tool for rapid screening of mines for geothermal heat extraction". In: *Applied Energy* 360, p. 122786. DOI: 10.1016/j.apenergy.2024.122786.

Mourik, Mikey van (May 7, 2025). *Operational findings from the UK's first multi-megawatt mine water geothermal heating schemes at Lanchester Wines*. Presentation (video link) at the 2025 Mine Water Geothermal Energy Symposium (online). IEA Geothermal. URL: https://www.iea-gia.org/workshops-and-symposium/2025-mine-water-geothermal-energy-symposium (visited on 12/17/2025).

Muffler, P and Raffaele Cataldi (1978). "Methods for regional assessment of geothermal resources". In: *Geothermics* 7.2-4, pp. 53–89. DOI: 10.1016/0375-6505(78)90002-0.

National Coal Board (1982). *The Treatment of Disused Mine Shafts and Adits*. London: National Coal Board.

National Statistics, Office for (2025). *The impact of higher energy costs on UK businesses: 2021 to 2024*. Tech. rep. Released 19 May 2025. Office for National Statistics.

Nicholson, Keith (1993). "Geothermal Systems". In: *Geothermal Fluids: Chemistry and Exploration Techniques*. Berlin, Heidelberg: Springer Berlin Heidelberg, pp. 1–18. ISBN: 978-3-642-77844-5. DOI: 10.1007/978-3-642-77844-5_1. URL: 10.1007/978-3-642-77844-5_1.

Nomis (2025). *Custom report: 2021 Census (compare area: E08000021)*. URL: https://www.nomisweb.co.uk/sources/census_2021/report?compare=E08000021 (visited on 12/16/2025).

North East LEP Mine Energy Taskforce (2024). *A Mine Energy White Paper: The Case for Mine Energy – unlocking deployment at scale in the UK*. White paper, commissioned by North East Local Enterprise Partnership and Mine Energy Taskforce. According to the Coal Authority, one quarter of the UK's homes and businesses are sited on former coalfields. URL: https://evidencehub.northeast-ca.gov.uk/report/a-mine-energy-white-paper.

North Sea Transition Authority (2018). *Consolidated Onshore Guidance*. Tech. rep. URL: https://www.nstauthority.co.uk/media/8015/29112017_consolidated-onshore-guidance-compendium_vfinal-002.pdf.

Nur, Suardi et al. (2023). "Determining optimal incentives for geothermal projects procured within PPP framework under the tariff constraints". In: *Renewable Energy Focus* 45, pp. 21–39. ISSN: 1755-0084. DOI: https://doi.org/10.1016/j.ref.2023.02.006. URL: https://www.sciencedirect.com/science/article/pii/S1755008423000236.

Nurmi, Pekka A. (2020). "The Geological Survey of Finland strengthening its role as a key player in mineral raw materials innovation ecosystems". In: *Geological Society, London, Special Publications* 499.1, pp. 149–163. DOI: 10.1144/SP499-2019-83. eprint: https://www.lyellcollection.org/doi/pdf/10.1144/SP499-2019-83. URL: https://www.lyellcollection.org/doi/abs/10.1144/SP499-2019-83.

O'Sullivan, Michael, Angus Yeh, and Warren Mannington (2010). "Renewability of geothermal resources". In: *Geothermics* 39.4. Special Issue on the Sustainable Utilization of Geothermal Energy, pp. 314–320. ISSN: 0375-6505. DOI: https://doi.org/10.1016/j.geothermics.2010.09.003. URL: https://www.sciencedirect.com/science/article/pii/S0375650510000428.

Olver, Thomas and Ryan Law (2025). "The United Downs Geothermal Power Plant, Cornwall, UK: combining the generation of geothermal electricity and heat, with the extraction of critical raw materials". In: *Proceedings of the 50th Workshop on Geothermal Reservoir Engineering, Stanford University, Stanford, California*.

Oppelt, Lukas et al. (2022). "Mine water geothermal energy: abandoned mines as a green energy source". In: *CLIMA 2022 conference*.

Oppelt, Lukas et al. (2025). "Mine Water as an Energy Source: Overview of Technical Basics, Existing Plants, and Monitoring Results". In: *Mine Water and the Environment*, pp. 1–25. DOI: 10.1007/s10230-025-01057-w.

Ordnance Survey (2025). *OS Terrain 5 DTM, July 2025*. Dataset. Scale 1:10,000, 5 m grid. Available via EDINA Digimap Ordnance Survey Service.

Østergaard, Dorte Skaarup et al. (2022). "Low-temperature operation of heating systems to enable 4th generation district heating: A review". In: *Energy* 248, p. 123529. ISSN: 0360-5442. DOI: 10.1016/j.energy.2022.123529. URL: https://www.sciencedirect.com/science/article/pii/S0360544222004327.

Partington, Gregor et al. (Jan. 2016). "A Review of Mineral Potential Modelling in NZ During the Past 15 Years". In: p. 53. ISBN: 978-1-925100-53-2.

Peng, Syd S. (2019). *Longwall mining*. eng. Third edition. London: CRCpress/Balkema, an imprint of the Taylor & Francis Group. ISBN: 0-429-52219-3.

Peralta Ramos, Eduardo, Klaus Breede, and Gioia Falcone (2015). "Geothermal heat recovery from abandoned mines: a systematic review of projects implemented worldwide and a methodology for screening new projects". In: *Environmental*

Earth Sciences 73, pp. 6783–6795. DOI: 10.1007/s12665-015-4285-y. URL: https://doi.org/10.1007/s12665-015-4285-y.

Perego, R. et al. (2022). "Intensive thermal exploitation from closed and open shallow geothermal systems at urban scale: unmanaged conflicts and potential synergies". In: *Geothermics* 103, p. 102417. DOI: 10.1016/j.geothermics.2022.102417.

Phillips, Geraint and Grant Wilson (2024). "Investigating Changes in Natural Gas Demand across Great Britain for Domestic Heating Using Daily Data: 2018 to 2024". In: *Energies* 17.19. ISSN: 1996-1073. DOI: 10.3390/en17194884. URL: https://www.mdpi.com/1996-1073/17/19/4884.

Preene, M. and Paul L. Younger (2014). "Can you take the heat?– geothermal energy in mining". In: *Mining Technology* 123, pp. 107–118. DOI: 10.1179/1743286314Y.0000000058.

Provision and Use of Work Equipment Regulations 1998 (1998). Statutory Instrument 1998/2306. UK legislation. URL: https://www.legislation.gov.uk/uksi/1998/2306/contents/made.

Quinao, Jaime Jose and Sadiq J Zarrouk (2014). "A Review of the Volumetric Stored-Heat Resource Assessment: One Method, Different Result". In: *Proceedings of 36th New Zealand Geothermal Workshop*, pp. 24–26.

Raymond, Jasmin and René Therrien (2008). "Low-temperature geothermal potential of the flooded Gaspé Mines, Québec, Canada". In: *Geothermics* 37.2, pp. 189–210.

Renz, A et al. (2009). "Numerical modeling of geothermal use of mine water: challenges and examples". In: *Mine Water and the Environment* 28.1, pp. 2–14.

Richter, A. (2023). *ThinkGeoEnergy's Top 10 Geothermal Countries 2022 Power Generation Capacity (MW)*. Accessed: 2023-07-12. URL: https://www.thinkgeoenergy.com/thinkgeoenergys-top-10-geothermal-countries-2022-power-generation-capacity-mw/.

Rodríguez, R. and M.B. Díaz (2009). "Analysis of the utilization of mine galleries as geothermal heat exchangers by means a semi-empirical prediction method". In: *Renewable Energy* 34, pp. 1716–1725. DOI: 10.1016/j.renene.2008.12.036.

Rossman, L. (2000). *Epanet 2 users manual*. Tech. rep. EPA/600/R-00/057. Cincinnati, OH: Environmental Protection Agency, National Risk Management Research Laboratory.

Santos, L., A. Dahi Taleghani, and D. Elsworth (2022). "Repurposing abandoned wells for geothermal energy: Current status and future prospects". In: *Renewable Energy* 194, pp. 1288–1302. ISSN: 0960-1481. DOI: https://doi.org/10.1016/j.renene.2022.05.138. URL: https://www.sciencedirect.com/science/article/pii/S0960148122007959.

Sanyal, Subir K and James B Koenig (1995). "Resource risk and its mitigation for the financing of geothermal projects". In: *Transactions International Geothermal Energy Conference, Florence, Italy*, pp. 2911–2915.

Shah, Manan et al. (2022). "A comprehensive study on modeling methods for gauging of resources in a geothermal reservoirs". In: *Modeling Earth Systems and Environment* 8.1, pp. 1391–1404. DOI: 10.1007/s40808-021-01162-z.

Shirani, Fiona et al. (2020). *Mine water heating in Caerau: Thoughts from local residents*. Tech. rep. FLEXIS Work Package 17: Social Acceptability & Responsible

Development of Energy Systems. Cardiff University / FLEXIS Project. URL: https://orca.cardiff.ac.uk/id/eprint/138639/1/minewater%5C%20report%5C%202021%5C%20incl%5C%20summary.pdf.

Soldo, Elena, Claudio Alimonti, and Davide Scrocca (2020). "Geothermal Repurposing of Depleted Oil and Gas Wells in Italy". In: *Proceedings* 58.1. ISSN: 2504-3900. DOI: 10.3390/WEF-06907. URL: https://www.mdpi.com/2504-3900/58/1/9.

Somogyi, V., V. Sebestyén, and G. Nagy (2017). "Scientific achievements and regulation of shallow geothermal systems in six European countries– a review". In: *Renewable and Sustainable Energy Reviews* 68, pp. 934–952. DOI: 10.1016/j.rser.2016.02.014.

Stelling, P. et al. (2016). "Geothermal systems in volcanic arcs: Volcanic characteristics and surface manifestations as indicators of geothermal potential and favorability worldwide". In: *Journal of Volcanology and Geothermal Research* 324, pp. 57–72. ISSN: 0377-0273. DOI: https://doi.org/10.1016/j.jvolgeores.2016.05.018. URL: https://www.sciencedirect.com/science/article/pii/S0377027316301238.

Stemmle, R et al. (2025). "Current research on aquifer thermal energy storage (ATES) in Germany". In: *Grundwasser*, pp. 1–18.

Stemmle, R. et al. (2024). "City-scale heating and cooling with aquifer thermal energy storage (ATES)". In: *Geothermal Energy* 12, p. 2. DOI: 10.1186/s40517-023-00279-x.

Sweeney, Alexandra et al. (2025). "The need to regulate thermal interference between mine water geothermal systems: a UK perspective". In: *Quarterly Journal of Engineering Geology and Hydrogeology* 58.2, qjegh2024–185.

Szalewska, M. (2021). "Legal aspects of geothermal energy use in Poland". In: *Comparative Law Review* 27, pp. 385–406. DOI: 10.12775/CLR.2021.017.

The Energy Act, 2019 (2019). Act of Parliament (Kenya). Republic of Kenya. URL: https://faolex.fao.org/docs/pdf/ken193499.pdf (visited on 12/23/2025).

The Geothermal Resources Act (1982). Primary Act cited in subsidiary legislation PDF (includes Act reference). Republic of Kenya. URL: https://www.kenyalaw.org/kl/fileadmin/pdfdownloads/LegalNotices/2007/130-GeothermalResourcesAct_Amendment_Regulations_2007.pdf (visited on 12/23/2025).

The Petroleum (Current Model Clauses) Order 1999 (Jan. 27, 1999). UK Statutory Instrument. UK Government. URL: https://www.legislation.gov.uk/uksi/1999/160/introduction/made (visited on 12/23/2025).

The Petroleum (Production) (Landward Areas) Regulations 1995 (May 25, 1995). UK Statutory Instrument. UK Government. URL: https://www.legislation.gov.uk/id/uksi/1995/1436 (visited on 12/23/2025).

The Water Environment (Controlled Activities) (Scotland) Regulations 2011, General Binding Rule 17 (2011). Scottish Statutory Instrument 2011 No. 209. UK legislation (Scotland). URL: https://www.legislation.gov.uk/ssi/2011/209/contents/made.

Tian, Xiaoming et al. (2024). "Dynamic geothermal resource assessment: Integrating reservoir simulation and Gaussian Kernel Density Estimation under geological uncertainties". In: *Geothermics* 120, p. 103017. DOI: 10.1016/j.geothermics.2024.103017.

Todd, Fiona et al. (2019). "Coupled hydraulic and mechanical model of surface uplift due to mine water rebound: implications for mine water heating and cooling schemes". In: *Scottish Journal of Geology* 55.2, pp. 124–133. DOI: 10.1144/sjg2018-028.

Todini, E. and S. Pilati (1988). "A gradient method for the solution of looped pipe networks". In: *Computer Applications in Water Supply. Vol. 1.* Ed. by B. Coulbeck and C.H. Orr. Letchworth: Research Studies Press, pp. 1–20.

Todini, Ezio and Lewis A. Rossman (2013). "Unified Framework for Deriving Simultaneous Equation Algorithms for Water Distribution Networks". In: *Journal of Hydraulic Engineering* 139.5, pp. 511–526. DOI: 10.1061/(ASCE)HY.1943-7900.0000703. eprint: https://ascelibrary.org/doi/pdf/10.1061/%28ASCE%29HY.1943-7900.0000703. URL: https://ascelibrary.org/doi/abs/10.1061/%28ASCE%29HY.1943-7900.0000703.

Tost, Michael et al. (Feb. 2021). *Social Licence to Operate (SLO) Guidelines for Europe*. Deliverable (D4.3). MIREU (Mining and Metallurgy Regions EU). URL: https://mireu.eu/sites/default/files/2021-05/D%204.3.pdf.

Townsend, David H et al. (2020). "On the Rocks–Exploring Business Models for Geothermal Heat in the Land of Scotch". In: *Proceedings World Geothermal Congress*.

Tsagarakis, K.P., L. Efthymiou, et al. (2020). "A review of the legal framework in shallow geothermal energy in selected European countries: need for guidelines". In: *Renewable Energy* 147, pp. 2556–2571. DOI: 10.1016/j.renene.2018.10.007.

Turnell, Helen et al. (2023). "Driving success towards zero carbon energy targets for UK's Local Authorities". In: *International Journal of Sustainable Energy Planning and Management* 38, p. 83.

UK Government (2024). *Coal Mining Data: Past Shallow Coal Mine Workings*. https://www.gov.uk/government/publications/coal-mining-data-past-shallow-coal-mine-workings. Accessed 2025.

Verhoeven, R. et al. (2014). "Minewater 2.0 Project in Heerlen, the Netherlands: transformation of a Geothermal Mine Water Pilot Project into a Full Scale Hybrid Sustainable Energy Infrastructure for Heating and Cooling". In: *Energy Procedia* 46, pp. 58–67. DOI: 10.1016/j.egypro.2014.01.158.

Vernon, Robert (2024). "An island of coal: the British National Coal Board and their 'Plans for coal' 1947 to 1987". In: *Comunicações Geológicas* 110, pp. 87–94.

Walls, David B. et al. (2021). "A review of the performance of minewater heating and cooling systems". In: *Energies* 14, p. 6215. DOI: 10.3390/en14196215.

Walls, David B. et al. (2022). "Heat recovery potential and hydrochemistry of mine water discharges from Scotland's coalfields". In: *Earth Science, Systems and Society* 2.1, p. 10056.

Walls, David B. et al. (2023). "Combining ground stability investigation with exploratory drilling for mine water geothermal energy development; lessons from exploration and monitoring". In: *Scottish Journal of Geology* 59.1-2, sjg2022–011. DOI: 10.1144/sjg2022-011. eprint: https://www.lyellcollection.org/doi/pdf/10.1144/sjg2022-011. URL: https://www.lyellcollection.org/doi/abs/10.1144/sjg2022-011.

Walls, David B. et al. (2024). "GIS analysis for the selection of optimal sites for mine water geothermal energy application: a case study of Scotland's mining regions". In: *Quarterly Journal of Engineering Geology and Hydrogeology* 57.3, qjegh2023–050. DOI: 10.1144/qjegh2023-050. eprint: https://www.lyellcollection.org/doi/pdf/10.1144/qjegh2023-050. URL: https://www.lyellcollection.org/doi/abs/10.1144/qjegh2023-050.

Wang, Huajun et al. (2024). "Analysis of geothermal heat recovery from abandoned coal mine water for clean heating and cooling: A case from Shandong, China". In: *Renewable Energy* 228, p. 120659. ISSN: 0960-1481. DOI: https://doi.org/10.1016/j.renene.2024.120659. URL: https://www.sciencedirect.com/science/article/pii/S0960148124007274.

Water (Northern Ireland) Order 1999 (1999). Statutory Instrument 1999 No. 662 (NI). UK legislation. URL: https://www.legislation.gov.uk/nisi/1999/662/contents/made.

Water Resources Act 1991 (1991). Chapter 57. UK legislation. URL: https://www.legislation.gov.uk/ukpga/1991/57/contents.

Watson, Sean M., Gioia Falcone, and Rob Westaway (2020). "Repurposing Hydrocarbon Wells for Geothermal Use in the UK: The Onshore Fields with the Greatest Potential". In: *Energies* 13.14. ISSN: 1996-1073. DOI: 10.3390/en13143541. URL: https://www.mdpi.com/1996-1073/13/14/3541.

Watzlaf, G. R. and T. E. Ackman (2006). "Underground Mine Water for Heating and Cooling using Geothermal Heat Pump Systems". In: *Mine Water and the Environment* 25, pp. 1–14. DOI: 10.1007/s10230-006-0103-9. URL: 10.1007/s10230-006-0103-9.

Westaway, Rob and Paul L. Younger (2016). "Unravelling the relative contributions of climate change and ground disturbance to subsurface temperature perturbations: Case studies from Tyneside, UK". In: *Geothermics* 64, pp. 490–515. ISSN: 0375-6505. DOI: https://doi.org/10.1016/j.geothermics.2016.06.009. URL: https://www.sciencedirect.com/science/article/pii/S0375650516300657.

White, Mark et al. (2024). "Numerical investigation of closed-loop geothermal systems in deep geothermal reservoirs". In: *Geothermics* 116, p. 102852. ISSN: 0375-6505. DOI: https://doi.org/10.1016/j.geothermics.2023.102852. URL: https://www.sciencedirect.com/science/article/pii/S0375650523002079.

Whittington, D. J. et al. (2025). "Frontier exploration for mine water energy resources". In: *Quarterly Journal of Engineering Geology and Hydrogeology* 58.4, qjegh2025–056. DOI: 10.1144/qjegh2025-056. eprint: https://www.lyellcollection.org/doi/pdf/10.1144/qjegh2025-056. URL: https://www.lyellcollection.org/doi/abs/10.1144/qjegh2025-056.

Whitworth, Keith R. (2002). "The monitoring and modelling of mine water recovery in UK coalfields". In: *Geological Society, London, Special Publications* 198.1, pp. 61–73. DOI: 10.1144/GSL.SP.2002.198.01.04. eprint: https://www.lyellcollection.org/doi/pdf/10.1144/GSL.SP.2002.198.01.04. URL: https://www.lyellcollection.org/doi/abs/10.1144/GSL.SP.2002.198.01.04.

Wieber, Georg and Marion Stemke (2019). "Pump Tests in Deep Ore Mine Shafts for the Evaluation of a Possible Geothermal Use". In: *Khayrulina E, Wolkersdorfer*

C, Polyakova S, Bogush A: Mine Water–Technological and Ecological Challenges. S, pp. 375–379.

Williams, Colin F, Marshall Reed, and Robert H Mariner (2008). *A Review of Methods Applied by the US Geological Survey in the Assessment if Identified Geothermal Resources*. US Department of Interior, US Geological Survey. DOI: 10.3133/ofr20081296.

Wyatt, Lee (Aug. 2022a). *Hydrogeological Conceptual Model for Algernon–Hebburn Mine Water Block (No. 19–20): Technical Note*. Tech. rep. Draft 1. Coal Authority and Environment Agency.

— (Aug. 2022b). *Hydrogeological Conceptual Model for Bates mine water block (No. 6): Technical Note*. Tech. rep. Draft 1.1. Coal Authority and Environment Agency.

— (Aug. 2022c). *Hydrogeological Conceptual Model for Central Durham North Mine Water Block (No. 24): Technical Note*. Tech. rep. Draft 1.1. Coal Authority and Environment Agency.

— (Aug. 2022d). *Hydrogeological Conceptual Model for Central Durham South mine water block (No. 32): Technical Note*. Tech. rep. Draft 1.1. Coal Authority and Environment Agency.

— (Aug. 2022e). *Hydrogeological Conceptual Model for East Consett mine water block (No. 29): Technical Note*. Tech. rep. Draft 1.1. Coal Authority and Environment Agency.

— (Aug. 2022f). *Hydrogeological Conceptual Model for Sherburn–Houghall mine water block (No. 37): Technical Note*. Tech. rep. Draft 1.1. Coal Authority and Environment Agency.

— (Aug. 2022g). *Hydrogeological Conceptual Model for Stanley mine water block (No. 31): Technical Note*. Tech. rep. Draft 1.1. Coal Authority and Environment Agency.

— (Aug. 2022h). *Hydrogeological Conceptual Model for Throckley mine water blocks (No. 8 and 16): Technical Note*. Tech. rep. Draft 1.1. Coal Authority and Environment Agency.

— (Aug. 2022i). *Hydrogeological Conceptual Model for Walker Mine Water Block (No. 18): Technical Note*. Tech. rep. Draft 1.1. Coal Authority and Environment Agency.

— (Aug. 2022j). *Hydrogeological Conceptual Model for West of Wear mine water block (No. 36): Technical Note*. Tech. rep. Draft 1.1. Coal Authority and Environment Agency.

Wyatt, Lee, Sally Gallagher, and Rhiannon Marchi-Smith (Aug. 2023a). *Hydrogeology of the North East England Coalfield*. Tech. rep. Draft 3.10. Coal Authority and Environment Agency.

Wyatt, Lee, John Leyland, and Ian A. Watson (2023b). *Long-term mine water management of abandoned coal mines in the United Kingdom: almost 30 years of process, experience, and lessons learned*.

Wyatt, Lee et al. (2025). "Drilling into coal mine workings: overview and experience from Britain's coalfields". In: *Quarterly Journal of Engineering Geology and Hydrogeology* 58.3, qjegh2025–016. DOI: 10.1144/qjegh2025-016. eprint:

https://www.lyellcollection.org/doi/pdf/10.1144/qjegh2025-016. URL: https://www.lyellcollection.org/doi/abs/10.1144/qjegh2025-016f.

Younger, Paul L. (2004). *'Making water': the hydrogeological adventures of Britain's early mining engineers*. Vol. 225. The Geological Society of London. ISBN: 1862391556.

— (2015). "Geothermal Energy: Delivering on the Global Potential". In: *Energies* 8.10, pp. 11737–11754. ISSN: 1996-1073. DOI: 10.3390/en81011737. URL: https://www.mdpi.com/1996-1073/8/10/11737.

Younger, Paul L. and R. Adams (1999). *Predicting Mine Water Rebound*. R&D Technical Report W179. Co-funded by the Environment Agency, Northumbrian Water Ltd, and University of Newcastle upon Tyne. Bristol, UK: Environment Agency, UK.

Zeyen, Elisabeth, Veit Hagenmeyer, and Tom Brown (2021). "Mitigating heat demand peaks in buildings in a highly renewable European energy system". In: *Energy* 231, p. 120784. DOI: 10.1016/j.energy.2021.120784.

Zhao, Jian and Heinz Konietzky (2021). "An overview on flooding induced uplift for abandoned coal mines". In: *International Journal of Rock Mechanics and Mining Sciences* 148, p. 104955. ISSN: 1365-1609. DOI: https://doi.org/10.1016/j.ijrmms.2021.104955. URL: https://www.sciencedirect.com/science/article/pii/S1365160921003385.

APPENDIX A

Appendix for Chapter 2

A.1 ArcGIS map layer construction

Here are in-depth detail of the methods applied in ArcGIS Pro.

A.1.1 MiRAS

Raster C12 is a combination of the first two criteria, areas of overlapping workings (C1) without <30 m BGL workings present (C2). C1 is established in four steps using the Underground workings dataset (Table 2.4) The underground workings . First, the "Union" tool is applied to the underground-workings polygons. Everywhere one polygon overlaps another it is subdivided into distinct pieces; this overlay preserves all input boundaries and attributes, which ensures that each unique ground footprint is explicitly represented. Second, "Multipart To Singlepart" converts any multipart features into individual features, so there is exactly one record for each polygon piece. Third, "Spatial Join" is used, the single-part layer is joined to itself using the “are identical to” relationship, which matches features that have exactly the same geometry. This operation adds a Join_Count attribute that records, for each piece, how many workings share that identical footprint. Areas that satisfy

Criterion 1 were then identified as those with Join_Count greater than or equal to two.

To implement C2, shallow workings are removed from the Criterion 1 result. The shallow-workings layer represents workings with depth less than 30 m below ground level. The Erase tool is used, with the Criterion 1 layer as the input features and the shallow-workings layer as the erase features. The output retains only those overlapping pieces that do not intersect shallow workings, yielding a polygon layer of overlapping worked seams with shallow areas excluded. This is converted to a raster where these areas have a value of 1.

C3 identifies locations where the mine water head lies within 0–60 m BGL. The workflow uses point measurements of mine water head elevation in m OD, mine water discharge points, and a DTM in m OD.

Mine water head points are compiled from a series of Mining Remediation Authority hydrogeology reports covering the mine water blocks in the region (Wyatt 2022a; Wyatt 2022b; Marchi-Smith 2022; Wyatt 2022c; Wyatt 2022d; Marchi-Smith and Wyatt 2022a; Wyatt 2022e; Marchi-Smith and Wyatt 2024a; Wyatt 2022f; Cowley 2022; Marchi-Smith and Wyatt 2022b; Wyatt 2022g; Wyatt 2022h; Wyatt 2022i; Wyatt 2022j; Marchi-Smith and Wyatt 2024b). For each block, the report map showing sampling locations is imported, georeferenced to the project coordinate system, and digitised to create a new point dataset. Head elevations in m OD are transcribed from the accompanying report into attribute fields for the corresponding points. Where multiple measurements exist for the same location, the most recent value is retained and earlier values are discarded. Where discharge locations are reported without a head elevation, the head is assumed to be at ground surface at that point and is set equal to the digital terrain model elevation.

A continuous mine water surface is then interpolated from these points using Empirical Bayesian Kriging as per Walls et al. (2024).

A mine water surface raster in m BGL is derived as DTM elevation minus the previously created mine water surface using Raster Calculator. This is then reclassified into 10-metre depth bands from >0–60 m BGL, assigning class values of 1 through 7 for the ranges >0, 0–10, 10–20, 20–30, 30–40, 40–50, and 50–60 metres

respectively, and assigning a value of 0 to depths greater than 60 metres. The result is a raster that retains only locations with acceptable head depth, encoded in 10-metre increments for subsequent combination with the other criteria.

C4 identifies locations where worked seams are not excessively deep. The procedure uses in-seam level points with seam elevation in metres Ordnance Datum and a digital terrain model (DTM) in metres Ordnance Datum (Ordnance Survey 2025) to derive depth below ground level, interpolates those depths to a continuous raster, and applies a threshold of 250 m. Surface elevation at each In Seam Level (ISL) point is sampled from the DTM using Extract Values to Points. A new numeric field named Depth_BGL is calculated as DTM elevation minus seam elevation, the result is the depth of the worked seam point in m BGL. Depth_BGL point values are interpolated to a continuous raster using inverse distance weighting with power equal to two and a variable search neighbourhood of twelve nearest points. The output cell size is selected to match the analysis resolution and the snap raster so that subsequent map algebra aligns without resampling. The interpolated depth raster is converted to a binary display, with classes 0–250 m BGL mapped to 1 and >250 mapped to 0.

These three maps are multiplied together using the raster calculator (Equation A.1.1) to produce the final map.

$$\text{Raster output} = C_{12} \times C_3 \times C_4, \qquad \text{where } C_{12} = 0 \text{ or } 1,\ C_3 = 1, \ldots, 7,\ C_4 = 0 \text{ or } 1. \tag{A.1.1}$$

A.1.2 GeoResources Cornwall, Geothermal Screening Assessment

The GRC method requires the locations of the mines in the target area, the depths of the mine workings, the geothermal gradient, and the current and potential future heat demand in the areas being evaluated.

Mine locations and depths

The Underground Workings dataset from the MRA is used to identify the locations of the mine workings. However, these do not have depth data.

To find this, additional processing was done. Both the In Seam Level point dataset (contains the depth data) and the Underground Workings dataset contain the attribute SE_CODE, which identifies the coal seam being worked. The ISL points which overlapped with the UW polygons are extracted. The ISL points which have a matching SE_CODE with UW polygon they were co-located with provide the depth (DPTH_SL) for that polygon. When there are multiple points for the same polygon the mean of the point depths are used (Figure 2.9).

There are some UW polygons that have no ISL points associated with them (865 of 2719 in the Newcastle case study) and therefore no depth. A different approach is used for these values (Figure 2.10). For each seam, polygons which have depth values are treated as training data and converted to representative points. These are used to construct a continuous depth surface via spatial interpolation (IDW). This seam-specific interpolated surface is intersected with polygons of the same seam that lack depth values, and a mean depth is derived for each polygon based on the interpolated values within its footprint. These estimated depths are written back into the original polygon dataset only where values are missing. This results in a unified Underground Workings layer in which depth is provided either by the ISL points, or the seam-specific IDW layer.

These depths are converted to BGL using a DTM (Figure 2.11 before being categorised into <203.5 m BGL, 203.5-290.7 m BGL, and 290.7-405.9 m BGL. These depths translate to <16°C, 16-19°C, and 19-23°C when using a average surface temperature of 9°C and the local geothermal gradient of 34.4°C km^{-1} (Farr et al. 2021). The original method also has a category for >25°C, but there are no mines predicted to be above 23°C.

Heat Demand

Heat demand was mapped using the Heat Demand Densities layer from Möller et al. 2022 which maps the demand from the residential and service sector as was in 2015

(in TJ Km^{-1}).

The final map shows the heat demand and the mine workings within each depth category. The deeper, hotter, more prospective mines are drawn on top of the shallower mines to allow the more prospective areas to be more easily identified.

A.1.3 MRA, Mine Water Heat Opportunity Mapping

The MRA method uses 7 maps to go through the decision process flowchart in Figure 2.2 to produce the final map. How each of these maps was produced is described below.

Mine Workings Present:

The underground workings file is converted to a raster which is defines workings are present as 1, and no workings as 0 (Figure 2.16).

Multiple overlapping seams:

The same analysis is used here as in the MiRAS C1 assessment, identifying where the overlapping seams are. This produces a map where 2 or more overlapping seams are given a value of 1, everything else is 0 (Figure 2.17.

Depth to workings:

The same process of finding the depth of each mine working polygon is used as for the GRC method. After determining the depth for each mine working polygon the depths are classified. The MRA method uses shallow workings only (<30 m bgl), >30 - 300 m bgl, 300 - 500 m bgl, and >500 m bgl. The area being assessed is broken down into cells, for each cell the depths of every mine polygon that is present is the cell is assessed. If there are only workings shallower than 30 m, that is classed as category 0. If there is at least on seam between 30 and 300 m bgl the cell is category 1. If the cell does not meet the test for category 0, or 1, but has at least one mine polygon between 300 - 500 m bgl, it becomes category 2. If the cell does not meet the test for category 0, 1, or 2, but has at least one mine polygon > 500 m bgl, it becomes category 3.

```
1
2  # Python Script and Feedback for adding seam depth to null underground workings
       polygons.
3
4  # - NE120E had been done previously when testing this script. When the process worked
       the other SE_CODEs where written in.
5  ------------------------------------------------------------------------------------
6
7  import arcpy
8  from arcpy.sa import Idw, ZonalStatisticsAsTable
9
10 # ---------------------------------------------------------------------
11 # SETTINGS - your setup
12 # ---------------------------------------------------------------------
13 gdb = r"J:\ArcGISInput\Projects\MRA_DU_Data\MRA_DU_Data.gdb"
14 fc = "Newcastle_undergroundworkings" # polygon feature class in that gdb
15 cell_size = 15 # interpolation cell size (m)
16
17 # Attribute field names
18 seam_field = "SE_CODE" # seam code field
19 depth_field = "MeanDpth_Manual" # depth field to fill
20 key_field = "OBJECTID_Polygon" # stable polygon ID shared across datasets
21
22 # Only process these seam codes (name codes that need values):
23 target_seams = [
24     "NE140H",
25     "NE170H",
26     "NE190H",
27     "NE210H",
28     "NE217H",
29     "NE230H",
```

```
    "NE260H",
    "NE280H",
    "NE290H",
    "NE310H",
    "NE330H",
    "NE350H",
    "NE370H",
    "NE400H",
    "NE427H",
]

# ---------------------------------------------------------------------
# ENVIRONMENT
# ---------------------------------------------------------------------
arcpy.env.workspace = gdb
arcpy.env.overwriteOutput = True

arcpy.CheckOutExtension("Spatial")

arcpy.env.snapRaster = r"J:\ArcGISInput\Projects\MRA_DU_Data\ne_dtm"
arcpy.env.cellSize = cell_size
arcpy.env.extent = fc
arcpy.env.mask = fc

print("Target seams:", target_seams)

for se_code in target_seams:
    print("\n=== Processing seam: {} ===".format(se_code))
    try:
        # Make a fresh layer
        lyr = "workings_lyr"
        if arcpy.Exists(lyr):
            arcpy.Delete_management(lyr)
```

```
63          arcpy.MakeFeatureLayer_management(fc, lyr)
64
65          # ---- count NULLs for this seam ----
66          where_nulls = f"{seam_field} = '{se_code}' AND {depth_field} IS NULL"
67          arcpy.SelectLayerByAttribute_management(lyr, "NEW_SELECTION", where_nulls)
68          null_count = int(arcpy.GetCount_management(lyr)[0])
69          print(f" Polygons with NULL depth for {se_code}: {null_count}")
70
71          if null_count == 0:
72              print(f" -> No NULLs for seam {se_code}; skipping.")
73              continue
74
75          # ---- training polygons (have depth) ----
76          where_train = (
77              f"{seam_field} = '{se_code}' AND {depth_field} IS NOT NULL"
78          )
79          arcpy.SelectLayerByAttribute_management(lyr, "NEW_SELECTION", where_train)
80          train_count = int(arcpy.GetCount_management(lyr)[0])
81          print(f" Training polygons: {train_count}")
82
83          if train_count < 3:
84              print(f" -> Skipping seam {se_code}: only {train_count} training polygons
                    .")
85              continue
86
87          # Training points
88          train_pts = f"{gdb}\\train_{se_code}_pts"
89          if arcpy.Exists(train_pts):
90              arcpy.Delete_management(train_pts)
91          arcpy.FeatureToPoint_management(lyr, train_pts, "INSIDE")
92
93          field_names = [f.name for f in arcpy.ListFields(train_pts)]
94          print(" Training point fields:", field_names)
```

```
        if depth_field not in field_names:
            print(f" !! Depth field {depth_field} not on {train_pts}")
            continue

        # ---- IDW raster ----
        print(" Creating IDW surface...")
        idw_ras = Idw(train_pts, depth_field, cell_size)

        out_ras = f"{gdb}\\IDW_{se_code}"
        if arcpy.Exists(out_ras):
            arcpy.Delete_management(out_ras)
        idw_ras.save(out_ras)
        print(f" Saved IDW raster as {out_ras}")

        # ---- target (NULL) polygons again ----
        arcpy.SelectLayerByAttribute_management(lyr, "NEW_SELECTION", where_nulls)
        tgt_count = int(arcpy.GetCount_management(lyr)[0])
        print(f" Target (NULL) polygons: {tgt_count}")

        if tgt_count == 0:
            print(f" -> No NULL polygons for seam {se_code} (after re-check).")
            continue

        tgt_fc = f"{gdb}\\{se_code}_tgtpolys"
        if arcpy.Exists(tgt_fc):
            arcpy.Delete_management(tgt_fc)
        arcpy.CopyFeatures_management(lyr, tgt_fc)

        # ---- Zonal Statistics ----
        zonal_table = f"{gdb}\\{se_code}_zonal"
        if arcpy.Exists(zonal_table):
            arcpy.Delete_management(zonal_table)

```

```
        print(" Running Zonal Statistics as Table (MEAN)...")
        ZonalStatisticsAsTable(
            in_zone_data=tgt_fc,
            zone_field=key_field,
            in_value_raster=out_ras,
            out_table=zonal_table,
            ignore_nodata="DATA",
            statistics_type="MEAN"
        )

        if not arcpy.Exists(zonal_table):
            print(" !! Zonal table was not created.")
            continue

        row_count = int(arcpy.management.GetCount(zonal_table)[0])
        print(f" Zonal table rows: {row_count}")

        depth_by_id = {}
        with arcpy.da.SearchCursor(zonal_table, [key_field, "MEAN"]) as zcur:
            for poly_id, mean_val in zcur:
                depth_by_id[poly_id] = mean_val
        non_null_means = sum(1 for v in depth_by_id.values() if v is not None)
        print(f" Non-null MEANs: {non_null_means}")

        # ---- update polygons ----
        updated = 0
        with arcpy.da.UpdateCursor(fc, [key_field, seam_field, depth_field]) as ucur:
            for poly_id, code, depth in ucur:
                if (
                    code == se_code
                    and depth is None
                    and poly_id in depth_by_id
                    and depth_by_id[poly_id] is not None
```

```
            ):
                ucur.updateRow((poly_id, code, depth_by_id[poly_id]))
                updated += 1

        print(f" Updated {updated} polygons for seam {se_code}.")
        print(f"=== Finished seam: {se_code} ===")

    except Exception as e:
        import traceback
        print(f"!! ERROR while processing seam {se_code}: {e}")
        traceback.print_exc()

print("\n*** SCRIPT FINISHED ***")
Target seams: ['NE140H', 'NE170H', 'NE190H', 'NE210H', 'NE217H', 'NE230H', 'NE260H', '
    NE280H', 'NE290H', 'NE310H', 'NE330H', 'NE350H', 'NE370H', 'NE400H', 'NE427H']
```

```
    Python script for converting UW depths from sealevel to BGL

import arcpy
from arcpy.sa import ZonalStatisticsAsTable

# ---------------------------------------------------------------------
# SETTINGS - adjust if any names change
# ---------------------------------------------------------------------
gdb = r"J:\ArcGISInput\Projects\MRA_DU_Data\MRA_DU_Data.gdb"
fc = "Newcastle_undergroundworkings" # polygon feature class in that gdb
dtm = r"J:\ArcGISInput\Projects\MRA_DU_Data\ne_dtm" # DTM raster

key_field = "OBJECTID_Polygon" # unique polygon ID (used before)
seam_field = "SE_CODE"
seam_elev_field = "MeanDpth_Manual" # seam elevation relative to MSL
mean_dtm_field = "MeanDTM" # new field to hold mean surface elevation
depth_bgl_field = "MeanDepth_BGL" # new field: depth below ground level
```

```
18
19 # ----------------------------------------------------------------------
20 # ENVIRONMENT
21 # ----------------------------------------------------------------------
22 arcpy.env.workspace = gdb
23 arcpy.env.overwriteOutput = True
24
25 arcpy.CheckOutExtension("Spatial")
26
27 arcpy.env.snapRaster = dtm
28 arcpy.env.cellSize = arcpy.Describe(dtm).meanCellWidth
29 arcpy.env.extent = fc # limit to workings extent
30 arcpy.env.mask = fc # clip stats to workings polygons
31
32 # ----------------------------------------------------------------------
33 # 1. Compute mean DTM per polygon (Zonal Statistics as Table)
34 # ----------------------------------------------------------------------
35 zonal_table = f"{gdb}\\Workings_DTMmean"
36
37 print("Running Zonal Statistics as Table (MEAN DTM per polygon)...")
38 if arcpy.Exists(zonal_table):
39     arcpy.Delete_management(zonal_table)
40
41 ZonalStatisticsAsTable(
42     in_zone_data=fc,
43     zone_field=key_field,
44     in_value_raster=dtm,
45     out_table=zonal_table,
46     ignore_nodata="DATA",
47     statistics_type="MEAN"
48 )
49
50 print("Zonal statistics table created:", zonal_table)
```

```
51
52 # ---------------------------------------------------------------------
53 # 2. Join mean DTM back to polygons
54 # ---------------------------------------------------------------------
55 print("Joining mean DTM values back to polygon feature class...")
56
57 # This will copy the "MEAN" field from the zonal table onto the FC
58 arcpy.JoinField_management(
59     in_data=fc,
60     in_field=key_field,
61     join_table=zonal_table,
62     join_field=key_field,
63     fields=["MEAN"]
64 )
65
66 # ---------------------------------------------------------------------
67 # 3. Add fields for MeanDTM and MeanDepth_BGL (if they do not exist)
68 # ---------------------------------------------------------------------
69 existing_fields = [f.name for f in arcpy.ListFields(fc)]
70
71 if mean_dtm_field not in existing_fields:
72     arcpy.AddField_management(fc, mean_dtm_field, "DOUBLE")
73     print(f"Added field: {mean_dtm_field}")
74
75 if depth_bgl_field not in existing_fields:
76     arcpy.AddField_management(fc, depth_bgl_field, "DOUBLE")
77     print(f"Added field: {depth_bgl_field}")
78
79 # ---------------------------------------------------------------------
80 # 4. Populate MeanDTM and MeanDepth_BGL
81 # MeanDTM = MEAN (from zonal stats)
82 # MeanDepth_BGL = MeanDTM - MeanDpth_Manual
83 #
```

```
# Note: MeanDpth_Manual is an elevation (negative below MSL, positive above).
# ---------------------------------------------------------------------
print("Calculating MeanDTM and MeanDepth_BGL...")

update_fields = [key_field, "MEAN", mean_dtm_field, seam_elev_field, depth_bgl_field]

updated_count = 0
no_dtm_count = 0
no_seam_elev_count = 0

with arcpy.da.UpdateCursor(fc, update_fields) as ucur:
    for poly_id, mean_dtm_raw, mean_dtm_val, seam_elev, depth_bgl in ucur:

        # Copy MEAN from zonal table into MeanDTM where available
        if mean_dtm_raw is not None:
            mean_dtm_val = mean_dtm_raw
        else:
            # No valid DTM cells under this polygon
            no_dtm_count += 1
            # Leave existing MeanDTM / MeanDepth_BGL as-is
            ucur.updateRow((poly_id, mean_dtm_raw, mean_dtm_val, seam_elev, depth_bgl))
            continue

        # Need both surface and seam elevation to compute depth
        if seam_elev is None:
            no_seam_elev_count += 1
            depth_bgl = None
        else:
            # Depth below ground level = surface elevation - seam elevation
            depth_bgl = mean_dtm_val - seam_elev
            updated_count += 1

        ucur.updateRow((poly_id, mean_dtm_raw, mean_dtm_val, seam_elev, depth_bgl))
```

```
117
118 print(f"Updated MeanDepth_BGL for {updated_count} polygons.")
119 print(f"Polygons with no valid DTM (MEAN is null): {no_dtm_count}")
120 print(f"Polygons with no seam elevation (MeanDpth_Manual is null): {no_seam_elev_count
    }")
121
122 print("\nDone computing mean depth below ground level.")
```

```
1  #Script to create raster of working depths (MRA)
2
3  #-1 - no workings
4  #0 - all workings <30 mBGL
5  #1 - at least one working between 30 - 300 m
6  #2 - not -1, 0, or 1, and at least 1 working between 300 - 500
7
8  #There are no workings in Newcastle deeper than 500 m. If there were:
9  3 - not -1, 0, 1, or 2, and at least 1 working deeper that 500 mBGL.
10
11 import arcpy
12
13 # ----------------------------------------------------------------
14 # 0. USER INPUTS - EDIT THESE
15 # ----------------------------------------------------------------
16 gdb = r"J:\ArcGISInput\Projects\MRA_DU_Data\MRA_DU_Data.gdb" # <-- change to your file
       gdb
17 boundary_fc = "Newcastle_Boundary" # polygon extent
18 workings_fc = "Newcastle_undergroundworkings" # mine workings polygons
19 depth_field = "MeanDepth_BGL" # depth attribute (m bgl)
20 dtm_raster = "ne_dtm" # snap raster
21 cell_size = 15 # cell size in metres
22
23 # Output names (inside the same gdb)
24 fishnet_fc = "Grid15m"
```

```
fishnet_clip_fc = "Grid15m_Clipped"
intersect_fc = "Grid_Workings_Intersect"
stats_table = "CellDepthSummary"
depth_class_field = "DepthClass"
depth_raster = "Depth_to_workings"

# ---------------------------------------------------------------------
# 1. Set environment
# ---------------------------------------------------------------------
arcpy.env.workspace = gdb
arcpy.env.overwriteOutput = True
arcpy.env.snapRaster = dtm_raster
arcpy.env.cellSize = cell_size
arcpy.env.extent = boundary_fc
arcpy.env.mask = boundary_fc

print("Workspace set to:", gdb)

# ---------------------------------------------------------------------
# 2. Create 15 m fishnet over Newcastle_Boundary
# ---------------------------------------------------------------------
desc = arcpy.Describe(boundary_fc)
ext = desc.extent

origin_coord = f"{ext.XMin} {ext.YMin}"
y_axis_coord = f"{ext.XMin} {ext.YMin + 10}" # arbitrary point "up"
corner_coord = f"{ext.XMax} {ext.YMax}"

print("Creating fishnet...")
arcpy.management.CreateFishnet(
    out_feature_class=fishnet_fc,
    origin_coord=origin_coord,
    y_axis_coord=y_axis_coord,
```

```
    cell_width=cell_size,
    cell_height=cell_size,
    number_rows="",
    number_columns="",
    corner_coord=corner_coord,
    labels="NO_LABELS",
    template=boundary_fc,
    geometry_type="POLYGON"
)

# Clip to boundary so we only keep cells inside Newcastle_Boundary
print("Clipping fishnet to boundary...")
arcpy.analysis.Clip(fishnet_fc, boundary_fc, fishnet_clip_fc)

# Add CellID field and populate with unique integers
print("Adding CellID...")
if "CellID" not in [f.name for f in arcpy.ListFields(fishnet_clip_fc)]:
    arcpy.management.AddField(fishnet_clip_fc, "CellID", "LONG")

with arcpy.da.UpdateCursor(fishnet_clip_fc, ["CellID"]) as cur:
    cid = 1
    for row in cur:
        row[0] = cid
        cur.updateRow(row)
        cid += 1

print("Fishnet ready:", fishnet_clip_fc)

# ---------------------------------------------------------------------
# 3. Intersect fishnet with workings polygons
# ---------------------------------------------------------------------
print("Intersecting fishnet with workings...")
arcpy.analysis.Intersect(
```

```
    in_features=[fishnet_clip_fc, workings_fc],
    out_feature_class=intersect_fc,
    join_attributes="ALL",
    cluster_tolerance="",
    output_type="INPUT"
)

# ---------------------------------------------------------------------
# 4. Add depth band flags (lt30, 30_300, 300_500, gt500)
# ---------------------------------------------------------------------
flag_fields = ["lt30", "d30_300", "d300_500", "gt500"]
existing_fields = [f.name for f in arcpy.ListFields(intersect_fc)]

for fld in flag_fields:
    if fld not in existing_fields:
        arcpy.management.AddField(intersect_fc, fld, "LONG")

print("Populating depth band flags on intersect...")
with arcpy.da.UpdateCursor(
    intersect_fc,
    [depth_field, "lt30", "d30_300", "d300_500", "gt500"]
) as cur:
    for row in cur:
        depth = row[0]
        # Initialise
        lt30 = d30_300 = d300_500 = gt500 = 0

        if depth is not None:
            if depth < 30:
                lt30 = 1
            elif 30 <= depth < 300:
                d30_300 = 1
            elif 300 <= depth < 500:
```

```
                d300_500 = 1
            elif depth >= 500:
                gt500 = 1

        row[1] = lt30
        row[2] = d30_300
        row[3] = d300_500
        row[4] = gt500
        cur.updateRow(row)

print("Depth band flags populated.")

# ---------------------------------------------------------------------
# 5. Summary Statistics by CellID
# ---------------------------------------------------------------------
print("Running Summary Statistics by CellID...")
arcpy.analysis.Statistics(
    in_table=intersect_fc,
    out_table=stats_table,
    statistics_fields=[
        ["lt30", "SUM"],
        ["d30_300", "SUM"],
        ["d300_500", "SUM"],
        ["gt500", "SUM"]
    ],
    case_field="CellID"
)

print("Summary table created:", stats_table)

# ---------------------------------------------------------------------
# 6. Join stats back to fishnet
# ---------------------------------------------------------------------
```

```
print("Joining stats back to fishnet...")
arcpy.management.JoinField(
    in_data=fishnet_clip_fc,
    in_field="CellID",
    join_table=stats_table,
    join_field="CellID",
    fields=["SUM_lt30", "SUM_d30_300", "SUM_d300_500", "SUM_gt500"]
)

print("Join complete.")

# ---------------------------------------------------------------------
# 7. Classify each cell into depth bands (FINAL LOGIC)
# ---------------------------------------------------------------------
if depth_class_field not in [f.name for f in arcpy.ListFields(fishnet_clip_fc)]:
    arcpy.management.AddField(fishnet_clip_fc, depth_class_field, "SHORT")

print("Calculating DepthClass...")

with arcpy.da.UpdateCursor(
    fishnet_clip_fc,
    ["SUM_lt30", "SUM_d30_300", "SUM_d300_500", "SUM_gt500", depth_class_field]
) as cur:
    for row in cur:
        n_lt30 = row[0] or 0
        n_30_300 = row[1] or 0
        n_300_500 = row[2] or 0
        n_gt500 = row[3] or 0

        total = n_lt30 + n_30_300 + n_300_500 + n_gt500

        # Default: no workings
        depth_class = -1
```

```
190
191         if total > 0:
192             # CLASS 0: all ?30
193             if (n_lt30 > 0 and
194                 n_30_300 == 0 and
195                 n_300_500 == 0 and
196                 n_gt500 == 0):
197                 depth_class = 0
198
199             # CLASS 1: at least one 30-300
200             elif n_30_300 > 0:
201                 depth_class = 1
202
203             # CLASS 2: no 30-300, but at least one 300-500
204             elif n_300_500 > 0:
205                 depth_class = 2
206
207             # CLASS 3: no 30-500, but at least one >500
208             elif n_gt500 > 0:
209                 depth_class = 3
210
211         row[4] = depth_class
212         cur.updateRow(row)
213
214 print("DepthClass calculation finished.")
215
216 # ---------------------------------------------------------------------
217 # 8. Convert fishnet polygons to raster using DepthClass
218 # ---------------------------------------------------------------------
219 print("Converting fishnet to raster...")
220 arcpy.conversion.PolygonToRaster(
221     in_features=fishnet_clip_fc,
222     value_field=depth_class_field,
```

```
    out_rasterdataset=depth_raster,
    cell_assignment="MAXIMUM_AREA",
    priority_field="",
    cellsize=cell_size
)

print("Done. Depth_to_workings raster created as:", depth_raster)
```

Opencast workings:

The Unlicenced Opencast workings dataset from the MRA was used to identify areas of opencast workings.

Mine water levels:

Mine water depth data is from the Mining Remediation Authority 2024a and the series of Hydrogeological reports produced by the MRA, for the NE of England, and the mine block there within (Wyatt 2022a; Wyatt 2022b; Marchi-Smith 2022; Wyatt 2022c; Wyatt 2022d; Marchi-Smith and Wyatt 2022a; Wyatt 2022e; Marchi-Smith and Wyatt 2024a; Wyatt 2022f; Cowley 2022; Marchi-Smith and Wyatt 2022b; Wyatt 2022g; Wyatt 2022h; Wyatt 2022i; Wyatt 2022j; Marchi-Smith and Wyatt 2024b; Wyatt et al. 2023a). The maps showing the mine blocks and the locations of discharge and monitoring points are imported into GIS software, georeferenced and digitised. The mine water heights contained in the report are reported in m AOD. If there was a discharge point with no associated height, it was presumed to be at the AOD height taken from the DTM, i.e. ground level. The water level in each mine block is considered separately. If there is only one data point this is taken as the mine water height across the whole mine block. If there are 3 or less points, a mean value is taken. If there are more than 3 an IDW surface created and used. These were joined together to create a raster that could be subtracted from the regional DTM to create a mine water surface in m bgl. This was then classified according to the MRA conditions, <75 m bgl, 75 - 100 m bgl, and >100 m bgl.

```
    Script to assign AOD depths to Mine block polygons or create IDW surfaces.
```

```
2
3  import arcpy
4  from arcpy.sa import Idw
5
6  # ----------------------------------------------------------
7  # SETTINGS - paths and field names
8  # ----------------------------------------------------------
9
10 gdb = r"J:\ArcGISInput\Projects\MRA_DU_Data\MRA_DU_Data.gdb"
11
12 # Feature classes in the GDB
13 mineblocks_fc = gdb + r"\MineBlocks" # polygons
14 created_pts_fc = gdb + r"\CreatedMineWater" # points with MineBlock + DepthAOD_no
15
16 # DTM raster (outside the gdb)
17 dtm = r"J:\ArcGISInput\Projects\MRA_DU_Data\ne_dtm"
18
19 # Field names
20 block_name_field = "MineBlockName" # in MineBlocks
21 point_block_field = "MineBlock" # in CreatedMineWater
22 depth_field = "DepthAOD_no" # in CreatedMineWater (from Minewater_height)
23
24 # Output fields on MineBlocks (only used for blocks with <=3 points)
25 out_depth_field = "MW_DepthAOD" # final mine water level per block (mean of <=3 pts)
26 out_count_field = "MW_PtCount" # number of points used per block
27
28 # Where to save IDW rasters (here: same GDB)
29 idw_workspace = gdb # change to a folder path if you prefer GeoTIFFs
30
31 cell_size = 15 # IDW cell size
32
33 # ----------------------------------------------------------
34 # ENVIRONMENT SETUP
```

```
# ------------------------------------------------------------
arcpy.env.workspace = gdb
arcpy.env.overwriteOutput = True

arcpy.CheckOutExtension("Spatial")

arcpy.env.snapRaster = dtm
arcpy.env.cellSize = cell_size

oid_field_blocks = arcpy.Describe(mineblocks_fc).OIDFieldName
oid_field_pts = arcpy.Describe(created_pts_fc).OIDFieldName

print("OID field for MineBlocks:", oid_field_blocks)
print("OID field for CreatedMineWater:", oid_field_pts)

# ------------------------------------------------------------
# BUILD LOOKUP: MineBlock -> list of point OIDs and depths
# ------------------------------------------------------------
print("Building point lookup from CreatedMineWater ...")

block_points = {} # { block_name: {'oids': [...], 'depths': [...]} }

with arcpy.da.SearchCursor(created_pts_fc, [oid_field_pts, point_block_field,
    depth_field]) as cur:
    for pt_oid, blk, depth in cur:
        if blk is None or depth is None:
            continue
        if blk not in block_points:
            block_points[blk] = {'oids': [], 'depths': []}
        block_points[blk]['oids'].append(pt_oid)
        block_points[blk]['depths'].append(depth)

print("Found points for {} unique blocks".format(len(block_points)))
```

```
67
68  # ------------------------------------------------------------
69  # ADD OUTPUT FIELDS TO MineBlocks IF NEEDED
70  # ------------------------------------------------------------
71  existing_fields = [f.name for f in arcpy.ListFields(mineblocks_fc)]
72
73  if out_depth_field not in existing_fields:
74      arcpy.AddField_management(mineblocks_fc, out_depth_field, "DOUBLE")
75      print("Added field:", out_depth_field)
76
77  if out_count_field not in existing_fields:
78      arcpy.AddField_management(mineblocks_fc, out_count_field, "LONG")
79      print("Added field:", out_count_field)
80
81  # ------------------------------------------------------------
82  # MAKE REUSABLE LAYERS
83  # ------------------------------------------------------------
84  if arcpy.Exists("blocks_lyr"):
85      arcpy.Delete_management("blocks_lyr")
86  if arcpy.Exists("pts_lyr"):
87      arcpy.Delete_management("pts_lyr")
88
89  arcpy.MakeFeatureLayer_management(mineblocks_fc, "blocks_lyr")
90  arcpy.MakeFeatureLayer_management(created_pts_fc, "pts_lyr")
91
92  # ------------------------------------------------------------
93  # HELPER: make a safe raster name from a block name
94  # ------------------------------------------------------------
95  def make_safe_name(blk_name, blk_oid):
96      if blk_name is None or blk_name == "":
97          base = f"Block_{blk_oid}"
98      else:
99          base = blk_name
```

```
    # Replace bad chars with underscore
    safe = "".join(c if c.isalnum() or c == "_" else "_" for c in base)
    # No leading digit
    if not safe[0].isalpha():
        safe = "B_" + safe
    # Limit length for GDB names
    if len(safe) > 25:
        safe = safe[:25]
    # Prefix to avoid collisions with other datasets
    return "IDW_" + safe

# ---------------------------------------------------------
# LOOP OVER BLOCKS AND APPLY YOUR RULE
# ---------------------------------------------------------
updated_mean = 0
made_idw = 0
no_points = 0

with arcpy.da.UpdateCursor(mineblocks_fc,
                           [oid_field_blocks,
                            block_name_field,
                            out_depth_field,
                            out_count_field]) as ucur:

    for blk_oid, blk_name, cur_depth, cur_count in ucur:
        new_depth = cur_depth
        pt_count = 0

        info = block_points.get(blk_name)

        # No points for this block
        if info is None:
            pt_count = 0
```

```
133             no_points += 1
134             ucur.updateRow((blk_oid, blk_name, new_depth, pt_count))
135             continue
136
137         depths = info['depths']
138         oids = info['oids']
139         pt_count = len(depths)
140
141         # Case 1: 1-3 points: simple mean of DepthAOD_no (store on polygon)
142         if pt_count <= 3:
143             mean_val = sum(depths) / float(pt_count)
144             new_depth = mean_val
145             updated_mean += 1
146             ucur.updateRow((blk_oid, blk_name, new_depth, pt_count))
147             continue
148
149         # Case 2: >3 points: per-block IDW, masked to that block, SAVE raster only
150         print(f"Block '{blk_name}' (OID {blk_oid}): {pt_count} points -> IDW raster
                only")
151
152         # Select this block into its own layer
153         if arcpy.Exists("block_temp_lyr"):
154             arcpy.Delete_management("block_temp_lyr")
155         arcpy.MakeFeatureLayer_management(
156             mineblocks_fc,
157             "block_temp_lyr",
158             f"{oid_field_blocks} = {blk_oid}"
159         )
160
161         # Restrict processing to this block
162         arcpy.env.extent = "block_temp_lyr"
163         arcpy.env.mask = "block_temp_lyr"
164
```

```
        # Select this block's points in pts_lyr
        oid_list = ",".join(str(o) for o in oids)
        where_pts = f"{oid_field_pts} IN ({oid_list})"
        arcpy.SelectLayerByAttribute_management("pts_lyr", "NEW_SELECTION", where_pts)

        # Build IDW
        print(" Running IDW...")
        idw_ras = Idw("pts_lyr", depth_field, cell_size)
        print(" IDW finished.")

        # Save the IDW raster with the name of the block (sanitized)
        idw_name = make_safe_name(blk_name, blk_oid)
        out_idw_path = idw_workspace + "\\" + idw_name

        if arcpy.Exists(out_idw_path):
            arcpy.Delete_management(out_idw_path)

        idw_ras.save(out_idw_path)
        print(" Saved IDW raster:", out_idw_path)

        # For IDW blocks, we do NOT change MW_DepthAOD (leave as-is / null),
        # but we still record the point count.
        made_idw += 1
        ucur.updateRow((blk_oid, blk_name, new_depth, pt_count))

# Reset env to global defaults
arcpy.env.extent = None
arcpy.env.mask = None

print("\n--- Summary ---")
print(f"Blocks with no points: {no_points}")
print(f"Blocks updated from mean of <=3 points (MW_DepthAOD): {updated_mean}")
print(f"Blocks with IDW rasters created (>3 points): {made_idw}")
```

```
198 print("Done.")
```

Recovery:

The recovery status of the mine water block is assessed using information from the Hydrogeology of the North East England Coalfield report (Wyatt et al. 2023a). For the purposes of the methodology, water levels must be classified as either recovering or recovered. However, the report explicitly assigns these categories to only a limited number of mine blocks. It is therefore interpreted that areas where pumping is actively used to control water levels are unlikely to have pumping reduced to permit further recovery; such areas can consequently be considered artificially "recovered." All remaining areas are also classified as recovered to avoid overestimating the opportunities available (Table 2.5).

Flooding

A raster of flooded workings was derived to indicate whether underground mine workings within each grid cell are likely to be inundated by mine water. For each cell, the depths of intersecting mine workings (MeanDepth_BGL) were compared with the corresponding mine water level (MW_BGL), both expressed in metres below ground level (m bgl). A working was classified as flooded where its depth was greater than the mine water depth in that cell (i.e. the working lies below the water level). The resulting Flooded_workings raster is binary: a value of 1 indicates that there is at least one flooded working within the cell, while a value of 0 indicates that no workings in the cell are flooded (either because there are no workings present, or because all workings lie above the mine water level).

To provide additional information on the depth range of any flooded workings, a second raster (Flooded_band) was generated. Mine working depths were grouped into four bands: <30 m bgl, 30–300 m bgl, 300–500 m bgl, and >500 m bgl. For each cell, flooded workings were identified within these bands using the same depth comparison (working depth > MW_BGL). The cell was then assigned a single code based on the deepest flooded band of interest present, using a simple priority scheme.

A value of -1 denotes that no flooded workings occur in the cell. A value of 0 indicates flooded workings shallower than 30 m bgl only. A value of 1 indicates at least one flooded working in the 30–300 m bgl band (regardless of whether shallower flooded workings are also present). A value of 2 indicates no flooded workings in 30–300 m bgl, but at least one flooded working between 300–500 m bgl. A value of 3 indicates no flooded workings in the shallower bands, but at least one flooded working deeper than 500 m bgl. Together, these two rasters distinguish between areas with no flooded workings, areas where workings are flooded, and the characteristic depth range of any flooded workings present.

Final map

These layers are converted into raster and given numeric values which were inputted into the raster calculator to produce the final map. The final classification raster R was created by applying an ordered set of rules to each cell, following the Coal Authority methodology. In summary, cells were assigned to four classes (no opportunity = 1, good = 4, possible = 3, challenging = 2) according to combinations of: the presence of underground workings, whether multiple seams are present,the depth band of the workings,the presence of opencast workings, the mine water level and flooding status, and the mine water recovery status.

The precise implementation used in ArcGIS Pro's Raster Calculator is as follows:

```
Con(
    ( ("Newc_workings_Clip" == 0) |
      ( ("Newc_workings_Clip" == 1) & ("Newc_multiseam_Clip" == 0) & ("Flooded_band" !=
           0) ) |
      ( ("Newc_workings_Clip" == 1) & ("Newc_multiseam_Clip" == 1) & ("
          Depth_to_workings" == 0) )
    ),
    1,

Con(
    ( ("Newc_workings_Clip" == 1) &
      ("Newc_multiseam_Clip" == 1) &
```

```
      ("Depth_to_workings" == 1) &
      ("Newc_Opencast_RClip" == 0) &
      ("Newc_Minewaterlevel_Clip" == 1)
    ),
    4,

Con(
    ( ("Newc_workings_Clip" == 1) &
      ("Newc_multiseam_Clip" == 1) &
      (
          ( ("Depth_to_workings" == 1) & ("Newc_Opencast_RClip" == 1) )

        | ( ("Depth_to_workings" == 1) &
            ("Newc_Opencast_RClip" == 0) &
            ("Newc_Minewaterlevel_Clip" == 3) &
            ("Newc_RecoveryC_Clip" == 0) )

        | ( ("Depth_to_workings" == 1) &
            ("Newc_Opencast_RClip" == 0) &
            ("Newc_Minewaterlevel_Clip" == 2) )

        | ( ("Depth_to_workings" == 2) &
            ("Newc_Opencast_RClip" == 1) )

        | ( ("Depth_to_workings" == 2) &
            ("Newc_Opencast_RClip" == 0) &
            ("Newc_Minewaterlevel_Clip" == 1) )

        | ( ("Depth_to_workings" == 2) &
            ("Newc_Opencast_RClip" == 0) &
            ("Newc_Minewaterlevel_Clip" == 2) )

        | ( ("Depth_to_workings" == 2) &
```

```
            ("Newc_Opencast_RClip" == 0) &
            ("Newc_Minewaterlevel_Clip" == 3) &
            ("Newc_RecoveryC_Clip" == 0) )
      )
    ),
    3,

Con(
    (
        ( ("Newc_workings_Clip" == 1) &
          ("Newc_multiseam_Clip" == 1) &
          ("Depth_to_workings" == 1) &
          ("Newc_Opencast_RClip" == 0) &
          ("Newc_Minewaterlevel_Clip" == 3) &
          ("Newc_RecoveryC_Clip" == 1) )

      | ( ("Newc_workings_Clip" == 1) &
          ("Newc_multiseam_Clip" == 1) &
          ("Depth_to_workings" == 2) &
          ("Newc_Opencast_RClip" == 0) &
          ("Newc_Minewaterlevel_Clip" == 3) &
          ("Newc_RecoveryC_Clip" == 1) )

      | ( ("Newc_workings_Clip" == 1) &
          ("Newc_multiseam_Clip" == 0) &
          ("Flooded_band" == 0) )
    ),
    2,
    0
)))
```

Listing A.1: ArcGIS Raster Calculator expression used to classify mine water heat opportunities in Newcastle